

NOTICE: When government or other drawings, specifications or other data are used for any purpose other than in connection with a definitely related government procurement operation, the U. S. Government thereby incurs no responsibility, nor any obligation whatsoever; and the fact that the Government may have formulated, furnished, or in any way supplied the said drawings, specifications, or other data is not to be regarded by implication or otherwise as in any manner licensing the holder or any other person or corporation, or conveying any rights or permission to manufacture, use or sell any patented invention that may in any way be related thereto.

CATALOGED BY DDC

AS AD No. 450598

4 5 0 5 9 8

RESEARCH TRIANGLE INSTITUTE
Durham, North Carolina

FINAL REPORT: VOLUME II, Specific Considerations and
Supporting Documents

R-OU-156

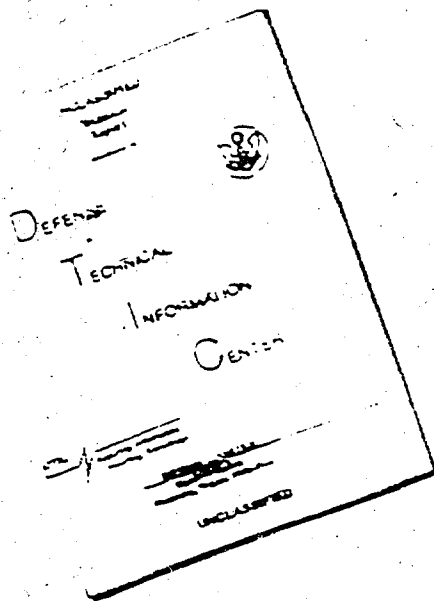
Radiological Recovery Concepts, Requirements,
and Structures

by

J. T. Ryan, J. D. Douglass, Jr., and H. E. Campbell
October 16, 1964

DDC
RECEIVED
NOV 10 1964
RESOLVED
DDC-IRA A

DISCLAIMER NOTICE



THIS DOCUMENT IS BEST
QUALITY AVAILABLE. THE COPY
FURNISHED TO DTIC CONTAINED
A SIGNIFICANT NUMBER OF
PAGES WHICH DO NOT
REPRODUCE LEGIBLY.

REPRODUCED FROM
BEST AVAILABLE COPY

THE RESEARCH TRIANGLE INSTITUTE
Operations Research and Economics Division

OCD Review Notice

This report has been reviewed in the Office of Civil Defense and approved for publication. Approval does not signify that the contents necessarily reflect the views and policies of the Office of Civil Defense.

RESEARCH TRIANGLE INSTITUTE
Durham, North Carolina

FINAL REPORT: VOLUME II, Specific Considerations and
Supporting Documents

R-OU-156

Radiological Recovery Concepts, Requirements,
and Structures

by

J. T. Ryan, J. D. Douglass, Jr., and H. E. Campbell
October 16, 1964

Prepared for

Office of Civil Defense
United States Department of the Army

under

Office of Civil Defense Contract No. OCD-PS-64-56
OCD Subtask 2233B
RTI Project OU-156

FINAL REPORT: VOLUME II, Specific Considerations
and Supporting Documents

Radiological Recovery Concepts, Requirements,
and Structures

Prepared for

Office of Civil Defense

United States Department of the Army

under

Office of Civil Defense Contract No. OCD-PS-64-56

OCD Subtask 3233B

RTI Project OU-156

by

J. T. Ryan

J. D. Douglass, Jr.

and

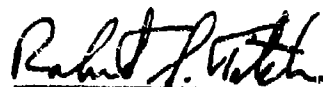
H. E. Campbell

THE RESEARCH TRIANGLE INSTITUTE
Operations Research and Economics Division
Post Office Box 490
Durham, North Carolina

Approved by:



Edgar A. Parsons
Director



Robert S. Titchen
Deputy Director

October 16, 1964

PREFACE

This is Volume II of two separately bound volumes that report the research completed under the general terms of the Office of Civil Defense Subtask No. 32338, "Radiological Recovery Concepts, Requirements and Structures." This volume describes five supporting studies all previously reported to the Office of Civil Defense in research memoranda. Volume I describes the general aspects of the investigations and presents the conclusions and recommendations. The abstract for each of the volumes is presented on the following pages.

The authors are pleased to acknowledge the valuable computer assistance of Mr. Quentin Ludgin of the Research Triangle Institute during the course of the project.

ABSTRACT FOR VOLUME 1

This study examines the effectiveness and costs associated with the application of decontamination to accelerating recovery of an activity in a postattack fallout environment. The effectiveness is measured in two ways: first, by the fractional reduction in dose rate that can be achieved by decontamination, and second, when the dose received during the activity is specified, by the fractional reduction in denial time that can be achieved by decontamination. The costs are described in terms of the personnel and equipment required for the decontamination, the radiation doses received by the personnel, and the water required by the operation. The recovery of an activity is defined in terms of radiation doses received by the activity personnel in performing the activity. When these doses are reduced to an acceptable safety level by reducing the dose rate in the activity area, the activity is said to be recovered. The above dose constraints are expressed both in terms of the maximum total dose and in terms of the maximum equivalent residual dose. The primary conclusion reached, that decontamination is as vital to recovery as shelters are to survival in a fallout environment, is the basis for recommending further studies analyzing the application of decontamination to integrated whole-city recovery.

ABSTRACT FOR VOLUME II

Volume II contains five studies concerned with determining the costs and effectiveness of decontamination applied to postattack recovery in a fallout environment. These studies cover the following subjects:

(1) The Effect of Early Decontamination on Total Dose: This study describes the effect of a single (discrete) reduction in radiation intensity (as by decontamination) on an individual's dose history in a $t^{-1.2}$ radiation field;

(2) The Effect of Early Decontamination on ERD: This analysis is like the first in describing the effect of a single reduction in radiation intensity, except that an individual's dose is measured in terms of his ERD;

(3) Total Dose Approximations for Brief Exposure in a Fallout Environment: Two approximations to the expression used to calculate total dose for a finite exposure time in a t^{-k} radiation field are developed and the resultant error is estimated. The approximations are then used to determine the earliest time of entry (for a fixed allowable dose) when a countermeasure operations such as decontamination is employed;

(4) The Effectiveness of Radiological Countermeasures in Accelerating Postattack Recovery: This study develops the parametric relationships that determine the extent to which radiological countermeasures could accelerate the postattack recovery process; e.g., time saved in recovering an activity as a function of the duration of the activity, the time when the activity was to have commenced, the allowable dose received by the activity personnel, the fallout reference intensity, and the effect of decontamination of the intensity.

(5) Studies of Decontamination Effectiveness: This analysis is primarily concerned with the costs and effectiveness of decontamination on and around nine NFSS structures, in reducing the dose rate inside or near the structures.

A parametric analysis of fictitious structures is also included to examine certain parameters (floor and wall weights, story of the detector, number and size of apertures, etc.) in a controlled manner to determine their contribution to dose rate reduction. A similar parametric analysis is made of streets and intersections in an urban area.

VOLUME II CONTENTS

	<u>Page</u>
PREFACE.	iii
ABSTRACT FOR VOLUME I.	iv
ABSTRACT FOR VOLUME II	v
INTRODUCTION	1
APPENDIX A: <u>The Effect of Early Decontamination on Total Dose</u>	A- 1
I. Introduction and Summary	A- 1
II. Analysis.	A- 3
III. Alternative Buildup Functions	A-61
References.	A-65
APPENDIX B: <u>The Effect of Early Decontamination on Equivalent Residual Dose</u>	B- 1
I. Introduction and Summary.	B- 1
II. ERD Without Decontamination	B- 2
A. General Expression for ERD.	B- 3
B. Intensity Function.	B- 4
C. Weighting Function.	B- 8
D. ERD Function without Decontamination.	B- 9
III. ERD With Decontamination.	B-13
A. Intensity Function with Decontamination	B-13
B. ERD Function with Decontamination	B-18
C. Maximum ERD with Decontamination.	B-19
IV. Reduction in ERD Due to Decontamination	B-35
A. Introduction and Derivation	B-35
B. Discussion of Results	B-39
References.	B-40
APPENDIX C: <u>Total Dose Approximations for Brief Exposure in a Fallout Environment</u>	C- 1
I. Introduction and Summary.	C- 1
A. Total Dose Expression	C- 1
B. First Approximation	C- 2
C. Second Approximation.	C- 5
D. Summary of Examples of the Use of the Approximations.	C- 7

VOLUME II CONTENTS (Cont'd)

	<u>Page</u>
II. First Approximation Error Analysis	C- 8
III. Second Approximation Error Analysis.	C-12
IV. Time Saved Using Total Dose Approximations.	C-14
A. Entry Time.	C-14
B. Time Saved.	C-16
APPENDIX D: <u>The Effectiveness of Radiological Countermeasures</u> <u>in Accelerating Postattack Recovery</u>	D- 1
I. Summary	D- 1
II. Analysis.	D- 3
A. Introduction.	D- 3
B. Dose Rate	D- 4
C. Countermeasure Effectiveness.	D- 6
D. Activity Performance Dose	D- 6
E. Activity Entry Lead Time.	D-18
F. Countermeasure Effect on Lead Time.	D-21
III. Discussion of Results	D-39
References.	D-52
APPENDIX E: <u>Studies of Decontamination Effectiveness.</u>	E- 1
I. Introduction.	E- 1
A. Objectives.	E- 1
B. Decontamination Data.	E- 3
C. Structures Analyzed	E- 5
D. Intensity Reduction Calculation	E- 5
E. Practical Considerations.	E-17
F. Non-Uniform Distributions	E-22
II. Individual Decontamination Studies.	E-24
A. Introduction.	E-24
B. Six-Floor Apartment Building.	E-44
C. Six-Floor Apartment Building.	E-52
D. Twenty-one Story Office Building.	E-58
E. General Dyestuffs Corporation	E-64
F. High School Gymnasium	E-70

VOLUME II CONTENTS (Cont'd)

	<u>Page</u>
G. Simonds Press Building.	E-74
H. Department of Interior.	E-80
I. A Three-Story Department Store Building	E-84
J. Bell Telephone Building	E-88
K. Fictitious Building - Parametric Study.	E-93
L. Unshielded Detector on Streets - Parametric Study	E-101
References.	E-105

LIST OF TABLES

<u>Table</u>		<u>Page</u>
E-I	Cost and Effectiveness Data for Selected Mass Reduction Factors for Various Decontamination Methods - Decontamination of Pavements (Asphalt or Concrete)	E-28
E-II	Cost and Effectiveness Data for Selected Mass Reduction Factors for Various Decontamination Methods - Decontamination of Roofs	E-29
E-III	Combined Ideal Intensity Reduction Factors for Nine Selected Structures	E-34
E-IV	Summary of Combined Practical Intensity Reduction Factor and Associated Costs for Nine Selected Structures	E-35
E-V	Summary of Outside Detector Analysis Data.	E-41
E-VI	Designation of Surfaces which can be Decontaminated.	E-95
E-VII	Building Data for Hypothetical Building Study. . . .	E-96
E-VIII	The $f_{i,j}^*$ Values for Parametric Study I	E-97
E-IX	The $f_{i,j}^*$ Values for Parametric Study II.	E-98
E-X	The $f_{i,j}^*$ Values for Parametric Study III	E-99
E-XI	The $f_{i,j}^*$ Values for Parametric Study IV.	E-100
E-XII	Equivalent PF Obtained by Removing all Contamination Except on Straight Road.	E-101
E-XIII	Equivalent PF Obtained by Removing all Contamination Except that on T - Shaped Intersection	E-102
E-XIV	Equivalent PF Obtained by Removing all Contamination Except that on Four-way Intersection	E-103
E-XV	Equivalent PF from Typical Contaminated Streets. . .	E-104

LIST OF FIGURES

Figure		Page
A-1	Variation in Dose Rate With Time	A-4
A-2	Relationships Considered in Selecting t_p	A-6
A-3	Model of Intensity Behavior.	A-7
A-4	Curve for Determining Total Dose as a Function of Time After Detonation.	A-9
A-5	Curve for Determining Total Dose as a Function of $(t-t_a + 1)$	A-11
A-6	Curves for Determining Total Dose as a Function of Time After Arrival	A-13
A-7	Normalized Total Dose as a Function of Time After Arrival.	A-15
A-8	Dose Received as a Function of Time of Arrival	A-18
A-9	Theoretical Effect of Instantaneous Decontamination or Dose Accumulation	A-19
A-10	Theoretical Effect on Finite Time Decontamination on Dose Accumulation	A-22
A-11	t_{eff} vs $t_d + \frac{1}{2}T$ for Finite Time Decontamination. . . .	A-25
A-12	Generalized Total Dose Curve	A-26
A-13	R_∞ vs t_d Trade Offs for Constant f_d	A-27
A-14	R_∞ vs f_d Trade Offs for Constant t_d	A-28
A-15	t_d vs f_d Trade Offs for Constant R_∞	A-29
A-16	ERD Weighting Function and Approximation	A-32
A-17	Comparison of $D_R(t)$ with $D_t(t)$	A-33
A-18	t_{max} as a Function of Time of Arrival	A-34
A-19	Normalized Max ERD as a Function of Time of Arrival	A-36
A-20	f_d vs t_d Trade Offs for Constant R_x	A-40
A-21	R_{336} vs f_d Trade Offs for Constant t_d	A-41
A-22	t_a vs t_d Trade Offs for Constant R_{336} with $f_d = 0$. .	A-42
A-23a	R_{336} vs t_d Trade Offs for Fixed f_d and $t_a = 1/3$ hour. .	A-45
A-23b	R_∞ vs t_d Trade Offs for Fixed f_d and $t_a = 1/3$ hour . .	A-46
A-24a	R_{336} vs t_d Trade Offs for Fixed f_d and $t_a = 1$ hour . .	A-47
A-24b	R_∞ vs t_d Trade Offs for Fixed f_d and $t_a = 1$ hour . .	A-48
A-24c	R_{175} vs t_d Trade Offs for Fixed f_d and $t_a = 1$ hour . .	A-49

LIST OF FIGURES (Cont'd)

Figure		Page
A-25a	R_{336} vs t_d Trade Offs for Fixed f_d and $t_a = 3$ hours	A-50
A-25b	R_{∞} vs t_d Trade Offs for Fixed f_d and $t_a = 3$ hours	A-51
A-25c	R_{236} vs t_d Trade Offs for Fixed f_d and $t_a = 3$ hours	A-52
A-26a	R_{336} vs t_d Trade Offs for Fixed f_d and $t_a = 9$ hours	A-53
A-26b	R_{∞} vs t_d Trade Offs for Fixed f_d and $t_a = 9$ hours	A-54
A-26c	R_{330} vs t_d Trade Offs for Fixed f_d and $t_a = 9$ hours	A-55
A-27	Effect of x on R_x Variation	A-56
A-28	f_d vs t_d Trade Offs to Achieve .9R Perfect with $t_a = 1/3$ hours	A-57
A-29	f_d vs t_d Trade Offs to Achieve .9R Perfect with $t_a = 1$ hour.	A-58
A-30	f_d vs t_d Trade Offs to Achieve .9R Perfect with $t_a = 3$ hours	A-59
A-31	f_d vs t_d Trade Offs to Achieve .9R Perfect with $t_a = 9$ hours	A-60
A-32	General Buildup Function	A-61
A-33	Alternative Buildup Function	A-62
A-34	Alternative Buildup Function	A-63
B-1	Intensity Behavior without Decontamination	B-6
B-2	ERD Weighting Function and Approximation	B-10
B-3	Comparison of $D_r(t)$ with $D_t(t)$	B-12
B-4	Time of Max ERD (t_{max}) as a Function of Time of Arrival	B-14

LIST OF FIGURES (Cont'd)

Figure		Page
B-5	Max ERD as a Function of Time of Arrival	B-15
B-6	Intensity Behavior with Decontamination	B-17
B-7	Effect of t_d on t_{max}	B-22
B-8	Effect of f_d on t_{max}	B-23
B-9	Locus of f_d , t_d Combinations	B-25
B-10a	Step 1 in the Solution for t_{max}	B-27
B-10b	Step 1 in the Solution for t_{max}	B-28
B-10c	Step 1 in the Solution for t_{max}	B-29
B-11	Step 2 in the Solution for t_{max}	B-30
B-12a	The Time of Maximum ERD as a Function of Time of Decontamination for Selected Levels of Decontamination $t_a = 1$ hour.	B-32
B-12b	The Time of Maximum ERD as a Function of Time of Decontamination for Selected Levels of Decontamination $t_a = 3$ hours	B-33
B-12c	The Time of Maximum ERD as a Function of Time of Decontamination for Selected Levels of Decontamination $t_a = 9$ hours	B-34
B-13a	Reduction in Maximum ERD Due to Decontamination as a Function of t_d for Selected f_d 's $t_a = 1$ hour. . .	B-36
B-13b	Reduction in Maximum ERD Due to Decontamination as a Function of t_d for Selected f_d 's $t_a = 3$ hours . .	B-37
B-13c	Reduction in Maximum ERD Due to Decontamination as a Function of t_d for Selected f_d 's $t_a = 9$ hours . .	B-38
C-1	Comparison of Total Dose and Approximations D_1 and D_2	C-3
C-2	Error When the Function D_1 is Used to Approximate the Dose D	C-4
C-3	Error When the Function D_2 is Used to Approximate the Dose D	C-6
C-4	Earliest Time of Entry Calculated Using D_1 for Dose. .	C-17
C-5	Earliest Time of Entry Calculated Using D_2 ($k = 1.2$) for Dose	C-18
C-6	Per Cent Savings Realized.	C-21
C-7	T_m = Time Saved with Perfect Decontamination	C-22

LIST OF FIGURES (Cont'd)

Figure		Page
D-1	Normalized Effective Intensity versus Time of Entry . . .	D-9
D-2	Weighting Function Approximation.	D-10
D-3	Normalized Effective Intensity versus Time of Entry . . .	D-12
D-4	Weighting Function Approximation.	D-14
D-5	Time of Maximum ERD versus Entry Time	D-15
D-6	Entry Time versus Time of Maximum ERD	D-16
D-7	Normalized Maximum ERD versus Time of Entry	D-17
D-8	Normalized Effective Intensity versus Time of Entry . . .	D-19
D-9	Normalized Dose versus Entry Time	D-20
D-10	Activity Parameters Δt and t_e when $\frac{f_d H}{D}$ is held Constant: Comparison of Total Dose and ERD Approach. .	D-22
D-11	Potential Maximum Time Saved ($I_e = \frac{D}{\Delta t}$) versus H	D-25
D-12	Fraction of Maximum Time Saved as a Function of f_d . . .	D-26
D-13	Effect of Biological Recovery	D-27
D-14	Total Dose Criterion Time Saved	D-29
D-15	Time Saved Performance Curves With $\frac{H}{D} = 6.25$ <u>roentgens/hr</u> roentgens	D-31
D-16	Time Saved Performance Curves With $\frac{H}{D} = 12.5$ <u>roentgens/hr</u> roentgens	D-32
D-17	Time Saved Performance Curves With $\frac{H}{D} = 25$	D-33
D-18	Time Saved Performance Curves With $\frac{H}{D} = 50$	D-34
D-19	Time Saved Performance Curves With $\frac{H}{D} = 100$	D-35
D-20	Time Saved Performance Curves With $\frac{H}{D} = 200$	D-36
D-21	Time Saved Performance Curves With $\frac{H}{D} = 400$	D-37
D-22	Time Saved Performance Curves With $\frac{H}{D_T} = 800$	D-38
D-23	H versus T Performance Curve	D-40
D-24	H versus I_e Performance Curve With $f_d = .9$	D-41
D-25	H versus I_e Performance Curve With $f_d = .8$	D-42
D-26	H versus I_e Performance Curves With $f_d = .7$	D-43
D-27	H versus I_e Performance Curves With $f_d = .6$	D-44
D-28	H versus I_e Performance Curves With $f_d = .5$	D-45
D-29	H versus I_e Performance Curves With $f_d = .4$	D-46

LIST OF FIGURES (Cont'd)

<u>Figure</u>		<u>Page</u>
E-1	Location Map of Decontamination Areas.	E-7
E-2	Efficiencies of Decontamination Methods.	E-9
E-3	Sensitivity of F_j to E_i	E-19
E-4	Maximum Error in F_j if $E = .06$	E-21
E-5	Error in F_j Using the Approximation $f_{i,j} = f_{i,j}^* + E_i$	E-23
E-6	Location Map of Decontamination Areas.	E-47
E-7	View of Building from West 182nd Street (Note: fireplug).	E-48
E-8	West 182nd Street (Note: large drain on corner).	E-48
E-9	View of Roof	E-49
E-10	View of Side Alley	E-49
E-11	View of Adjacent Roofs	E-50
E-12	View of Playground and Garden Area (Note: iron fence around garden)	E-50
E-13	Location Map of Decontamination Areas.	E-54
E-14	A View of West 52nd Street	E-55
E-15	A View of the Narrow Alley Behind Building	E-55
E-16	View of Garage Roof and Parking Lot.	E-56
E-17	View of Tunnel to Rear Alley	E-56
E-18	View of Building from West 52nd Street	E-57
E-19	View of Roof (Note: three foot lip at edge).	E-57
E-20	Location Map of Decontamination Areas.	E-60
E-21	View of Park Avenue (Note: Island with Garden in Center of Road).	E-61
E-22	View of East 49th Street	E-61
E-23	View of Park Avenue Showing Iron Gate Around Center Island.	E-62
E-24	View of Sidewalk and Fireplug on East 49th Street.	E-62
E-25	View of Roof (Non-contributing surface).	E-63
E-26	A Drain on the Roof.	E-63

LIST OF FIGURES (Cont'd)

<u>Figure</u>		<u>Page</u>
E-27	Location Map of Decontamination Areas.	E-66
E-28	View of Building from Hudson Street (Note: Sewer drain)	E-67
E-29	View of Intersection of Hudson Street and Morton Street. (Note: brick pavement, fireplace and sewer. . .	E-67
E-30	View of Building Roofs Across Leroy Street	E-68
E-31	Playground (Note: two drains in center).	E-68
E-32	View of Hudson Street and Sidewalk Areas from Roof . .	E-69
E-33	View of Parking Lot and Adjacent Garage Roof. (Note: depression area on garage roof).	E-69
E-34	Location Map of Decontamination Areas.	E-72
E-35	View of Building from Bennett Street	E-73
E-36	Playground	E-73
E-37	Location Map of Decontamination Areas.	E-76
E-38	View of Building from South Water Street	E-77
E-39	View of Building from Ely Street (Note: steep grade) .	E-77
E-40	View of Building from South Avenue	E-78
E-41	View of Building from Intersection of South Avenue and Ely Street	E-78
E-42	Location Map of Decontamination Areas.	E-82
E-43	Location Map of Decontamination Areas.	E-86
E-44	View of Building from Main Street.	E-87
E-45	View of Building from Capitol Avenue	E-87
E-46	Location Map of Decontamination Areas.	E-90
E-47	View of Building from Intersection of 11th Street and Chestnut Street.	E-91
E-48	View of Building from Pine Street.	E-91
E-49	View of Building from 10th Street and Chestnut Street.	E-92
E-50	View of the Building from 11th Street.	E-92
E-51	Location Map of Parametric Study	E-94
E-52	Straight Road.	E-101
E-53	T - Shaped Street Intersection	E-102
E-54	Full Four-way Intersection	E-103

Radiological Concepts, Requirements, and Structures
Volume II. Specific Considerations and Supporting Documents

INTRODUCTION

This volume reports five studies performed under Office of Civil Defense subtask 3233B, Radiological Recovery Concepts, Requirements, and Structures. It is addressed to technical personnel concerned with the planning of postattack recovery operations as summarized and described in Volume I of this report. All of the studies presented in Volume II are concerned with examining the effectiveness and costs that describe the application of decontamination to accelerating recovery of an activity in a postattack environment. The studies, by analyzing operations, situations, develop sets of operational planning guides that take the form of:

- (1) Operational points of view and associated rules of thumb that place in perspective the important aspects and parameters that govern the value of the operation,
- (2) Specific analytical approaches and performance curves that provide the necessary background of theory and detailed data.

The first type of planning guide is presented in Volume I, General Considerations, while the second type of planning guide is presented in this Volume II, Specific Considerations and Supporting Documents. The paragraphs below summarize the five supporting documents reported in this volume.

1. General Considerations (Volume I, Chapter 1)

2. Decontamination of Personnel (Volume II, Chapter 2)

3. Decontamination of Equipment (Volume II, Chapter 3)

effects of fallout arrival time, fallout buildup function, initiation time of decontamination operation, duration of the operation, and effectiveness (dose reduction) of the operation are displayed both analytically and graphically. Fallout arrival times from .2 hours to 10 hours are considered. General buildup functions are used. Decontamination operations are considered only when they begin after fallout deposition has ceased. Both zero and finite operation duration times are considered. Finally, all possible dose reductions are considered. The results are, in general, displayed by means of the ratio of the maximum total dose with the operation to the total dose without the operation. The major assumption in this study is that the radioactive decay is adequately approximated by an exponential decay $I(t)e^{-1.2t}$ curve.

Appendix B: The Effect of Early Decontamination on EED

The purpose of this study is to determine the effect of early decontamination intensity reductions on an individual's equivalent residual dose, EED. The individual and combined effects of fallout arrival time, fallout buildup function, initiation time of decontamination operation, duration of the operation, and effectiveness (dose reduction) of the operation are displayed both analytically and graphically. Fallout arrival times from .2 hours to 10 hours are considered. General buildup functions are used. Decontamination operations are considered only when they begin after fallout deposition has ceased. Both zero and finite operation duration times are considered. Finally, all possible dose reduction are considered. The results are, in general, displayed by means of the ratio of the maximum EED with the operation to the maximum EED without the operation. The major

assumption in the analysis is that the radioactive decay is approximately approximated by an approximate $I(t) = I_0 e^{-\lambda t}$ curve.

Appendix C: Total Dose Approximation for Brief Exposure in a Fallout Environment

The purpose of this study is to determine the effect of the use of approximations for total dose. An individual entering a fallout zone, whose dose rate is $\frac{I(t)}{PF} t^{-k}$, at time t_e and leaving it at time $t_e + \Delta t$ receives a certain dose $D(t_e, \Delta t, k)$. Two approximations of this dose, $\frac{\Delta I(t)}{PF} t_e^{-k}$ and $\frac{\Delta I(t)}{PF} (t_e + \frac{\Delta t}{2})^{-k}$, are examined to determine the resultant error. This error is developed and graphed as a function of k and $\frac{\Delta t}{t_e}$. The approximations are then used when the allowable dose is fixed to determine the earliest time of entry and to determine the amount by which this entry time can be reduced when countermeasure operations such as decontamination are employed.

Appendix D: The Effectiveness of Radiological Countermeasures in Accelerating Postattack Recovery

This study develops the relationships that determine the extent to which radiological countermeasures can accelerate the postattack recovery process. The recovery of an activity is specified in terms of the duration of the activity, the time when the activity is to commence, the allowable dose received by the activity personnel, the fallout field characteristics, and the effect of the countermeasure on these field characteristics. The acceleration of the recovery is specified by the difference between the time when the activity may commence if the countermeasure is not employed and the time when the activity may commence if the countermeasure is employed. This difference, the time saved, is analyzed as a function of the other

parameters. Finally, the analysis is examined in a general manner to determine the range of situations where countermeasures appear to be potentially most valuable.

Appendix F: Studies of Decontamination Effectiveness

This study examines, by theory and by analysis of real structures, the reductions in intensity inside and outside NPS buildings that can be brought about by decontaminating the accessible surfaces on and around the buildings. Specifically, the report presents the theory and applies it to nine different NPS buildings in order to:

- (1) Determine the intensity reductions that can be achieved by decontamination methods applied to practical situations involving real physical structures.
- (2) Determine the intensity reductions that can be achieved when the detector is located inside a structure and when the detector is located outside the structure.
- (3) Determine the decontamination costs (equipment, manpower, water, radiation dose received by the decontamination crews) in achieving the intensity reductions.
- (4) Determine the sensitivity of the achieved intensity reduction to the cleaning efficiency of the decontamination operation (and, therefore, to the type of decontamination method).
- (5) Determine the relative importance of the various surfaces (roofs, paved roads, parking lots, etc.) that can be decontaminated to the intensity reduction that can be achieved.

Appendix A

The Effect of Early Decontamination on Total Dose

This Appendix was originally submitted to OCD as Research Memorandum RM 156-1,* except for minor editorial changes.

L. B. Douglass, Jr. The Effect of Decontamination on Total Dose.
Research Memorandum RM 156-1. Durham, North Carolina: Research
Institute, Operations Research Division, 12 March 1964

Appendix A

The Effect of Early Decontamination on Total Dose

I. INTRODUCTION AND SUMMARY

In a postattack environment, radiation from the radioactive fallout may be sufficiently hazardous to force a cut back or curtailment in certain activities involving personnel. Fortunately, the hazard posed by the radioactivity does not remain invariant but, rather, diminishes with time as radioactive decay takes place. This process of natural decay in field intensity enables the curtailed activity to be resumed at some future time, which depends on the amount and type of radioactive material. If it is desirable or necessary to resume activities before sufficient time has elapsed for the requisite reduction in intensity to have occurred naturally, then the intensity must be reduced by other means. Decontamination is one means of forcing such a reduction. This study analyzes the effect of a forced reduction in the intensity in a facility (which may be the result of decontaminating on or about the facility) on the total dose of the personnel within the facility.

In the absence of a forced reduction, the total dose received by an individual up to time t is the area under his intensity vs. time curve up to time t . Here, the intensity is that within the facility and therefore the protection factor of the facility is absorbed into the reference intensity factor $I(1)$. The intensity curve in this study (Figure A-3) uses a linear function to describe the buildup of intensity and the function

$I(1)t^{-1.2}$ to describe the subsequent decay. For any time t , the total dose as a function of reference intensity, $I(1)$, and time of arrival, t_a , presented in Figure A-12. This "normal" total dose is used in the subsequent development as a reference. That is, the total dose at some time after decontamination has been performed will be compared with the "normal" total dose that otherwise would have been received up to the same time.

Decontamination enters the analyses as an instantaneous reduction in intensity that takes place at time t_d . Before time t_d , the intensity is not affected. For all times after time t_d , the intensity magnitude is multiplied by a factor f_d whose value lies between zero and one. The resultant decrease in total dose (for fixed time of arrival) will depend on t_d , on f_d , and, in addition, on the time after t_d at which the total dose is examined. At the conclusion of the analysis, the total dose is examined at infinity, at two weeks, and at the time at which the equivalent residual dose associated with the "normal" total dose is a maximum. For each examination and for various times of arrival, the ratio of total dose with decontamination to normal total dose is presented as a function of time of decontamination (t_d) and amount of decontamination (f_d). The effects of variations in these parameters comprise the primary objectives of this analysis and are presented in Figures A-20 through A-26.

In the analysis, fallout arrival times from .2 hours to 10 hours are considered. Only times of decontamination operations beginning after the time at which fallout deposition ceases are considered. Both zero and finite operation duration times are considered. All possible intensity reductions are considered. The results are displayed by the ratio of the

total dose with the operation to the total dose without the operation. This ratio is evaluated at specific times that are applicable to the value range of interest; for instance, short range (weeks) or long range (months). Finally a method is presented so that the results can be applied to any desired buildup function.

II. ANALYSIS

The majority of fallout operations studies have used the common fallout decay law to describe the constraining radioactive environment. This decay law approximates the radiation intensity at a point by $I(1)t^{-1.2}$, where $I(1)$ is a reference constant and t is the time after detonation in hours. This expression is assumed to be valid in describing the radiation intensity at a point from the time at which the fallout deposition is completed to 4000 hours after detonation. In actual operations it is necessary to consider the effect of natural fallout deposition. This gradual buildup of the fallout field begins at the time of arrival of the first fallout particles, t_a , reaches a peak in radiation intensity at t_p , and is completed when deposition ceases, t_c . The resultant behavior of intensity with time is illustrated in Figure A-1.

Devaney (Reference A-1) references LaRiviere as suggesting the following approximate relationships among t_a , t_p , and t_c :

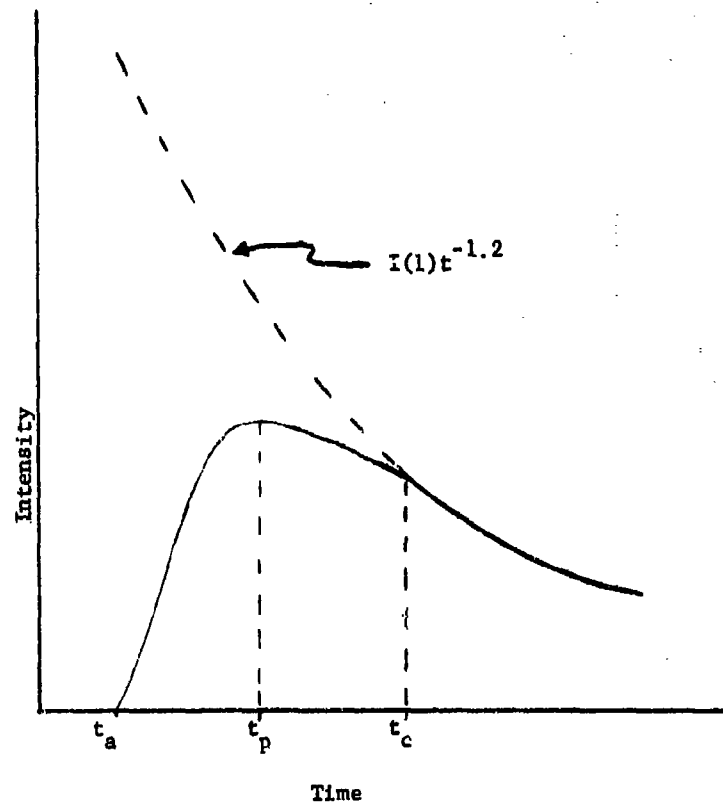
$$t_p = 2 t_a \quad t_a \leq 13 \text{ hr.} \quad (\text{A-1})$$

$$t_c = 5 t_a^{0.7} \quad t_a \leq 13 \text{ hr.} \quad (\text{A-2})$$

In addition, he suggests that, between t_a and t_p , the log intensity increases

FIGURE A-1

Variation in Dose Rate With Time



linearly with log time. That is, he suggests the following formulation of intensity be applied to the interval of time from t_a to t_p :

$$I = I_a(t-t_a)^k, \quad (A-3)$$

where k and I_a are constants that depend on the particular situation.

These suggestions provide a useful basis for constructing a model that includes the effect of t_a on operations planning. The time of arrival is selected for emphasis because: 1) it strongly affects the dose magnitude that a community can expect to receive; and 2) it is potentially valuable as a reference time from the viewpoint of a community that is about to schedule recovery operations. With this direction in mind, it is convenient to begin by simplifying the above suggestions and combining them into a fallout intensity model.

First, examine Equations A-1 and A-2 as displayed by the solid lines in Figure A-2. Rather than use these two equations for t_p and t_c assume that t_p and t_c occur simultaneously and use the broken line in Figure A-2 to represent both t_p and t_c . That is, let $t_p = t_c = 2.5 t_a$. The constant 2.5 is selected to place the broken line between the solid lines for $t_a \leq 10$ and thus partially compensate for letting t_p equal t_c . The resultant variation of intensity with time is illustrated in Figure A-3.

In Figure A-3, the following relation must hold:

$$I_a(t-t_a) = I(1)t^{-1.2} \text{ when } t = 2.5 t_a. \quad (A-4)$$

This equation determines I_a in terms of $I(1)$ and t_a as follows:

FIGURE A-2

Relationships Considered in Selecting t_p

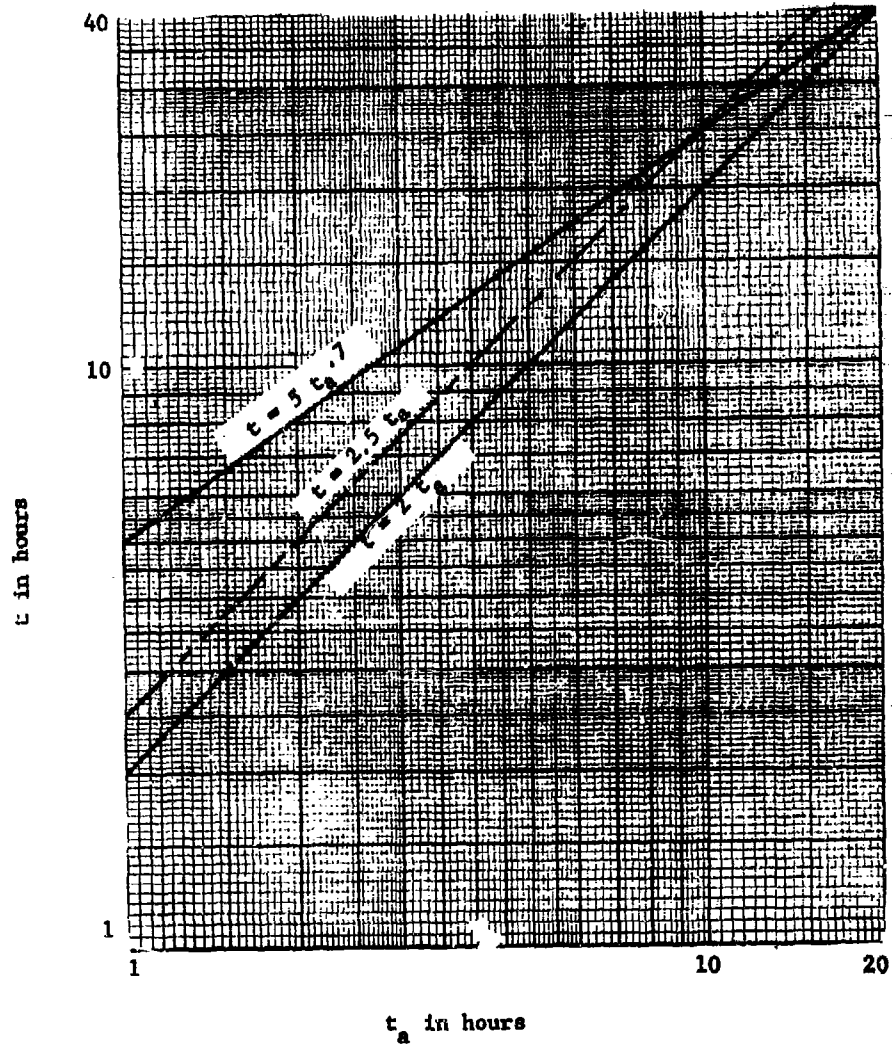
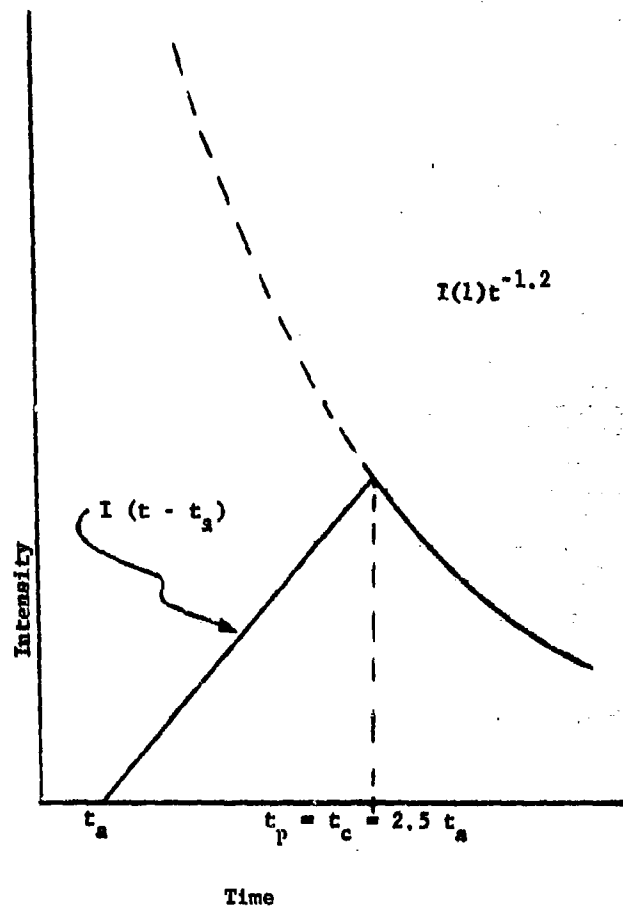


FIGURE A-3

Model of Intensity Behavior



$$I_a = \frac{I(1) (2.5t_a)^{-1.2}}{1.5t_a} = .222 t_a^{-2.2} I(1) \quad (A-5)$$

Equation A-5 and Figure A-3 combine to define the total dose, $D_t(t)$ as a function of time as follows:

$$\frac{D_t(t)}{I(1)} = \begin{cases} .222 t_a^{-2.2} \int_{t_a}^t (x-t_a) dx & \text{for } t_a \leq t \leq 2.5 t_a \\ .222 t_a^{-2.2} \int_{t_a}^{2.5t_a} (x-t_a) dx \\ + \int_{2.5t_a}^t x^{-1.2} dx & \text{for } t \geq 2.5 t_a \end{cases} \quad (A-6)$$

which reduces to

$$\frac{D_t(t)}{I(1)} = \begin{cases} .111 t_a^{-2.2} (t-t_a)^2 & \text{for } t_a \leq t \leq 2.5 t_a \\ 4.41 t_a^{-0.2} - 5 t^{-0.2} & \text{for } t \geq 2.5 t_a \end{cases} \quad (A-7)$$

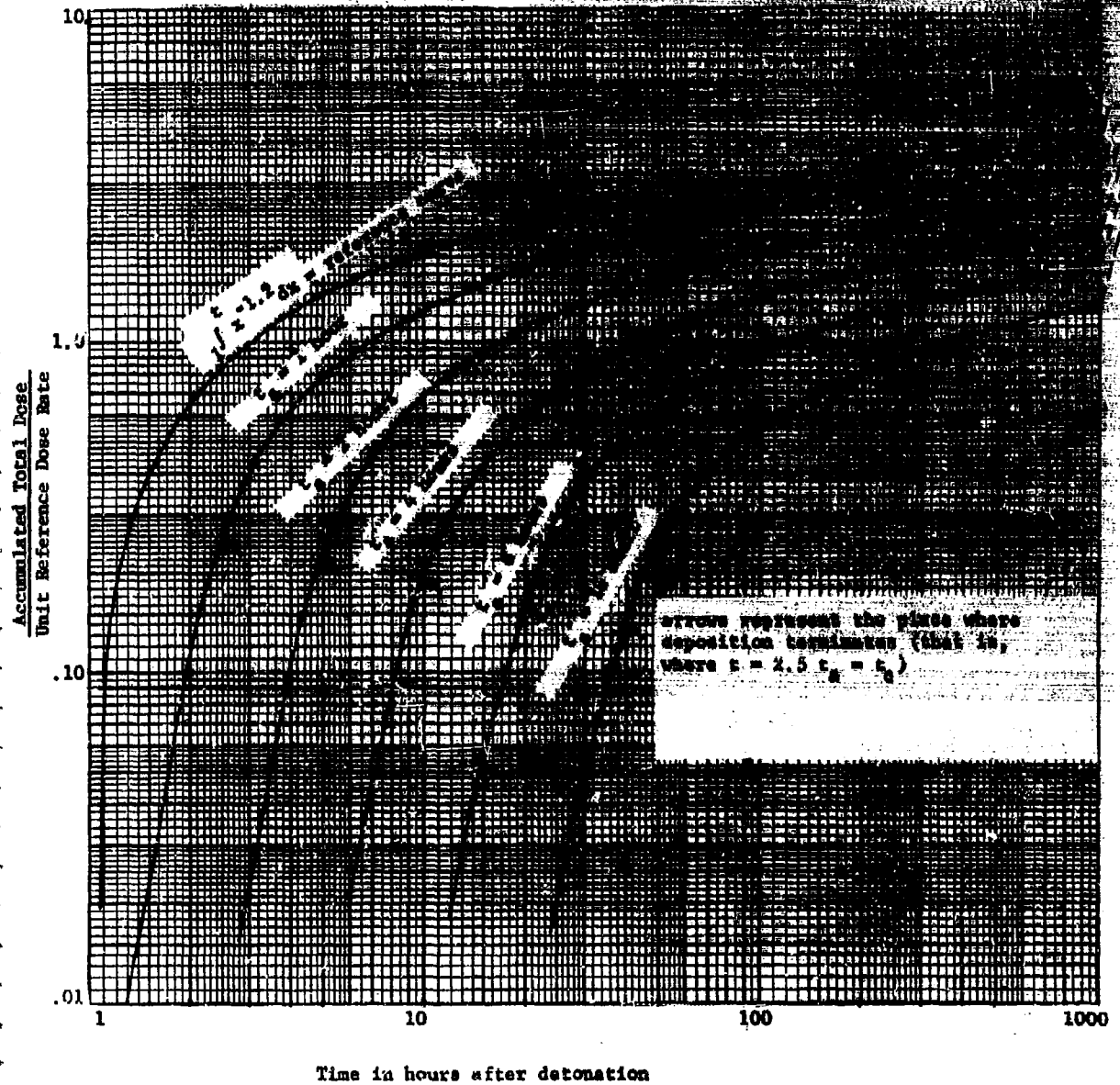
This expression for total dose* will be used in the subsequent discussion. It will be used to analyze operations within the first few weeks after fallout arrives. Equation A-7 is shown in Figure A-4 by five curves, each of which assumes a specific value for t_a . The values selected for t_a are, in hours, 1, 2, 4, 8, and 16. In addition to these five curves, a sixth curve representing the equation

$$\frac{D_t(t)}{I(1)} = \int_1^t x^{-1.2} dx \quad (A-8)$$

*An analysis using the more complicated ERD is presented in Appendix B.

FIGURE A-4

Curve for Determining Total Dose as a Function of Time After Detonation



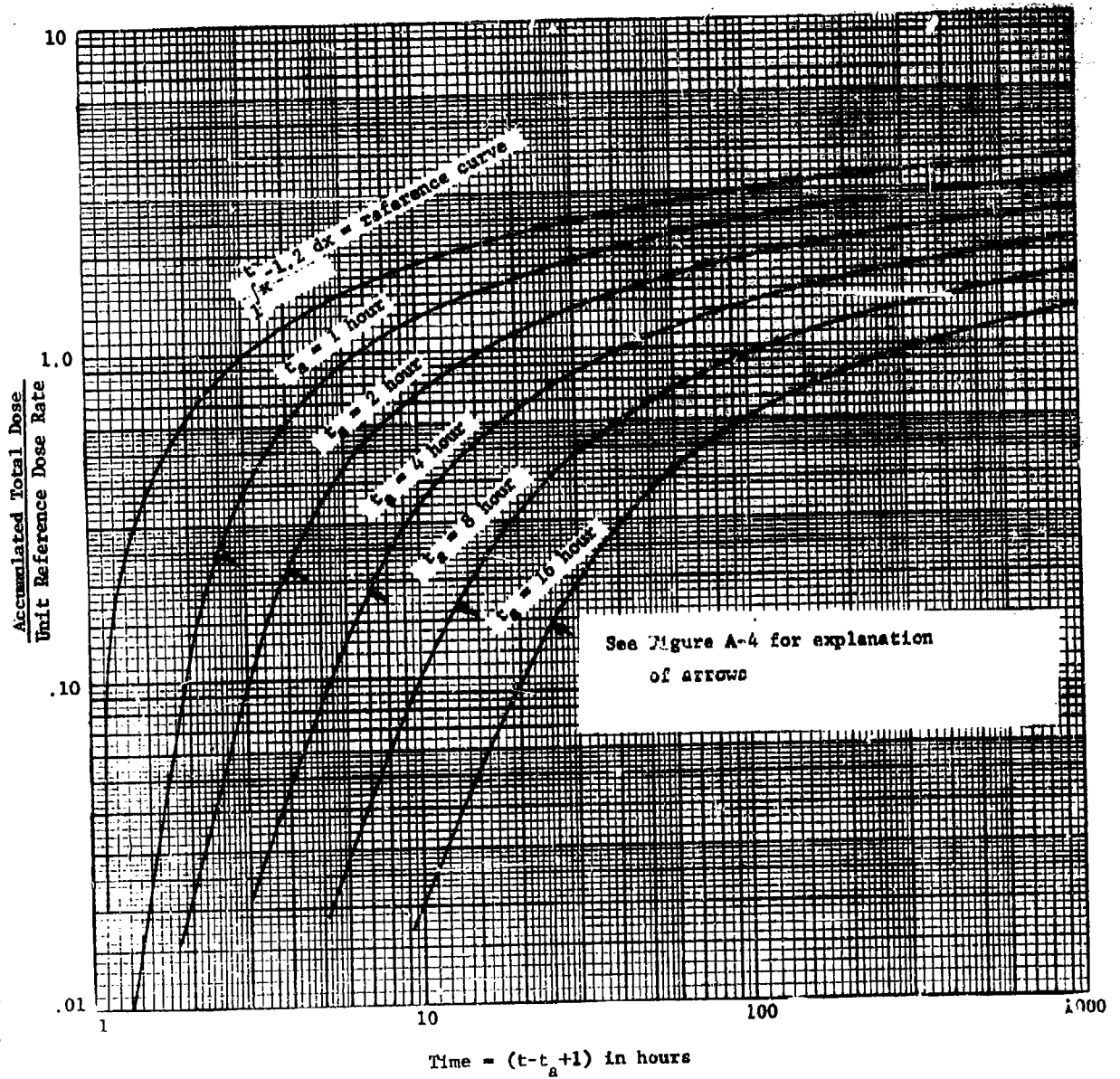
is also presented. This sixth curve is the total dose curve that does not account for the buildup period. This curve assumes that all fallout is instantaneously deposited at $t = 1$ hour; that is, at one hour following detonation. On each of the five curves that do account for the buildup period, an arrow is placed to indicate when $t_c = t_p$ occurs. From the curves in Figure A-4, the total dose as a function of time can be determined for any applicable reference intensity, $I(1)$, and any of the specified times of arrival.

A prediction of the radiation hazard (total dose) for a particular community begins with the selection of a reference curve on the basis of the weapon, the burst height, ground zero, induced radiation effects, and the weather conditions. This curve, labeled "reference curve" in Figure A-4 assumes that all fallout deposition that will occur naturally does, in fact, occur instantaneously at $t = 1$ hour. It does not account for the natural buildup of the fallout material. Therefore, the reference curve then must be modified to account for time of arrival and buildup period. In Figure A-4, the five curves for selected values of t_a illustrate such a modification for different times of arrival. It can be seen that this modification is independent of $I(1)$, which is one reason for presenting the curves in a normalized form (by dividing each by the reference intensity, $I(1)$).

Figure A-4 views the dose history of a community from the eyes of an outsider because the reference time, $t = 0$, is the time of detonation. Therefore it is worthwhile to modify these curves so that they reflect the view point of an insider whose reference time is more conveniently taken in terms of the time of arrival, t_a . This is done in Figure A-5, where the

FIGURE A-5

Curve for Determining Total Dose as a Function of $(t-t_a+1)$

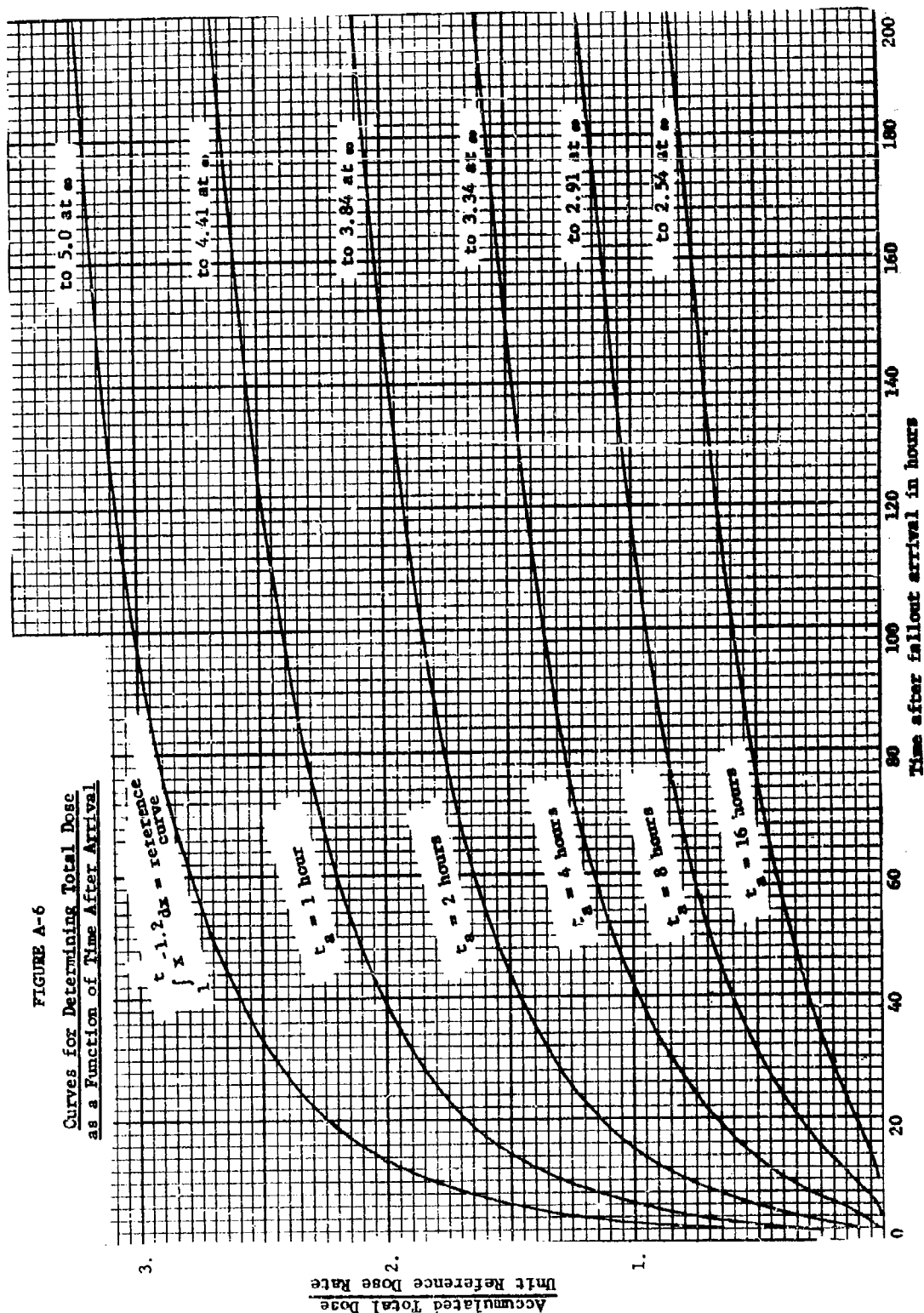


data in Figure A-4 are reinterpreted so that for all cases the insider first notes the arrival of fallout at time one hour. Therefore, in Figure A-5, the labels on the curves ($t_a = 1, t_a = 2, \dots$) indicate the number of hours before $t_a - 1$ that the detonation actually occurred. This is the only difference between Figures A-4 and A-5; that is, the viewpoint or reference time distinguishes Figure A-4 from Figure A-5. As in Figure A-4, the arrows in Figure A-5 indicate when the insider witnesses the cessation of fallout deposition. The effect of t_a as shown in Figure A-5 becomes more evident when uniform scales are used rather than logarithmic scales. Therefore, the curves in Figure A-5 are redrawn to form Figure A-6 by merely changing the type of scales. In this figure it is interesting to note the wide variation due to t_a in the total dose that would result from an indefinite ($t = \infty$) stay in the area if the decay law remains valid out to $t = \infty$. For all curves, the same reference intensity, $I(1)$, would have been predicted; only the actual time of arrival is varied.

From the data presented in Figure A-6, a new set of data can be obtained by normalizing the curves so that the total dose resulting from an indefinite stay in the area, rather than the reference intensity, is the same for all curves. This situation is illustrated in Figure A-7 where the fraction of potential ($t = \infty$) dose is presented as a function of time. It should be clear that all curves asymptotically approach unity. This set of curves illustrates the effect of t_a and the buildup period on the dose history when the potential dose is held invariant.

The arrows in Figure A-7 again represent the times at which fallout deposition ceases. This cessation of fallout deposition for all five cases

FIGURE A-6
Curves for Determining Total Dose
as a Function of Time After Arrival



in Figure A-7 is seen to occur when approximately 6% of the infinity dose has been received. This effect can also be seen in Equation A-7 as follows:

$$D_t(t = \infty) = 4.41 t_a^{-.2} I(1) , \quad (A-9)$$

$$D_t(t = 2.5 t_a) = 4.41 t_a^{-.2} I(1) - 5 (2.5 t_a)^{-.2} I(1) = .245 t_a^{-.2} I(1) , \quad (A-10)$$

and therefore

$$\frac{D_t(t = 2.5 t_a)}{D_t(t = \infty)} = \frac{.245 t_a^{-.2} I(1)}{4.41 t_a^{-.2} I(1)} = .056 \approx .06 \quad (A-11)$$

This interesting "result" is a characteristic of the particular model that is represented by Figure A-3 and Equation A-5. If the model is reasonable, then the dose received prior to cessation of fallout deposition is predicted to be approximately 6% of the infinity dose or, more conservatively, less than 10% of the infinity dose. In subsequent analysis of operations that begin at $t = 2.5$ and $t_a = t_p$, the actual calculated value, 5.6%, will be used to represent the percent of infinity dose that is received during the buildup period.

From Figure A-6 it is interesting to rework the data and display the effect of t_a in a slightly different manner. Consider the ratio of dose received within a fixed interval of time beginning at time t_p to dose received up to time t_p . This ratio as a function of t_a is displayed in Figure A-8 where four intervals of time (5, 10, 15, and 20 hours) are considered. From this figure and Figure A-7 it is easy to see that the rate at which dose accumulates is strongly dependent on the time of arrival, t_a .

The preceding discussion displays the effect of fallout arrival time on

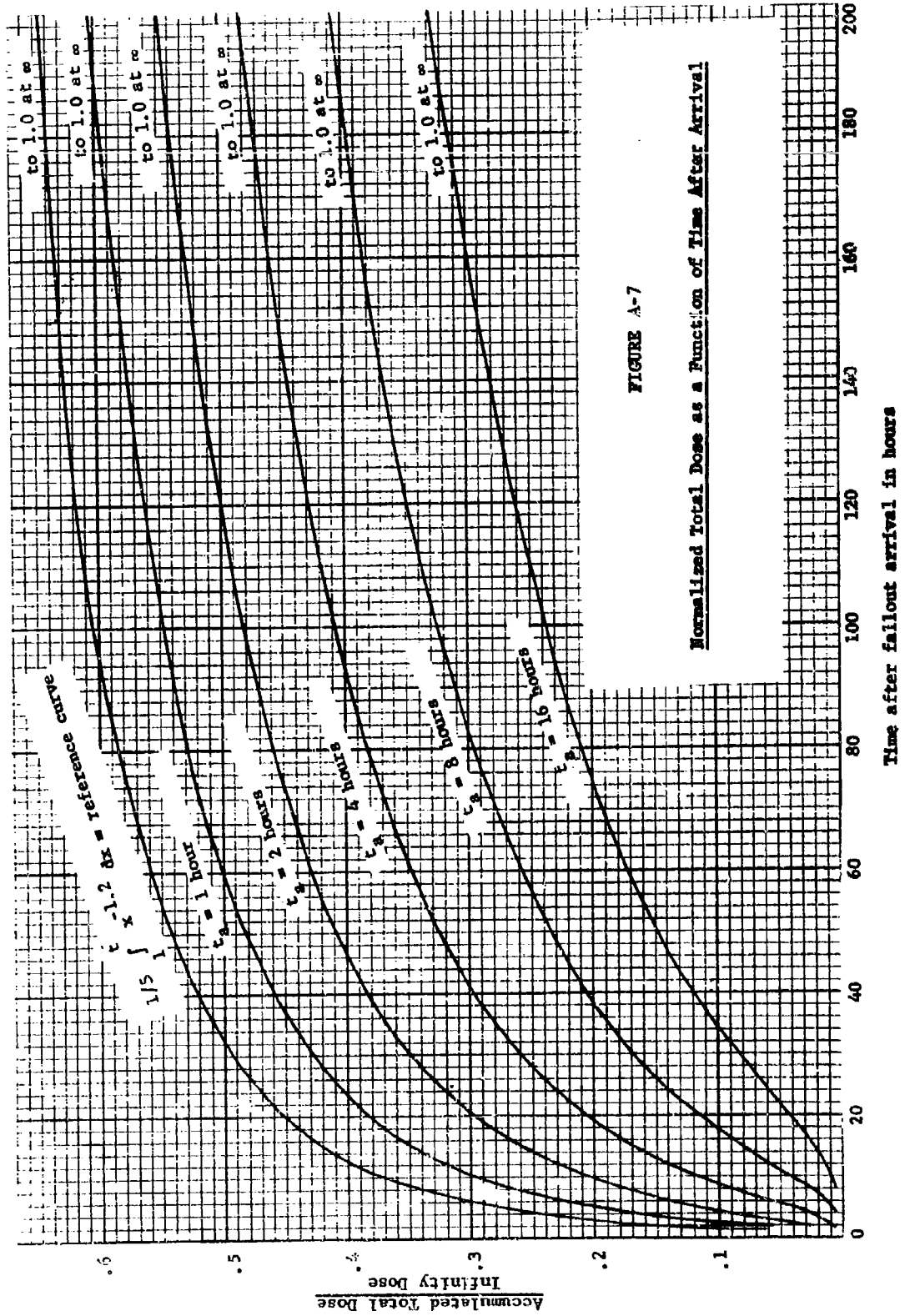


FIGURE A-7

Normalized Total Dose as a Function of Time After Arrival

Time after fallout arrival in hours

the manner in which radiation dose is received. The presented data are applicable to any predicted $H + 1$ reference intensity, $I(1)$. The applicability of the data is, therefore, independent of any material attenuation of the radiation that may exist. The curves may be applied to people in or out of facilities by merely dividing $D(t)$ by the appropriate protection factors of the facilities of interest.

The data developed in the preceding discussion can also be used to display the effect on the individual of a reduction in intensity brought about by an operation such as shielding, decontaminating, and so forth. In the following discussion, the operation will be assumed to be decontamination. Its effectiveness, f_d , is measured in terms of the reduction in intensity where the individual is located, due to the decontamination operation. That is, if the intensity in the absence of any decontamination operation would be $I(t)$ for any t , then the intensity at some time, t^* , after the performance of a decontamination operation whose effectiveness is f_d would be $I^*(t^*)$ where

$$I^*(t^*) = f_d I(t^*) \quad . \quad (A-12)$$

The effect of this process on the individual is displayed by giving the individual's dose curve both with decontamination and without decontamination and by then comparing the two curves. This comparison is developed first for the simple case where decontamination is assumed to occur instantaneously; that is, where zero time is required for the entire process of decontamination. The finite time will be developed later in this appendix.

Consider the dose that is received as a function of time when the time of arrival, $t_a = 2$ hours. This curve in Figure A-7 is redrawn and presented as Curve 1 in Figure A-9. Next, assume that the fallout cloud itself is decontaminated and that $f_d = 1/3$. The resultant dose as a function of time is presented as Curve 2 in Figure A-9. Curve 2 is merely $1/3$ times Curve 1. Curves 1 and 2 therefore bound the region in which any dose curve corresponding to decontamination at time t_d with $f_d = 1/3$ must lie. When t_d is greater than $2.5 t_a$ then the actual dose curve can be constructed by appropriately combining Curves 1 and 2.

The appropriate combination is very easy to construct. As an example, let $t_d = 10$ hours, and $f_d = 1/3$. This means that at $t = 10$ hours, the intensity in the facility is instantaneously reduced by a factor of $1/3$. Prior to $t = 10$, point a, Curve 1 describes the dose history. After $t = 10$, point b, Curve 2 describes the behavior of dose history. To describe the dose history after $t = 10$, Curve 2 must be shifted upwards until point b is superimposed on point a. Curve 3 is Curve 2 shifted up to meet this condition. The combination of Curves 1 and 3 that describes the dose history is indicated by the dotted portion of the two curves in Figure A-9. If t_d had been greater than 10, then it would have been necessary to shift Curve 2 up further to meet the necessary condition as follows: Curve 2 is shifted upwards until Curves 1 and 2 intersect at t_d . This process results in the correct dose curve only when $t_d \geq 2.5 t_a$.

For $t \geq 2.5 t_a$, Curve 1 is given in Equation A-7 as follows:

$$D_{t1}(t) = I(1) (4.41 t_a^{-.2} - 5t^{-.2}) \quad (A-13)$$

FIGURE A-8

Dose Received as a Function of
Time of Arrival

$$R = \frac{D(t_p + x) - D(t_p)}{D(t_p)}$$

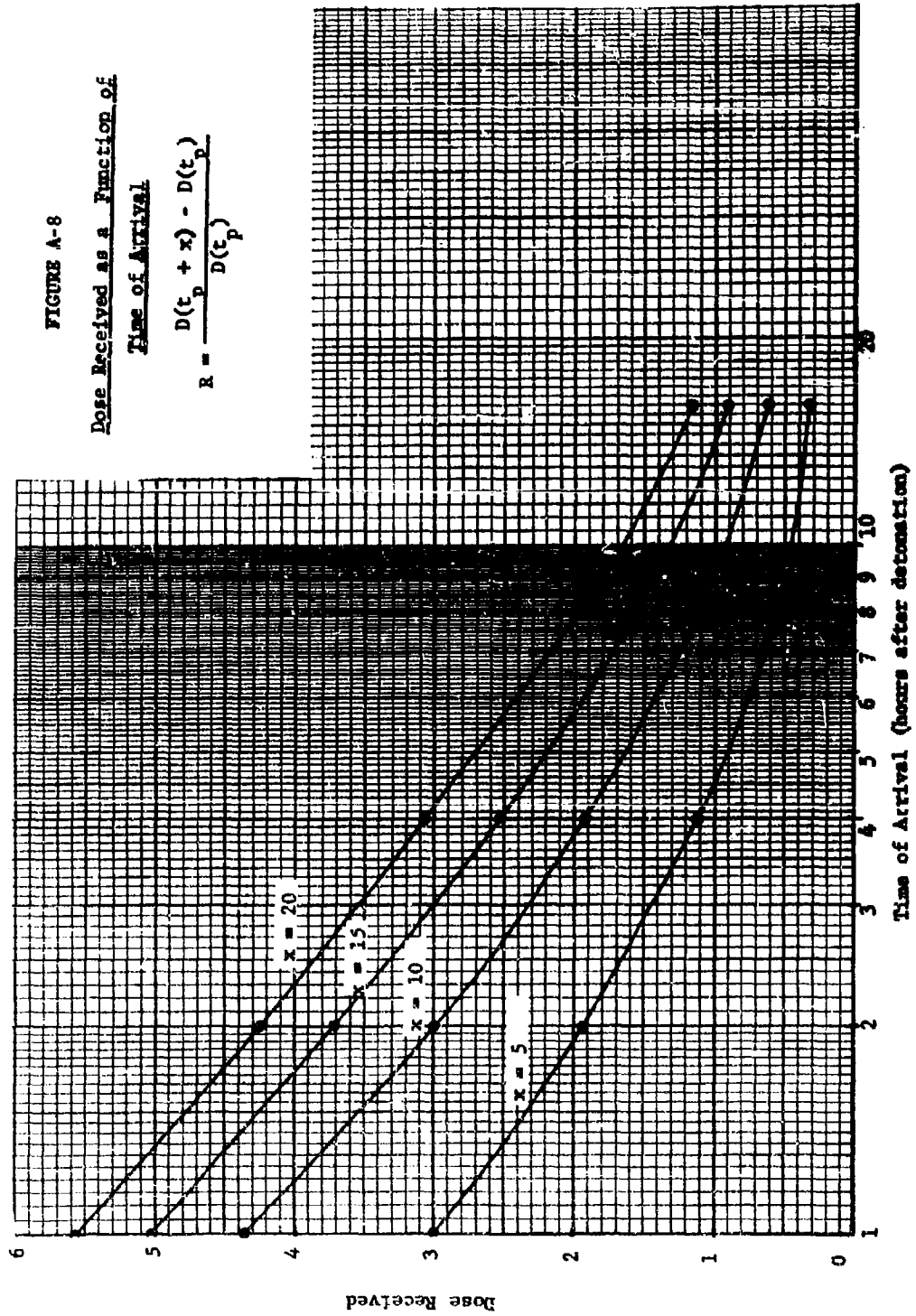
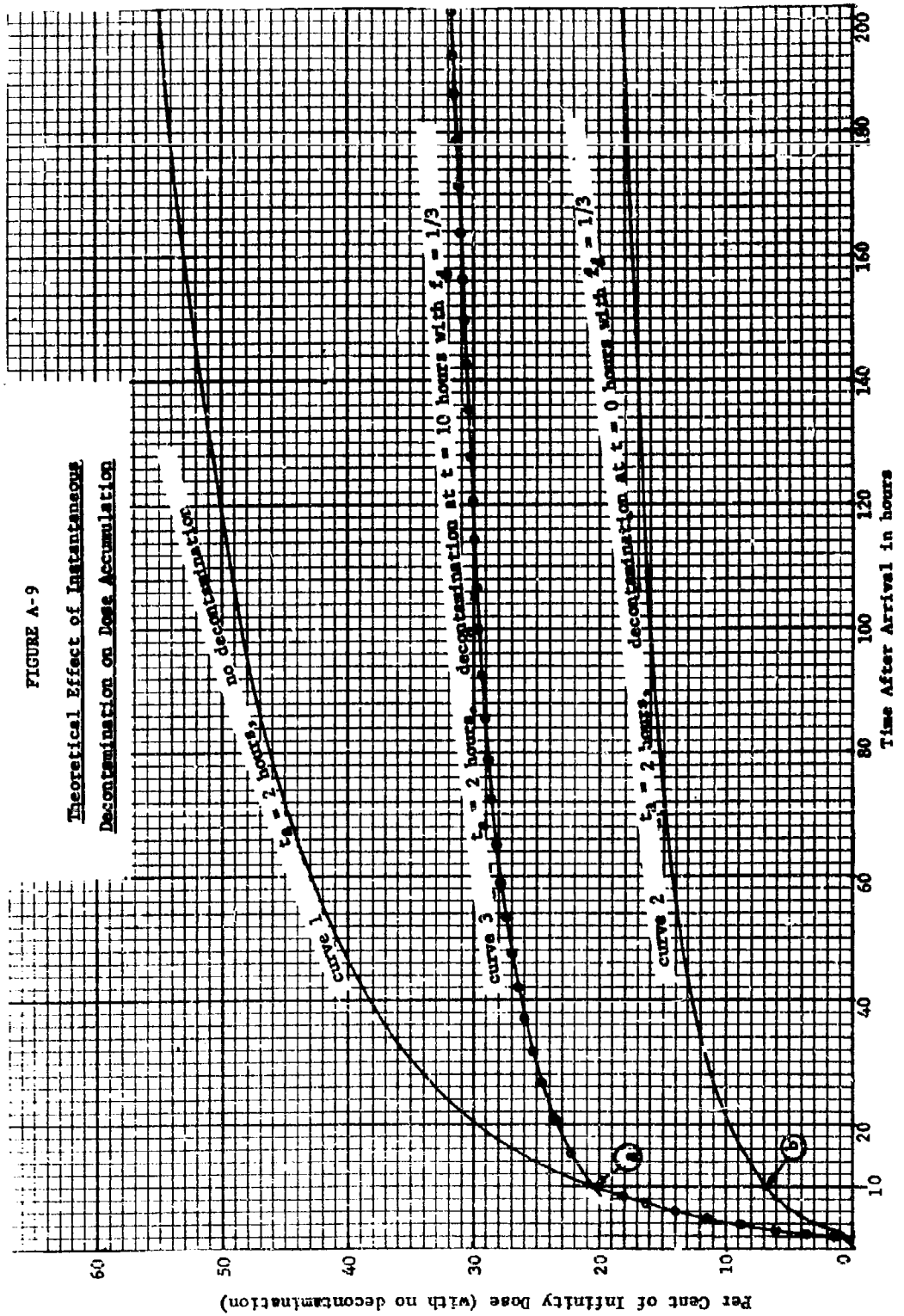


FIGURE A-9
Theoretical Effect of Instantaneous
Decontamination on Dose Accumulation



Curve 2 is, for $t \geq 2.5 t_a$,

$$D_{t2}(t) = f_d I(1) (4.41 t_a^{-.2} - 5t^{-.2}) \quad (A-14)$$

Therefore, Curve 3 is,

$$D_{t3}(t) = \begin{cases} D_{t1}(t) & t \leq t_d \\ D_{t1}(t_d) + D_{t2}(t) - D_{t2}(t_d) & t > t_d \end{cases}$$

$$= \begin{cases} D_{t1}(t) & t \leq t_d \\ (1 - f_d) D_{t1}(t_d) + f_d D_{t1}(t) & t > t_d \end{cases} \quad (A-15)$$

The value of decontamination can be measured by the ratio of infinity dose with decontamination to infinity dose without decontamination; that is, by the value ratio R_∞ where

$$R_\infty = \frac{D_{t3}(t = \infty)}{D_{t1}(t = \infty)}$$

$$= f_d + (1 - f_d) \frac{D_{t1}(t_d)}{D_{t1}(\infty)} \quad (A-16)$$

However, from Equation A-13

$$D_{t1}(\infty) = 4.41 I(1) t_a^{-.2} \quad (A-17)$$

and

$$D_{t1}(t_d) = I(1) (4.41 t_a^{-.2} - 5 t_d^{-.2}) \quad (A-18)$$

so that

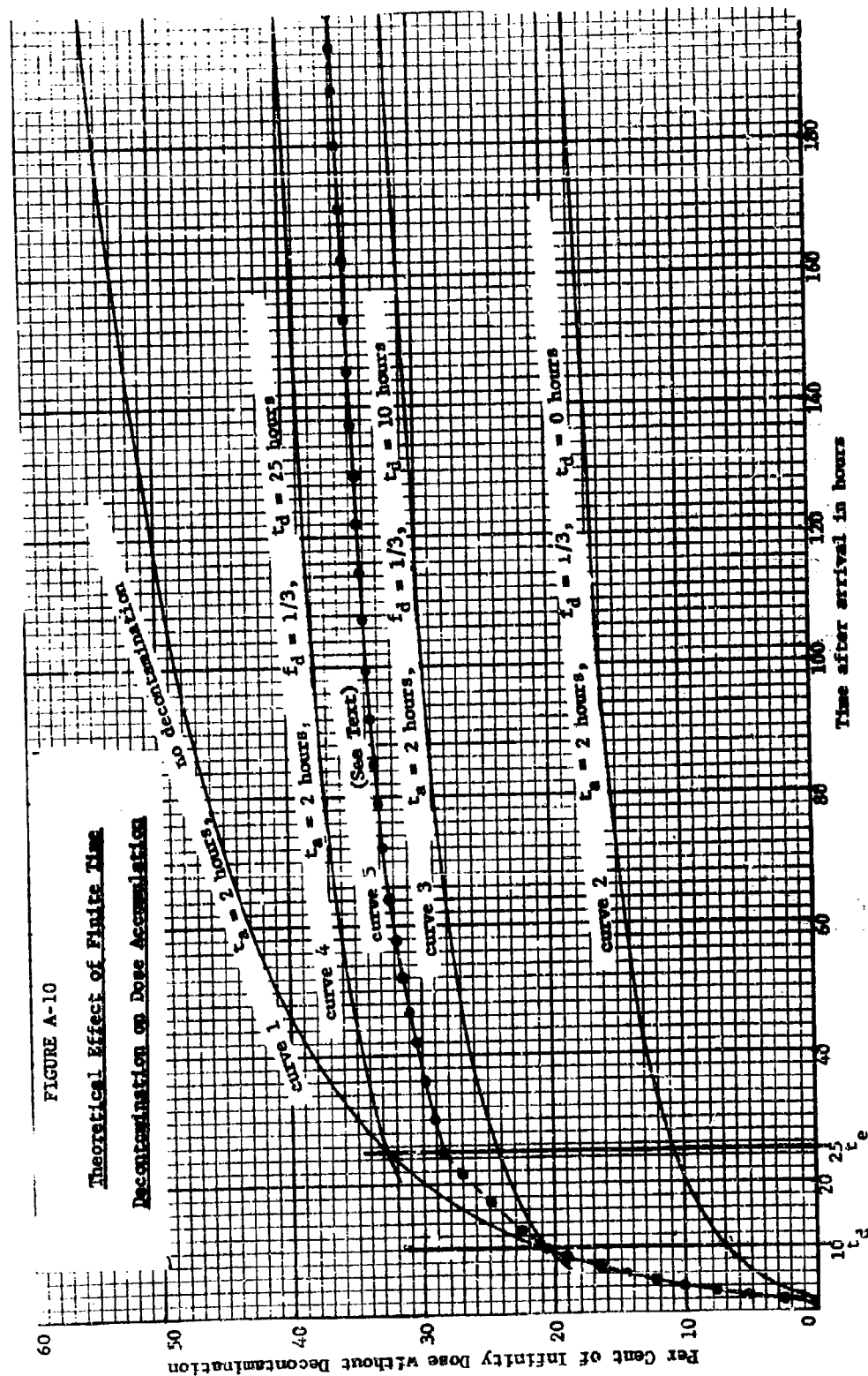
$$R_{\infty} = f_d + (1 - f_d) \left(1 - 1.13 \left(\frac{t_a}{t_d}\right)^2\right). \quad (A-19)$$

This equation expresses the effectiveness of instantaneous decontamination, R_{∞} , as a function of decontamination effectiveness, f_d ; time of arrival, t_a ; and time of decontamination, t_d . This relationship is displayed in Figures A-13 through A-15. Together, these figures display the result of any instantaneous decontamination effectiveness, f_d , that becomes effective at any time $t_d \geq 2.5 t_a$, for any time of arrival t_a , and any initial reference intensity, $I(1)$. However, before interpreting and discussing these figures, it is worthwhile first to examine decontamination that does not occur instantaneously and show how it may be related to instantaneous decontamination.

When the decontamination process requires a finite time, T , the process will be said to begin at time t_d and to end at time $t_d + T = t_e$. The resultant dose will be described in conjunction with Figure A-10. In Figure A-10, Curves 1, 2, and 3 are the same as the corresponding curves in Figure A-9. Curve 4 is the curve that would apply if the decontamination occurred instantaneously at time $t_d = 25$. Therefore, if $t_d = 10$, and $T = 15$ so that $t_d + T = t_e = 25$, then the appropriate dose curve would lie between Curves 3 and 4 and would be identical in shape to Curves 3 and 4 for $t \geq 25$. The curve that will be assumed appropriate is labeled Curve 5 and is located midway between Curves 3 and 4. In constructing Curve 5, the only new assumption used is the dose history between $t = 10$ and $t = 25$. It is assumed that during the process the dose will be halfway between the curve for no decontamination, Curve 1, and the curve for instantaneous decontamination, Curve 3. Therefore, Curve 5 is located midway between Curves 1 and 3 at the conclusion of the process, $t_e = 25$; and, this locates Curve 5 midway

FIGURE A-10

Theoretical Effect of Finite Time
Decontamination on Dose Accumulation



between Curves 3 and 4. The resultant curve is therefore represented by the dotted portions of the several curve segments.

Once again, it is useful to examine the value of this decontamination in the same manner that the value of instantaneous decontamination was examined. Let Curves 1, 2, . . . , 5 in Figure A-10 be represented by $D_{t1}(t)$, $D_{t2}(t)$, . . . , $D_{t5}(t)$. As before, $D_{t2}(t)$ is merely $f_d D_{t1}(t)$. The value of decontamination is then the ratio, R_∞ , of infinity dose with decontamination to infinity dose without decontamination; that is,

$$R_\infty = \frac{D_{t5}(t = \infty)}{D_{t1}(t = \infty)} \quad (A-20)$$

For $t \geq 25$, the following holds:

$$D_{t5}(t) = D_{t4}(t) - 1/2 [D_{t1}(t_e) - D_{t3}(t_e)] \quad (A-21)$$

$$= f_d D_{t1}(t) + (1-f_d) D_{t1}(t_e) - 1/2 [D_{t1}(t_e) - f_d D_{t1}(t_e) - (1-f_d) D_{t1}(t_d)]$$

$$= f_d D_{t1}(t) + \frac{1-f_d}{2} [D_{t1}(t_d) + D_{t1}(t_e)] \quad (A-22)$$

and therefore,

$$R_\infty = f_d + \frac{(1-f_d)}{2} \frac{D_{t1}(t_d) + D_{t1}(t_e)}{D_{t1}(\infty)} \quad (A-23)$$

Recall from Equation A-13 that

$$D_{t1}(t) = I(1) (4.41 t_a^{-.2} - 5 t^{-.2}) \quad (A-24)$$

for $t \geq t_d$.

Combining Equations A-23 and A-24 the ratio R_∞ becomes,

$$R_{\infty} = f_d + (1-f_d) \left[1 - \frac{1.13}{t_a^{-.2}} \left(\frac{t_d^{-.2} + t_e^{-.2}}{2} \right) \right] . \quad (A-25)$$

Now, define an effective decontamination time, t_{eff} , as follows:

$$t_{eff}^{-.2} = 1/2 (t_d^{-.2} + t_e^{-.2}) . \quad (A-26)$$

Using this effective time, t_{eff} , the ratio, R_{∞} , becomes

$$R_{\infty} = f_d + (1-f_d) (1-1.13 \left(\frac{t_{eff}}{t_a} \right)^{-.2}) , \quad (A-27)$$

which is the same as the R_{∞} for instantaneous decontamination as given by Equation A-19. This is the reason for delaying the interpretation and discussion of Figures A-13 through A-15. Although developed for instantaneous decontamination, they also apply to finite time decontamination by merely selecting an effective time on the basis of t_d and $-T$ according to Equation A-26. Figure A-11 has been drawn to represent Equation A-26. It gives t_{eff} as a function of $t_d + 1/2 T$ for selected values of T .

The preceding analysis can be summarized with four figures. The first, Figure A-12, replaced Figures A-1 through A-6. When the time of arrival, t_a , is specified, the total dose $D_t(t)$ can be determined from the figure for any time, t , less than one thousand hours, and for any reference intensity, $I(1)$. This figure represents the following equation:

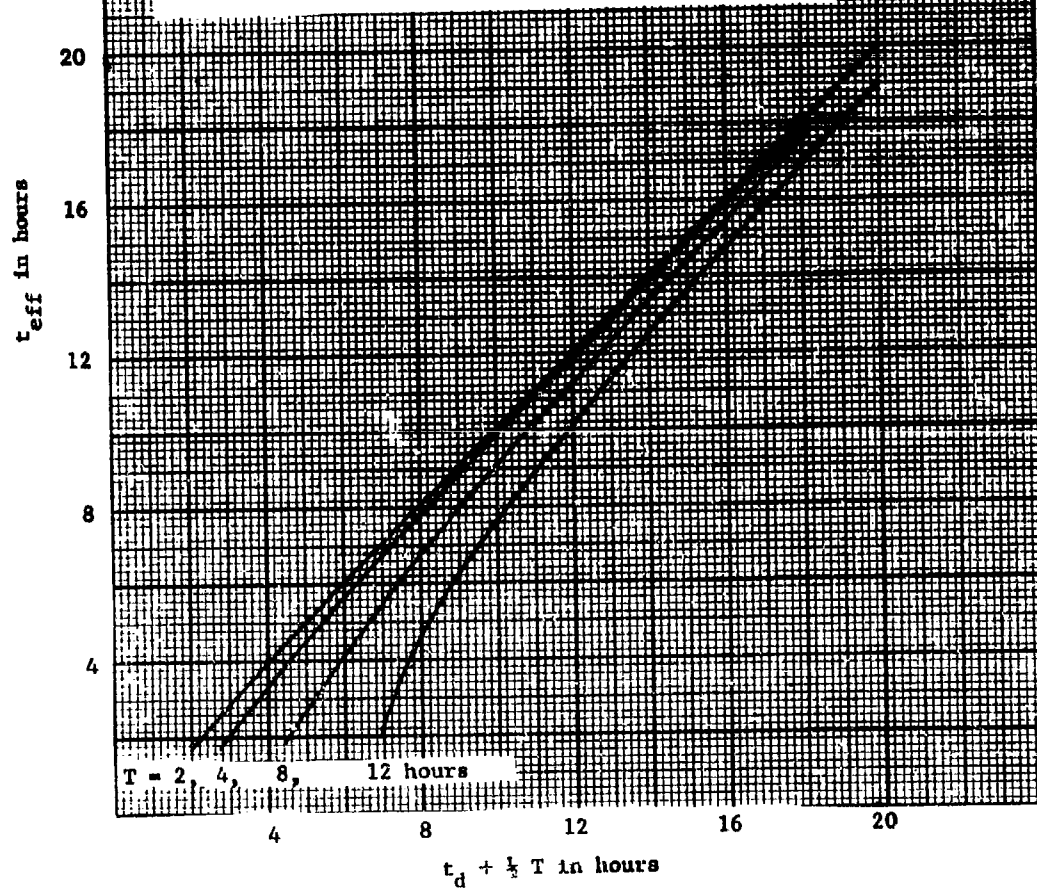
$$\frac{t_a^{-.2} D_t(t)}{I(1)} = 4.41 - 5 \left(\frac{t_a}{t} \right)^{.2} \text{ for } \frac{t}{t_a} \geq 2.5 . \quad (A-28)$$

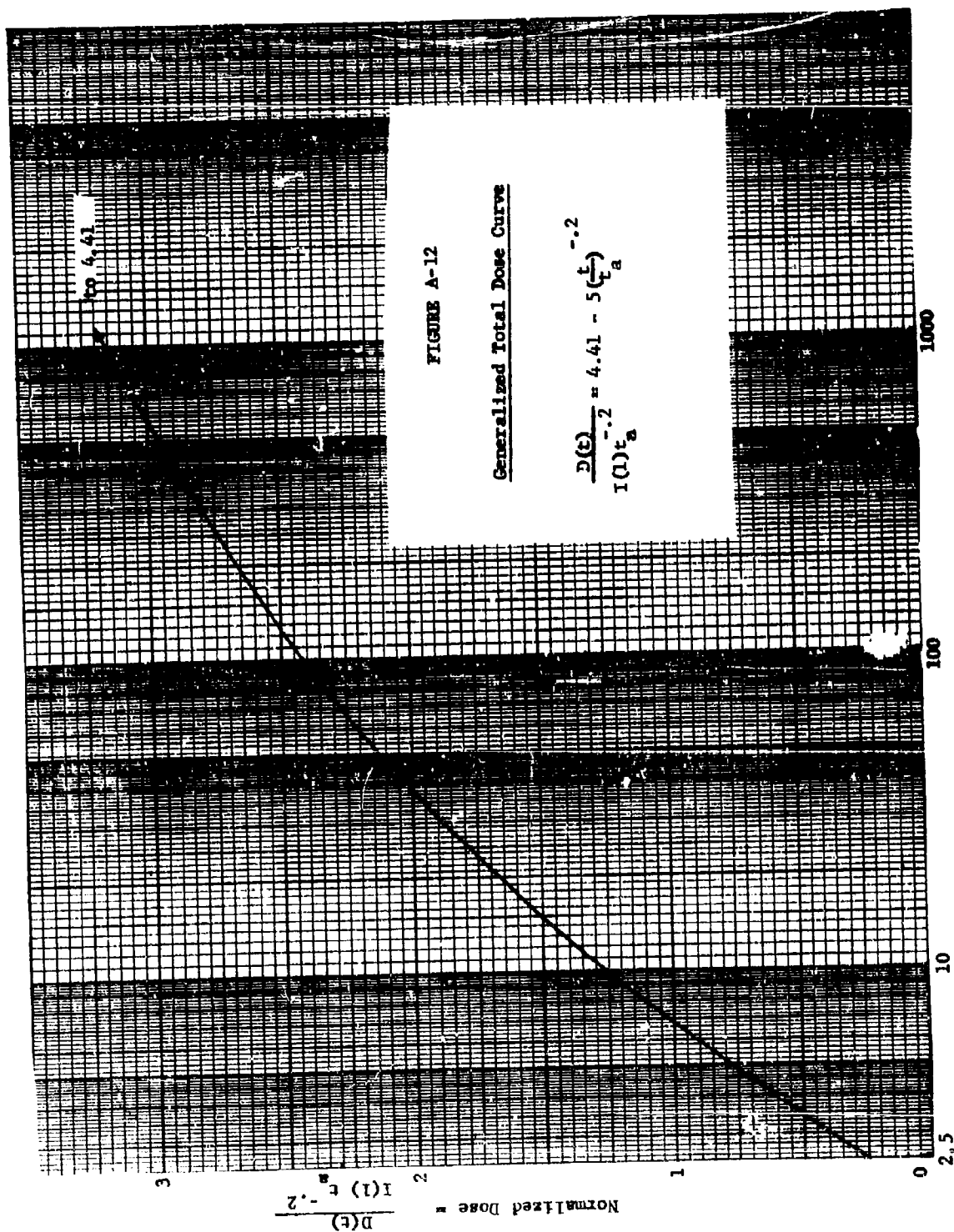
This curve will be called the generalized total dose curve. It is normalized both with respect to t_a and with respect to $I(1)$.

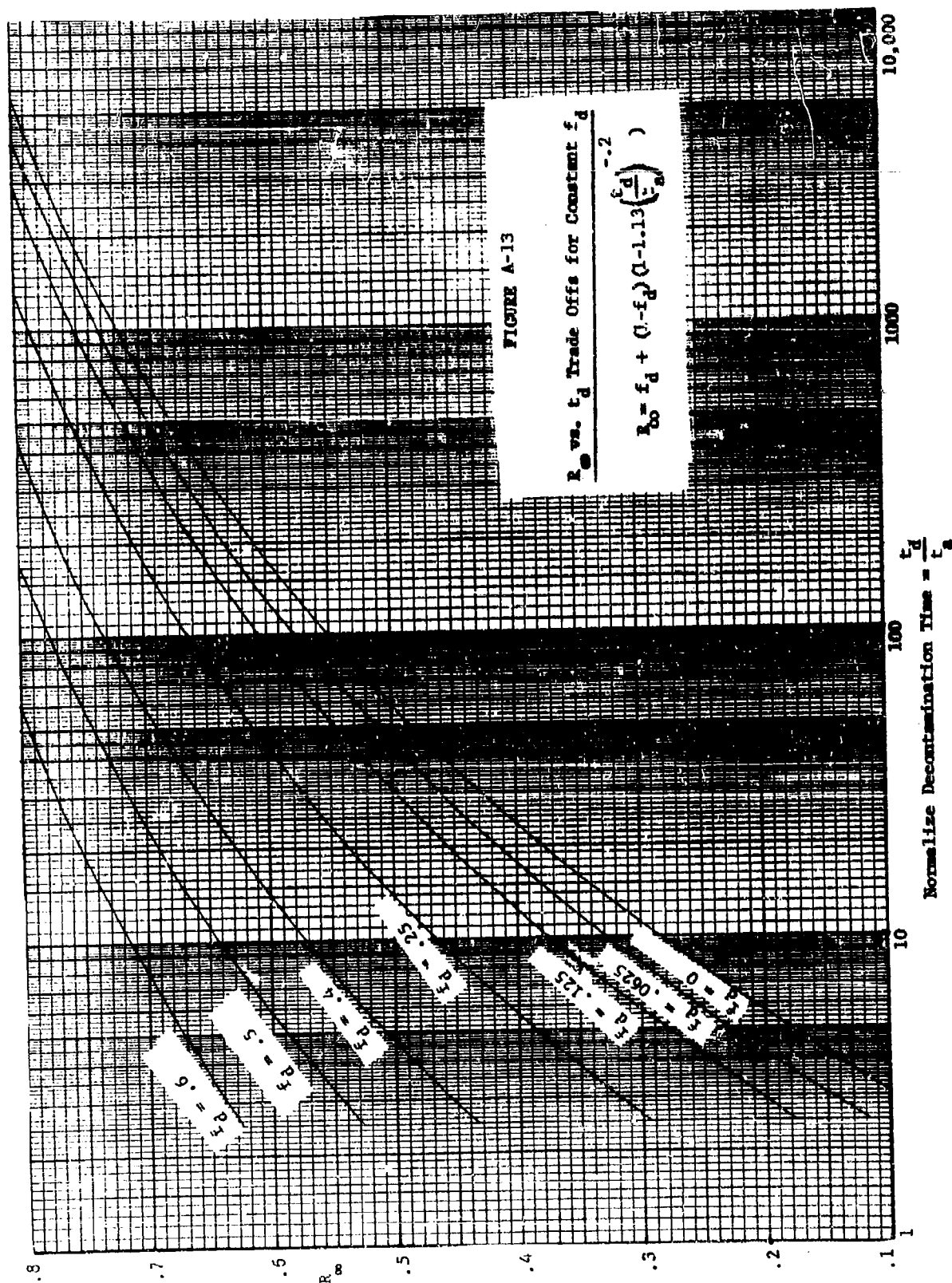
FIGURE A-11

t_{eff} vs. $t_d + \frac{1}{2}T$ for Finite Time Decontamination

$$\frac{1}{2} \left[t_d^{-0.2} + (t_d + T)^{-0.2} \right] = t_{eff}^{-0.2}$$







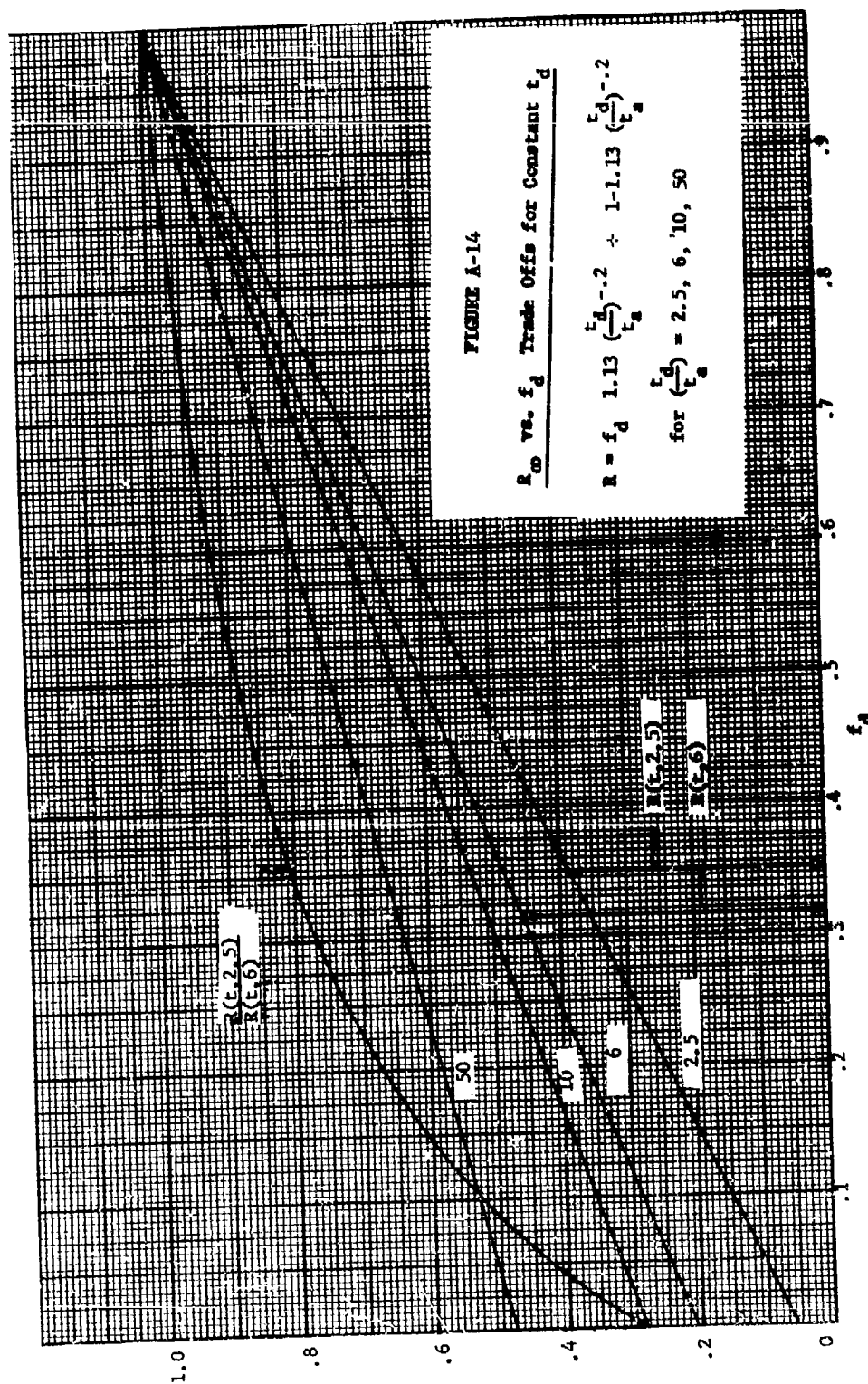
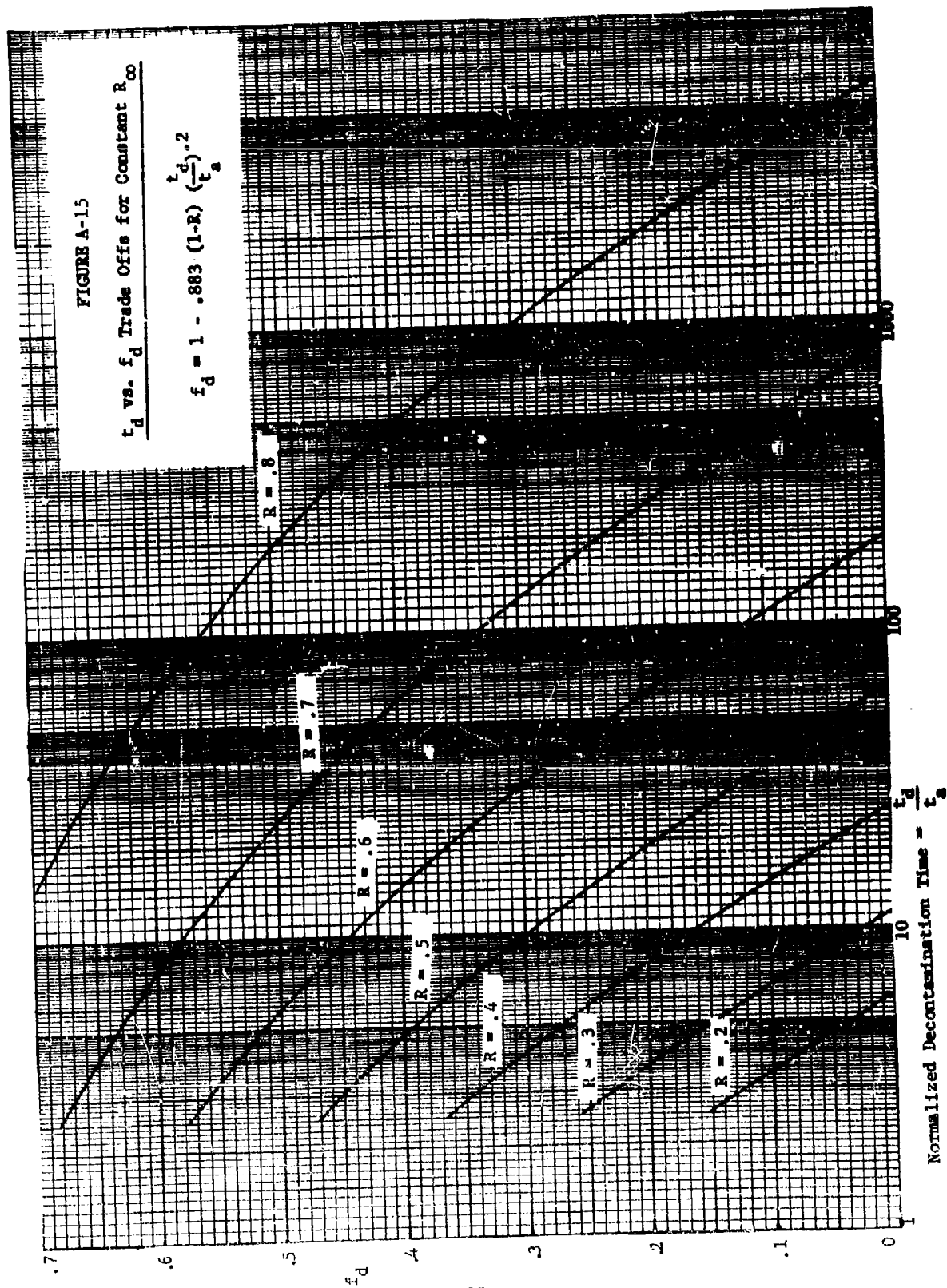


FIGURE A-14

R vs. f_d Trade Offs for Constant t_d

$$R = f_d \cdot 1.13 \left(\frac{t_d}{t_a} \right)^{-0.2} + 1 - 1.13 \left(\frac{t_d}{t_a} \right)^{-0.2}$$

for $\left(\frac{t_d}{t_a} \right) = 2.5, 6, 10, 50$



Figures A-13 through A-15 express the following forms of Equation A-19:

$$R_{\infty} = f_d + (1-f_d)(1-1.13 \left(\frac{t_d}{t_a}\right)^{-.2}) , \quad (A-29)$$

$$R_{\infty} = \left[1-1.13 \left(\frac{t_a}{t_d}\right)^{.2} \right] + f_d \left[1.13 \left(\frac{t_a}{t_d}\right)^{.2} \right] \quad (A-30)$$

and

$$f_d = 1 - .883 (1-R_{\infty}) \left(\frac{t_d}{t_a}\right)^{.2} , \quad (A-31)$$

all for $\frac{t_d}{t_a} \geq 2.5$. These three figures display the various trade-offs of interest that exist in the decontamination process. Figure A-13 shows the relationship between the value ratio, R_{∞} , and the time of decontamination, t_d , for fixed levels of decontamination effectiveness, f_d . Figure A-14 shows the relationship between the decontamination effectiveness, f_d , and the value ratio, R_{∞} , for a fixed times of decontamination, t_d . Figure A-15 shows how t_d and f_d can be varied without changing the value ratio, R_{∞} . All three figures are presented for cases where f_d and R_{∞} are less than 1.0. However, it should be recognized that the presentation could have covered cases where f_d and R_{∞} were greater than 1.0 because the governing equations are valid for both situations.

These figures are most useful in obtaining an uncluttered appreciation of the trade-offs that exist along with a rough approximation of their behavior. Although the curves are exact, they must be viewed as a rough approximation because the value ratio is evaluated in terms of infinity dose ($t = \infty$) whose applicability has not yet been discussed. The ratio was evaluated at $t = \infty$ to obtain a simple approximation of the trade-offs and their general behavior. To obtain a second approximation it is worthwhile

to determine a more appropriate time at which to evaluate the value ratio. Such a time will be selected on the basis of equivalent residual dose, $D_R(t)$, rather than total dose, $D_t(t)$.

The Blair theory regarding the rate of recovery as quoted in Devaney (Reference 1) is shown as curve W_1 in Figure A-16 along with an approximation curve which will be used in the following discussion, curve W . This approximation is used throughout the interval of time, 0 to 500 hours, which, as will be seen, encompasses the time interval of interest in this analysis. Using this approximation, the equivalent residual dose, $D_R(t)$ can be expressed as follows:

$$D_R(t) = \int_0^t \{ .1 + .9 (1 - \alpha(t - x)) \} I(x) dx \quad (A-32)$$

where, from Figure A-16, α is .00085. Inserting $I(x)$ as expressed in Figure A-3 and Equation A-5 this becomes

$$D_R(t) = (1 - .9\alpha t) I(1) (4.41 t_a^{-.2} - 5 t^{-.2}) + .9\alpha I(1) (2.4 t_a^{.8} + 1.25 t^{.8}). \quad (A-33)$$

This equation in a normalized form is displayed along with $D_t(t)$ in Figure A-17 for $t_a = 1, 2, 4$, and 8 hours. In this figure it can be seen that the maximum equivalent residual dose occurs prior to $t = 300$ hours. More specifically, the maximum can be determined by setting the derivative equal to zero. This process results in the following equation for t_{max} :

$$t_{max}^{-.2} + 262 t_{max}^{-1.2} = .883 t_a^{-.2}, \quad (A-34)$$

which is presented in Figure A-18. From this figure, the maximum is seen to lie between 175 hours and 336 hours when t_a lies between 1 hour and 10 hours.

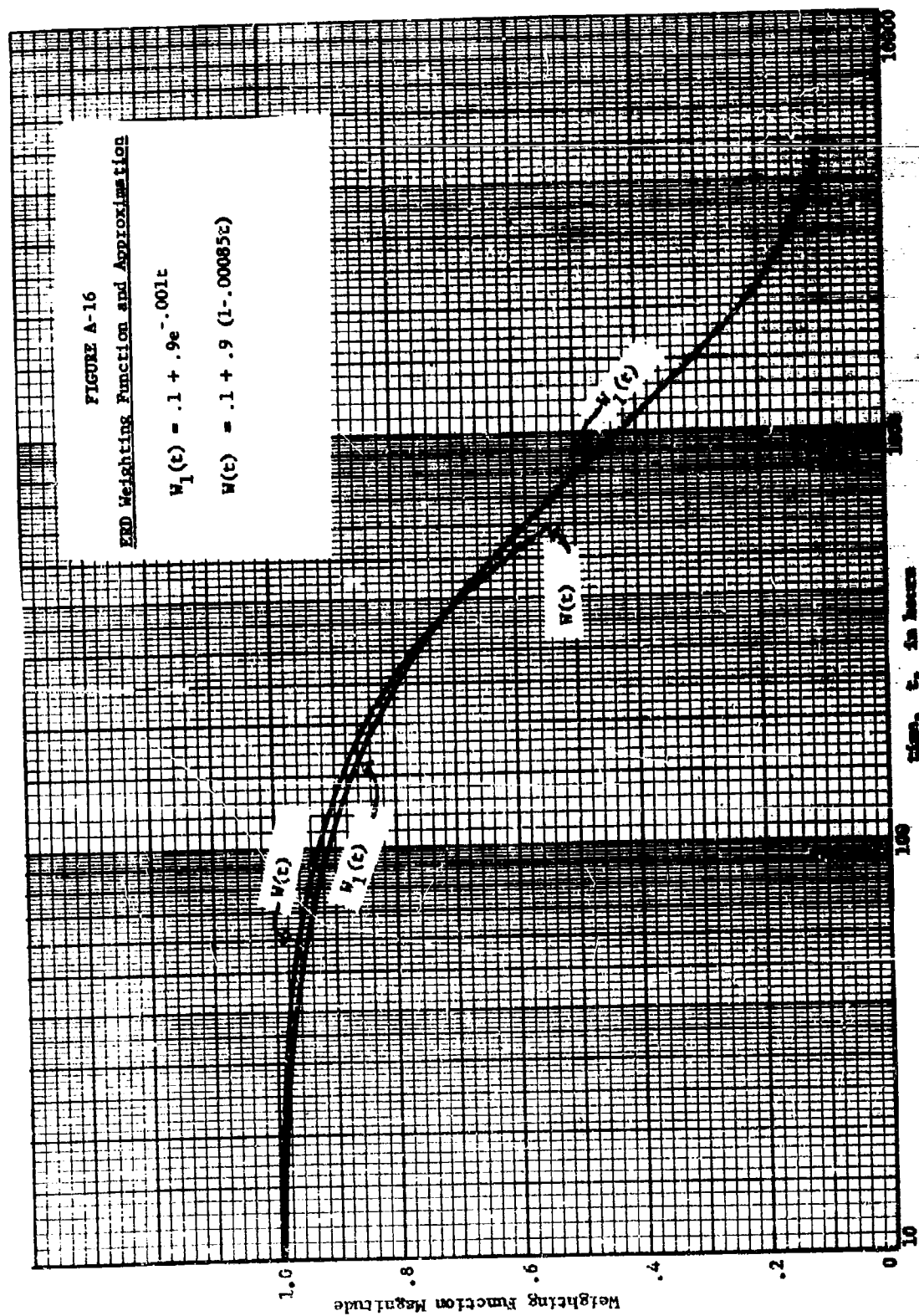
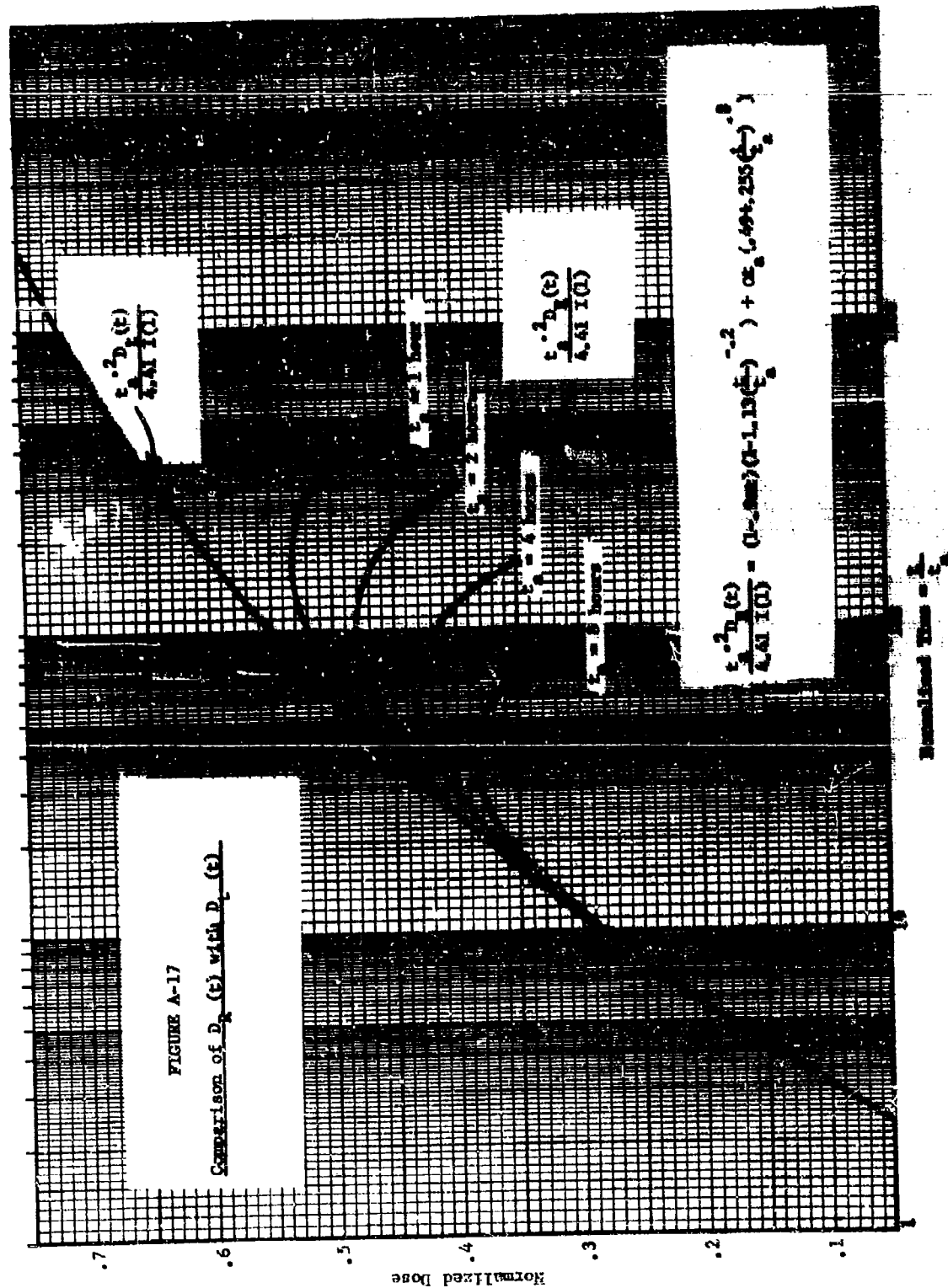
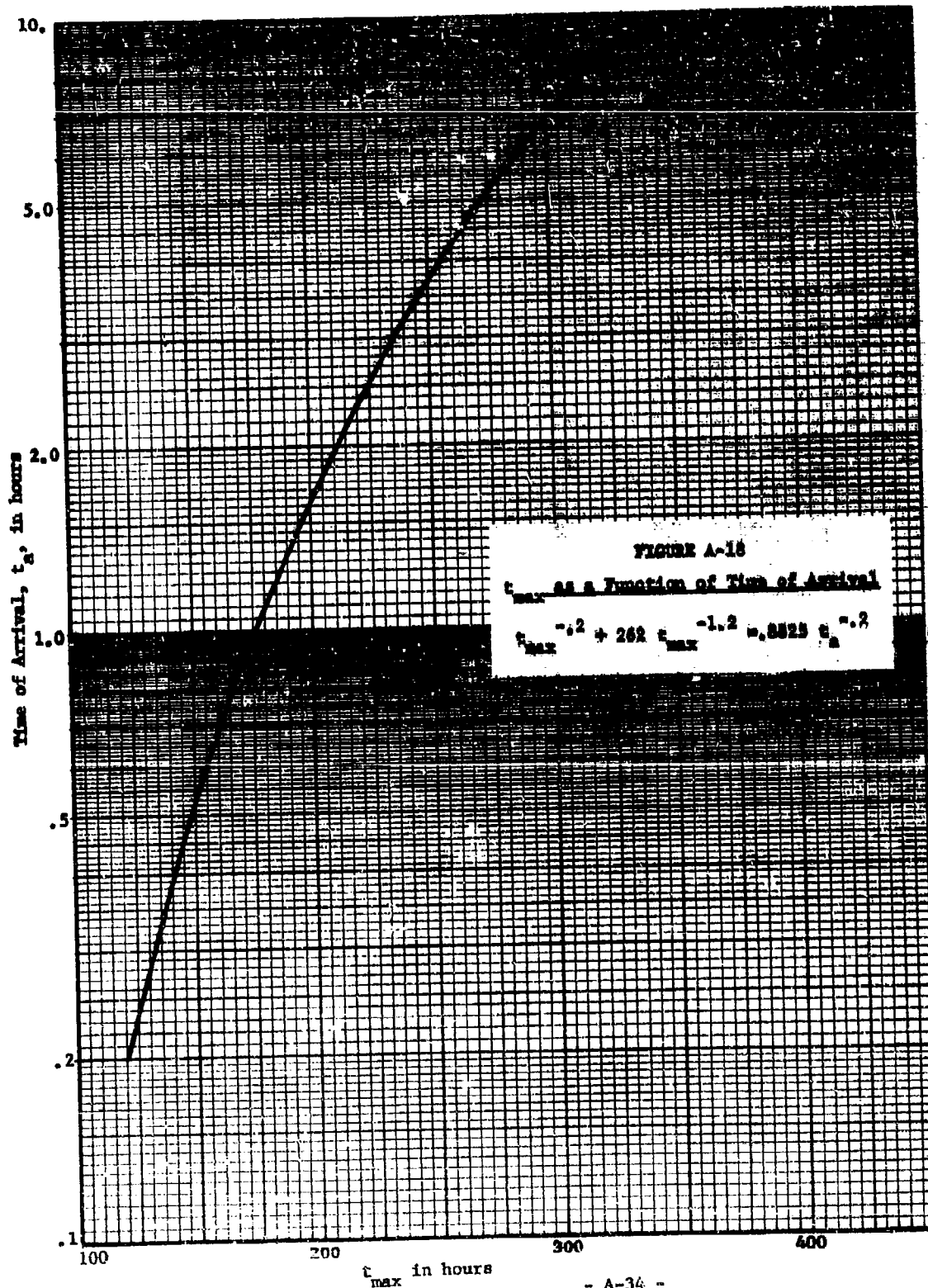


FIGURE A-16
FED Weighting Function and Approximation

$$W_1(t) = .1 + .9e^{-.001t}$$

$$W(t) = .1 + .9 (1 - .00085t)$$





The normalized value of $D_R(t)$ when $t = t_{\max}$ is presented in Figure A-19 as a function of time of arrival, t_a .

From the resultant times at which $\max D_R(t)$ occurs, it is obvious that the validity range of the expression used to approximate the recovery process is more than sufficient. In addition, it can be seen that the $\max D_R(t)$ will occur before two weeks (336 hours) for $t_a \leq 10$ hours. For this reason, two weeks, or 336 hours, is selected as the evaluation time for a second approximation. This time, 336 hours, is selected as a logical time that is independent of t_a at which to evaluate the decontamination value ratio.

In addition, the value ratio will be evaluated at that time when, for a given time of arrival, the equivalent residual dose, $D_R(t)$, reaches a maximum. Obviously this latter evaluation time will not be independent of t_a .

For these last two approaches to the value ratio, Equation A-16 can be rewritten as,

$$R_x = f_d + (1 - f_d) \frac{D_{t1}(t_d)}{D_{t1}(x)}, \quad (\text{A-35})$$

where x is the time at which the value ratio is to be evaluated. Upon substituting Equation A-13 for $D_{t1}(\cdot)$, the above expression becomes:

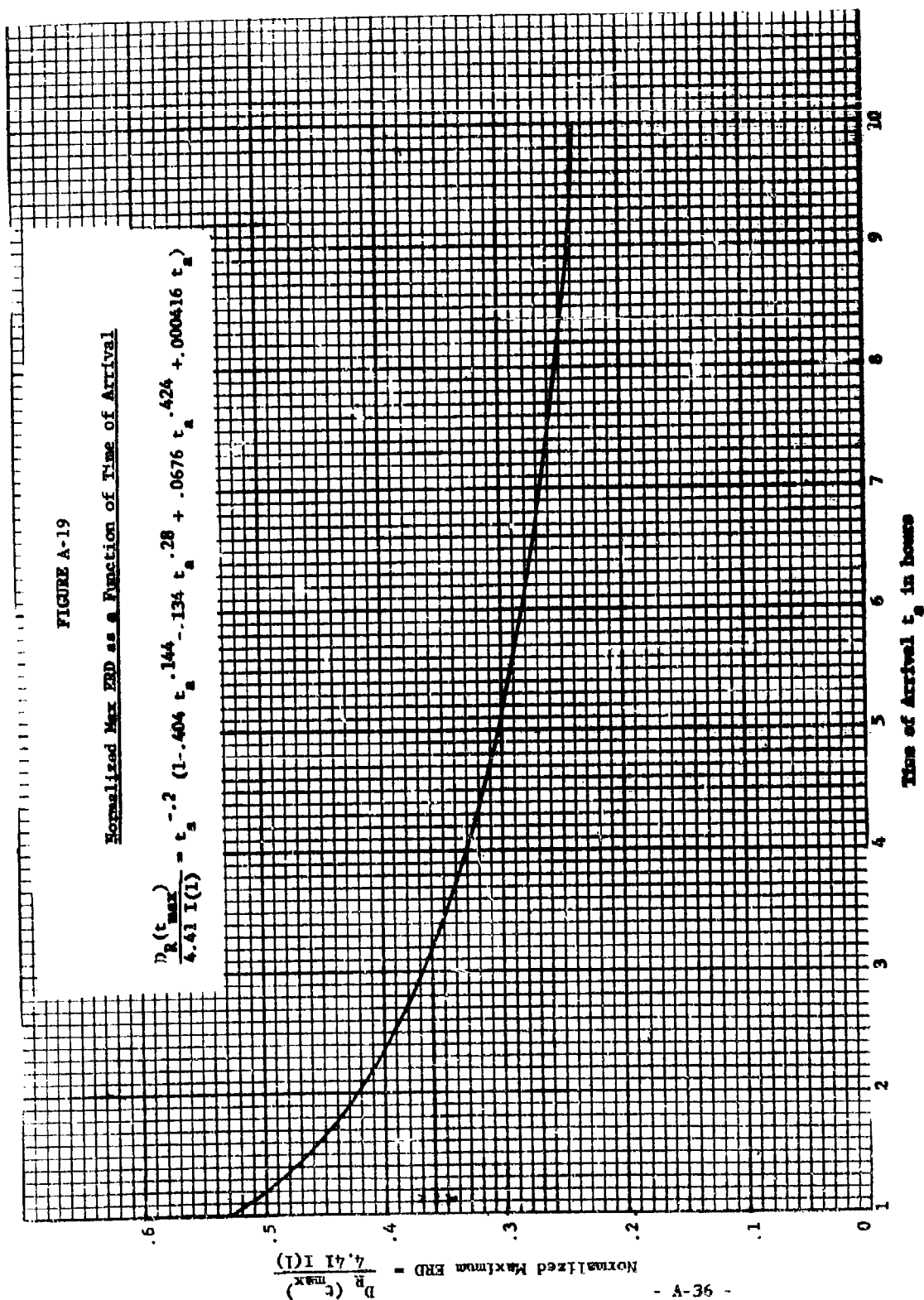
$$R_x = f_d + (1 - f_d) \frac{1 - 1.13 t_a^{.2} t_d^{-.2}}{1 - 1.13 t_a^{.2} x^{-.2}}. \quad (\text{A-36})$$

When x is sufficiently large, this expression reduces to Equation A-19 for R_{∞} .

FIGURE A-19

Normalized Max ERD as a Function of Time of Arrival

$$\frac{D_R(t_{\max})}{4.41 I(1)} = t_a^{-0.2} (1 - .404 t_a^{.144} - .134 t_a^{.28} + .0676 t_a^{.424} + .000416 t_a^2)$$



The above equation expresses the trade-offs that exist among R_x , f_d , t_a , and t_d . Before graphically displaying these trade-offs, it is worthwhile to review the meaning of, and constraints on, the various parameters and the equation itself. The least complicated parameters are f_d and t_d . Together, they describe the decontamination (or similar type) operation. As a result of the operation, the intensity is reduced by a factor f_d . When the operation is ineffective, $f_d = 1$. When the operation is perfect, $f_d = 0$. This operation takes place at some time t_d , which must be after the deposition of fallout has ceased or, mathematically, must be during that time when the intensity behavior is adequately described by the $t^{-1.2}$ decay law. Because fallout deposition ceases at time $t = 2.5 t_a$ in the buildup function used to develop the equation, the equation holds when t_d is greater than $2.5 t_a$. That is, if the time of arrival is one hour, then decontamination is not performed before $2\frac{1}{2}$ hours; if the time of arrival is 3 hours, then decontamination is not performed before $7\frac{1}{2}$ hours. Briefly, the equation assumes that decontamination will not be performed before the fallout is all deposited.

Contrary to expectation, the buildup model (Figure A-3) used to develop Equation A-36 does not preclude the application of the equation to other fallout situations. The buildup model is only used as a vehicle for introducing the parameter t_a into the equation. The equation is valid for any different buildup model that uses a time of arrival, t_a^* . In such a case it is only necessary to determine the proper correspondence between t_a^* and the t_a used in Equation A-36. This correspondence may be determined from the following expression:

$$t_a^{-1.2} = \frac{1}{4.41 I(1)} \int_{t_a^*}^{t_c^*} f(x) dx + 1.13 t_c^{*-1.2}, \quad (A-37)$$

where t_a^* is the time of arrival,
 t_c^* is the time of deposition cessation, and

$f(x)$ is the intensity-time behavior of the new buildup model.

This expression will be completely developed in Section III below.

The two remaining parameters, R_x and x , are the most complicated parameters in Equation A-36. To keep R_x compatible with Equation A-16,

R_x is:

$$R_x = \frac{D_t(x) \text{ with decontamination}}{D_t(x) \text{ without decontamination}} \quad (A-38)$$

where x is the time at which the total dose expressions in the ratio are evaluated. The complication lies in selecting the proper x , or equivalently, in interpreting the results that arise when a particular x is selected. In either case, both the selection and interpretation are tantamount to value judgments. When concern is focused on short range recovery and survival, the tendency may be to examine the ratio evaluated at short range times; that is, at lesser values of x . When concern is focused on long range recovery, the tendency may be to examine the ratio evaluated at long range time; for instance, at $x = \infty$. Three examples of appropriate x 's are presented; $x = \infty$, $x = 2 \text{ weeks} = 336 \text{ hours}$, and $x = \text{that time when the ERD is a maximum (between 330 hours and 175 hours, depending on } t_a^*)$. The ratio R_x for particular values of x is the fractional reduction in total dose (and, therefore, irreparable dose) that results from the performance of the operation (see Equation A-38). Because the actual interpretation will depend on the manner in which Equation A-36 and the descriptive curves are actually used, the preceding remarks are brief and intended only as examples of

considerations that will arise in using the displays that follow. The first display, Figure A-20, shows the trade-offs that exist between f_d and t_d for specified values of R_{336} and t_a . The corresponding display for R_∞ was presented in Figure A-15. These curves define the limits of operation performance that will achieve a specified result. For example, consider a particular geographical area where the time of fallout arrival, t_a , and reference intensity, $I(1)$, combine to produce a very serious situation. When these two parameters t_a and $I(1)$ are specified, Figure A-12 will predict the dose received up to any time t . Figure A-20 shows the range of reduction operation that can be performed (t_d and f_d) to achieve the particular dose reduction when concern is short range ($x = 336$). As an example, let $t_a = 4$ hours and $I(1) = 1000$ R/hr. From Figure A-12, at $t = 336$ hours, the predicted dose is $2.35 I(1)t_a^{-.2} = 2.35 \times 1000 \times .76 = 1786$ roentgens. If it were desired to reduce this to 600 roentgens, or by a factor of $\frac{600}{1786} = .34$, then the f_d and t_d combinations that would achieve this result are located using the labeled dashed curve on Figure A-20. Figure A-15 showed the trade-offs when the concern was long range ($x = \infty$).

The second display, Figures A-21 and A-22, shows how the fractional reduction in dose, R_{336} , varies when the reduction in intensity, f_d , is changed for specific times of arrival, t_a , and of decontamination, t_d . (The long range consideration, $x = \infty$, was displayed in Figure A-14.) The two figures work together. Figure A-21 presents the trade-off for $t_a = 1$ hour and Figure A-22 is used to interpret the Figure A-21 curves for other times of arrival. That is, from Equation A-36 it can be seen that each curve in Figure A-21 is not restricted to the time t_a and t_d with which

FIGURE A-20
 f_d vs. t_d Trade Offs for Constant R_x

$$f_d = \frac{t_d^{-0.2} (R_x - 1) + 1.13 (t_d^{-0.2} - R_x t_d^{-0.2})}{1.13 (t_d^{-0.2} - t_d^{-0.2})}$$

$R_x = .75, .5, .25$
 $t = 336. = x$

(all time in hours)

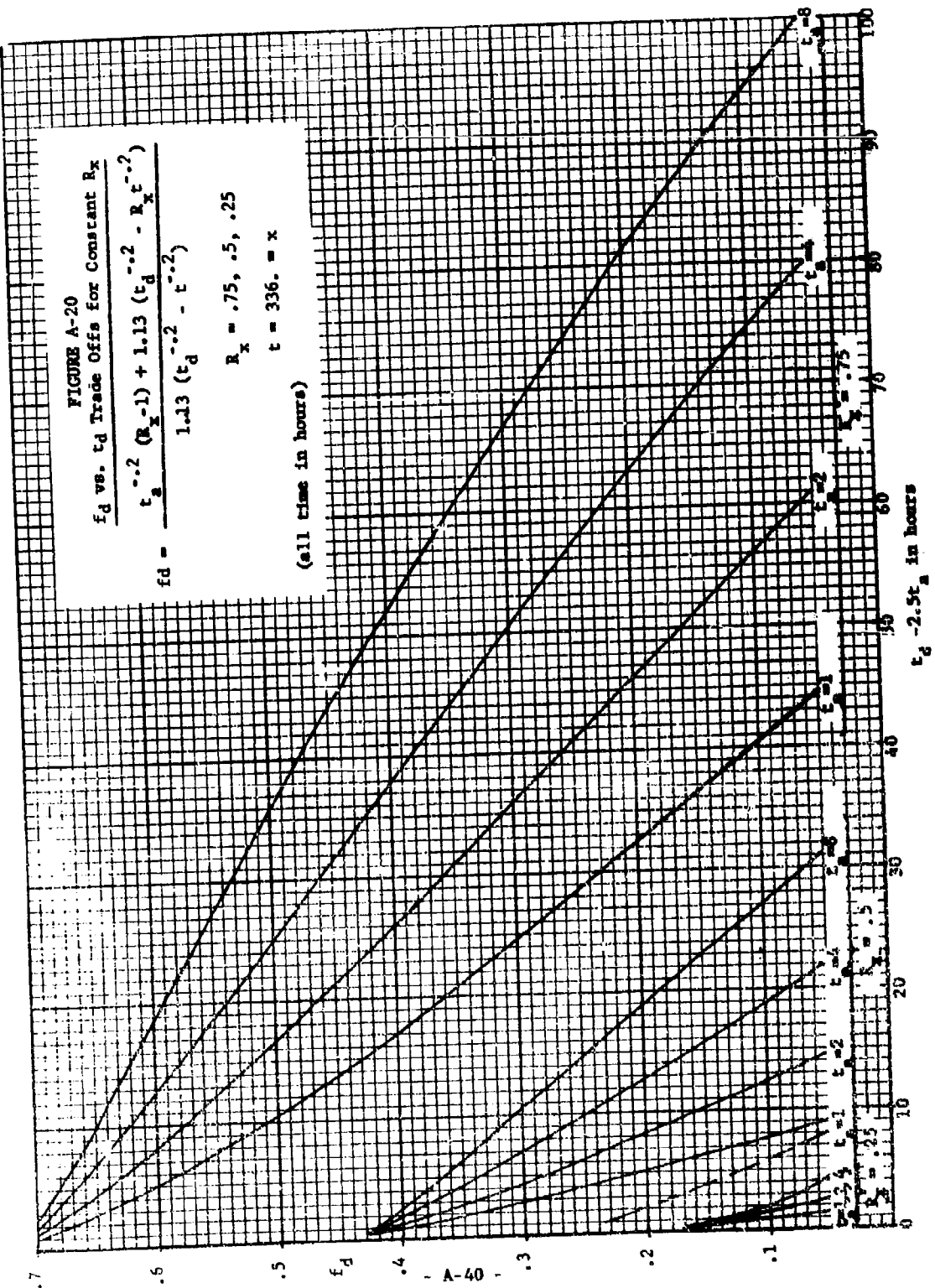
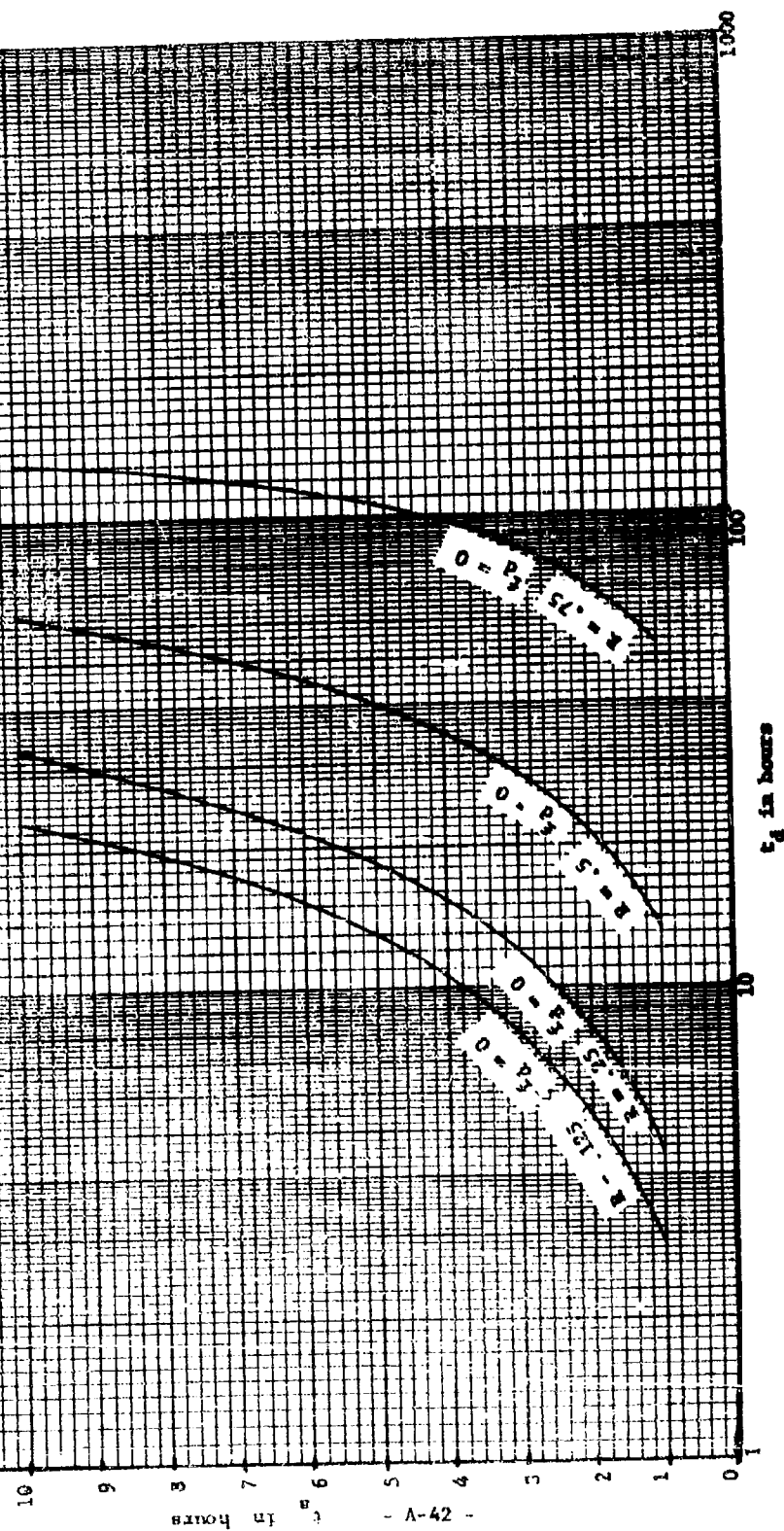


FIGURE A-22

$$R_{336}(F_d \rightarrow 0) = \frac{1-1.13 \left(\frac{F_d}{F_c}\right)^{-0.2}}{1-1.13 \left(\frac{F_{d0}}{F_c}\right)^{-0.2}}$$



they are labeled. Instead, each curve is applicable to a multitude of t_a , t_d combinations. The set of combinations that applies to each curve in Figure A-21 is given by each of the four corresponding curves in Figure A-22. The curves in both Figures are labeled 1, 2, 3, and 4 to establish easy recognition of the proper correspondence.

The third display, Figures A-23 through A-26, shows how a given intensity reduction, f_d , will achieve different dose reductions when the operation time, t_d , is varied. This effect is portrayed for times of arrival 1/3, 1, 3, and 9 hours and for value ratio evaluation times of ∞ , 336 hours, and the times when the equivalent residual dose is maximum (see Figure A-18). From this set of curves it is easy to determine the wide variation that exists in the magnitude of the value ratio and that results from f_d , t_d , t_a , and, most vividly, x . These variations in the value ratio, R_x , are of two distinct and different types. Most important for operation planning is the variation that results when f_d , t_d , and t_a are varied. These variations result from the manner in which the decontamination operation is performed. In contrast to these are the variations in R_x that occur when x is varied. These variations have nothing to do with the decontamination operation. They only reveal the effect of the time at which the value ratio is examined. To emphasize this effect, several of the curves for $f_d = 0$ and $f_d = .8$ are combined and presented in a different manner in Figure A-27. For $t_a = 1$, Figure A-27 shows the variation that results when the time at which the value ratio is evaluated is changed. It can be seen that the variation is greatly dependent on the reduction in intensity, f_d . For low values of f_d , the

variation due to x is greater than it is at high values of f_d .

Figures A-28 to A-31 show an entirely different effect. An examination of Figures A-23 through A-26 reveals that as one goes to lower and lower values of f_d , the return as measured by R_x becomes less and less. This effect is displayed in Figures A-28 to A-31, one for each of the times of arrival 1/3, 1, 3, and 9 hours. The value ratio, R_x , was presented as a function of f_d in Equation A-36. The limiting R_x (or "best" R_x) is reached when $f_d = 0$ and can be expressed as R_x^* as follows:

$$R_x^* = \frac{1 - 1.13 t_a^{.2} t_d^{-.2}}{1 - 1.13 t_a^{.2} x^{-.2}} \quad (A-39)$$

Consider the t_d 's and f_d 's that result in a value ratio that is within 10% of the theoretical limit. That is, let

$$R_x = 1.1 R_x^* \quad (A-40)$$

Substituting the equation for R_x and R_x^* (Equations A-36 and A-39) into Equation A-40 results in the following relation among t_d , f_d , and x :

$$11.3 f_d = \frac{t_a^{-.2} - 1.13 t_d^{-.2}}{t_d^{-.2} - x^{-.2}} \quad (A-41)$$

This relationship is displayed in Figure A-28 through A-31 for 2 values of x and 4 values of t_a . These displays show the f_d that must be achieved to result in a value ratio that is 90% of the theoretical limit when the time of decontamination t_d is fixed. This may be interpreted as one possible curve for diminishing returns in the value of f_d . The shaded portion of each Figure is the region swept out by the curve as x goes from 336 hours to ∞ .

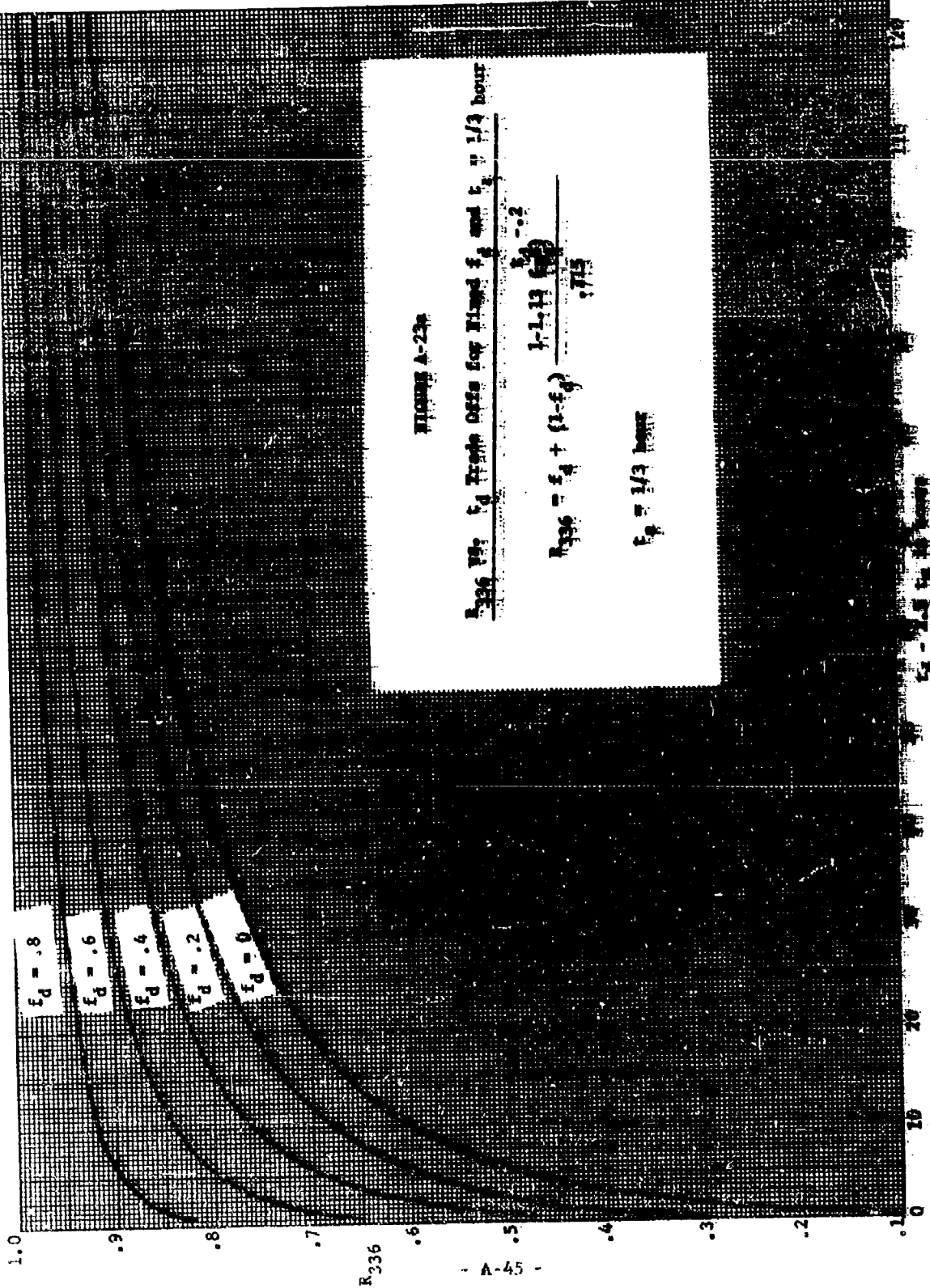


FIGURE A-23a

R_{336} vs. t_d Trade Offs for Fixed f_d and $t_d = 1/3$ hour

$$R_{336} = f_d + (1-f_d) \frac{1-1.13 \left(\frac{t_d}{1.13} \right)^{0.2}}{1.13}$$

$$t_d = 1/3 \text{ hour}$$

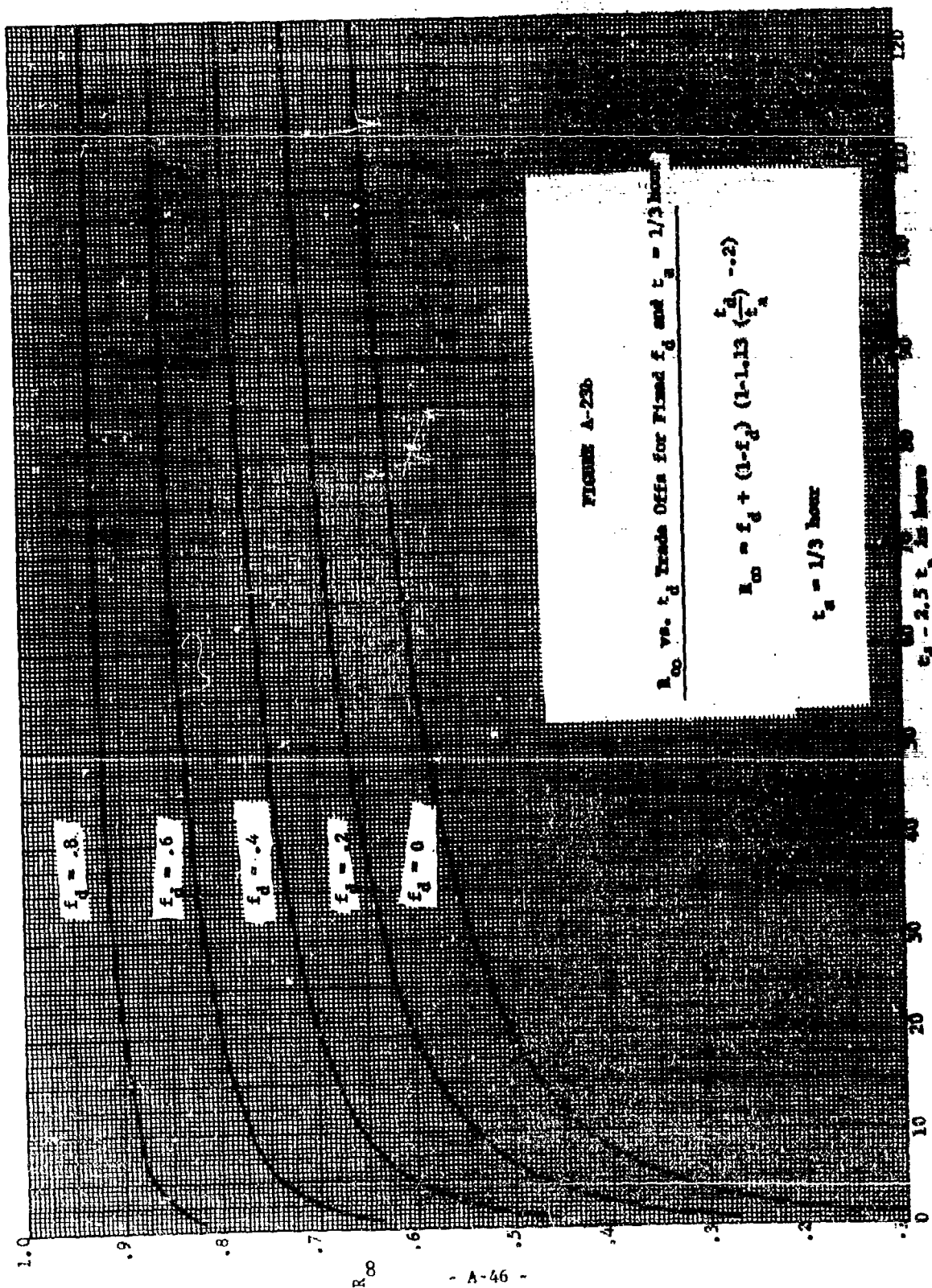


FIGURE A-23b

R_{∞} vs. t_d Trade Offs for Fixed f_d and $t_a = 1/3$ hour

$$R_{\infty} = f_d + (1-f_d) \left(1 - 1.13 \left(\frac{t_d}{t_a}\right)^{-0.2}\right)$$

$$t_a = 1/3 \text{ hour}$$

$t_d = 2.5 t_a$ 2.5 hours

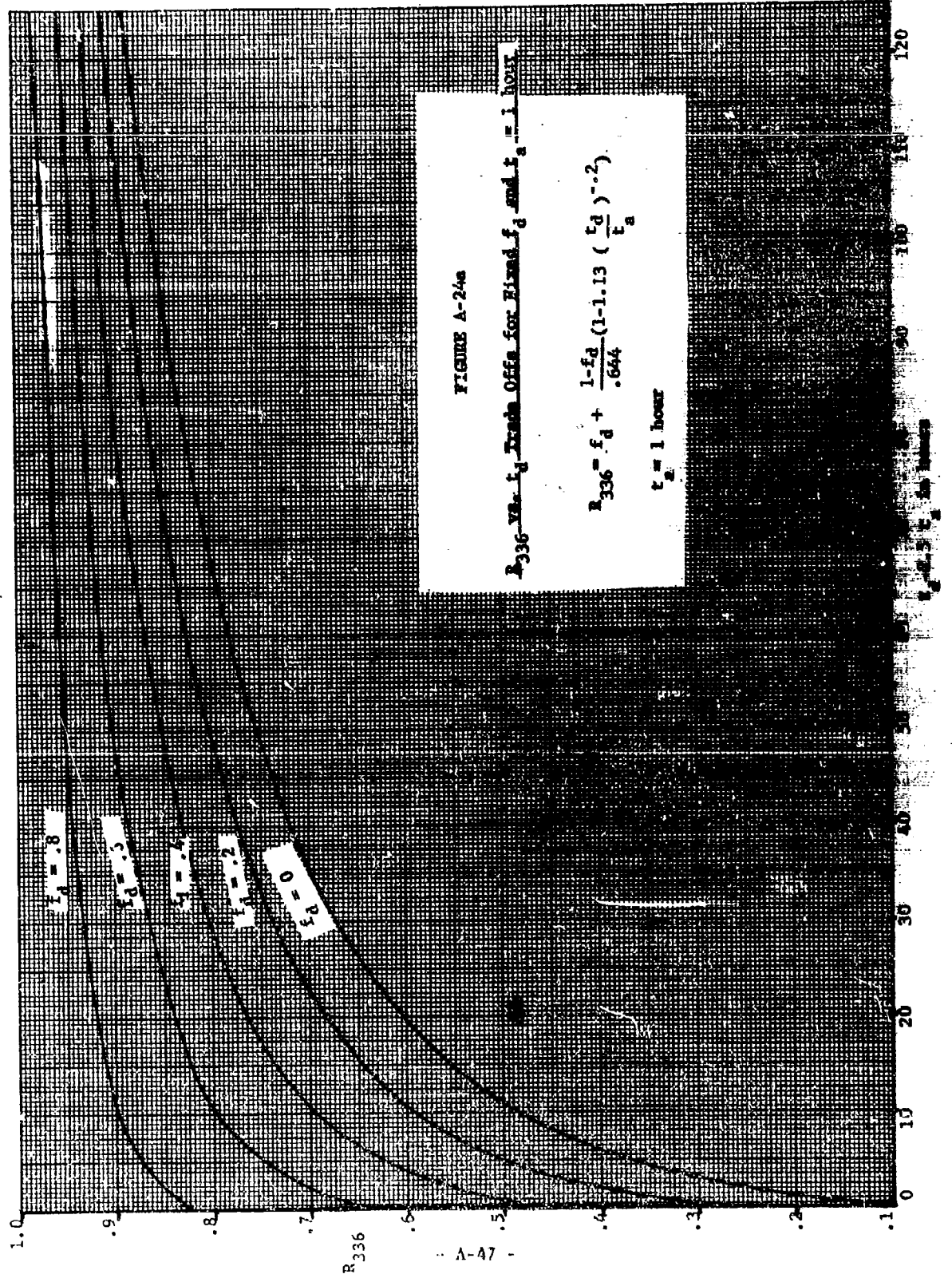


FIGURE A-24a

R_{336} vs. t_d Trade Offs for Fixed f_d and $t_a = 1$ hour

$$R_{336} = f_d + \frac{1-f_d}{.644} \left(1 - 1.13 \left(\frac{t_d}{t_a}\right)^{-0.2}\right)$$

$t_a = 1$ hour

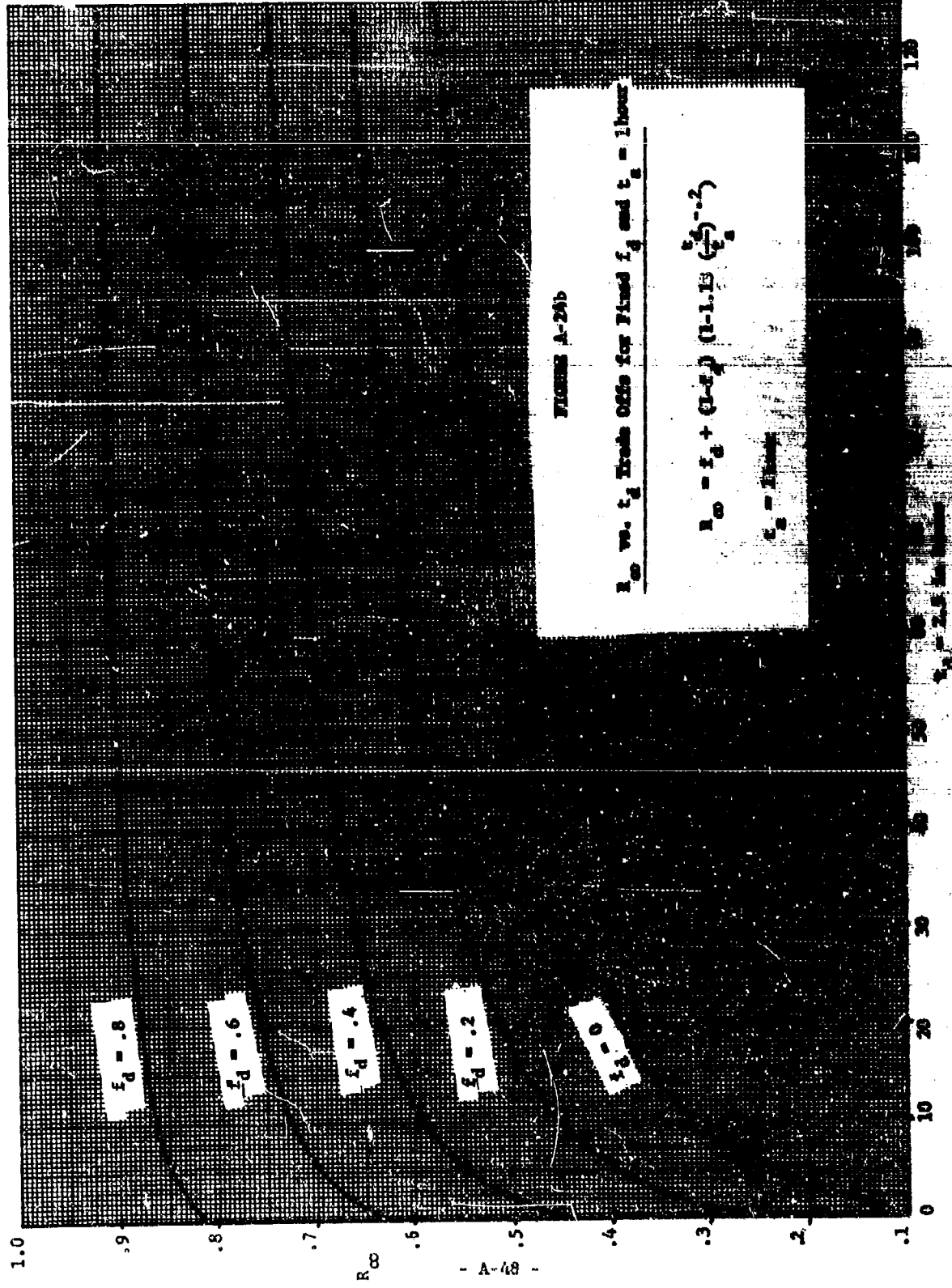


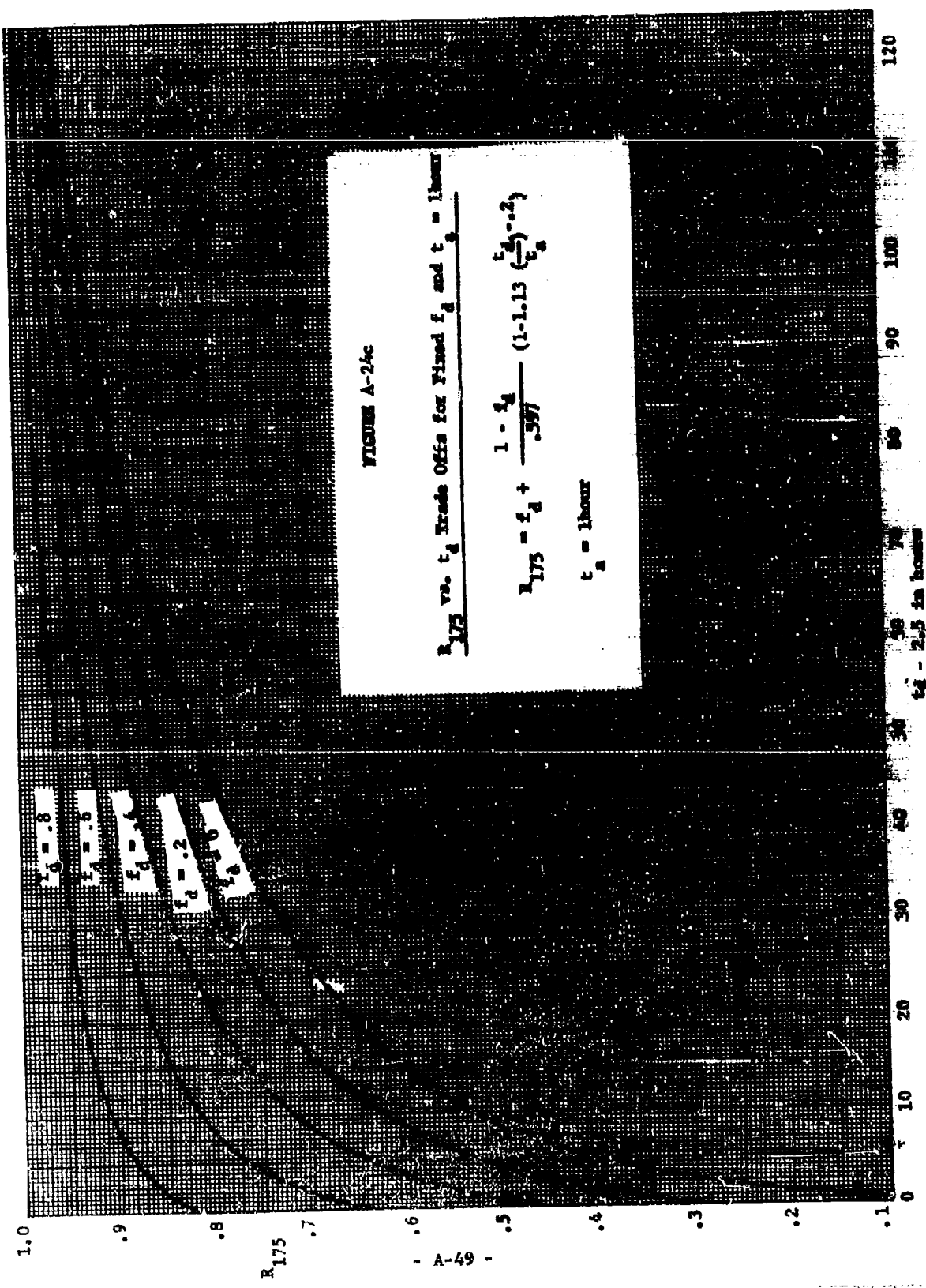
FIGURE A-20b

R_{∞} vs. t_d Trade Offs for Fixed f_d and $t_e = 1$ hour

$$R_{\infty} = f_d + (1-f_d) \left(1 - \frac{t_d}{t_e}\right)^{-2}$$

$$t_e = 1 \text{ hour}$$

$t_d = 2.5 \text{ hr}$



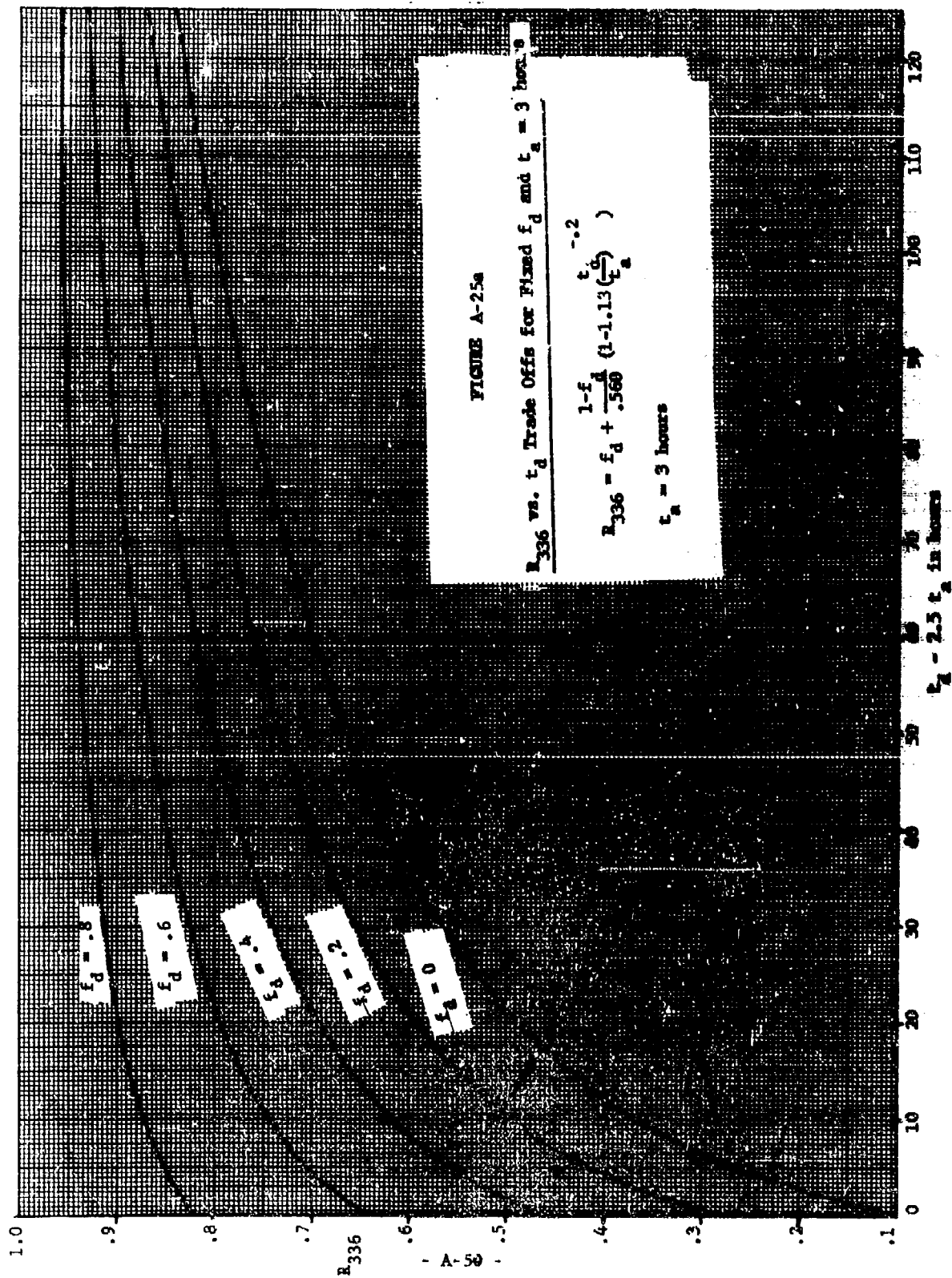


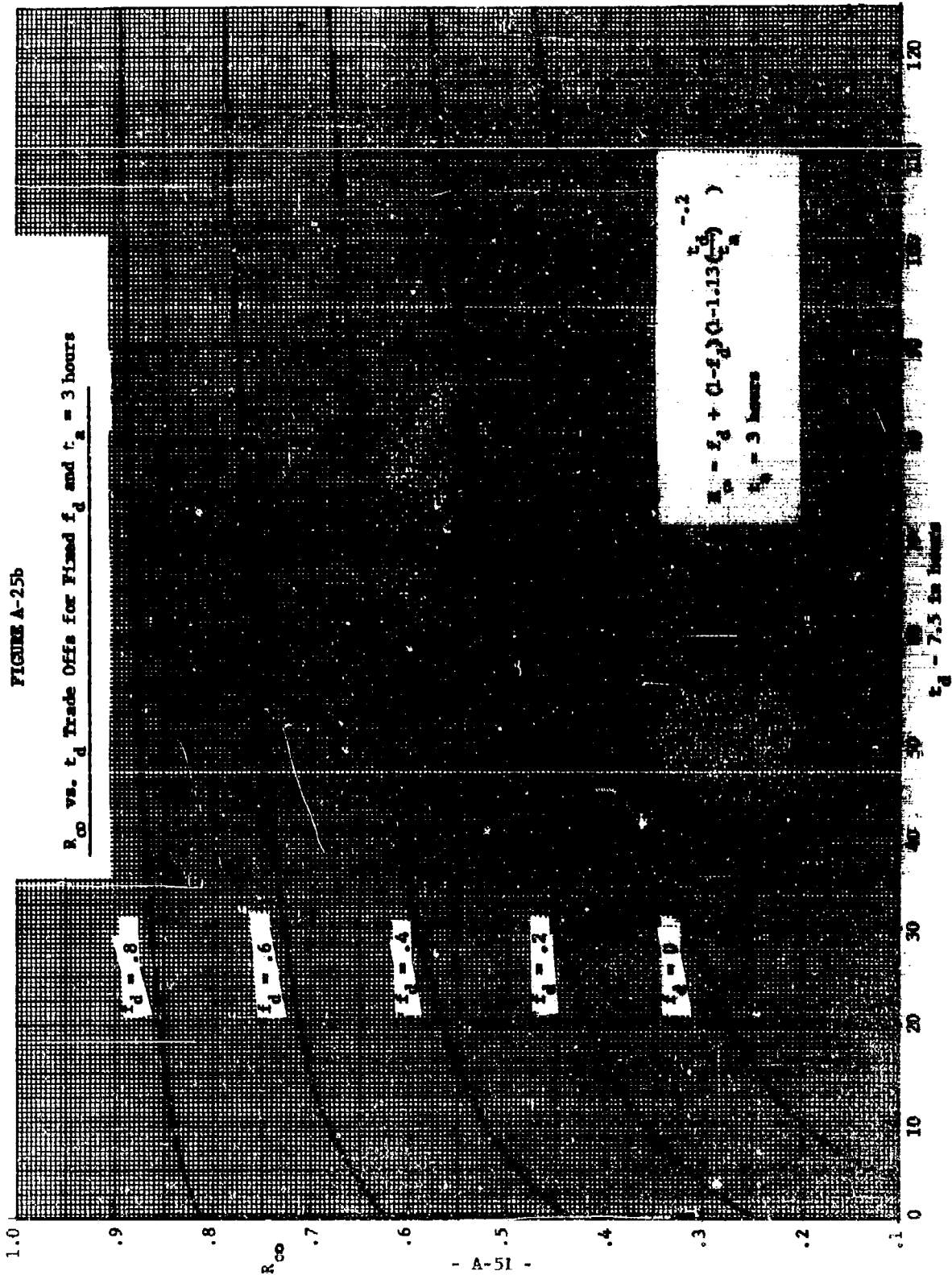
FIGURE A-25a

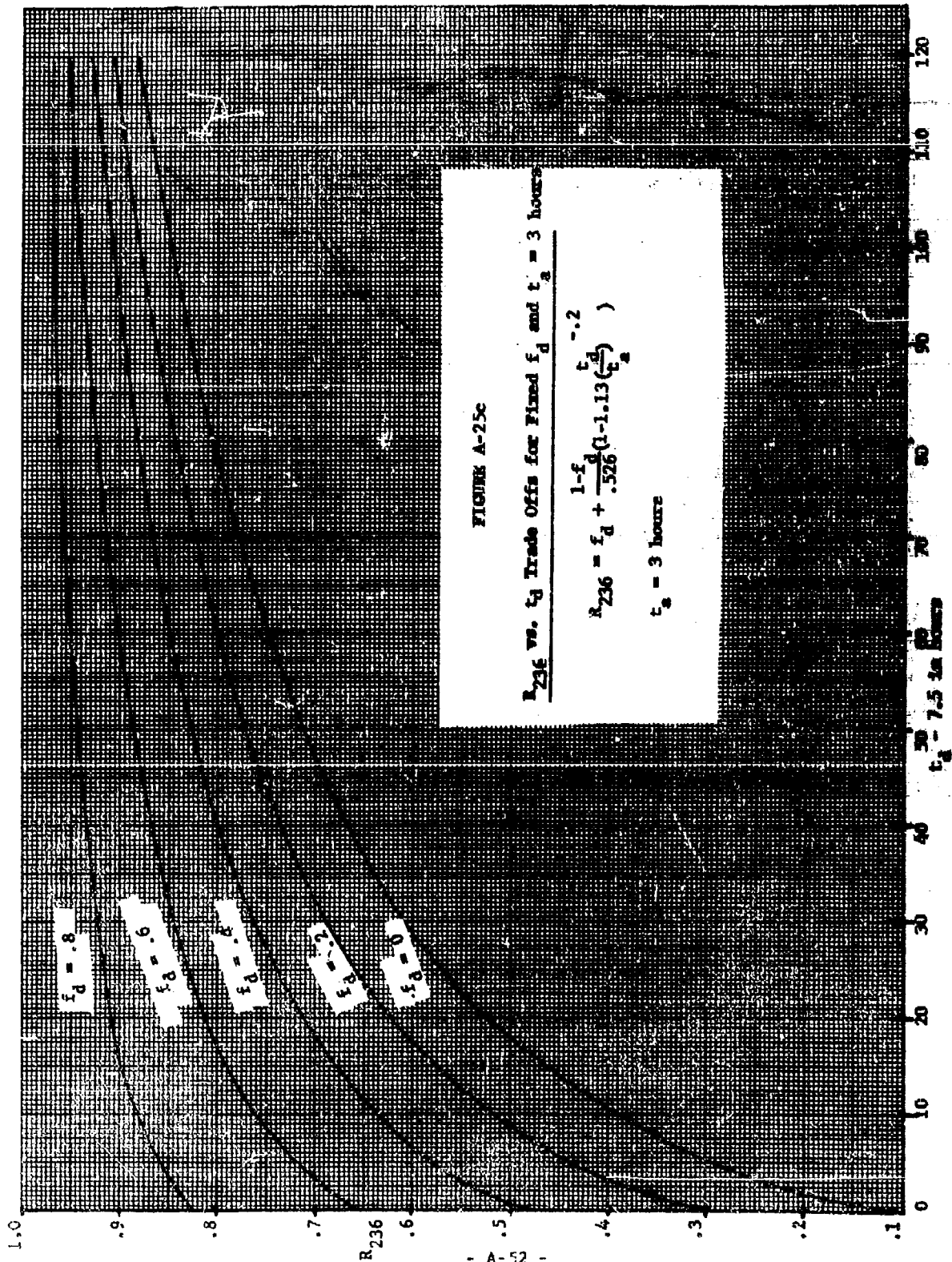
R_{336} vs. t_d Trade Offs for Fixed f_d and $t_a = 3$ hours

$$R_{336} = f_d + \frac{1-f_d}{.560} \left(1 - 1.13 \left(\frac{t_d}{t_a} \right)^{-0.2} \right)$$

$t_a = 3$ hours

$t_d - 2.5 t_a$ in hours





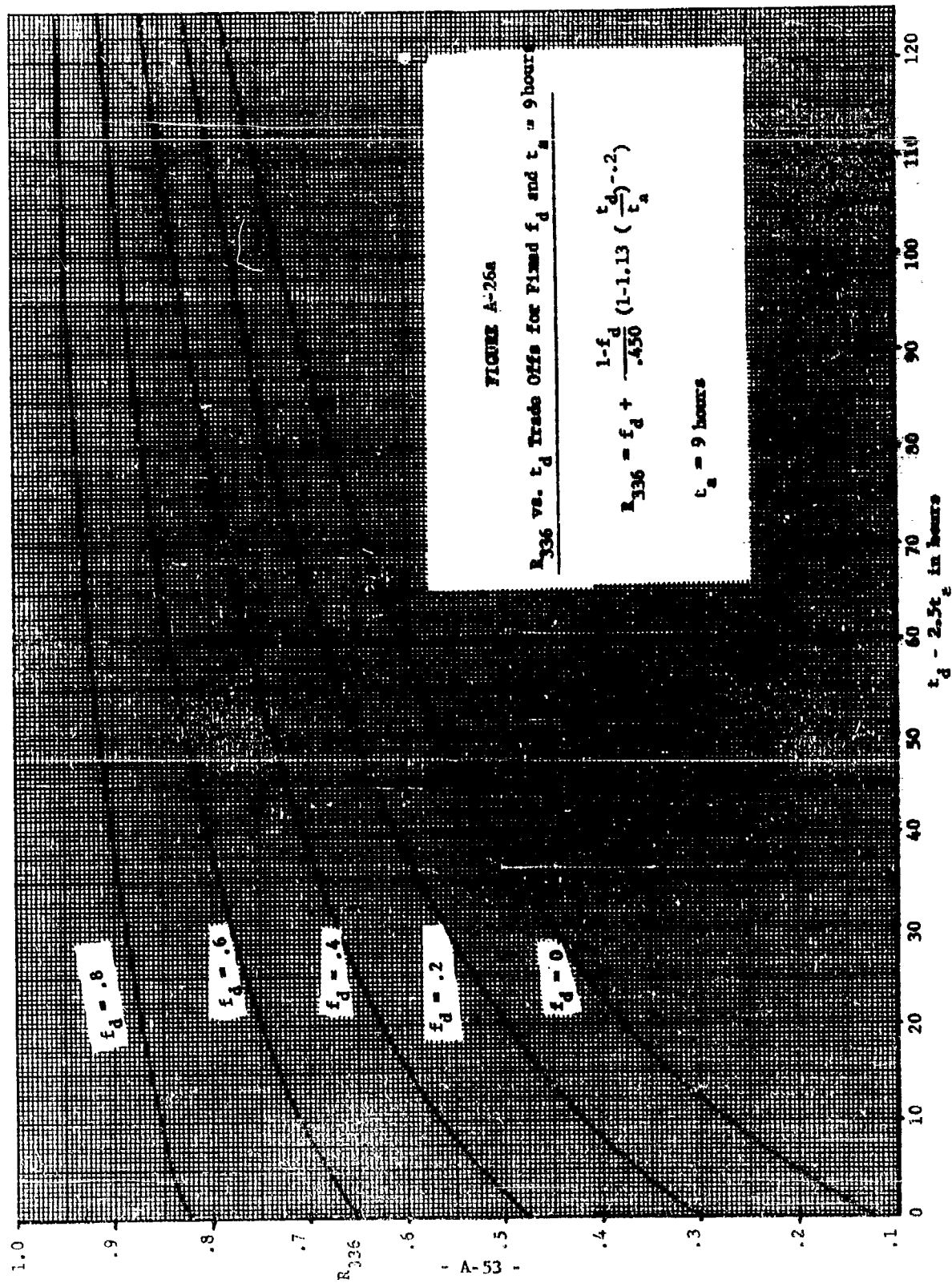
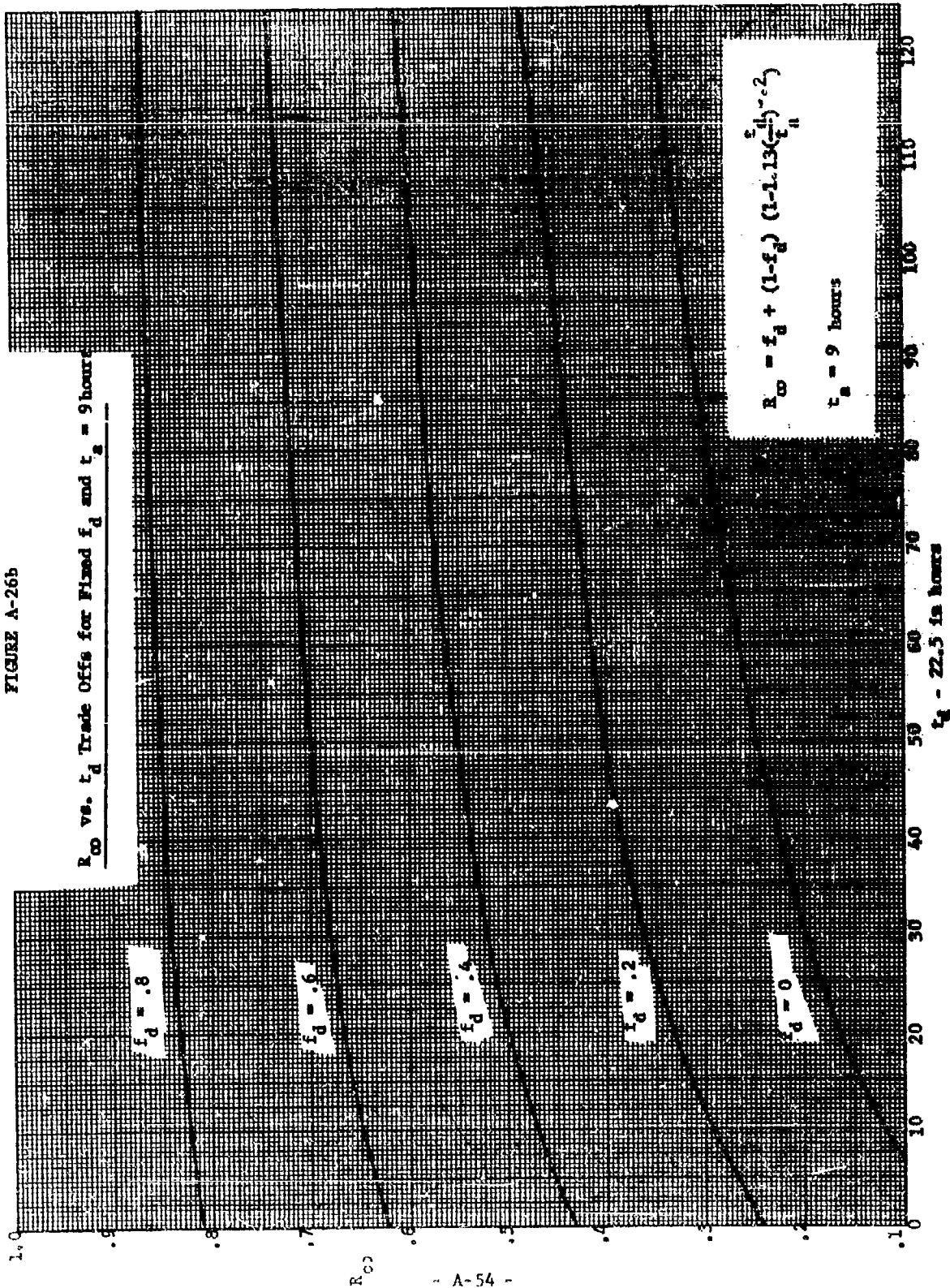


FIGURE A-26b



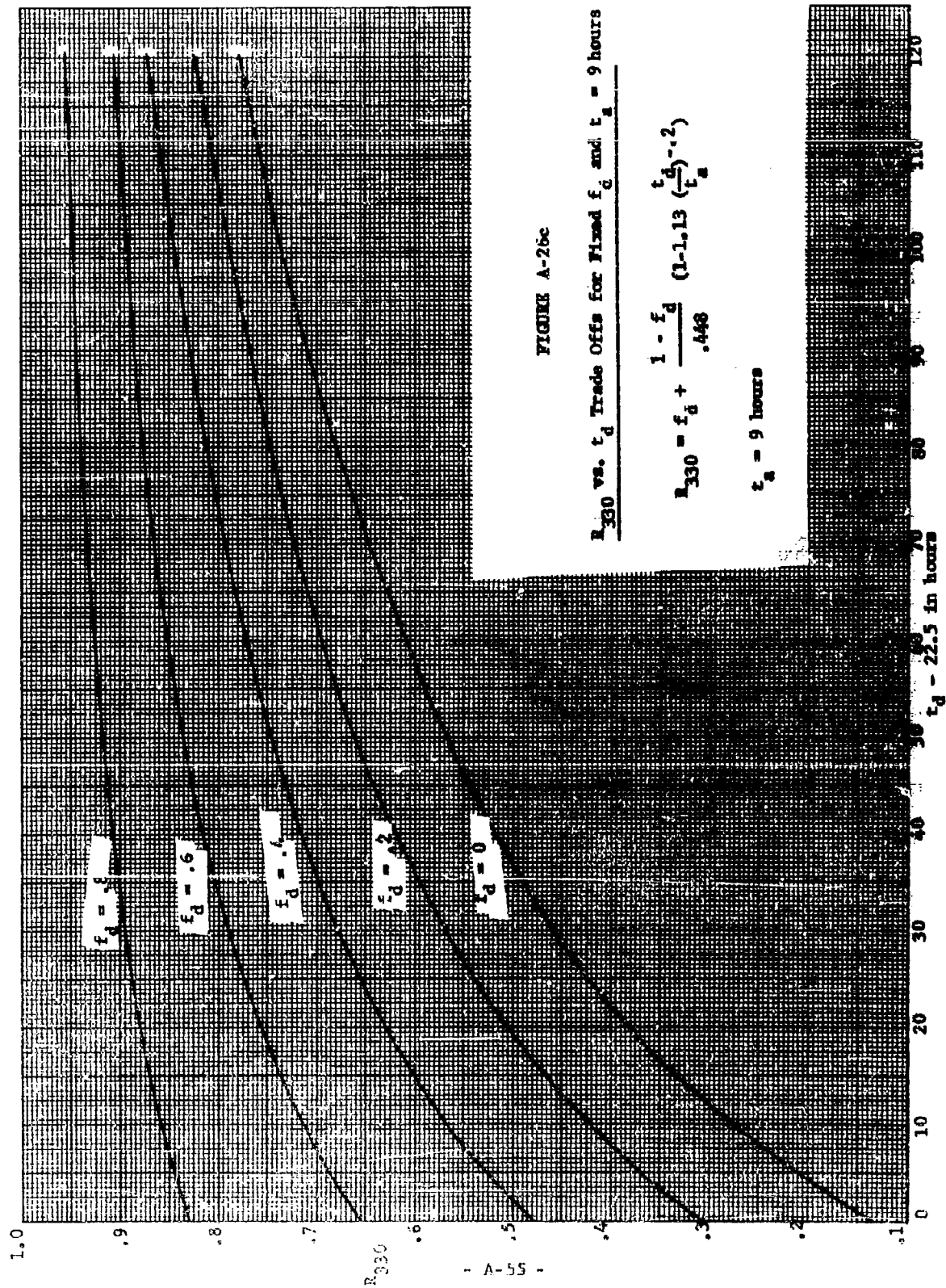


FIGURE A-26c

R_{330} vs. t_d Trade Offs for Fixed f_d and $t_a = 9$ hours

$$R_{330} = f_d + \frac{1 - f_d}{.448} \left(\frac{t_d}{t_a} \right)^{-1.2}$$

$t_a = 9$ hours

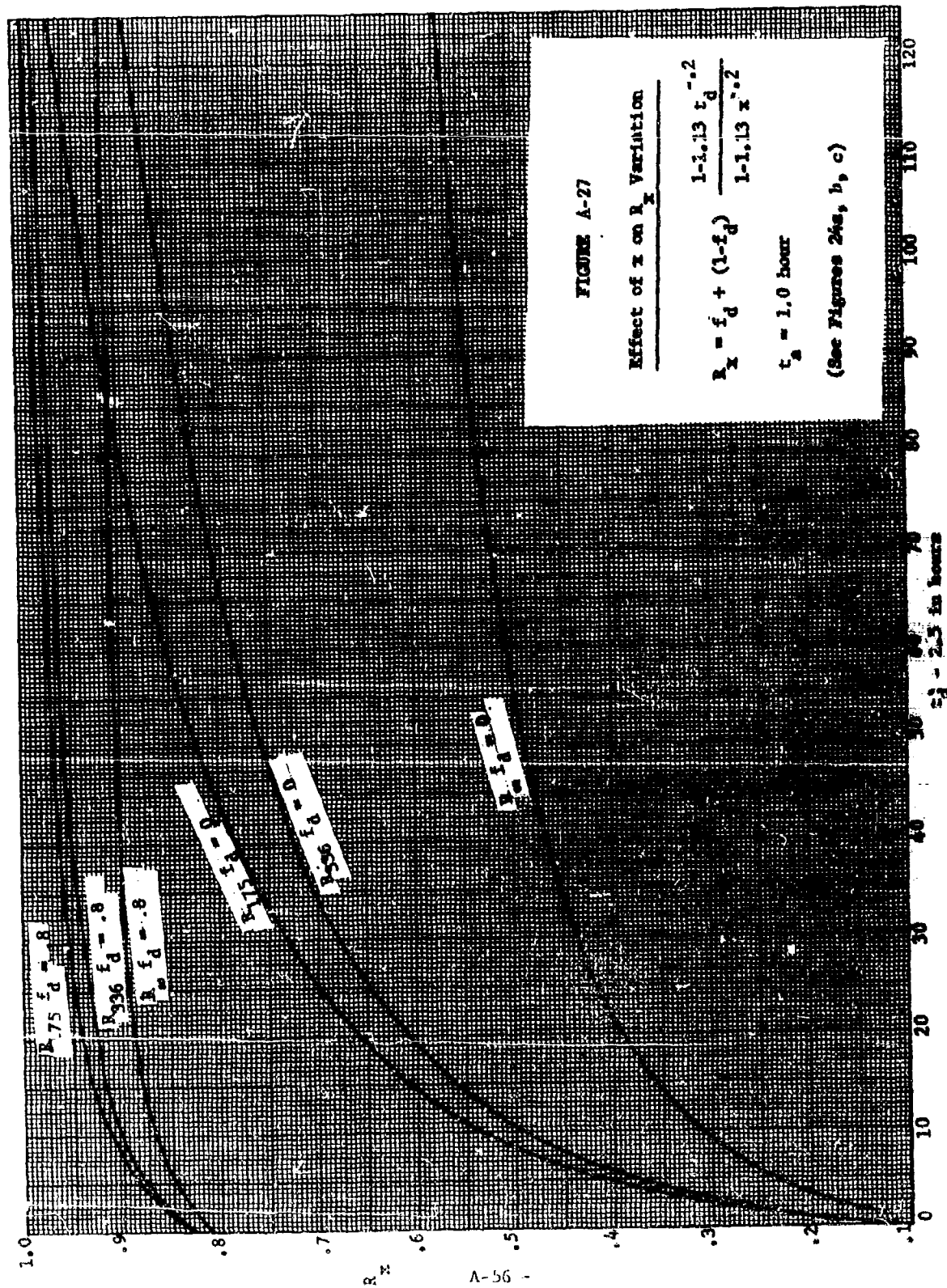


FIGURE A-27

Effect of z on R_z Variation

$$R_z = f_d + (1-f_d) \frac{1-1.13 z_d^{-0.2}}{1-1.13 z_d^{-0.2}}$$

$t_d = 1.0$ hour

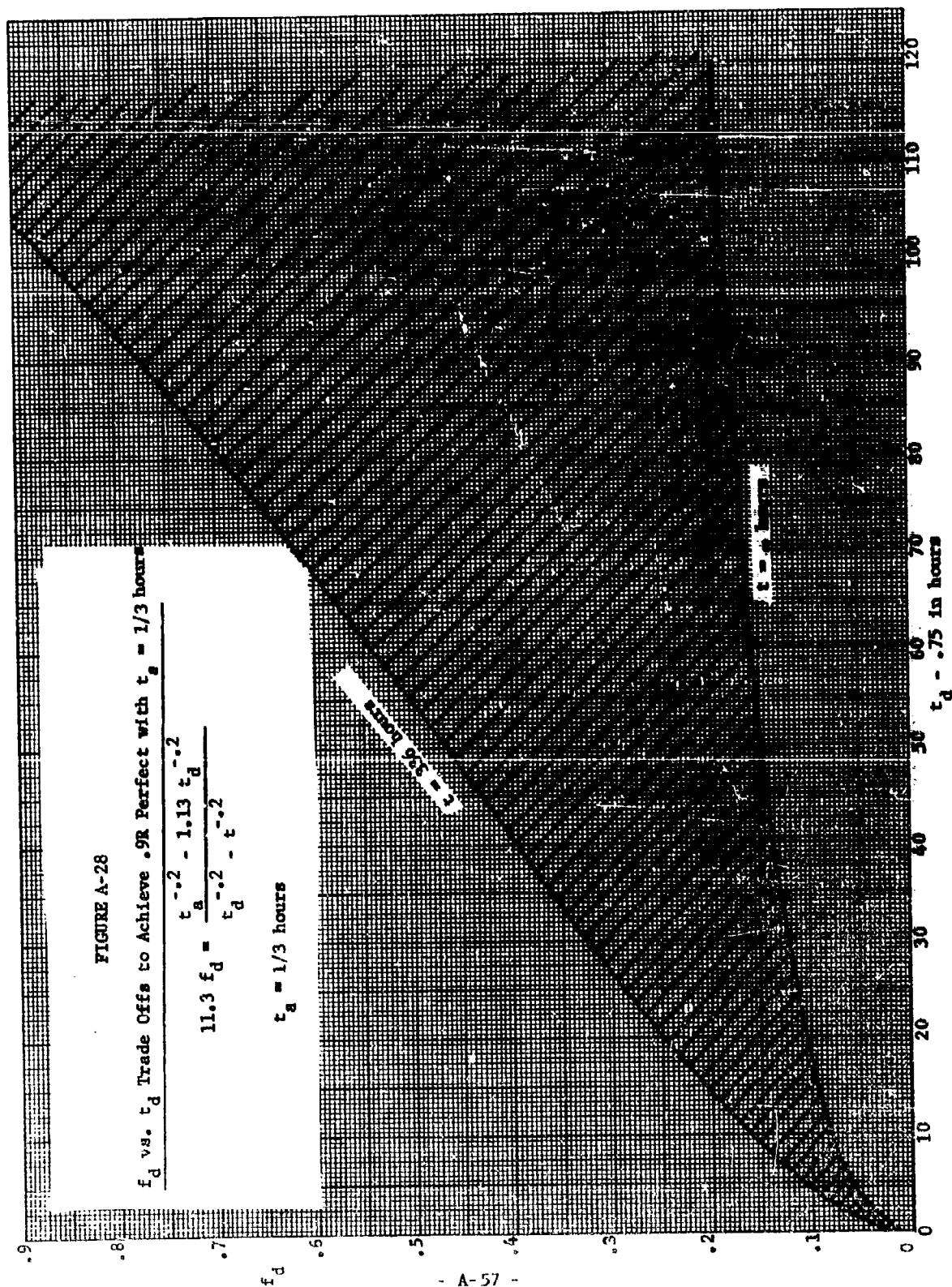
(See Figures 24a, b, c)

FIGURE A-28

f_d vs. t_d Trade Offs to Achieve .9R Perfect with $t_a = 1/3$ hours

$$11.3 f_d = \frac{t_a^{-0.2} - 1.13 t_d^{-0.2}}{t_d^{-0.2} - t_a^{-0.2}}$$

$t_a = 1/3$ hours



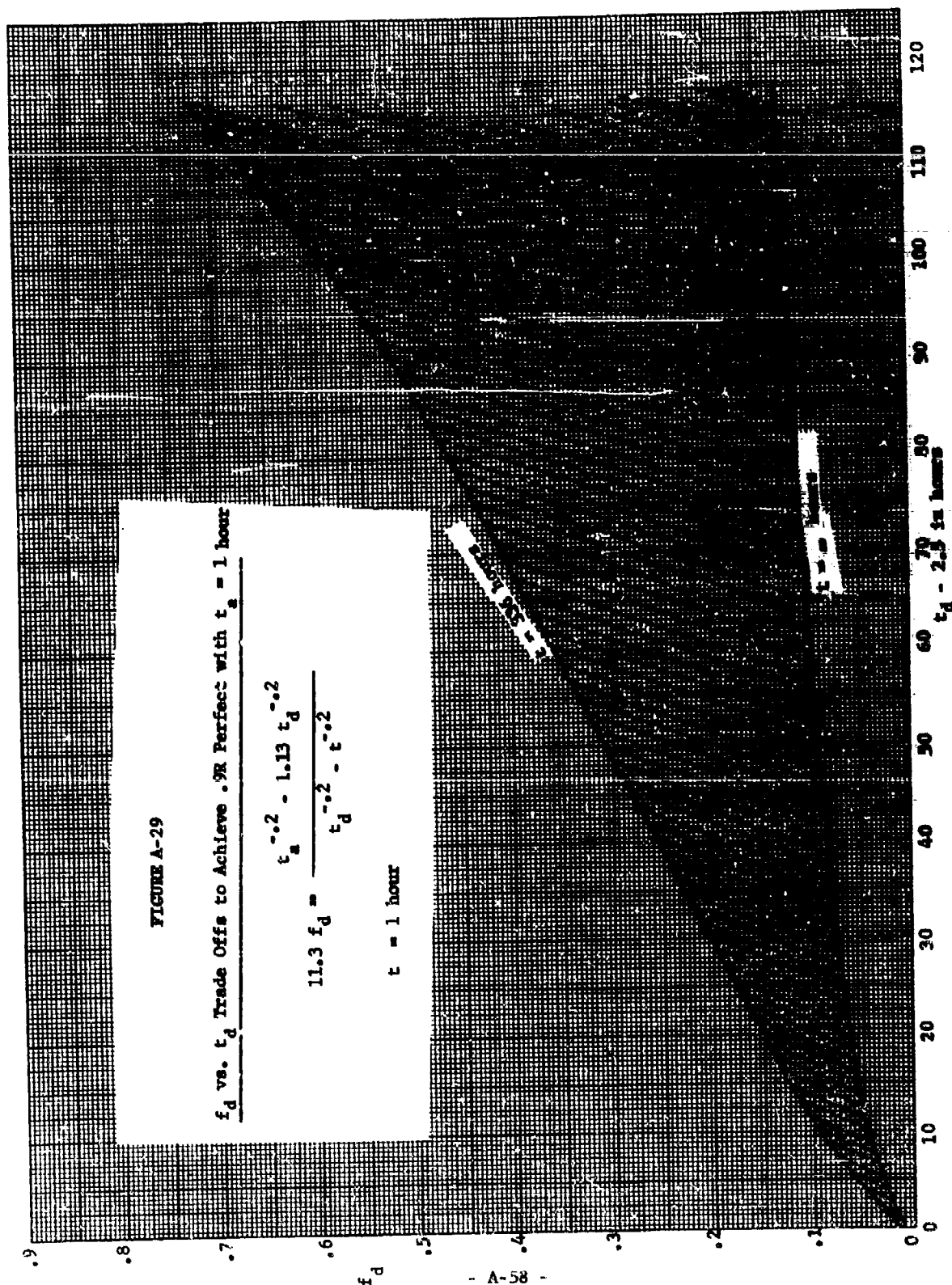


FIGURE A-30

f_d vs. t_d Trade Offs to Achieve .92 Perfect with $t_a = 3$ hours

$$11.3 f_d = \frac{t_a^{-0.2} - 1.13 t_d^{-0.2}}{t_d^{-0.2} - t_a^{-0.2}}$$

$t_a = 3$ hours

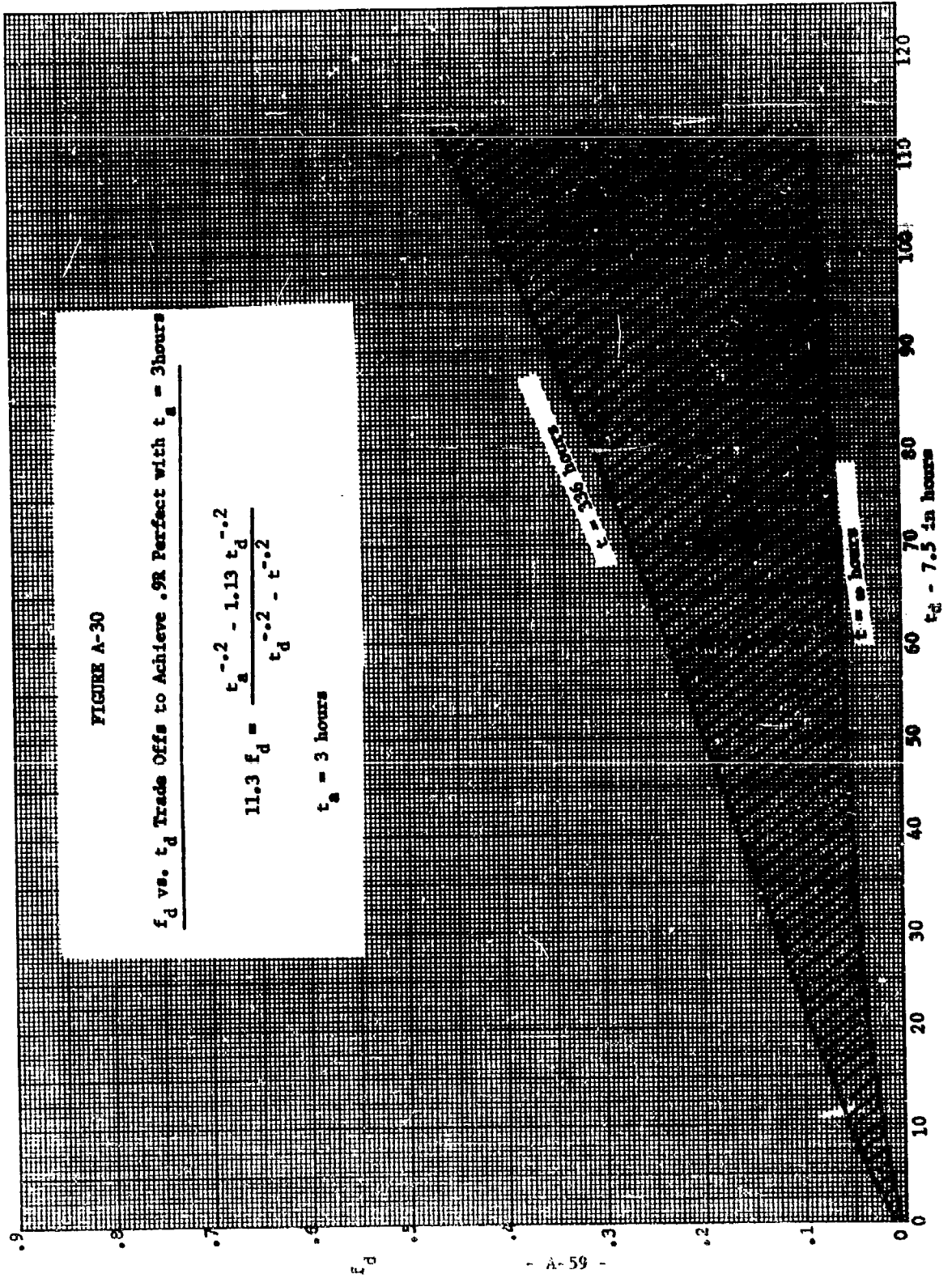


FIGURE A-31

f_d vs. t_d Trade Offs to Achieve .9R Perfect with $t_g = 9$ hours

$$11.3 f_d = \frac{t_g^{-0.2} - 1.13 t_d^{-0.2}}{t_d^{-0.2} - t_g^{-0.2}}$$

$t_g = 9$ hours

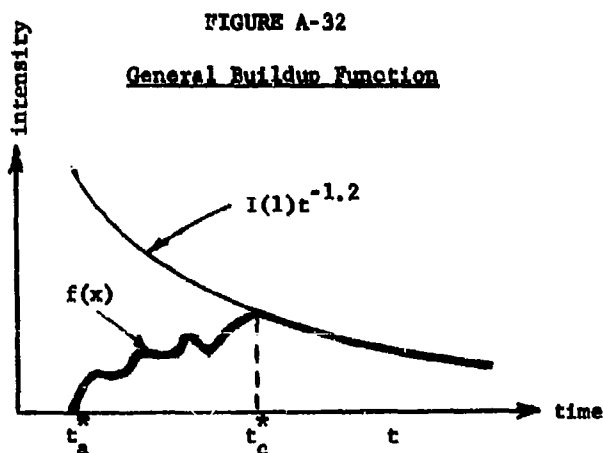
$t = 35$ hours

$t = 0$ hours

$t_d = 22.5$ hours

III. ALTERNATIVE BUILDUP FUNCTIONS

The effectiveness of decontamination operations in reducing total dose received by an individual has been approached using a linear function to approximate fallout radiation intensity buildup (See Figure A-3). As previously stated, this linear approximation was used only as a vehicle to introduce the parameter t_a into the final results. It does not limit the results to situations where the buildup is linear. For example, consider the buildup function illustrated in Figure A-32.



At some time t ($t \geq t_c^*$) (See Figure A-32) the total dose is,

$$D_t^*(t) = \int_{t_a}^{t_c^*} f(x) dx + \int_{t_c^*}^t I(1)^{-1.2} dt \quad (A-42)$$

At this same time t , the total dose for the model used in Section II (Figure A-3) is, for $t \geq 2.5 t_a$,

$$D_t(t) = I(1) (4.41 t_a^{-.2} - 5t^{-.2}) \quad (A-43)$$

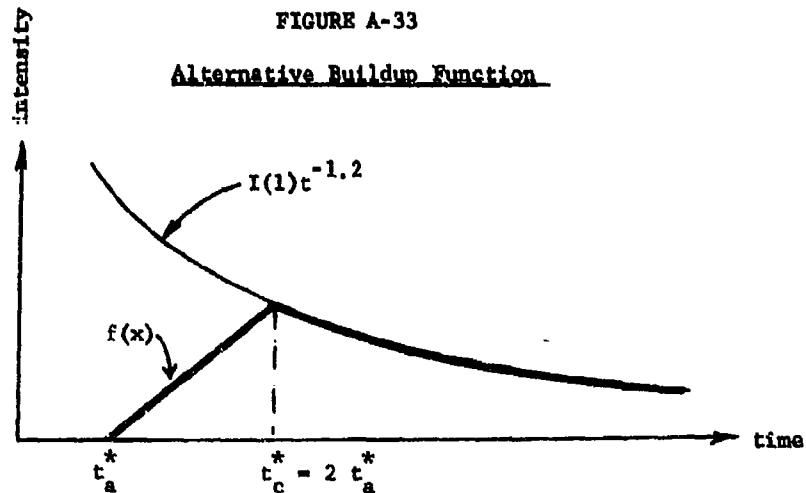
If there exists a $t_a(t_a^*)$ such that $D_t^*(t) = D_t(t)$, then the results of Section II may be applied to situations where the buildup is given by Figure A-32. The function $t_a(t_a^*)$ exists and is found as follows:

$$I(1) (4.41 t_a^{-.2} - 5 t^{-.2}) = \int_{t_a^*}^{t_c^*} f(x) dx + 5 I(1) (t_c^{*- .2} - t^{-.2}), \quad (A-44)$$

or,

$$t_a^{-.2} = \frac{1}{4.41 I(1)} \int_{t_a^*}^{t_c^*} f(x) dx + 1.13 t_c^{*- .2}, \quad (A-45)$$

which is the desired function for the new buildup function $f(x)$. As an example, consider the function in Figure A-33.



Let $f(x) = (x - t_a^*) I(1) t_a^{*-2.2} 2^{-1.2}$. Equation A-45 then becomes

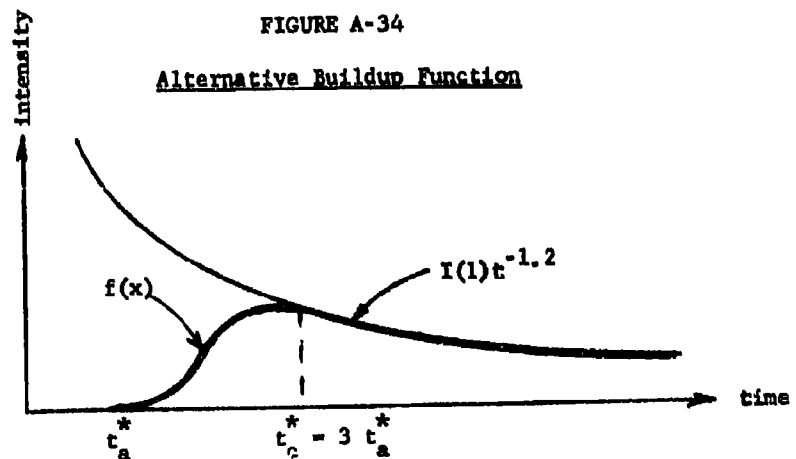
$$\begin{aligned} t_a^{-.2} &= \frac{2^{-1.2} I(1) t_a^{*-2.2}}{4.41 I(1)} \int_{t_a^*}^{2 t_a^*} (x - t_a^*) dx + 1.13 (2 t_a^*)^{-.2} \\ &= 1.033 t_a^{*- .2} \\ &= (.85 t_a^*)^{-.2} \end{aligned} \quad (A-46)$$

or

$$t_a = .85 t_a^* \quad (A-47)$$

Therefore, the curves $t_a = 1, 3, 9$ would be read as $t_a^* = 1.18, 3.53, 10.6$.

As a second example, consider the function in Figure A-34.



To maintain continuity, if $f(x)$ is a sine function in the interval $[t_a^*, 3 t_a^*]$,

then,

$$f(t) = \frac{I(1)}{2} (3 t_a^*)^{-1.2} \left[1 + \sin \frac{\pi}{2 t_a^*} (t - 2 t_a^*) \right] \quad (A-48)$$

Therefore, Equation A-45 becomes

$$t_a^{-.2} = \frac{1}{4.41 I(1)} \int_{t_a^*}^{3 t_a^*} \frac{I(1)}{2} (3 t_a^*)^{-1.2} [1 + \sin \frac{\pi}{2 t_a^*} (t - 2 t_a^*)] dt \quad (A-49)$$

$$+ 1.13 (3 t_a^*)^{-.2} \\ = \left(\frac{3^{-1.2}}{4.41} + 3^{-.2} 1.13 \right) t_a^{*-1.2} \quad (A-50)$$

$$= (1.183 t_a^*)^{-.2} , \quad (A-51)$$

or

$$t_a = 1.183 t_a^* . \quad (A-52)$$

Therefore, the curves $t_a = 1, 3, 9$ would be read as $t_a^* = .845, 2.53, 7.6$, respectively. From the examples and preceding discussion, it can be seen that time of arrival and nature of the buildup function are used for presentation convenience and the results obtained do not depend on them. The main assumption in the development is the $t^{-1.2}$ decay law. The precision implicit in the results depends on the precision with which the $t^{-1.2}$ decay law models reality. However, in the process of using the results for prediction and planning, any error that results from using this decay assumption will be minor when compared to the error due to other assumptions that must be made in attempting to apply the theory.

APPENDIX A REFERENCES

- A-1 J. F. Devaney. Operations in Fallout. OCDM-SA-61-13. Washington: Office of Civil Defense Mobilization, June 1961.
- A-2 J. D. Douglass, Jr., and H. E. Campbell. The Effect of Decontamination on Equivalent Residual Dose. RM-156-2. Durham, North Carolina: Research Triangle Institute, Operations Research Division, April, 1964. See Appendix B.

The Effect of Early Decontamination
on Equivalent Residual Dose

This Appendix was originally
submitted to OCD as Research
Memorandum RM 156-2nd, except
for minor editorial changes.

Appendix B

The Effect of Early Decontamination on Equivalent Residual Dose

I. INTRODUCTION AND SUMMARY

Appendix A analyzed the effect of a reduction in the intensity in a facility (which might be the result of decontaminating on or about the facility) on the total dose of the personnel within the facility. To complement this information, the present study analyzes the effect of a reduction in the intensity in a facility on the equivalent residual dose (ERD) of the personnel remaining within the facility over the whole time period of interest.

The ERD of an individual at time t is the area under the appropriate portion of a weighted intensity vs. time curve. Here, the intensity is that within the facility, and therefore the protection factor of the facility is absorbed into the reference intensity factor, $I(1)$. The intensity curve used here employs a linear function to describe the buildup of intensity and the function $I(1)t^{-1.2}$ to describe the subsequent decay. For any time t , the ERD as function of reference intensity, $I(1)$, and time of arrival, t_a , is presented in Figure B-3. This "normal" ERD is used in the subsequent development as a reference. That is, the ERD at some time after decontamination has been performed will be compared with the "normal" ERD that otherwise would have been received up to the same time. Following this general development, attention is focused on the maximum value attained by the "normal" ERD as a function of the reference intensity and time of arrival. The behavior of this maximum ERD is illustrated in Figures B-4 and B-5.

Decontamination enters the analyses as an instantaneous reduction in intensity that takes place at time t_d . Before time t_d , the intensity is not affected. For all times after time t_d , the intensity magnitude is multiplied by a factor f_d whose value lies between zero and one. The resultant decrease in maximum ERD (for fixed time of arrival) will depend on t_d and f_d . For various times of arrival, the ratio of maximum ERD with decontamination to normal maximum ERD is presented as a function of time of decontamination (t_d) and amount of decontamination (f_d). The effects of variations in these parameters comprise the primary objectives of this analysis and are presented in Figures B-13 a, b, and c.

In the analysis, fallout arrival times from .2 hours to 10 hours are considered. Only times of operations later than the time at which fallout deposition ceases are considered. Both zero and finite operation duration times are considered. All possible intensity reductions are considered. The results are displayed by the ratio of the maximum ERD with the operation to the maximum ERD without the operation. In addition a method is presented so that the results can be applied to any desired buildup function.

II. ERD WITHOUT DECONTAMINATION

The effect of decontamination on an individual's ERD will be determined as a function of both the fallout intensity characteristics (time of arrival, buildup function, and reference intensity) and the decontamination operation characteristics (time of decontamination and effectiveness of decontamination). The effect of a particular decontamination operation will be viewed as the

change in an individual's maximum ERD resulting from the performance of the operation. To determine this change, it is first necessary to determine the behavior of an individual's maximum ERD as determined by the fallout intensity characteristics in the absence of any decontamination operations. This section determines this behavior.

A. General Expression for ERD

The following development postulates the occurrence of a single nuclear detonation at time $t = 0$ where t is in hours. As a result of this detonation, radioactive fallout material is deposited in the vicinity of the individual of interest. This material produces radiation whose intensity at the individual's location is $I(t)$ in roentgens per hour. This intensity is zero prior to $t = 0$. Because this intensity is at the individual's location, the protection factor of the facility in which the individual is located is incorporated into the intensity function $I(t)$.

Throughout the analysis, the individual remains at the location where the intensity is $I(t)$ for all $t > 0$. Therefore, at any time greater than zero the total dose he will have received is:

$$\text{Total Dose} = D_T(t) = \int_0^t I(x) dx \quad . \quad (B-1)$$

When the intensity is weighted to account for the natural biological repair that takes place, the resultant dose is called the equivalent residual dose, ERD. If $W(t-x)$ is the appropriate weighting function, then at any time greater than zero the individual's ERD is:

$$\text{ERD} = D_R(t) = \int_0^t W(t-x) I(x) dx \quad . \quad (B-2)$$

This is the general expression for ERD that is used throughout the remainder of this paper. In Section B, the intensity function $I(x)$ will be formulated to reflect the combined effects of fallout material deposition rate and radioactive decay. Prior to the completion of the deposition process, a buildup function will be chosen to represent the intensity behavior. For times after deposition has ceased, the common decay law, $I(t)t^{-1.2}$, will be used to represent the intensity behavior. In Section C the weighting function as suggested by Devaney (Reference B-1) and the National Committee on Radiation Protection (Reference B-2) will be approximated for subsequent analysis and evaluation of Equation B-2.

B. Intensity Function

The intensity function is developed for all times greater than zero by first dividing the times of interest into three intervals. The first interval is prior to t_a , the time of fallout arrival. Over this interval the intensity is assumed equal to zero. That is,

$$I(t) = 0 \text{ for } t < t_a \quad (B-3)$$

The second interval is from t_a to t_c , where t_c is the time at which fallout deposition ceases. During this time interval the intensity function, called the buildup function, must reflect the combined effect of material deposition and radioactive decay. Because of the many factors entering into such a determination, the appropriate function will vary according to the particular situation. Therefore, a convenient (linear and with $t_c = 2.5 t_a$)* function will be selected upon which the subsequent analysis

*For a more detailed discussion regarding the selection of this particular buildup function, see Reference B-2.

will be based. At the conclusion of this section the mathematics necessary to apply the analysis and results of this report to different buildup functions will be presented.

The analysis regards $I(t)$ as linear throughout the time interval t_a to t_c . That is,

$$I(t) = I(t - t_a) \text{ for } t_a \leq t \leq t_c = 2.5 t_a \quad (B-4)$$

is selected as a reference buildup function. Because in Equation B-4 the intensity is zero when $t = t_a$, the intensity function is continuous throughout the first two time intervals, zero to $2.5 t_a$. The constant I in Equation B-4 is chosen to make the intensity function continuous throughout the second and third intervals, t greater than t_a .

The third interval includes all times greater than $t_c = 2.5 t_a$. During this interval, the intensity behavior is assumed to follow the common radioactive decay law, $t^{-1.2}$. That is,

$$I(t) = I(1)t^{-1.2} \text{ for } 2.5 t_a < t \quad (B-5)$$

Here, $I(1)$ in roentgens per hour is the reference intensity constant. Although Equation B-5 is specified for all times greater than $2.5 t_a$, the analysis will only use the equation when t is between .2 hours and 4000 hours.

The intensity function development is completed by determining the constant I in Equation B-4 so that the intensity function is continuous for all t greater than zero. This is accomplished by combining Equations B-4 and B-5 and setting t equal to $2.5 t_a$ as follows:

$$I(1.5 t_a) = I(1) (2.5 t_a)^{-1.2} \quad (B-6)$$

or

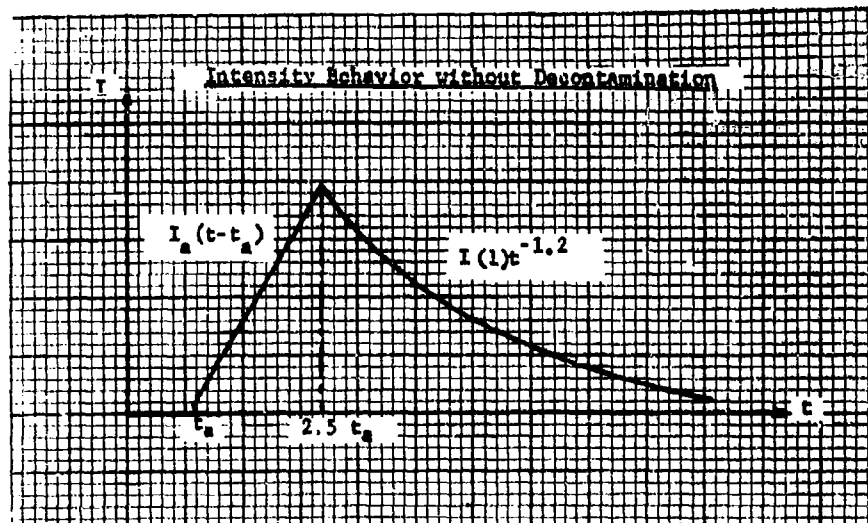
$$I = \frac{I(1) (2.5 t_a)^{-1.2}}{1.5 t_a} = .222 t_a^{-2.2} I(1) \quad (B-7)$$

Therefore, the complete intensity function for t greater than zero is:

$$I(t) = \begin{cases} 0 & \text{for } t < t_a \\ .222 t_a^{-2.2} I_0(t-t_a) & \text{for } t_a \leq t \leq 2.5 t_a \\ I(1)t^{-1.2} & \text{for } 2.5 t_a \leq t \end{cases} \quad (B-8)$$

This behavior is illustrated in Figure B-1.

FIGURE B-1



Although the subsequent analysis will use Equation B-8 to represent the intensity function, the results obtained can be applied to situations involving different buildup functions. In Appendix A (Chapter III) the process of applying similar results to intensity functions with different buildup functions was developed for the analysis of decontamination effects on total dose. In the present discussion, the analysis is concerned with ERD. However, if the fallout deposition is completed within 150 hours, then the ERD can be set equal to the total dose throughout the deposition process. For this case where the deposition interval, $1.5 t_a$, is less than 150 hours, or, for $0 \leq t_a < 100$ hours, the ERD for $t \geq 150$ hours may be written as:

$$D_R(t) = W(t-150) \int_0^{150} I(x) dx + \int_{150}^t W(t-x) I(x) dx \quad (B-9)$$

If $2.5 t_a$ is less than 150 hours, this becomes, using Equation B-8,

$$D_R = W(t-150) \int_0^{150} I(x) dx + \int_{150}^t W(t-x) I(1) x^{-1.2} dx \quad (B-10)$$

Let the desired alternative intensity function, using a different buildup function, be,

$$I^*(t) = \begin{cases} 0 & \text{for } t \leq t_a^* \\ I_A^*(t) & \text{for } t_a^* \leq t \leq t_c^* < 150 \\ I(1)t^{-1.2} & \text{for } t_c^* < t \end{cases} \quad (B-11)$$

where t_a^* is the alternative time of arrival and t_c^* is the corresponding time of deposition cessation. In this case ERD function for $t \geq 150$ is:

$$D_R^*(t) = W(t-150) \int_0^{150} I_A^*(x) dx + \int_{150}^t W(t-x) I(1) t^{-1.2} dx \quad (B-12)$$

The desired correspondence is obtained by setting $D_R(t)$ equal to $D_R^*(t)$, which results in the following expression:

$$\int_0^{150} I(x) dx = \int_0^{150} I_A^*(x) dx \quad (B-13)$$

This expression in Appendix A is reduced to:

$$t_a^{-.2} = \frac{1}{4.41 I(1)} \int_{t_a^*}^{t_c^*} I_A^*(x) dx + 1.13 t_c^*{}^{-.2} \quad (B-14)$$

This equation establishes the proper correspondence between times of arrival t_a used in the subsequent analysis and times of arrival t_a^* of alternative types of buildup functions, $I^*(t)$. Using this correspondence, examples of which are presented in Appendix A, the subsequent results may be applied to intensity functions using other types of buildup functions.

C. Weighting Function

The weighting function $W(t)$ used to account for biological repair and recovery is given in References B-1 and B-2 as follows:

$$W_1(t) = .1 + .9 e^{-.001t} \quad (B-15)$$

This function is shown as curve $W_1(t)$ in Figure B-2 along with an approximation that will be used in the following analysis:

$$W(t) = .1 + .9 (1 - .00085t) \quad (B-16)$$

This approximation will only be used when its value is within two per cent of $W_1(t)$. That is, $W(t)$ as given in Equation B-16 will be used when:

$$\left| W_1(t) - W(t) \right| \leq .02 W_1(t) . \quad (B-17)$$

This condition holds when t is between 0 and 400 hours. It will be seen that the maximum IRD occurs before time $t = 400$ hours if the time of arrival is less than 17 hours.

D. ERD Function without Decontamination

The equations developed in Sections B and C for $I(t)$ and $W(t)$ respectively, can now be incorporated into the general expression for ERD,

$$D_R(t) = \int_0^t W(t-x) I(x) dx .$$

First, substitute the expression for $W(t-x)$ given in Equation B-16 as follows:

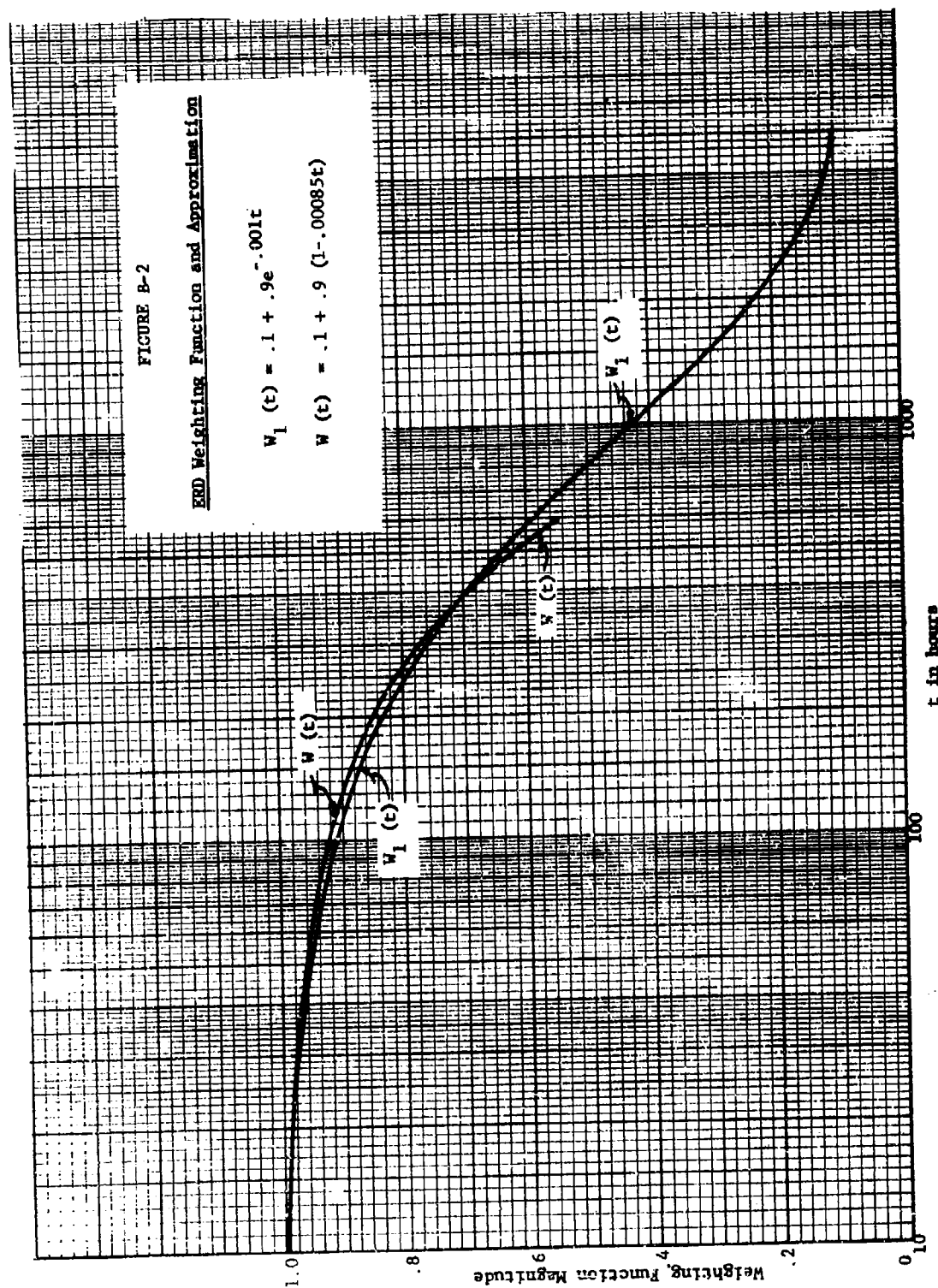
$$D_R(t) = \int_0^t \left[.1 + .9 (1 - \alpha(t-x)) \right] I(x) dx . \quad (B-18)$$

Second, substitute the expression given in Equation B-8 for $I(x)$ and evaluate the resultant expression for $t \geq 2.5 t_a$, as follows:

$$\begin{aligned} D_R(t) = & \int_{t_a}^{2.5 t_a} \left[.222 t_a^{-2.2} I(1) (x-t_a) \right] \left[.1 + .9 (1 - \alpha(t-x)) \right] dx \\ & + \int_{2.5 t_a}^t I(1) x^{-1.2} \left[.1 + .9 (1 - \alpha(t-x)) \right] dx . \end{aligned} \quad (B-19)$$

Integrating and dividing through by $I(1)$, this equation becomes, for $t \geq 2.5 t_a$,

$$\begin{aligned} \frac{D_R(t)}{I(1)} = & -5t^{-.2} (1-.0009563t) \\ & + 4.413 t_a^{-.2} (1-.000365t_a) \\ & - .003376t (t_a^{-.2}) . \end{aligned} \quad (B-20)$$



For comparison, the corresponding expression determined in Appendix A for total dose is:

$$\frac{D_T(t)}{I(1)} = -5t^{-.2} + 4.413t_a^{-.2} \quad (B-21)$$

These two equations B-20 and B-21 are presented in Figure B-3 to illustrate their behavior for selected times of arrival ($t_a = 1, 2, 4,$ and 8 hours).

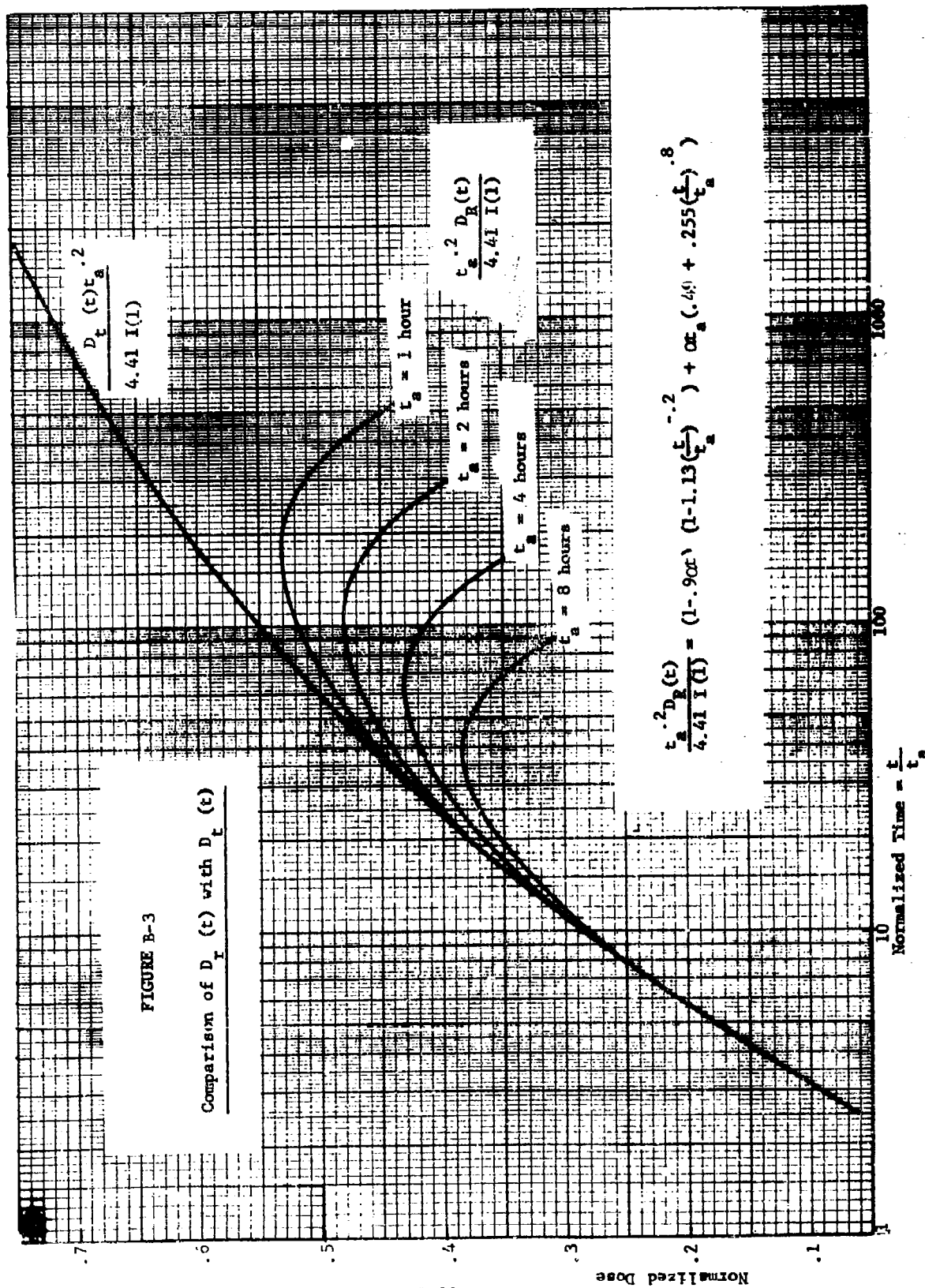
Although the subsequent analysis occasionally will be concerned with the general behavior illustrated in Figure B-3, primary interest is the time at which the ERD reaches a maximum, t_{\max} , and the value of the ERD maximum, $D_R(t_{\max})$. The behavior of t_{\max} as a function of t_a is determined by taking the derivative $\frac{d}{dt} D_R(t)$ and setting it equal to zero. This results in the following expression for t_{\max} :

$$t_{\max}^{-.2} + 262 t_{\max}^{-1.2} = .8825 t_a^{-.2} \quad (B-22)$$

A graph of this equation for t_a between .2 and 10 hours is presented in Figure B-4.

Equation B-22 (Figure B-4) and Equation B-20 can now be combined to show the maximum ERD, $D_R(t_{\max})$, as a function of time of arrival, t_a . The behavior of $D_R(t_{\max})$ is presented in Figure B-5 for times of arrival between .2 and 10 hours. From Figure B-5 the maximum ERD that an individual would experience can be determined for any predicted $I(1)$ and any time of arrival between .2 and 10 hours.

For the present, this concludes the basic analysis of ERD without decontamination. It will be extended later on in the analysis concerned with the effect of decontamination. Such extensions, when they occur, will



appear as the limit approached as the decontamination process becomes less and less effective. For the present it is sufficient to have obtained an expression for $D_R(t)$, Equation B-20, and to have examined the behavior of t_{\max} and $D_R(t_{\max})$, Figures B-4 and B-5 respectively.

III. ERD WITH DECONTAMINATION

The equations discussed in the preceding chapter were developed to describe the individual's maximum ERD as a function of the fallout intensity characteristics at the individual's location in the absence of any decontamination operations. In this chapter, the intensity function will be modified to include the effect of a decontamination operation (Section A). Then, in Section B, the ERD function will be redeveloped using the modified intensity function. Finally, in Section C, the maximum ERD with decontamination will be developed. By comparing this maximum ERD function with the maximum ERD function without decontamination (Chapter II) it will be possible to determine the effect on an individual's maximum ERD brought about by a decontamination operation.

Although the present discussion refers solely to decontamination operations, the equations and analysis apply to any operation that affects the intensity in a manner similar to that in which decontamination is assumed to affect the intensity.

A. Intensity Function with Decontamination

Decontamination has been referred to as "the action to reduce the dose rate in one area by removing the fallout contaminant from the area or by burying it within the area" (Reference B-1). In the subsequent

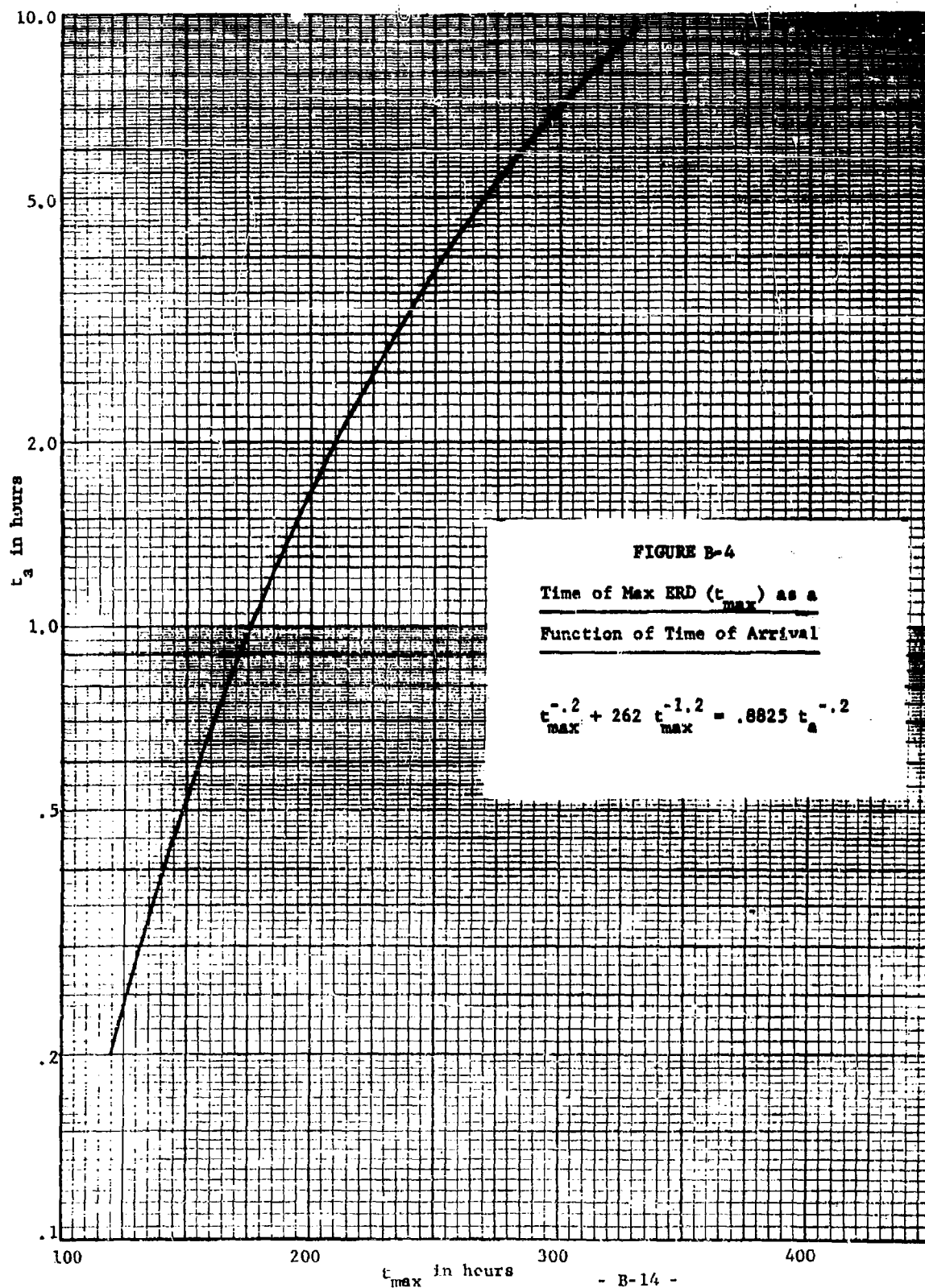
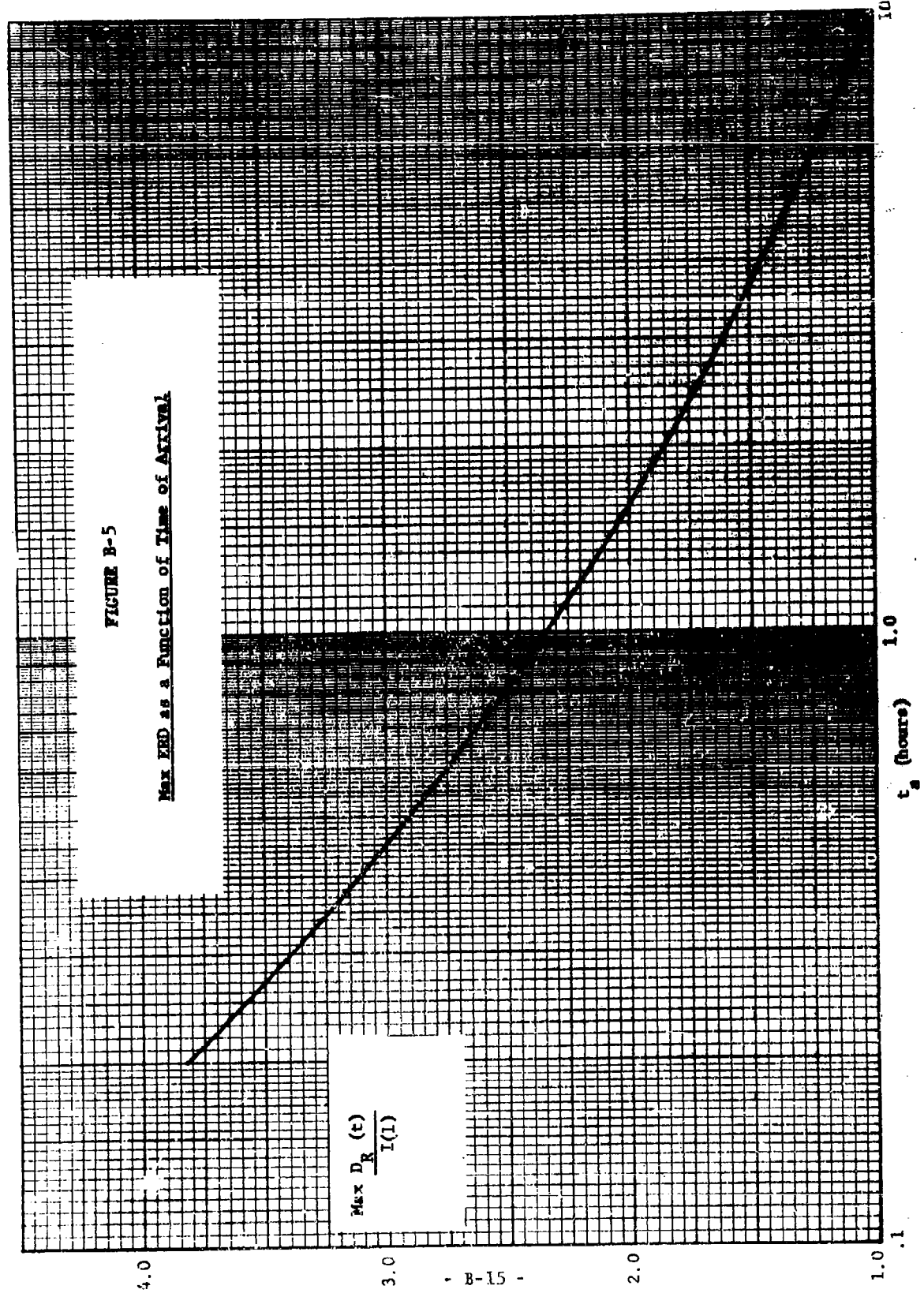


FIGURE B-5
Max EED as a Function of Time of Arrival



analysis, interest is restricted to the time at which the action takes place and to the reduction in intensity brought about by the action. In reality, such a reduction in intensity is achieved over some finite time interval required for the performance of the action. For the analysis in this paper, this process will be modeled by an idealized process whereby the reduction in intensity occurs instantaneously at time t_d where t_d is the time of decontamination in hours after detonation.* The intensity reduction brought about by the decontamination operation is called the decontamination effectiveness, f_d . If the intensity in the absence of any decontamination operation is $I(t)$ for $t \geq 0$ and if the intensity after decontamination is performed is $I_d(t)$ for $t \geq t_d$, then,

$$I_d(t) = f_d I(t) \quad (B-23)$$

for all t greater than t_d , the decontamination time. In the same sense that $I(t)$ is the intensity measured at the individual's location, the decontamination effectiveness, f_d , is measured at the individual's location, and in general, is not measured where the decontamination action actually takes place (i.e., outside the facility wherein the individual is located). In the analysis, f_d will vary between 0 (perfect decontamination) and 1 (completely ineffective decontamination). Furthermore, t_d will always be greater than $t_c = 2.5 t_a$ (time of deposition cessation) and, in this study, less than the time at which the individual's maximum ERD is reached.

*In Reference B-2, Chapter II, the problem of selecting a proper t_d to correspond to a real situation is discussed in detail. For the majority of cases, it is sufficient to select as t_d the center of the real process time interval.

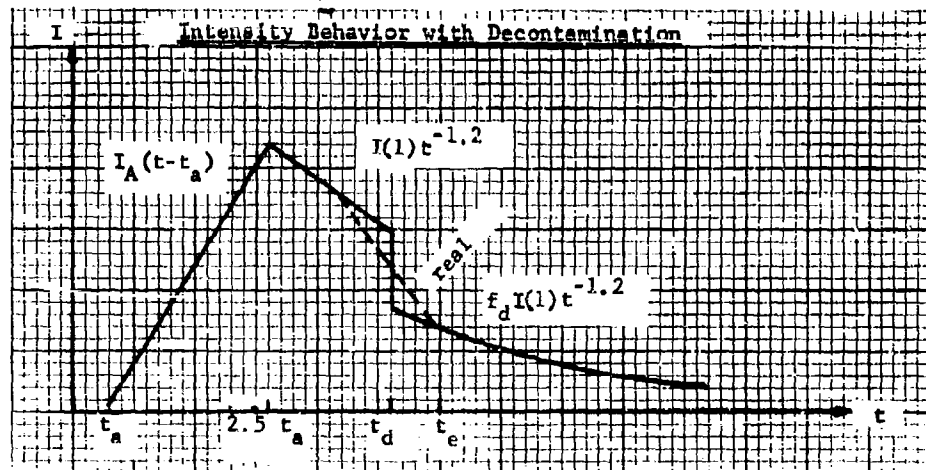
Obviously, if $t_d \geq t_{\max}$, then the decontamination operation does not affect the individual's maximum ERD.

Prior to the time of decontamination, t_d , the intensity at the individual's location is given by Equation B-8. After t_d , the intensity becomes f_d times the intensity given by Equation B-8. That is, if a decontamination operation whose effectiveness is f_d takes place at time t_d , then the appropriate intensity function, $I(t)$, is:

$$I(t) = \begin{cases} 0 & \text{for } 0 \leq t < t_a \\ .222 t_a^{-2.2} I(1) (t-t_a) & \text{for } t_a \leq t < 2.5 t_a \\ I(1)t^{-1.2} & \text{for } 2.5 t_a \leq t < t_d \\ f_d I(1)t^{-1.2} & \text{for } t_d \leq t \end{cases}$$

This behavior is illustrated in Figure B-6.

FIGURE B-6



In Figure B-6, a dotted line labeled "real" has been included to illustrate the effect on intensity behavior of a decontamination process that takes a finite time to conduct. The error in intensity that arises from the instantaneous action model, although significant in the intensity function, will be insignificant in the ERD function, $D_R(t)$, when t is greater than t_e shown in Figure B-6.

B. ERD Function with Decontamination

The general expression for ERD with decontamination can be developed by merely substituting the expression for $I(t)$ given in Equation B-24 into Equation B-2. This substitution results in the following equation for ERD with decontamination.

$$\begin{aligned}
 D_R(t, t_a, t_d, f_d) = & \int_{t_a}^{2.5t} W(t-x) .222 t_a^{-2.2} I(1) (x-t_a) dx \\
 & + \int_{2.5t_a}^{t_d} W(t-x) I(1)x^{-1.2} dx \\
 & + \int_{t_d}^t W(t-x) f_d I(1)x^{-1.2} dx .
 \end{aligned} \tag{B-25}$$

As in Equation B-18, the weighting function, $.1 + .9(1-.00085(t-x))$, which accounts for biological repair and recovery, next to substituted for $W(t-x)$ in Equation B-25. When this substitution is made and the expression is integrated, the ERD function, for $t \geq t_d$, reduces to:

$$\begin{aligned} \frac{D_R(t, t_a, t_d, f_d)}{I(1)} &= (4.413 t_a^{-.2}) (1 - .000365 t_a) \\ &- 5 f_d t_a^{-.2} (1 - .0009563 t) \\ &- .003376 t \left[t_a^{-.2} - 1.133 (1 - f_d) t_d^{-.2} \right]. \end{aligned} \quad (B-26)$$

On the basis of this equation, an individual's ERD can be determined for specified combinations of t_a , f_d , t_d , and t . The only restrictions are that t_a be less than 17 hours and that t_d be greater than $t_c = 2.5 t_a$. In the subsequent section, this ERD function will be examined to determine the behavior of the individual's maximum ERD. In Section IV, this maximum ERD as a function of t_d and f_d will then be compared with the maximum ERD that would be received without any decontamination for a set of selected times of arrival.

C. Maximum ERD with Decontamination

In this section the ERD function developed in the previous section is evaluated to determine the behavior of the individual's maximum ERD as a function of t_a , t_d , and f_d . To achieve this, first, an expression is derived to indicate the time of the maximum ERD, t_{max} , as a function of these variables. Next, the behavior of the expression involving t_{max} is analyzed and the actual time, t_{max} , is computed as a function of t_d for selected f_d 's and t_a 's. Finally, the maximum ERD is determined as a function of t_d for these selected f_d 's and t_a 's by substituting the appropriate combinations of t_{max} , f_d , t_d , and t_a into Equation B-26.

1. Derivation of Expression for Time of Maximum ERD

In order to compute the magnitude of the maximum ERD as a function

of t_a , t_d , and f_d from Equation B-26, it is first necessary to determine the time of maximum ERD, t_{\max} , as a function of these variables. The general behavior of t_{\max} as a function of t_a , t_d , and f_d is obtained by first differentiating Equation B-26. This derivative is as follows:

$$\frac{1}{I(1)} \frac{dD_R}{dt} = f_d \left[t^{-1.2} + .003825 t^{-.2} - .003825 t_d^{-.2} \right] - \left[.003376 t_a^{-.2} + .003825 t_d^{-.2} \right] \quad (B-27)$$

for $t_d \leq t$.

The expression for the time of the maximum ERD as a function of t_a , t_d , and f_d can be obtained for $t_d \leq t_{\max}$ by simply equating this derivative to zero and replacing t by t_{\max} . This results in the following expression:

$$f_d (t_{\max}^{-.2} + 262 t_{\max}^{-1.2}) = .8825 t_a^{-.2} - (1-f_d) (t_d^{-.2}) \quad (B-28)$$

where t_{\max} is the time in hours at which the ERD is a maximum.

2. Behavior of the Time of Maximum ERD

Before numerically evaluating t_{\max} in Equation B-28 as a function of f_d , t_d , and t_a , it is worthwhile to observe the behavior of t_{\max} when f_d and t_d are allowed to vary and t_a is held invariant. This operation is necessary because Equation B-28 does not produce the correct t_{\max} for certain combinations of f_d and t_d . The reason

for this may be seen in Equation B-26. Equation B-26 is only valid for $t \geq t_d$. Therefore, Equation B-27 is only valid for $t \geq t_d$ and Equation B-28 is only valid for $t_{\max} \geq t_d$. Although mathematically valid for $-\infty < t_{\max} < \infty$ and therefore all f_d, t_d combinations, Equation B-28 only applies to the physical situation when $t_{\max} \geq t_d$. Therefore, it is useful to examine the behavior of t_{\max} as a function of t_d and f_d and to determine the range of t_d, f_d combinations such that t_{\max} can be determined from Equation B-28.

When Equation B-28 is a valid expression for t_{\max} , it can be seen that:

- (1) for fixed f_d , as t_d increases, t_{\max} decreases, and
- (2) for fixed t_d , as f_d decreases, t_{\max} decreases.

These two observations lead to the behavior of t_{\max} as a function of t_d and f_d as follows:

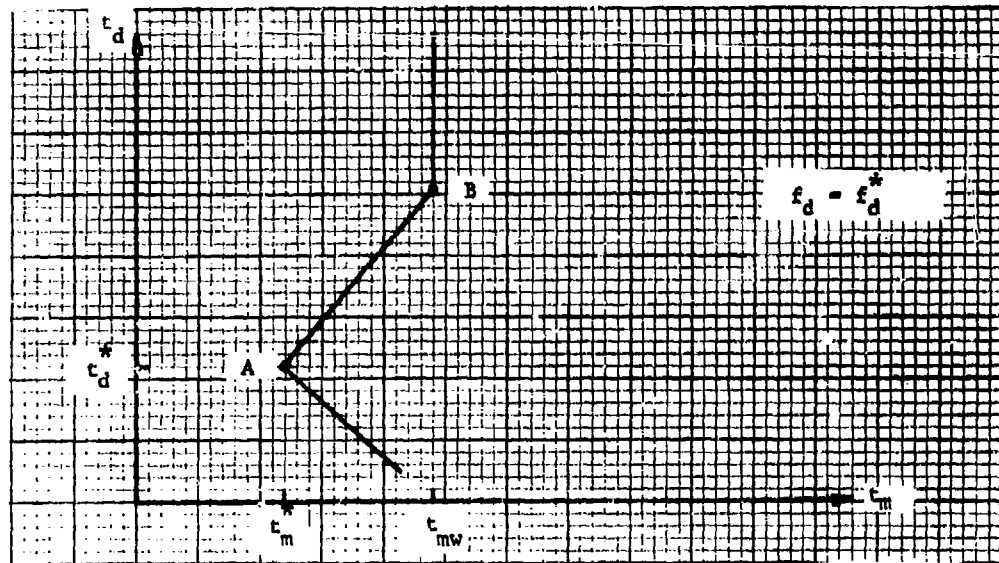
- (1) First, fix f_d at f_d^* and examine $t_{\max}(t_d)$ (see Figure B-7).

As t_d increases, t_{\max} decreases until Point A is reached when $t_d = t_{\max}$. Denote this time of maximum (i.e., minimum t_{\max} such that $t_d = t_{\max}$) by t_{\max}^* and this t_d by t_d^* . Therefore, at Point A, $t_d^* = t_{\max}^* = t_{\max}^*$. As t_d increases beyond t_d^* , t_{\max} also increases at the same rate until Point B is reached. That is, along the path AB, t_{\max} is equal to t_d . At Point B, t_{\max} is the same as the time of maximum without decontamination. Denote this time of maximum by t_{mw} . When t_d is greater than t_{mw} , the maximum will not be affected by the decontamination operation because the maximum was reached

before t_d . Therefore, as t_d increases beyond t_{mw} , t_{max} remains equal to t_{mw} .

FIGURE B-7

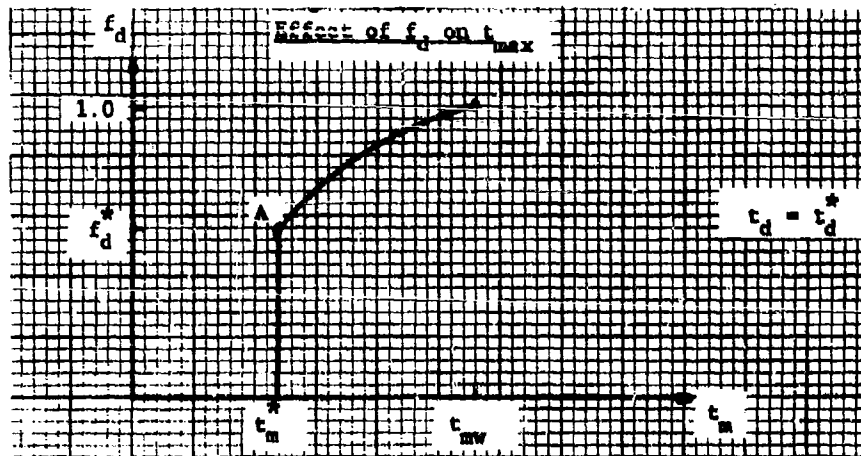
Effect of t_d on t_{max}



(2) Second, fix t_d at t_d^* and examine $t_{max}(f_d)$ (see Figure B-8).

When $f_d=1.0$, the decontamination operation is completely ineffective and t_{max} occurs at t_{mw} as it would in the absence of any decontamination. As f_d decreases from 1.0, t_{max} decreases until Point A is reached. Point A is the place where t_{max} becomes equal to t_d^* . Denote this time of maximum (i.e., minimum t_{max} such that $t_{max}=t_d^*$) by t_{max}^* and this f_d by f_d^* . As f_d decreases below f_d^* , t_{max} remains unchanged and equal to t_{max}^* .

FIGURE B-8



The important aspects to be inferred from these illustrations are:

- (1) For a given t_a and a pre-selected t_d , called t_d^* , there is an f_d^* such that for any $f_d \leq f_d^*$ neither the time nor the magnitude of the maximum ERD will be decreased below that achieved by using f_d^* . For any $f_d > f_d^*$ the maximum ERD can be reduced by applying a more effective f_d .
- (2) For a given t_a and a pre-selected f_d , called f_d^* , there is a t_d^* such that for any $t_d \geq t_d^*$, the time and magnitude of the maximum ERD will be the same as the time and magnitude of the ERD at the moment when the decontamination operation takes effect (t_d).

Then f_d^* , t_d^* combinations can be determined by setting $f_d = f_d^*$ and $t_{\max} = t_d = t_d^*$ in Equation B-28 (which gives t_{\max} as a function of t_a , t_d , and f_d). This substitution results in the following equation for f_d^* .

$$f_d^* = \frac{.8825 t_a^{-.2} - t_d^{*-2}}{262 t_d^{*-1.2}} \text{ for } t_d^* \geq 2.5 t_a \quad (B-29)$$

Thus, this equation represents the lowest value of f_d (that is, f_d^*) that must be considered in determining the time and magnitude of maximum ERD for any combination of $t_d = t_d^*$ and t_a . It will be used in the subsequent section to establish boundaries in evaluating t_{\max} as a function of t_a , t_d , and f_d . In addition, from an operational standpoint, the f_d^* represents the most effective f_d for a given t_a and t_d^* . That is, any f_d above the f_d^* indicated by this equation for a given t_a and t_d^* will result in a higher maximum ERD. Any better (smaller) f_d will not reduce the maximum ERD below that achieved by using f_d^* . This equation is graphed in Figure B-9 which gives f_d^* as a function of t_d^* for selected t_a 's of 1, 2, 3, 5, 7 and 9 hours.

3. Solution for t_{\max}

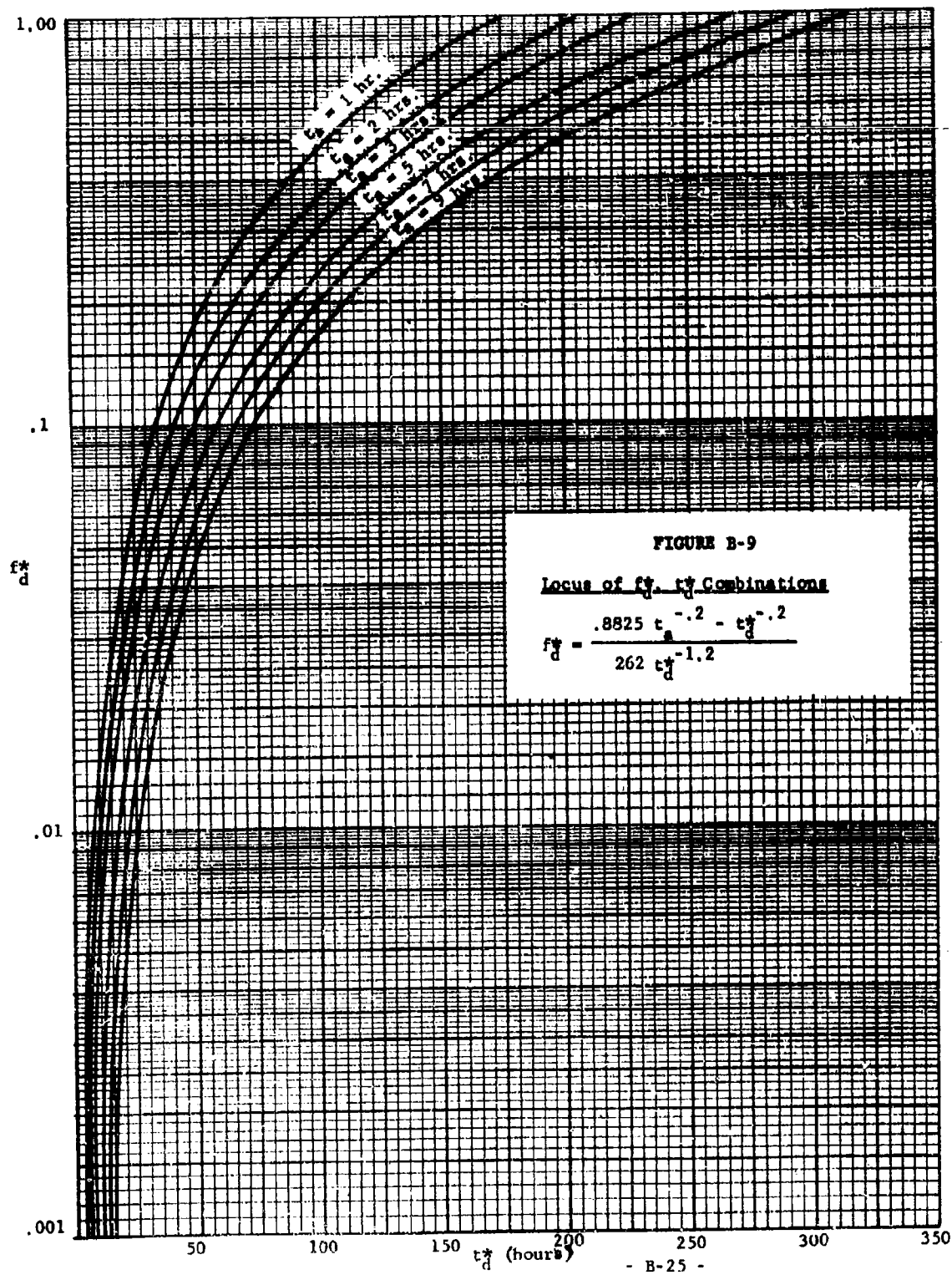
As previously mentioned, t_{\max} can be determined for various t_a , and t_d , and f_d combinations from Equation B-28 for $t_d \leq t$. The only other constraints that have been placed on the operation are that $t_d \geq 2.5 t_a$ and $t_a \leq 17$ hours. For the purpose of this analysis t_{\max} is determined as a function of t_d for selected t_a 's and f_d 's in the following manner.

The right side of Equation B-28 can be expressed as

$$x = .8825 t_a^{-.2} - (1-f_d) t_d^{-.2} \quad (B-30)$$

and similarly the left side can be expressed as,

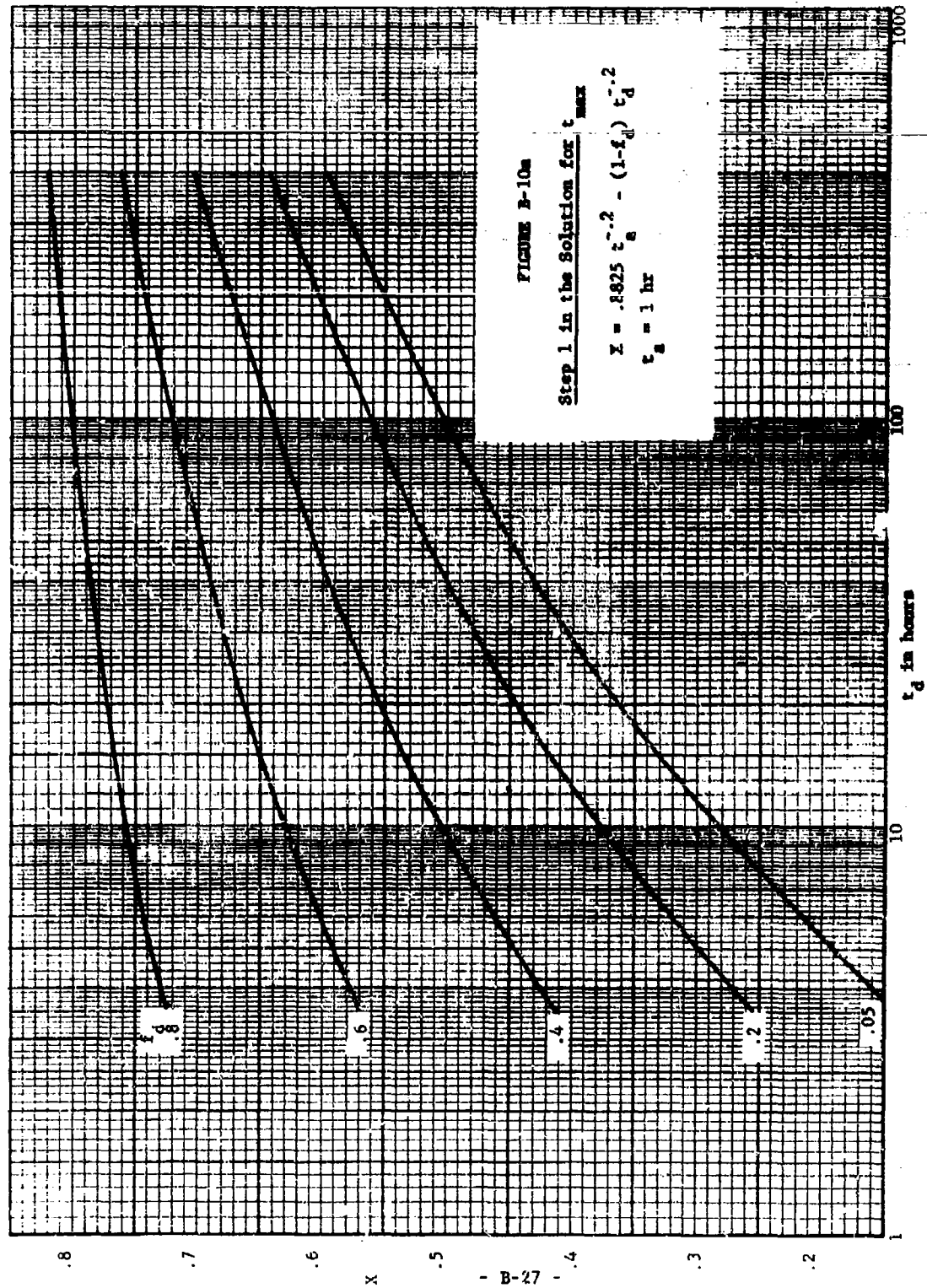
$$x = f_d (t_{\max}^{-.2} + 262 t_{\max}^{-1.2}) \quad (B-31)$$

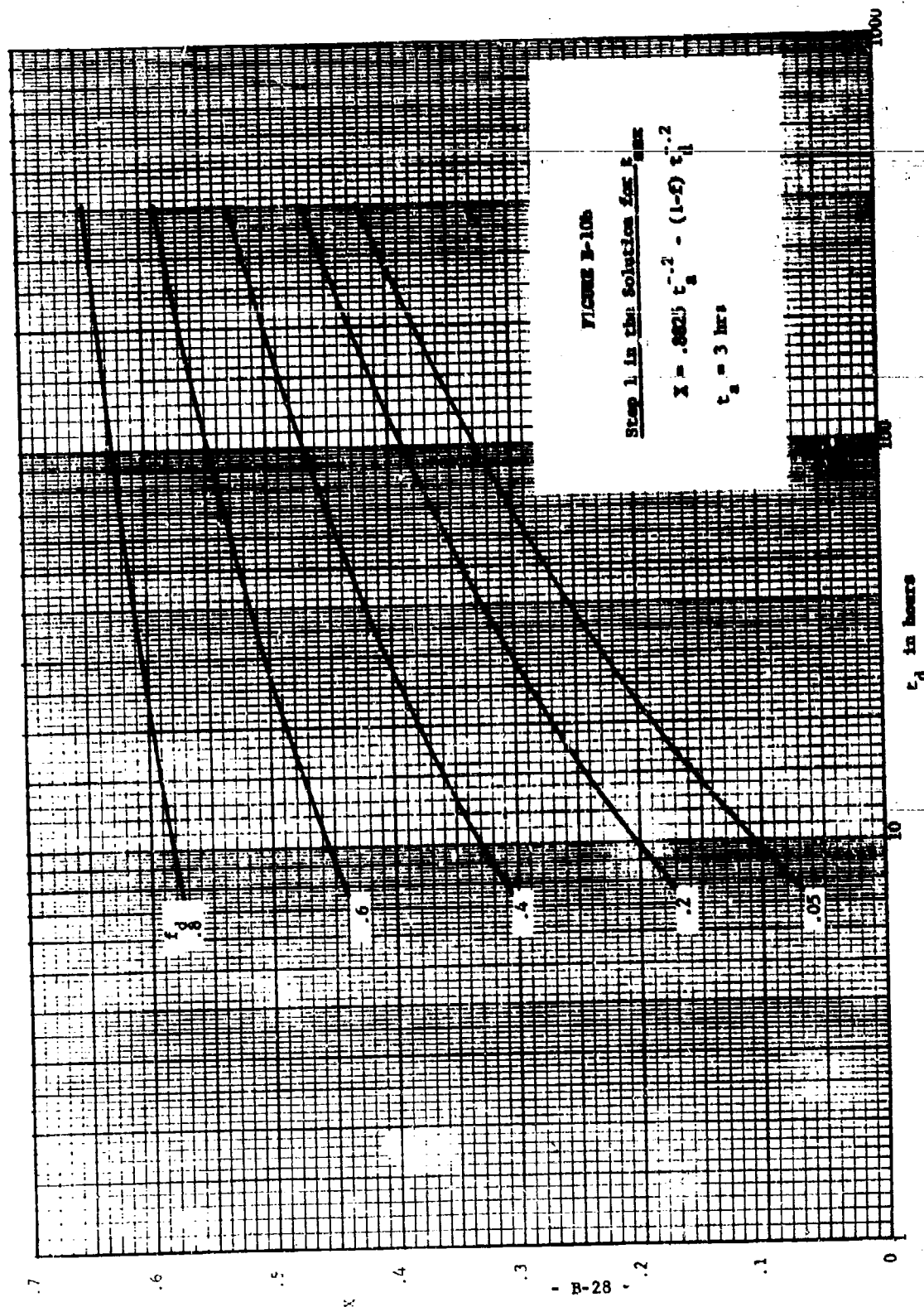


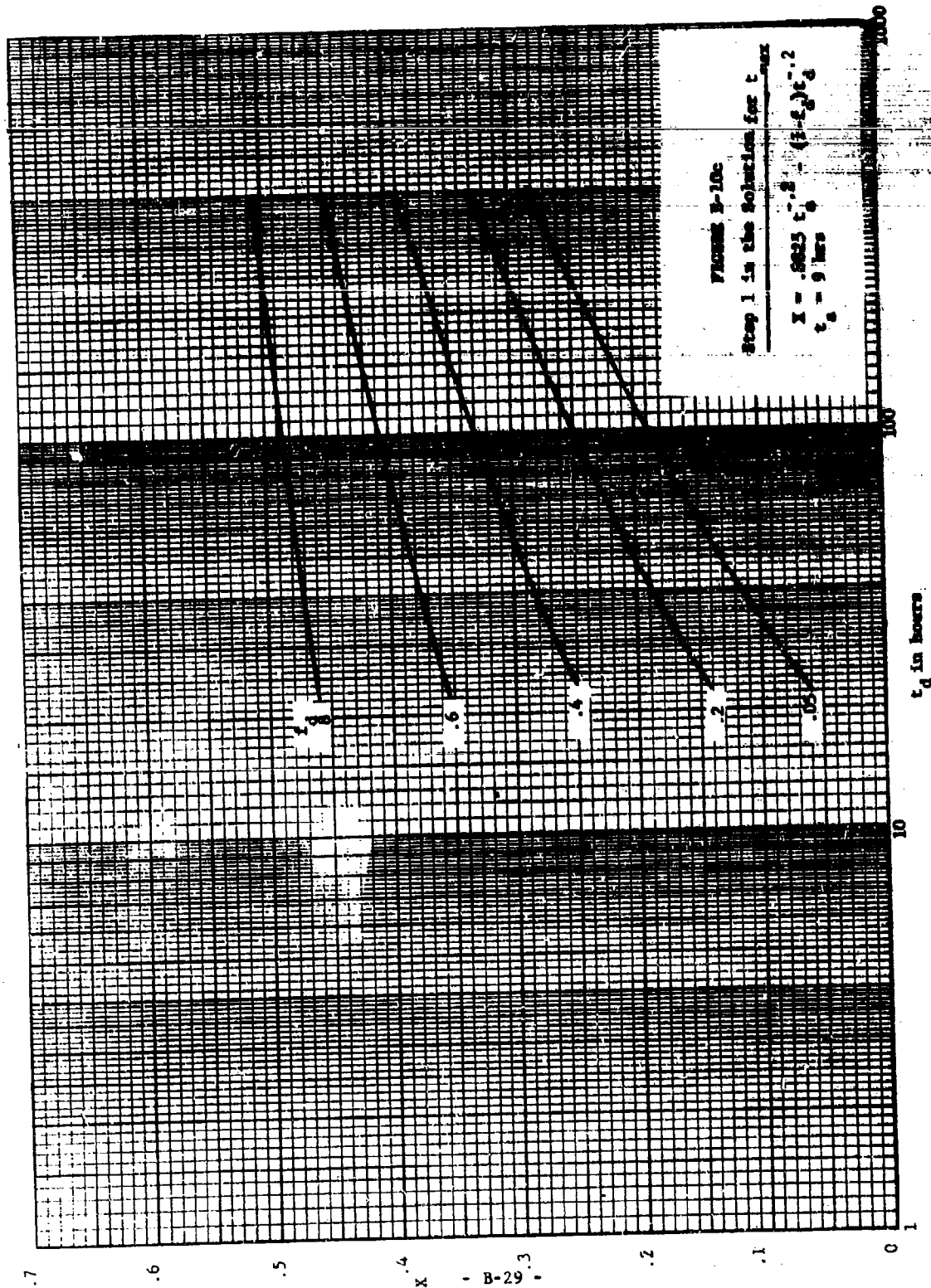
By fixing t_a in Equation B-30, t_d can be graphed as a function of x for selected f_d 's. Figures B-10a, B-10b, and B-10c show x as a function of t_d for f_d 's of .05, .2, .4, .6, and .8 for t_a 's of 1, 3, 9 hours respectively. From Equation B-31, t_{\max} also can be graphed, as is done in Figure B-11, as a function of x for the same f_d 's. From Figures B-10a, B-10b, and B-10c, the value of x corresponding to a fixed t_a and the desired combination of f_d and t_d can be determined. The t_{\max} corresponding to this combination can then be determined by locating this value of x in Figure B-11 for the same f_d , and then reading the appropriate t_{\max} .

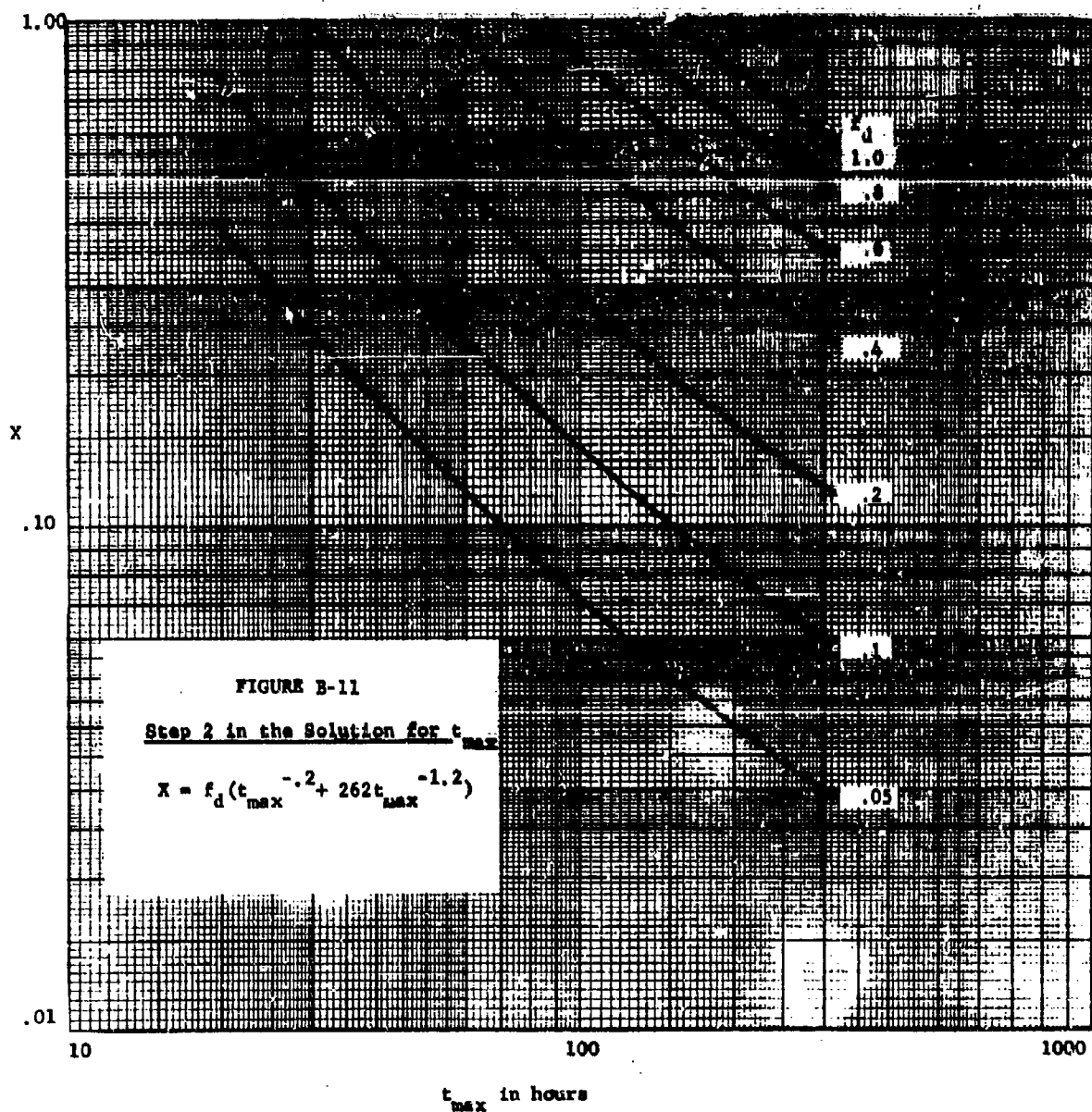
To assure that the pre-selected t_d is less than or equal to t_{\max} for the particular f_d of interest, Equation B-29 or Figure B-9 must be used. As previously discussed, the f_d^* given by this equation represents the minimum value of f_d that must be considered for a given t_d . Therefore to assure that the selected $t_d \leq t_{\max}$ for the desired f_d , f_d must be equal to or greater than f_d^* for that t_d . This can readily be determined from Figure B-9 for selected cases. For example, if $t_a=1$ and the selected t_d is 50 hours, then $f_d^* = .18$. For any $f_d \leq f_d^*$ for $t_d = 50$ hours, t_{\max} will be equal to t_d . Therefore only those $f_d \geq .18$ should be considered for a t_d of 50 hours and t_a of 1 hour.

Through the use of the above procedure, t_{\max} as a function of t_d has been determined for various f_d 's and t_a 's. The results are summarized in Figures B-12a, B-12b, B-12c, for $t_a = 1, 3, 9$ hours respectively. In each of these figures, t_{\max} is given for a fixed t_a as a function of t_d for f_d 's of 0, .05, .2, .4, .6 and .8. Both





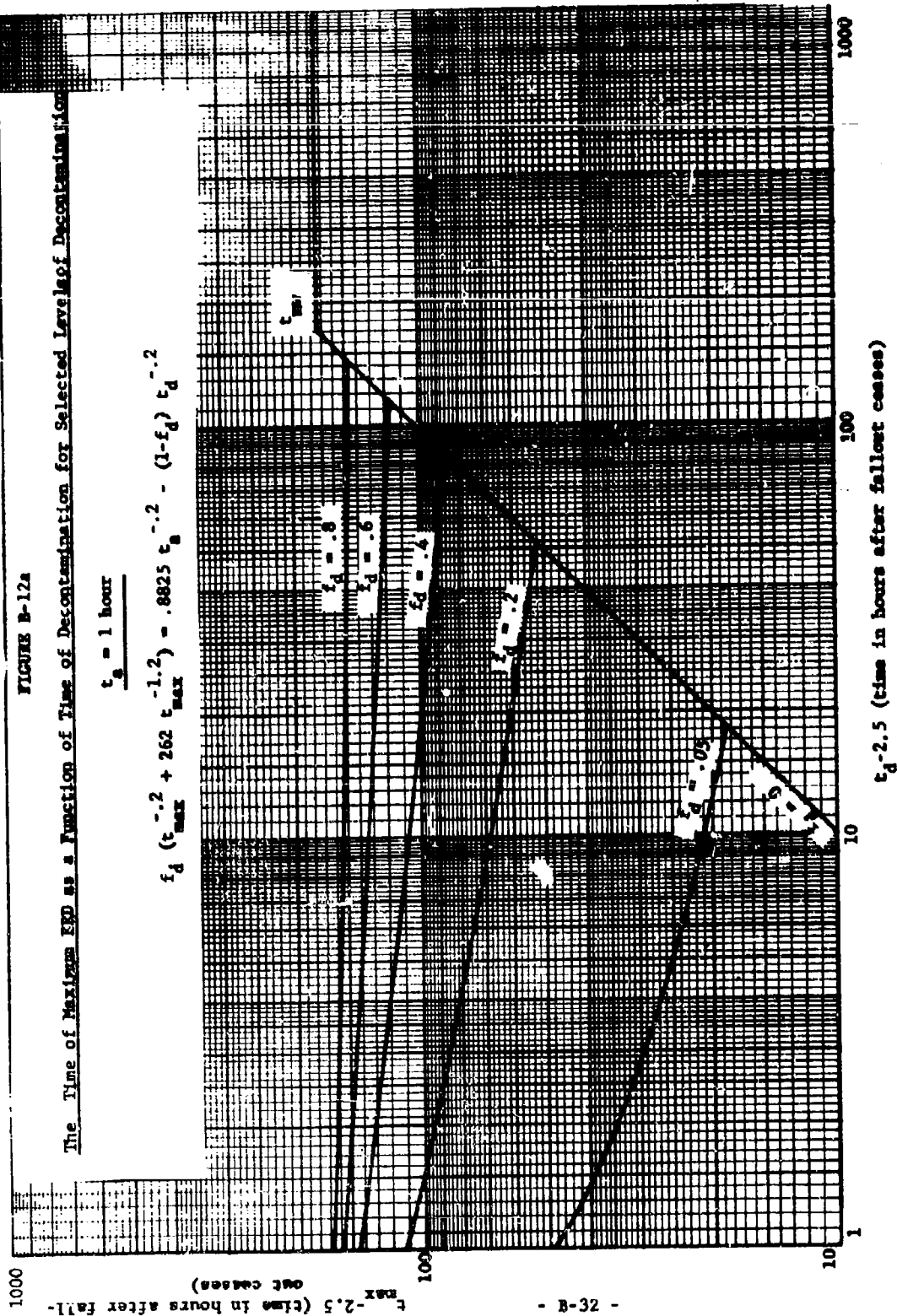




t_{\max} and t_d are expressed in hours after the time that deposition of fallout ceases (i.e., $t_{\max} = 2.5 t_g$ and $t_d = 2.5 t_a$). The $f_d = 0$ curves in these figures were derived by simple application of the fact that when all fallout is removed at a given t_d , the maximum ERD will occur at that t_d . That is, for all points on the $t_d = 0$ curves $t_d = t_{\max}$. The point of intersection of a given $f_d > 0$ curve with the $f_d = 0$ curve indicates that if decontamination is delayed until this time, any smaller f_d would not decrease the maximum ERD.

4. Computation of Maximum ERD

The magnitude of the maximum ERD can be computed by substituting the desired combinations of t_a , t_d , and f_d into Equation B-26 along with their corresponding t_{\max} 's. These t_{\max} 's as previously discussed are given as a function of t_d by Figures B-12a - B-12c for selected t_a 's and f_d 's. Equation B-26 has been evaluated for selected t_a 's and f_d 's. These results are graphically summarized in Figures B-13a, B-13b, and B-13c in the next section. The maximum ERD without decontamination is presented as a function of t_d for (right-hand scale) $t_a = 1, 3$, and 9 and $f_d = 0, .2, .4, .6$ and $.8$ for each t_a . Since $I(1)$ has been normalized, these curves allow computation of maximum ERD for any combination of $I(1)$ and PF as long as the individual remains in the same fallout field and at the same PF in which he first began accumulating radiation dose.



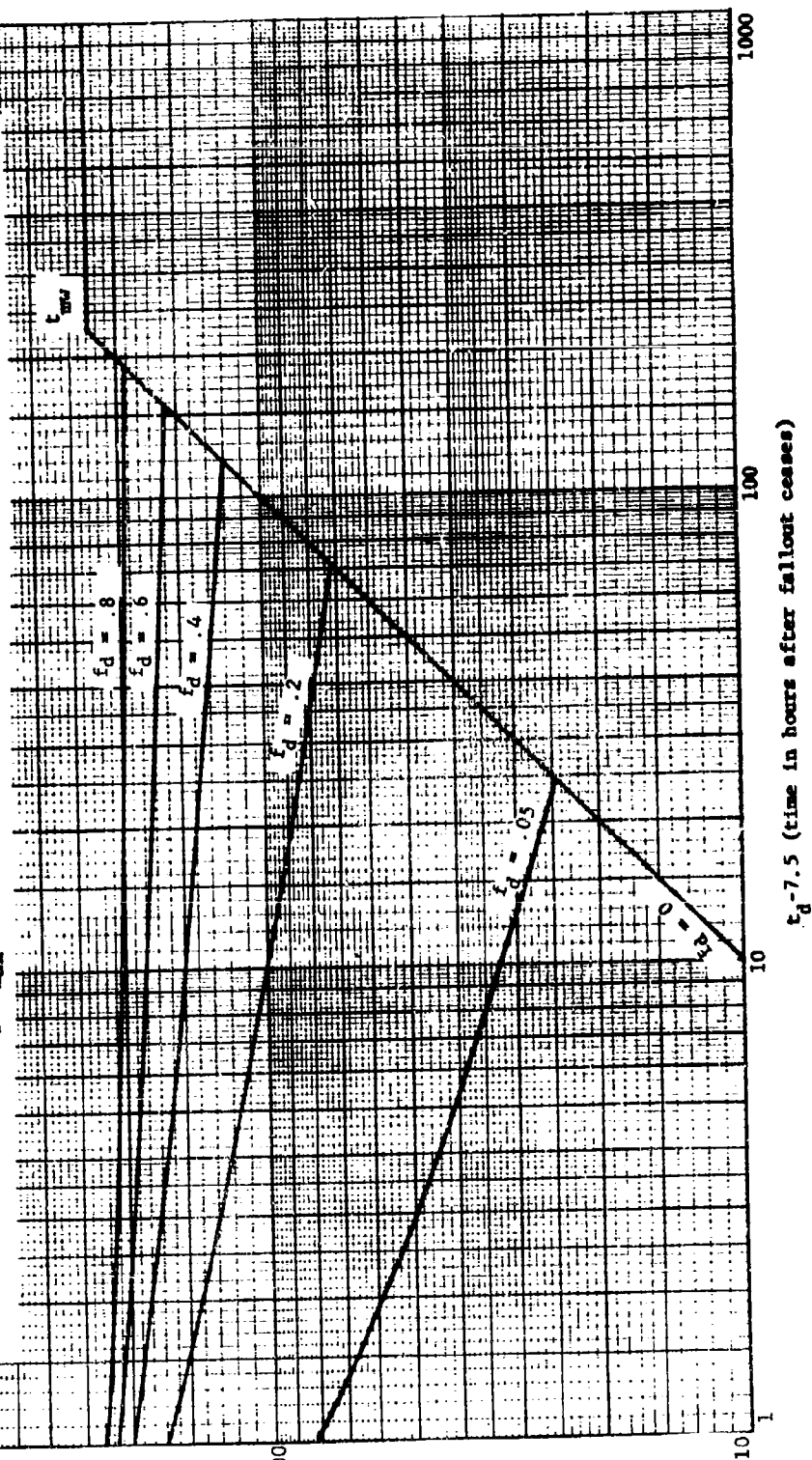
$t_{\max}^{-7.5}$ (time in hours after fallout ceases)

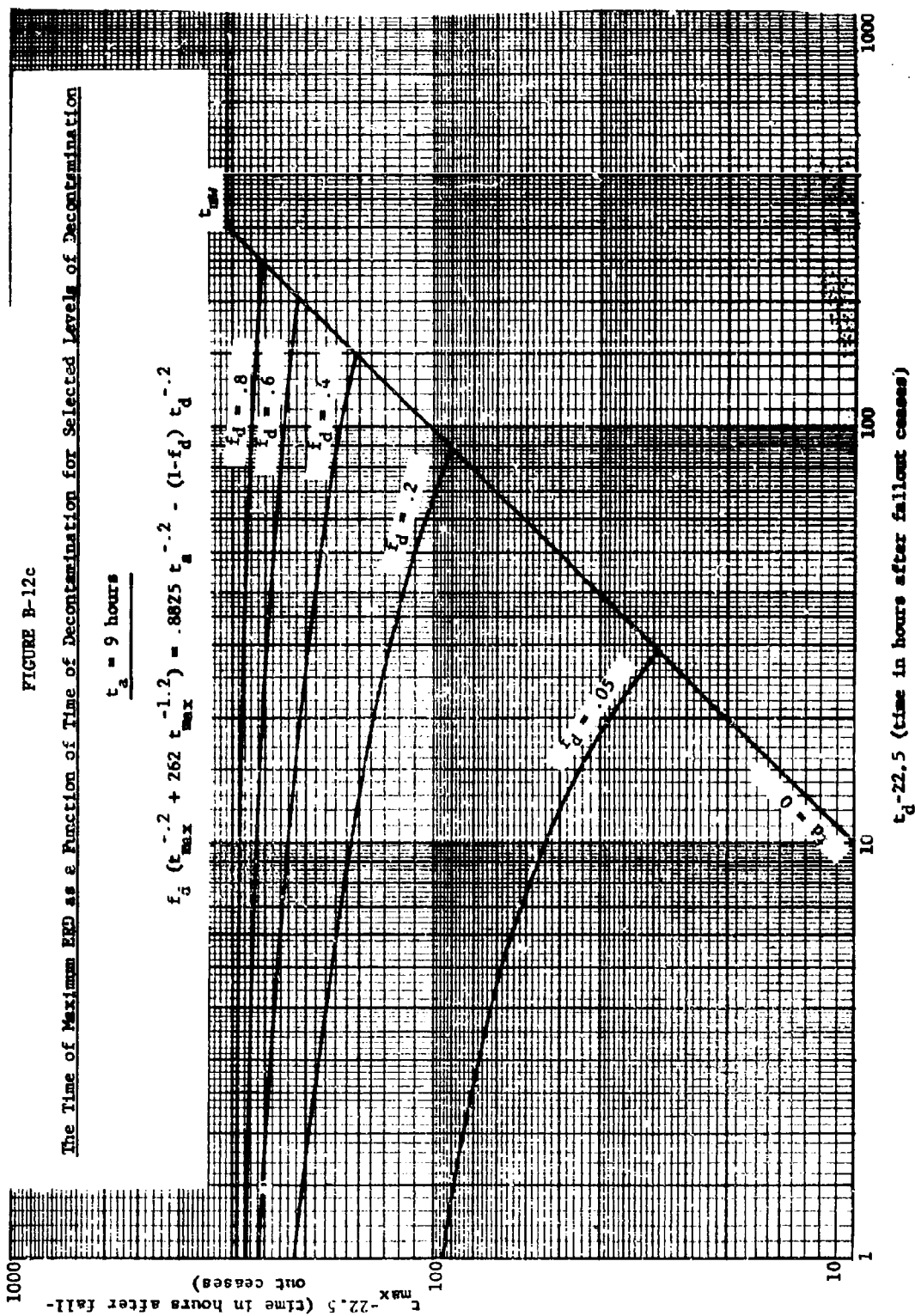
FIGURE B-12b

The Time of Maximum ERD as a Function of Time of Decontamination for Selected Levels of Decontamination

$$t_a = 3 \text{ hours}$$

$$f_d (t_{\max}^{-1.2} + 262 t_{\max}^{-1.2}) = .8825 t_a^{-.2} - (1-f_d) t_d^{-.2}$$





IV. REDUCTION IN ERD DUE TO DECONTAMINATION

A. Introduction and Derivation

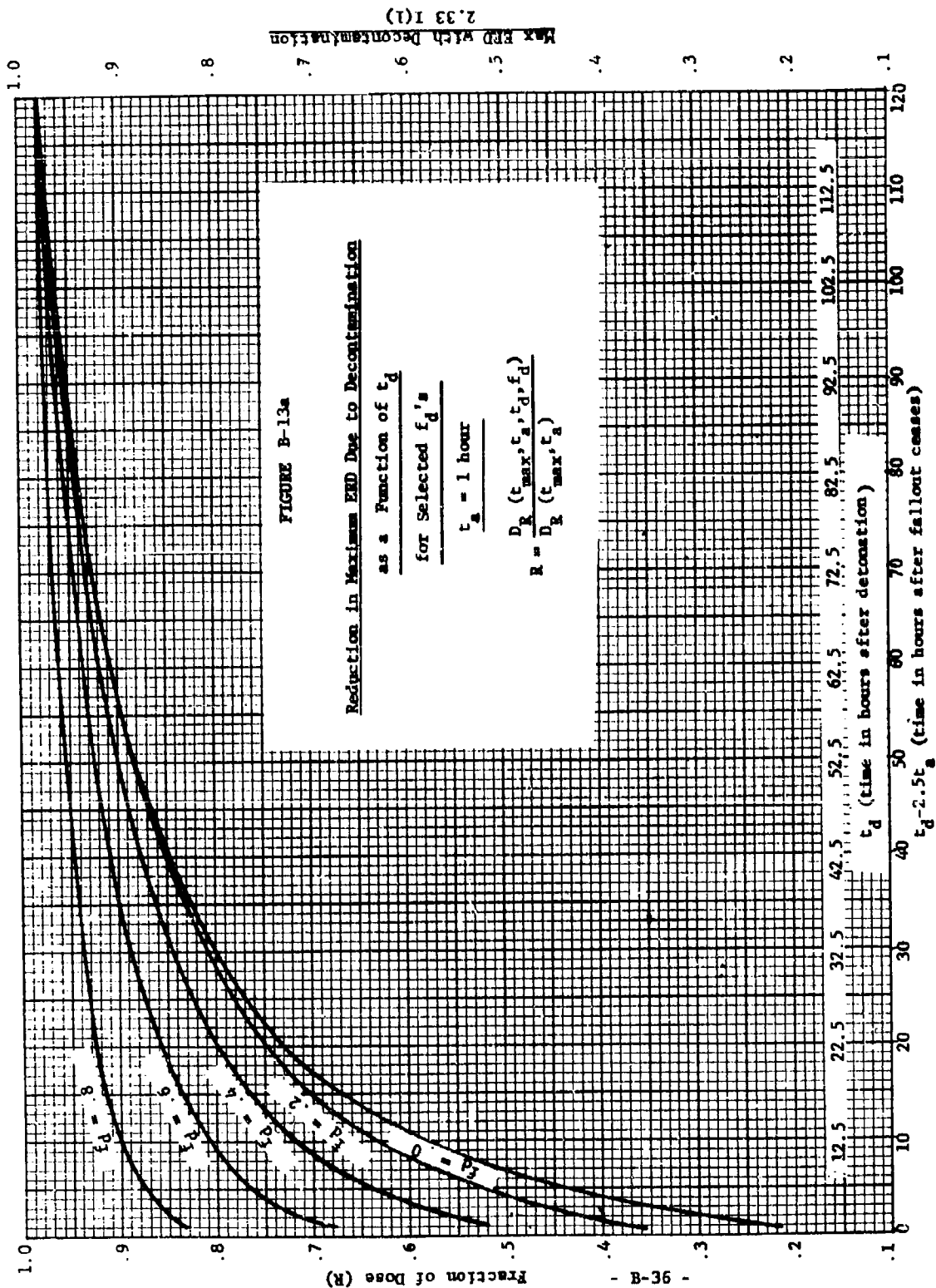
The previous derivations and evaluations of the ERD with and without decontamination provide a basis for ascertaining the value of decontamination (or similar operations) in reducing potential dose as a function of t_a , t_d , and f_d . This value can be conveniently measured by forming the ratio of the maximum ERD with decontamination to that with no decontamination, as follows:

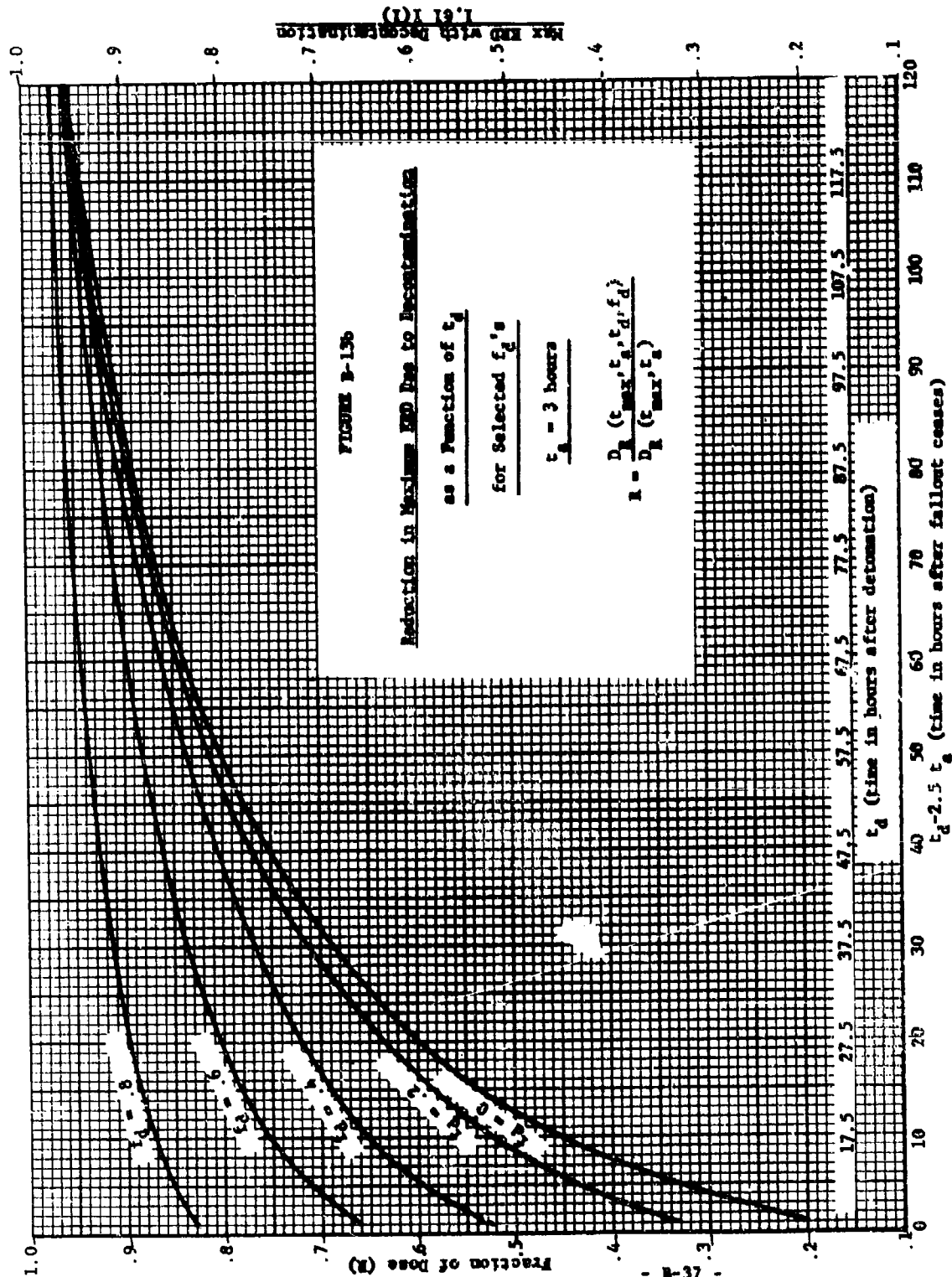
$$R = \frac{\text{max ERD with decontamination}}{\text{max ERD without decontamination}} = \frac{D_R(t_{\text{max}}, t_a, t_d, f_d)}{D_R(t_{\text{max}}, t_a)} \quad (\text{B-32})$$

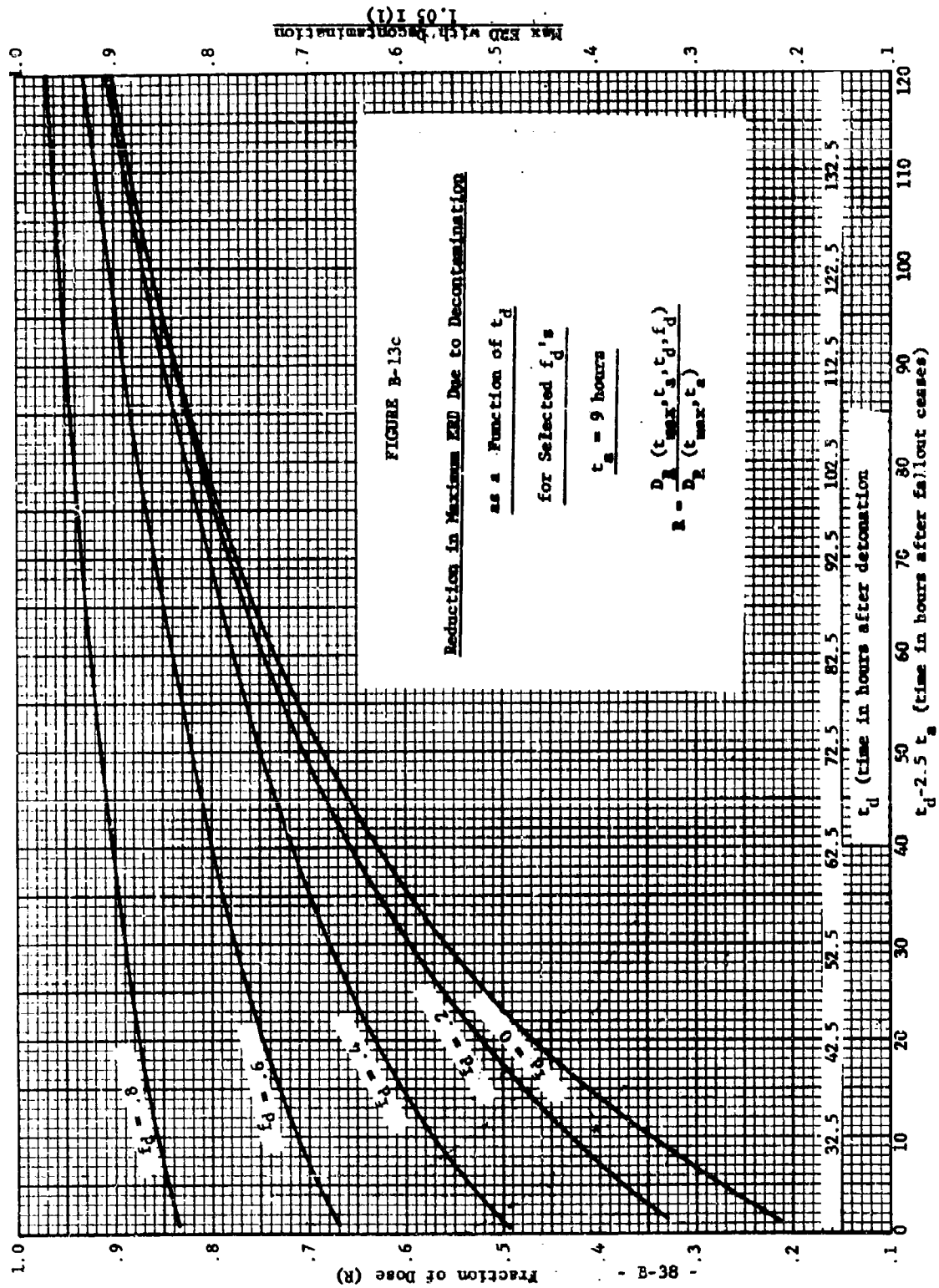
where R is denoted as the value ratio. The evaluation of R is given by appropriately combining the results of Sections II and III.

More specifically, the maximum ERD without decontamination, $D_R(t_m, t_a)$, is given as a function of t_a when Equations B-20 and B-22 are properly combined and evaluated at the time of maximum ERD without decontamination. The analogous results for the maximum ERD with decontamination, $D_R(t_m, t_a, t_d, f_d)$, are given by Equations B-26 and B-28 as a function of t_a , t_d , and f_d . By evaluating these expressions, the value of decontamination in reducing dose is obtainable. For this analysis R will be evaluated as a function of t_d for those t_a 's and f_d 's for which the numerator and denominator of Equation B-32 have previously been determined in Sections II and III.

The summarized results for R , determined by combining the values of maximum ERD from the right-hand scale of Figures B-13a, B-13b, and B-13c with those of Figure B-3, are presented in Figures B-13a, B-13b, B-13c (left-hand scale). The reduction in ERD due to decontamination is given as a function







of t_d and for $f_d = 0, .2, .4, .6, \text{ and } .8$ for each t_a ($t_a = 1, 3, \text{ and } 9$ hours). This reduction is expressed in terms of the fraction of the dose that would be received if decontamination is activated. Time of decontamination is given both as time after detonation (t_d) and time after the time at which fallout deposition ceases ($t_d - 2.5 t_a$).

B. Discussion of Results

Primarily, these results allow a simple and "uncluttered" view of the effectiveness of decontamination in reducing radiation dose (ERD) over most of the spectrum of important environmental parameters. In addition, they indicate the precise trade-offs between these parameters for a specified fractional reduction in ERD. For example, for t_a of 1 hour, f_d of .6, activated at 24 hours after cessation of fallout is equivalent to f_d of zero at 47 hours (estimated from Figure B-13a).

In interpreting these results it is worthwhile to bear in mind that they are applicable not only to decontamination, but any countermeasure which reduces the intensity in the same manner, (i.e., when the countermeasure affects the intensity the same as the defined f_d herein). It should be noted that these mathematical results are independent of the level of initial intensity considered for the individual or the PF of the shelter in which he is located when he begins to accumulate dose. For practical application, however, the ERD must remain below 200 R. It is also assumed that he remains in the same location throughout the time of interest (i.e., he remains in the same inside intensity field as the one in which he first began accumulating any dose).

APPENDIX B REFERENCES

- B-1 J. F. Devaney. Operations in Fallout. OCDM-SA-61-13. Washington: Office of Civil Defense Mobilization, June 1961.
- B-2 National Committee on Radiation Protection and Measurements. Exposure to Radiation in an Emergency. Report No. 29, Chicago: University of Chicago, Department of Pharmacology, Section of Nuclear Medicine, January 1962.

Appendix C

Total Dose Approximations for
Brief Exposure in a Fallout Environment

This Appendix was originally submitted to OCD as Research Memorandum RM 156-4,* except for minor editorial changes.

* J. D. Douglass, Jr. Calculating the Total Dose Received During a Brief Exposure in a Fallout Environment. Research Memorandum RM 156-4. Durham, North Carolina: Research Triangle Institute, Operations Research Division, 23 March 1964.

Appendix C

Total Dose Approximations for Brief

Exposure in a Fallout Environment

I. INTRODUCTION AND SUMMARY

A. Total Dose Expression

The modeling and analysis of operations in a fallout environment often requires an expression for the total dose received by an individual over a finite interval of time. When the individual is located in a facility whose protection factor is PF, the rate at which he accumulates dose is given by the expression

$$I(t) = \frac{I(1)}{PF} t^{-k} \text{ roentgens/hour} \quad (C-1)$$

where t is the time after detonation in hours, k is the decay constant (usually set equal to 1.2), and $I(1)$ is the $t = 1$ reference dose rate in the fallout field where the facility is located. The total dose received by an individual during the time he is in the facility is normally obtained by integrating the dose rate over this same period of time. If the individual is in the facility from time t_e to time $t_e + \Delta t$, then the dose received is

$$\begin{aligned} D(t_e, \Delta t) &= \int_{t_e}^{t_e + \Delta t} I(t) dt \\ &= \frac{I(1)}{PF} \frac{1}{k-1} (t_e^{1-k} - (t_e + \Delta t)^{1-k}) \text{ roentgens} \quad (C-2) \end{aligned}$$

where $k > 1$ is assumed. Although the process used to obtain this expression for total dose is simple, the expression itself is quite cumbersome for

many applications (for example, in determining t_e as a function of $I(1)$, PF, k, Δt , and the total dose, D).

Many difficulties associated with the expression for total dose given in Equation C-2 can be eliminated by using an appropriate approximation for the total dose received. This study considers two approximations that eliminate some of the difficulties. The two approximations that will be considered are illustrated in Figure C-1. For comparison, the "true" total dose is also illustrated in Figure C-1. It will be shown that the accuracy of both approximations depends on the size of the ratio $\frac{t_e}{\Delta t}$ and on the value of k. As the ratio increases, the accuracy increases. This study examines this accuracy of the two approximations in detail and presents several curves that illustrate the behavior of the error when $\frac{t_e}{\Delta t}$ and k are allowed to vary.

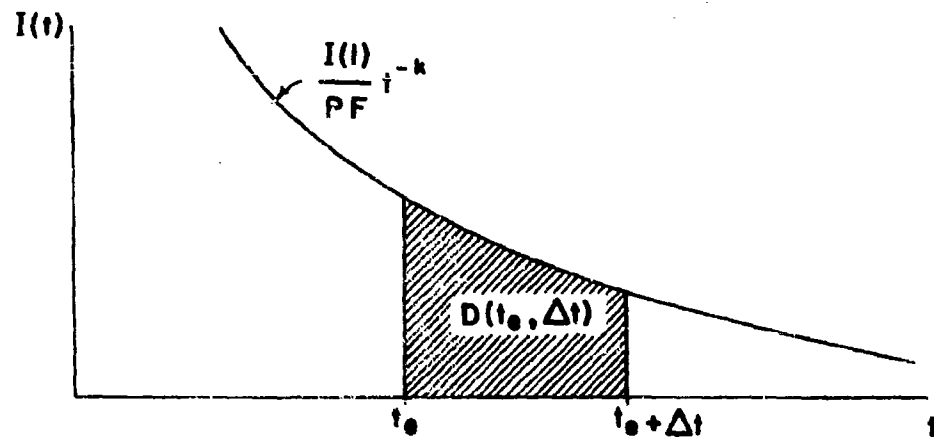
B. First Approximation

In the first example, the total dose received from time t_e to time $t_e + \Delta t$ is approximated by multiplying the duration of the exposure interval, Δt , by the dose rate at the center of the interval, $I(t_e + \frac{\Delta t}{2})$. If this approximation is called $D_1(t_e, \Delta t)$, then

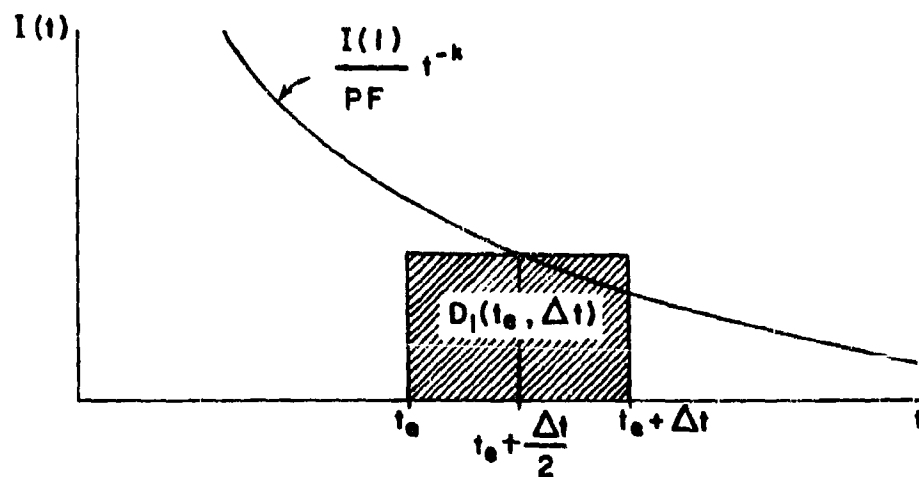
$$D_1(t_e, \Delta t) = \frac{I(1)}{PF} (t_e + \frac{\Delta t}{2})^{-k} \Delta t \text{ roentgens} \quad (C-3)$$

The error, $\delta_1 = \frac{D_1 - D}{D_1}$, that results when this approximation (Equation C-3) is used to determine the total dose is derived in Section II and the results are displayed in Figure C-2 as a function of the ratio $\frac{t_e}{\Delta t}$. In the derivation section it is shown that the resultant error δ_1 , decreases toward zero as the ratio $\frac{t_e}{\Delta t}$ increases. Therefore, when one is concerned with a range of

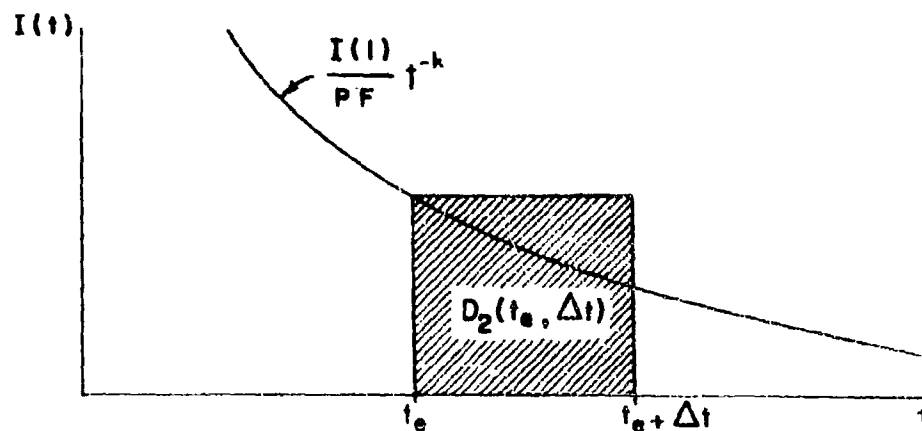
FIGURE C-1
Comparison of Total Dose and Approximations D_1 and D_2



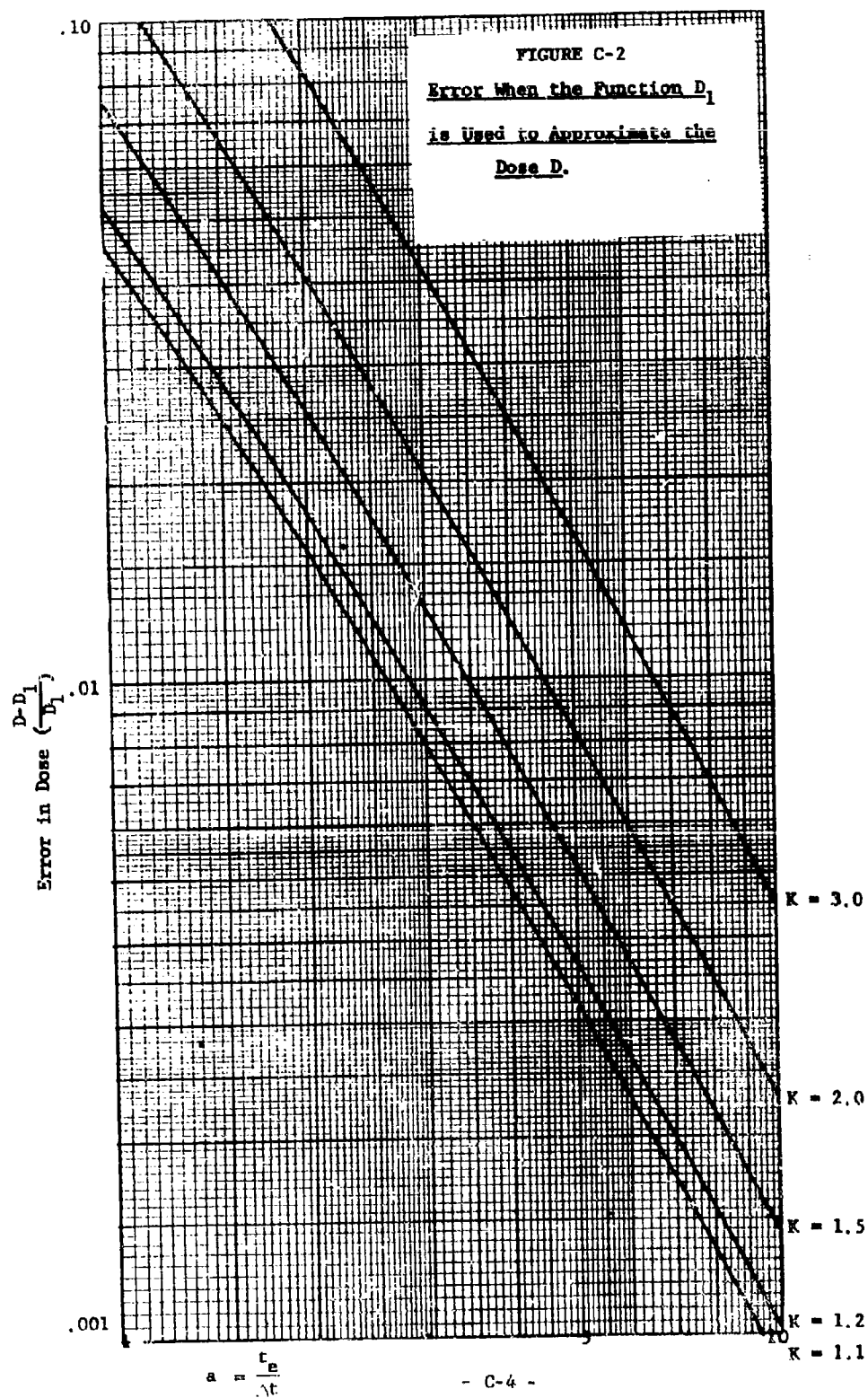
a)



b)



c)



values of $\frac{t_e}{\Delta t}$ ratios, the error is always less than the error associated with the smallest $\frac{t_e}{\Delta t}$ ratio in the range of interest (a range of values of $\frac{t_e}{\Delta t}$ ratios will be the case, for example, when t_e is being determined as a function of Δt and $D_1(t_e, \Delta t)$). In Figure C-2 when $k = 1.2$, the error that results when $\frac{t_e}{\Delta t}$ is equal to 2.85 is seen to be .01 (1%). That means that for any $\frac{t_e}{\Delta t}$ greater than 2.85, the resultant error will always be less than 1%. Similarly, if $\frac{t_e}{\Delta t}$ is greater than 1.0, then the error will always be less than .052 (5.2%) when $k = 1.2$.

C. Second Approximation

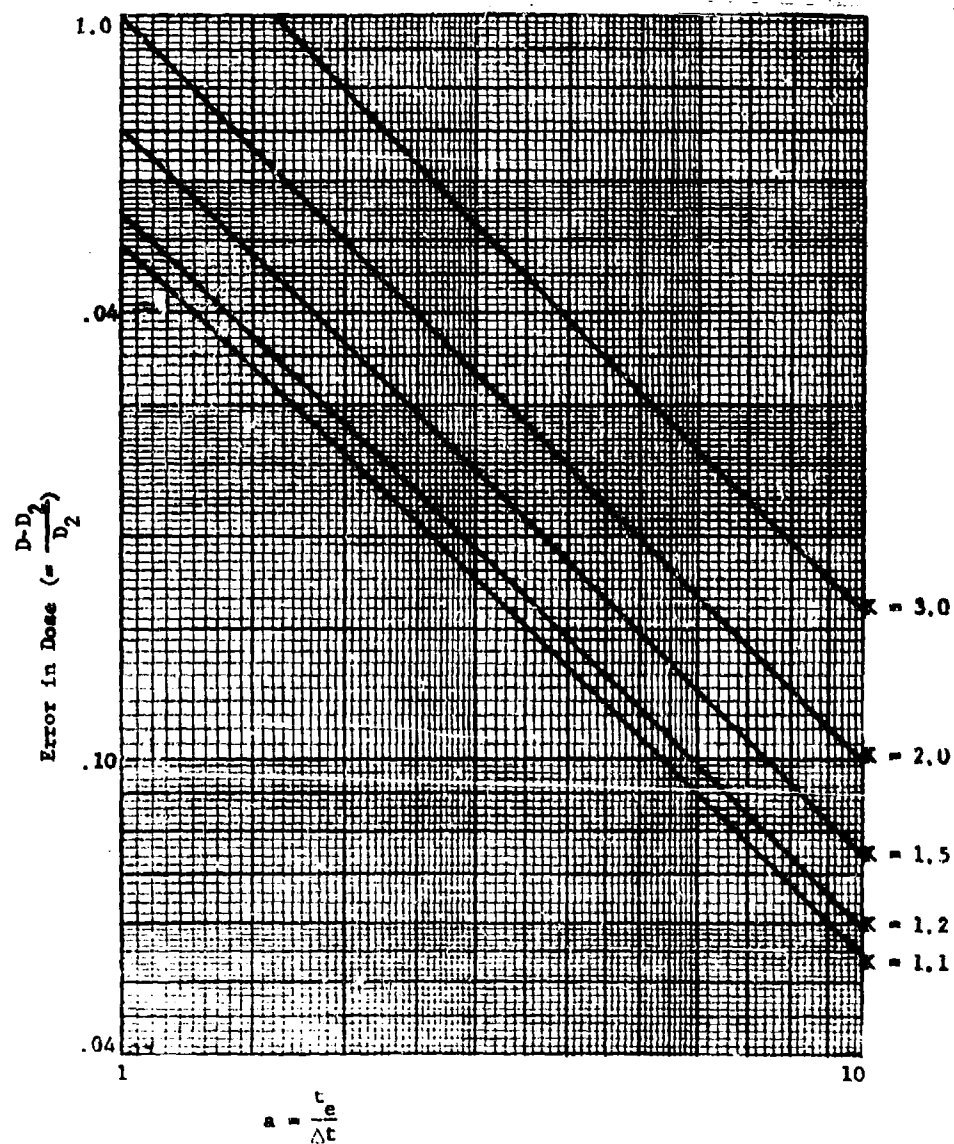
As a second example, the total dose received from time t_e to time $t_e + \Delta t$ can be approximated by multiplying the duration of the exposure interval, Δt , by the dose rate at the beginning of the interval, $I(t_e)$. If this approximation is called $D_2(t_e, \Delta t)$, then

$$D_2(t_e, \Delta t) = \frac{I(1)}{PF} (t_e)^{-k} \Delta t \text{ roentgens} \quad (C-4)$$

The error, $\epsilon_2 = \frac{D_2 - D}{D}$, that results when this approximation (Equation C-4) is used to determine the total dose is derived in Section III and the results are displayed in Figure C-3. This figure gives the error as a function of the ratio, $\frac{t_e}{\Delta t}$, for a set of decay constants, k . In Section III this error is shown to decrease toward zero as the ratio $\frac{t_e}{\Delta t}$ increases. For an example of the actual error, when $k = 1.2$, the error that results when $\frac{t_e}{\Delta t}$ is equal to 7.7 is, from Figure C-3, equal to .07 (that is, 7%). That means that for any $\frac{t_e}{\Delta t}$ greater than 7.7, the resultant error will always be less than 7%.

FIGURE C-3

Error When the Function D_2 is Used to Approximate the Dose D



D. Summary of Examples of the Use of the Approximations

The use of these approximations to achieve simple expressions that are applicable for operations analyses and planning is illustrated in the final section of this paper. There, the problem of determining the earliest time, t_e , of activity resumption or initiation is investigated. Expressions for t_e are developed to show the effect on t_e of changing the activity duration, the fallout field characteristics ($I(1)$ and k), and the allowable dose to be received in the performance of the activity.

Finally, this entry time is determined when radiological countermeasure operations such as decontamination are used to accelerate the recovery process by shortening the above entry time. When a countermeasure operation leads to a reduced entry time (with the allowable dose remaining unchanged), the amount of that time reduction is called the "time saved" in resuming or initiating a particular activity. By using the first approximation (Equation C-3) this time saved, T , is derived as the product of the maximum possible time saved and per cent savings realized. The maximum possible time saved is the time that would be saved if the countermeasure operation were ideal (for decontamination, complete removal of all fallout material). This maximum possible time saved--a function of $\frac{I(1)}{PF}$, activity duration, Δt , and allowable dose--is displayed in Figure C-7. As shown in Section IV, when the allowable dose is fixed, the maximum possible time saved is, indeed, not equal to t_e (without decontamination) but rather is equal to $t_e + \frac{\Delta t}{2}$. The per cent savings realized is the per cent of the maximum that is achieved with a non-ideal countermeasure. This per cent savings realized--a function of the countermeasure effectiveness (defined in Section III)--is displayed in Figure C-8.

II. FIRST APPROXIMATION ERROR ANALYSIS

Using the symbols defined in the preceding section, the actual total dose received between time t_e and $t_e + \Delta t$,

$$D(t_e, \Delta t) = \frac{I(1)}{PF} \left(\frac{1}{k-1} \right) (t_e^{1-k} - (t_e + \Delta t)^{1-k}) , \quad (C-2)$$

is to be approximated by the following:

$$D_1(t_e, \Delta t) = \frac{I(1)}{PF} (t_e + \frac{\Delta t}{2})^{-k} \Delta t . \quad (C-3)$$

The error, E_1 , that results when $D_1(t_e, \Delta t)$ is used in place of $D(t_e, \Delta t)$ is defined as follows:

$$E_1 = \left| \frac{D(t_e, \Delta t) - D_1(t_e, \Delta t)}{D(t_e, \Delta t)} \right| \quad (C-5)$$

$$= \left| 1 - \frac{D_1(t_e, \Delta t)}{D(t_e, \Delta t)} \right| . \quad (C-6)$$

To determine the error, E_1 , it is convenient to analyze the ratio R_1 , where

$$R_1 = \frac{D(t_e, \Delta t)}{D_1(t_e, \Delta t)} , \quad (C-7)$$

$$= \left(\frac{1}{k-1} \right) (t_e^{1-k} - (t_e + \Delta t)^{1-k}) (t_e + \frac{\Delta t}{2})^k \frac{1}{\Delta t} \quad (C-8)$$

$$= \left(\frac{1}{k-1} \right) \left(\left(\frac{t_e}{\Delta t} \right)^{1-k} - \left(1 + \frac{t_e}{\Delta t} \right)^{1-k} \right) \left(\frac{1}{2} + \frac{t_e}{\Delta t} \right)^k . \quad (C-9)$$

In Equation C-9, let $\frac{t_e}{\Delta t} = a$. Furthermore, let $t_e > \Delta t$ so that $a > 1$ will

bound the range of a in the subsequent analysis. Equation C-9 becomes

$$R_1 = \left(\frac{1}{k-1}\right) (a^{1-k} - (1+a)^{1-k}) \left(\frac{1}{2} + a\right)^k \quad (C-10)$$

Because $k > 1$ and $a > 1$, it is obvious that $R_1 > 0$. Additional information-- that R_1 approaches 1 as a increases--may be learned by changing the form of the expression for R_1 in Equation C-10 to

$$R_1 = \left(\frac{1+a}{k-1}\right) \left(\frac{1+\frac{1}{2a}}{1+\frac{1}{a}}\right)^k \left((1 + \frac{1}{a})^{k-1} - 1\right) \quad (C-11)$$

and then replacing the last two terms by the appropriate power series as follows:

$$R_1 = \left(\sum_{r=0}^{\infty} (-1)^r \binom{k}{r} \left(\frac{1}{2(a+1)}\right)^r \left(\frac{1+a}{k-1}\right) \left(\sum_{r=0}^{\infty} \binom{k-1}{r} \frac{1}{a^r} - 1\right)\right) \quad (C-12)$$

$$= \left(1 - \frac{k}{2(a+1)} + \frac{k(k-1)}{2!(2(a+1))^2} - \dots\right) (1+a) \left(\frac{1}{a} + \frac{k-2}{2!a^2} + \dots\right) \quad (C-13)$$

From Equation C-13, it can be seen that, for fixed k , $k > 1$, the value R_1 approaches 1 as the ratio $a = \frac{t_a}{\Delta t}$ increases.

In addition, R_1 monotonically decreases toward 1 as the fraction $a = \frac{t_a}{\Delta t}$ increases. This can be seen by examining the derivative of R_1 with respect to a as follows:

$$\frac{dR_1}{da} = \frac{1}{2} \left(\frac{1}{k-1}\right) \left(a + \frac{1}{2}\right)^{k-1} (a+1)^{-k} \left((1 + \frac{1}{a})^k (1 + 2a - k) - (1+2a+k)\right) \quad (C-14)$$

In the right hand side of Equation C-14, the first four factors are always positive. Therefore, it is only necessary to show that the one remaining factor, $((1 + \frac{1}{a})^k (1+2a-k) - (1+2a+k))$, is always negative. Call this factor F.

To show that $F < 0$ for the k 's of interest in this paper ($1 < k < 4$), expand $(1 + \frac{1}{a})^k$ in a power series, $\sum_{r=0}^k \binom{k}{r} \frac{1}{a^r}$, and retain only the first group of consecutive positive terms as follows:

for $1 < k \leq 2$

$$F \leq (1 + \frac{k}{a} + \frac{k(k-1)}{2! a^2}) (1 + 2a - k) - (1 + 2a + k) \quad (C-15)$$

$$\leq \frac{-k}{2a^2} (k^2 - 2k + 1) \quad (C-16)$$

$$\leq \frac{-k}{2a^2} (k-1)^2 \leq 0 \quad (C-17)$$

for $2 < k \leq 3$

$$F \leq (1 + \frac{k}{a} + \frac{k(k-1)}{2! a^2} + \frac{k(k-1)(k-2)}{3! a^3}) (1 + 2a - k) - (1 + 2a + k) \quad (C-18)$$

$$\leq \frac{k}{3! a^3} (-k^3 + (4-a)k^2 - 5k + 2 + a) \quad (C-19)$$

$$\leq \frac{k}{3! a^3} (1-k)(k^2 + (a-3)k + 2 + 2) \quad (C-20)$$

$$\leq \frac{k}{3! a^3} (1-k)((k-1)(k-2) + a(k+1)) \leq 0 \quad (C-21)$$

for $3 < k \leq 4$

$$F \leq (1 + \frac{k}{a} + \frac{k(k-1)}{2! a^2} + \frac{k(k-1)(k-2)}{3! a^3} + \frac{k(k-1)(k-2)(k-3)}{4! a^4}) (1+2a-k) - (1+2a+k) \quad (C-22)$$

$$\leq \frac{k(1-k)}{4! a^4} ((k^3 + (2a-6)k^2 + (4a^2 - 2a + 11)k + (4a^2 - 4a - 6)) \quad (C-23)$$

$$\leq \frac{k(1-k)}{4! a^4} ((k-1)(k-2)(k-3) + 2a(k-2)(k-1) + 4a^2(k+1)) \leq 0 \quad (C-24)$$

Therefore, $\frac{dR_1}{da}$ is negative when k is the range of interest, $1 < k < 4$, and when $a > 1$. Because this derivative is negative, R_1 monotonically decreases toward 1 as the ratio $a = \frac{t}{\Delta t}$ increases. In terms of the error, E_1 , as R_1 decreases toward 1, its reciprocal increases toward 1 and therefore, the error decreases toward zero. The actual error is easily determined by combining Equations C-6, C-7, and C-10 as follows:

$$E_1 = \left| 1 - \frac{1}{R_1} \right|, \quad (C-25)$$

$$= 1 - \frac{1}{R_1}, \quad (C-26)$$

$$= 1 - \frac{k-1}{\left(\frac{1+a}{2}\right)^k (a^{1-k} - (a+1)^{1-k})}. \quad (C-27)$$

To compare E_1 with R_1 , let

$$R_1 = 1 + \delta_1, \quad (C-28)$$

so that

$$E_1 = \frac{\delta_1}{1 + \delta_1}, \quad (C-29)$$

$$= \delta_1 - \delta_1^2 + \delta_1^3 - \dots, \quad (C-30)$$

$$\leq \delta_1. \quad (C-31)$$

The size of δ_1 , and therefore the bound on E_1 , depends on $a = \frac{t}{\Delta t}$ and on k . If for fixed k the error bound δ_1 is known for any a_x , then the error associated with any $a > a_x$ will be less than δ_1 . That is,

$$E_1(a_x, k) > E_1(a, k) \text{ for } a_x < a. \quad (C-32)$$

As a convenience, a selected set of bounds on the error as a function of k and a is presented in Figure C-2. In Figure C-2, for selected set of k ($k = 1.1, 1.2, 1.5, 2.3$) and error bounds, δ_1 , between .001 and .10, the minimum value of $a = \frac{t_e}{\Delta t}$ such that the error is less than the desired bound is presented. As an example, when $k = 1.2$, the error, δ_1 , will always be less than .03 (3%) if the ratio $a = \frac{t_e}{\Delta t}$ is greater than 1.46.

III. SECOND APPROXIMATION ERROR ANALYSIS

Continuing from Section I, the total dose received between time t_e and time $t_e + \Delta t$,

$$D(t_e, \Delta t) = \frac{I(1)}{PF} \left(\frac{1}{k-1} \right) (t_e^{1-k} - (t_e + \Delta t)^{1-k}), \quad (C-2)$$

is to be approximated by the following:

$$D_2(t_e, \Delta t) = \frac{I(1)}{PF} (t_e)^{-k} \Delta t. \quad (C-4)$$

The error, E_2 , that results when $D_2(t_e, \Delta t)$ is used in place of $D(t_e, \Delta t)$ is defined as follows:

$$E_2 = \left| \frac{D(t_e, \Delta t) - D_2(t_e, \Delta t)}{D(t_e, \Delta t)} \right|, \quad (C-33)$$

$$= \left| 1 - \frac{D_2(t_e, \Delta t)}{D(t_e, \Delta t)} \right| \quad (C-34)$$

As in the previous section, let

$$R_2 = \frac{D(t_e, \Delta t)}{D_2(t_e, \Delta t)} \quad , \quad (C-35)$$

$$= \left(\frac{1}{k-1}\right) \left(\frac{t_e}{\Delta t}\right) \left(1 - \left(\frac{\Delta t}{t_e} + 1\right)^{1-k}\right) \quad , \quad (C-36)$$

$$= \left(\frac{1}{k-1}\right) a \left(1 - \left(1 + \frac{1}{a}\right)^{1-k}\right) \quad . \quad (C-37)$$

where $a = \frac{t_e}{\Delta t}$. Again, if $k > 1$ and $a > 1$, then $R_2 > 0$. Expanding $\left(1 + \frac{1}{a}\right)^{1-k}$, Equation C-37 becomes,

$$R_2 = \left(\frac{a}{k-1}\right) \left(1 - \left(1 + \frac{1-k}{a} + \frac{(1-k)(1-k-1)}{2! a^2} + \dots\right)\right) \quad , \quad (C-38)$$

$$= 1 - \frac{k}{2! a} + \frac{k(k+1)}{2! a^2} - \frac{k(k+1)(k+2)}{4! a^3} + \dots \quad . \quad (C-39)$$

As the ratio $a = \frac{t_e}{\Delta t}$ increases, R_2 approaches 1 and $R_2 \leq 1$. The behavior of R_2 can be further understood by examining the derivative of R_2 with respect to a .

$$\frac{dR_2}{da} = \left(\frac{1}{k-1}\right) \left(1 - \left(1 + \frac{k}{a}\right) \left(1 + \frac{1}{a}\right)^{-k}\right) \quad . \quad (C-40)$$

This, as expected, is positive when $k > 1$ and $a > 1$. Therefore, R_2 monotonically increases toward 1 as the ratio $a = \frac{t_e}{\Delta t}$ increases. In terms of the error, E_2 , and R_2 increases toward 1, its reciprocal decreases toward 1, and therefore, the error decreases toward zero. The actual error may be determined by combining Equations C-34 and C-37 as follows:

$$E_2 = \left| 1 - \frac{1}{R_2} \right| = \frac{1}{R_2} - 1 \quad , \quad (C-41)$$

$$= \left(\frac{k-1}{a}\right) \left(1 - \left(1 + \frac{1}{a}\right)^{1-k}\right)^{-1} - 1 \quad . \quad (C-42)$$

To compare E_2 with R_2 , let

$$R_2^{-1} = 1 + \delta_2, \quad (C-43)$$

so that

$$E_2 = \delta_2. \quad (C-44)$$

The size of δ_2 , and therefore the bound on E_2 , depends on $a = \frac{t_a}{\Delta t}$ and on k . If for fixed k the error δ_2 is known for any a_x , then the error associated with any $a > a_x$ will be less than δ_2 . That is,

$$E_2(a_x, k) > E_2(a, k) \text{ for } a_x < a. \quad (C-45)$$

As a convenience, a selected set of bounds on the error as a function of k and a is presented in Figure C-3. In Figure C-3, for a selected set of k ($k = 1.1, 1.2, 1.5, 2.0, 3.0$) and error bounds, δ_2 , between .01 and 1.0, the minimum value of a such that the error is less than the desired bound is presented. As an example, when $k = 1.2$, the error δ_2 will always be less than .1 (10%) if the ratio $a = \frac{t_a}{\Delta t}$ is greater than 5.9.

IV. TIME SAVED USING TOTAL DOSE APPROXIMATIONS

A. Entry Time

An important problem commonly encountered in the analysis of fallout operations involves the time at which a particular activity can be initiated or resumed. In such problems, the fallout environment constrains activity performance through the limitations placed on the allowable dose the individual engaged in the activity may receive. As an example, assume an individual is to engage in a particular activity beginning at time t_e and lasting until

time $t_e + \Delta t$. Let the protection afforded the individual by the activity be PF so that the dose he will receive in performing the activity, $D_A(t_e, \Delta t)$ is,

$$D_A(t_e, \Delta t) = \frac{I(1)}{PF} \frac{1}{k-1} (t_e^{1-k} - (t_e + \Delta t)^{1-k}) \text{ roentgens.} \quad (C-2)$$

On the basis of the individual's exposure before and after the activity is performed, this dose $D_A(t_e, \Delta t)$, must be limited and hence the activity must be planned so that the dose is less than the imposed limit. If this limit is L_A , then the activity planning must provide that $D_A(t_e, \Delta t) \leq L_A$. The bounds on the activity performance can be determined by substituting L_A for $D_A(t_e, \Delta t)$ in Equation C-2. It is more convenient, however, to use one of the two approximations described in the preceding sections because they are much more readily solved for t_e . Using the first approximation, Equation C-3, the time at which the activity can be scheduled to begin is, as a function of the activity duration Δt ,

$$t_e = \left(\frac{\Delta t I(1)}{PF L_A} \right)^{1/k} - \frac{\Delta t}{2} \text{ hours.} \quad (C-46)$$

The concomitant error in t_e determined from Equation C-46 can be determined, for a range of decay constants k , from Figure C-2. This relationship, Equation C-46, is illustrated in Figure C-4 where t_e is presented as a function of Δt for a selected set of $\frac{I(1)}{PF L_A}$ values (2, 4, 8, 16, 32, 64, 128, and 256). Also included in this figure is an indication of the applicable error for each case.

In the determination of t_e , if either the parameters are such that $\frac{t_e}{\Delta t}$ tends to be large, or the error requirements are not stringent, then a simpler expression for t_e can be determined from the second approximation

by substituting L_A for $D_2(t_e, \Delta t)$ in Equation C-4. This procedure results in the following expression for t_e as a function of Δt :

$$t_e = \left(\frac{I(1) \Delta t}{PF L_A} \right)^{1/k} \text{ hours.} \quad (C-47)$$

In this case the concomitant error in t_e can be determined, for a range of decay constants k , from Figure C-3. This relationship, Equation C-47, is illustrated in Figure C-5 where t_e is presented as a function of Δt for a selected set of $\frac{I(1)}{PF L_A}$ values (2, 4, 8, 16, 32, 64, 128, and 256). Also included in this figure is an indication of the applicable error for each case.

B. Time Saved

In many cases of essential activities, the time at which the activity can begin (Equation C-46 or Equation C-47) may be undesirably late (large t_e). In these situations some form of radiological countermeasure is used to decrease the dose rate,

$$I(t) = \frac{I(1) t^{-k}}{PF} \text{ roentgens/hour,} \quad (C-1)$$

by decreasing the applicable value of $\frac{I(1)}{PF}$. As an example, decontamination of the facility may lead to such an effective decrease. Let the effect of such an operation be represented by multiplying the $\frac{I(1)}{PF}$ constant by a factor f_d , whose value lies between zero and one. After the decontamination operation is performed, the dose rate is

$$I(t) = f_d \frac{I(1)}{PF} t^{-k} \text{ roentgens/hour,} \quad (C-48)$$

and the approximation to the time at which the activity may commence becomes,

FIGURE C-4
Earliest Time of Entry Calculated Using D_1 for Dose

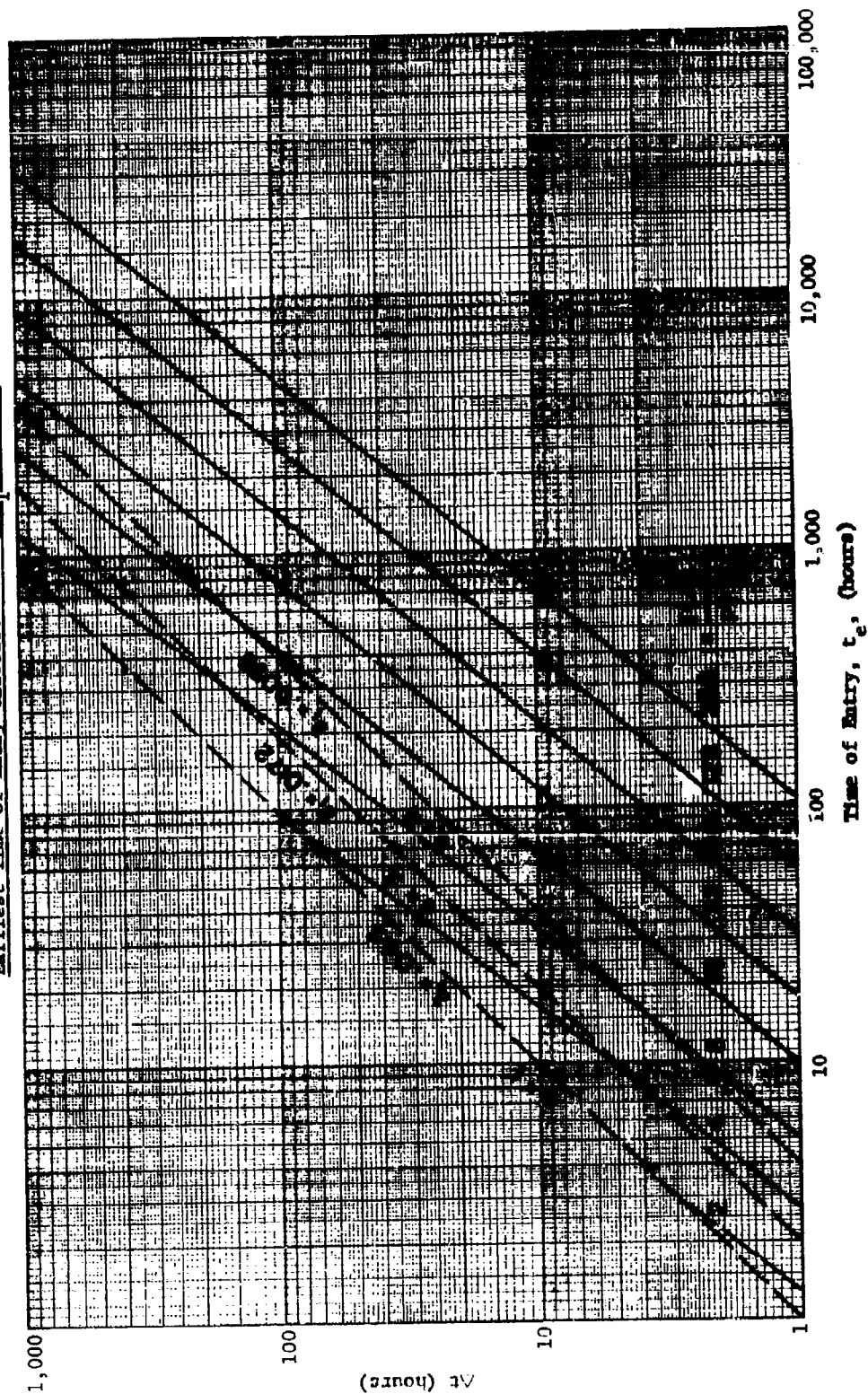
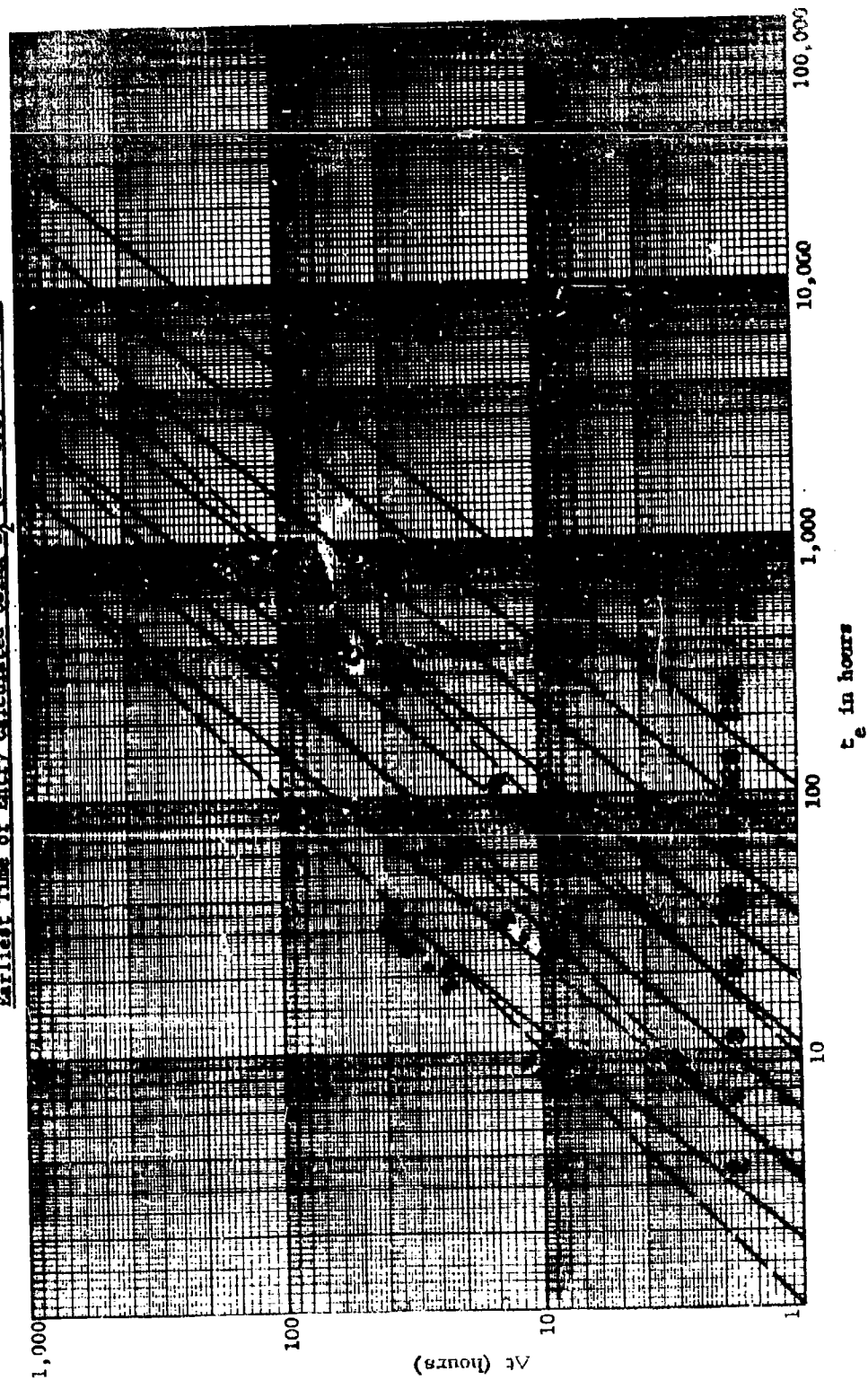


FIGURE C-5
Earliest Time of Entry Calculated Using D_2 ($k = 1.2$) for Dose



using $D_1(t_e, \Delta t)$,

$$t_e^* = \left(\frac{\Delta t I(1) f_d}{PF L_A} \right)^{1/k} - \frac{\Delta t}{2} \text{ hours.} \quad (C-49)$$

Here it is assumed that the operation leading to an $f_d < 1$ was performed at some time t_d prior to t_e^* .

It is easily seen in Equation C-49 that the decontamination operation decreased the required delay time for initiation or resumption of the activity. The actual time which has been saved as a direct result of decontamination is determined by subtracting t_e^* from t_e as follows:

$$T = t_e - t_e^* \text{ hours,} \quad (C-50)$$

$$= \left(\frac{\Delta t I(1)}{PF L_A} \right)^{1/k} (1 - f_d^{1/k}) \text{ hours,} \quad (C-51)$$

$$= T_{\max} \frac{PCSR}{100} \quad (C-52)$$

In Equation C-52, T has been interpreted as the product of two terms T_{\max} and $\frac{PCSR}{100}$. The first term T_{\max} is the limit approached by T as f_d approaches zero. Because $f_d = 0$ represents perfect or ideal decontamination, T_{\max} is called the maximum time saved using perfect decontamination.

Besides requiring $f_d = 0$, perfect decontamination requires $t_d = 0$. This latter requirement implies $t_e^* \geq 0$ and as a result places a practical bound on the effectiveness of f_d . That is, as the problem was stated, the dose to be received in the performance of the activity was fixed at L_A . If perfect decontamination were employed, the dose received would be zero and hence much lower than L_A . In such a case, a portion of the decontamination effort is used to meet the requirement $D(t_e^*, \Delta t) = L_A$ and the remaining portion of the decontamination effort is used to further reduce the dose to zero, below the

requirement. This effort used to reduce the dose from L_A to zero is not effective in meeting the problem requirement because the requirement has already been met. This is what is implied by the restriction $t_e^* \geq 0$. If this restriction is not adhered to, confusion will grow out of the inequality obtained from comparing T_{\max} with t_e ; that is,

$$T_{\max} = t_e + \frac{\Delta t}{2} \quad (C-53)$$

and therefore

$$T_{\max} \neq t_e \quad (C-54)$$

In the same sense that T_{\max} is the limit approached as f_d approaches zero, $\frac{PCSR}{100}$ is the fraction of the maximum that is realized with imperfect (non-ideal) decontamination. That is, PCSR is the per cent savings realized that results when f_d is a positive number greater than zero.

These two terms,

$$PCSR = 100 (1 - f_d^{1/k}) \quad (C-55)$$

and

$$T_{\max} = \left(\frac{\Delta t}{PF} \frac{I(1)}{L_A} \right)^{1/k} \text{ hours,} \quad (C-56)$$

are presented in Figures C-6 and C-7 respectively. Figure C-7 describes the maximum savings possible for given values of Δt , $I(1)$, PF , and L_A , and Figure C-6 describes the per cent of this that is realized for a given value of f_d .

As an example, assume that an activity is to be resumed where the $\frac{I(1)}{PF}$ value is 5000 roentgens per hour. In addition assume the individual engaged

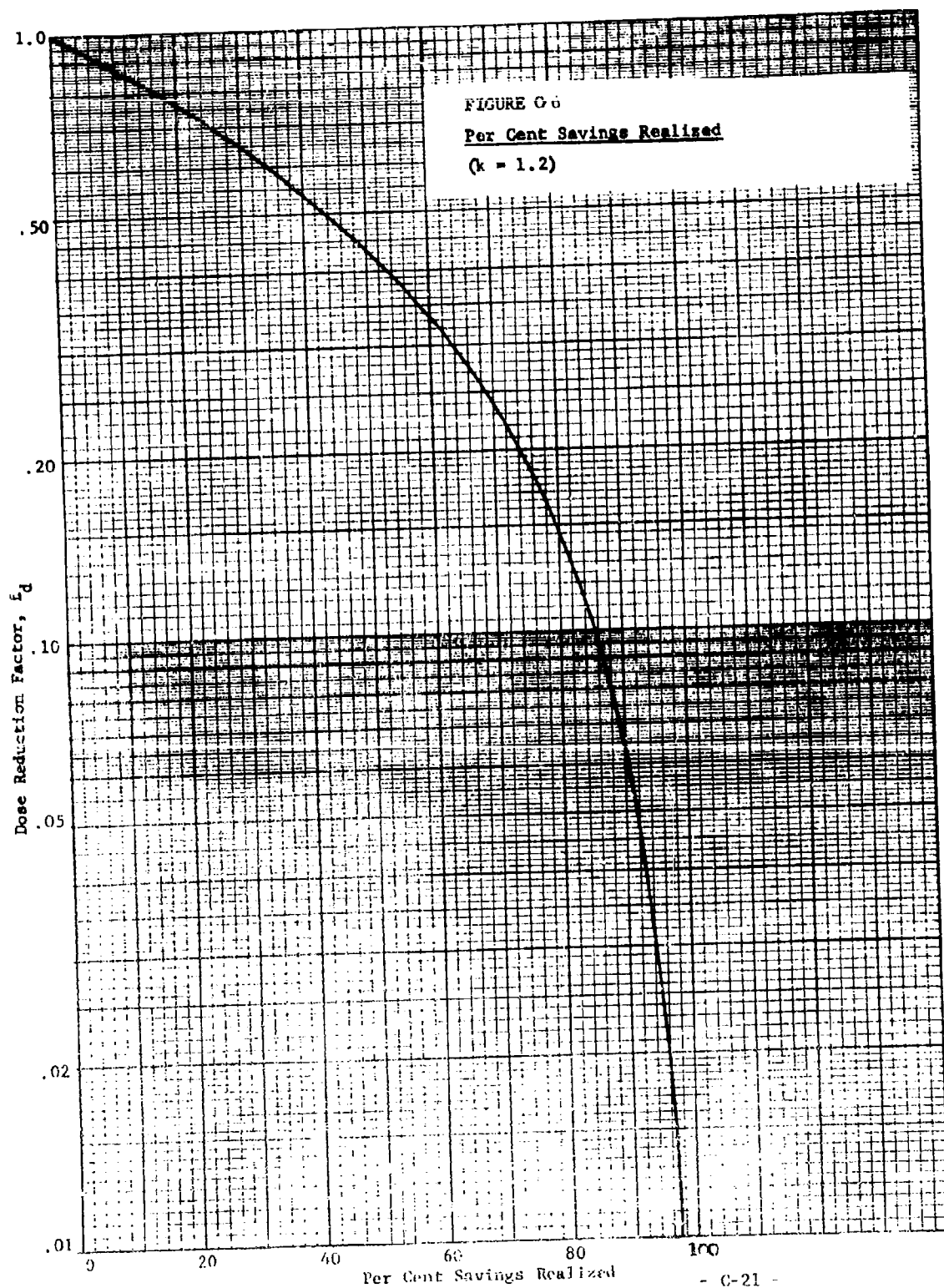
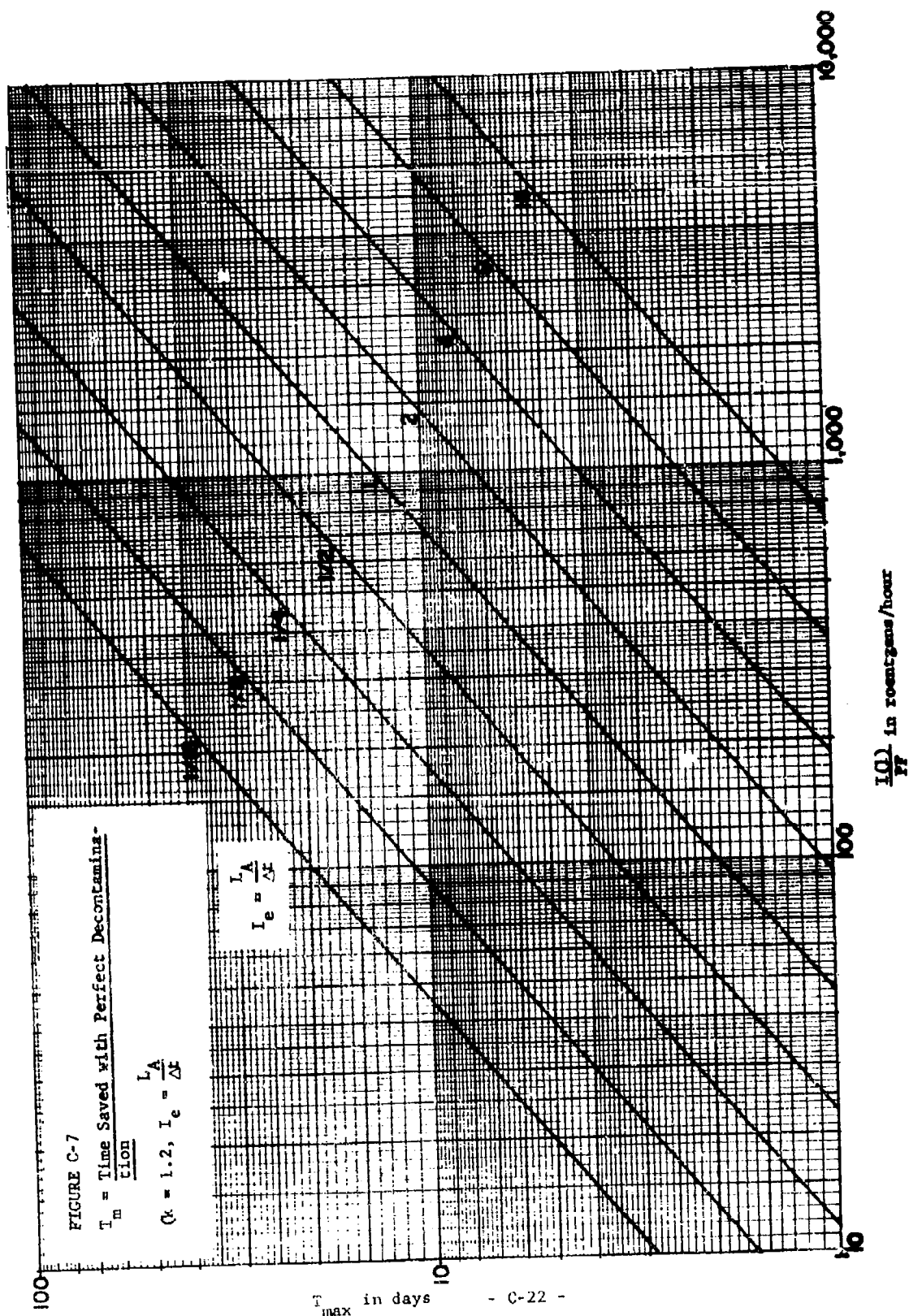


FIGURE C-7
T = Time Saved with Perfect Decontaminating

T^m = Time Saved with Perfect Decontamination

$$\frac{L_A}{\Delta t} = I_e$$

$$\frac{I_A}{I_e} = \Delta x$$



in the activity is to receive no more than 160 roentgens. From Figure C-7, if the planned duration of the activity was 10 hours, then the ratio $\frac{L_A}{\Delta t}$ is $\frac{160}{10} = 16$ and the maximum time saved, T_{\max} , is 120 hours. If the decontamination effectiveness, f_d , is .2, then the per cent realized is, from Figure C-6, 74%. Therefore, the time saved in resuming the activity is $.74 \times 120 = 89$ hours or approximately 4 days. This savings is a direct result of decontamination.

As a second example, assume that the activity has an $\frac{I(1)}{PF}$ value of 5000 roentgens per hour, that the individual is to receive no more than 120 roentgens, and that the duration of the activity will be five days or 120 hours. In this case, from Figure C-7, the maximum time saved is 50 days. If the decontamination effectiveness is .3, the time saved becomes $.638 \times 50 = 32$ days. From Figure C-4, the earliest time of activity resumption without decontamination would be 47.5 days. Therefore, with decontamination, the activity can be resumed at $47.5 - 32 = 15.5$ days after detonation--thus saving 32 days.

As expected, the above discussion presents an example of the simplicity that results from the use of the total dose approximations mentioned in the introductory section. Many different applications exist as well as different interpretations of the material presented above. The only constraint in using the approximations involves the allowable error (presented in Figures C-2 and C-3). Even this restriction can be relaxed considerably because the direction and magnitude of the error are known and therefore can be accounted for by biasing the interpretation of the results of the analysis when $\frac{t_e}{\Delta t}$ is low.

Appendix D

The Effectiveness of Radiological Countermeasures
in Accelerating Postattack Recovery

This Appendix was originally
submitted to OGD as Research
Memorandum RM 156-5,* except
for minor editorial changes.

* J. D. Douglass, Jr. The Effectiveness of Radiological Countermeasures
in Accelerating Postattack Recovery. Research Memorandum RM 156-5,
Durham, North Carolina: Research Triangle Institute, Operations Research
Division, 29 May 1964.

Appendix D

The Effectiveness of Radiological Countermeasures in Accelerating Postattack Recovery

I. SUMMARY

The material in this Appendix was developed to determine the extent to which radiological countermeasures could accelerate the postattack recovery process. In the development, the recovery of an activity is specified in terms of the duration of the activity, Δt , and the time when the activity is to commence, t_e . Other activity characteristics that affect the dose received by the performing personnel are absorbed into an activity intensity constant, H , which also accounts for the fallout radiation field characteristics. For the purpose of this summary, H may be considered to be the common H+1 reference intensity, $I(1)$, at the place where the personnel are located. The personnel performing the activity are specified in terms of the allowable radiation dose, D , one may receive in performing the activity. This dose specification is made in terms of either total dose or equivalent residual dose (ERD), or both, depending on the length of the activity duration. The countermeasure is specified by its effectiveness, f_d , in causing a reduction in dose received by an individual in performing a scheduled operation.

Obviously, the above parameters are not all independent. In particular, of the five (Δt , t_e , H , D , f_d), any four may be regarded as independent and the fifth can be expressed in terms of them. Such expressions are developed

Appendix D

The Effectiveness of Radiological Countermeasures in Accelerating Postattack Recovery

I. SUMMARY

The material in this Appendix was developed to determine the extent to which radiological countermeasures could accelerate the postattack recovery process. In the development, the recovery of an activity is specified in terms of the duration of the activity, Δt , and the time when the activity is to commence, t_e . Other activity characteristics that affect the dose received by the performing personnel are absorbed into an activity intensity constant, H , which also accounts for the fallout radiation field characteristics. For the purpose of this summary, H may be considered to be the common H+1 reference intensity, $I(1)$, at the place where the personnel are located. The personnel performing the activity are specified in terms of the allowable radiation dose, D , one may receive in performing the activity. This dose specification is made in terms of either total dose or equivalent residual dose (ERD), or both, depending on the length of the activity duration. The countermeasure is specified by its effectiveness, f_d , in causing a reduction in dose received by an individual in performing a scheduled operation.

Obviously, the above parameters are not all independent. In particular, of the five (Δt , t_e , H , D , f_d), any four may be regarded as independent and the fifth can be expressed in terms of them. Such expressions are developed

in the analysis section of this report. Although each parameter is treated as the dependent variable at some time in the analysis, the emphasis is placed on expressing t_e as a function of H , D , Δt , and f_d . There, the intent is to determine how the time when the activity may commence, t_e , varies as a function of the countermeasure effectiveness, f_d , and the operating constraints, Δt , H , and D . By holding these operating constraints constant, it is then possible to determine the difference between the time when the activity may commence if the countermeasure is not employed, t_e^* , and the time when the activity may commence if the countermeasure is employed, t_e .

This difference, $t_e^* - t_e$, is the time, T , that is saved in recovering an activity as a direct result of a particular countermeasure. This time saved is expressed in this appendix as a function of the operating constraints, Δt , D , and H , and the countermeasure effectiveness, f_d . Sets of performance curves that describe the behavior of T as the four parameters vary independently are presented at the end of the analysis section as Figures D-15 through D-27.

In the final section of this appendix, these figures are examined in a general manner to determine an impression of the range of situations where countermeasures appear to be most valuable. There, the measure of effectiveness is the time saved. The range of situations that is obtained uses the assumption that T should be at least one week, and that T should be at least 30 per cent of t_e^* . Under these two assumptions it is shown that the range of potentially valuable application is specified by two inequalities, $f_d \leq .7$ and $H\Delta t \geq k(f_d)D$. Here, $k(f_d)$ is a function of f_d whose value is

determined from one of the curves in Figures D-24 through D-29. When $f_d = .7$, $k(f_d) = 100$ and range of application is defined by the inequality $H\Delta t \geq 100D$. In addition, the greater the inequality of $H\Delta t$ and $100D$ is, the greater is the resultant amount of time saved.

II. ANALYSIS

A. Introduction

By using certain radiological countermeasures, it is possible to accelerate the process of postattack recovery. The amount by which the process is accelerated will depend on the effectiveness of the countermeasure, the amount and distribution of radioactive fallout present in the area where the recoverable activity and/or facility is located, and on the personnel--their dose history and the additional allowable dose that they may receive in performing the activity.

In the following analysis, the radioactive fallout hazard is measured, with respect to the facility wherein the activity is to be recovered, by the dose in roentgens that will be received by the individual performing the activity. This dose is called the performance dose. The effectiveness of the countermeasure is measured 1) by the fractional reduction in the performance dose brought about by the countermeasure when the timing of the activity is held constant, and 2) by the fractional reduction in the activity timing brought about by the countermeasure when the performance dose is held constant. The allowable dose to be received in performing the activity is defined in three ways, depending on the particular time duration of the activity: if the duration is less than thirty days, then

the total dose is used; if the duration is more than four days and less than thirty days, then the equivalent residual dose (ERD) at the end of the duration is used; if the duration is sufficiently long that the ERD reaches a maximum before the end of the duration, then the maximum ERD that is reached is used. Obviously, these three viewpoints are not mutually exclusive.

The following analysis combines the above concepts and arrives at a measure of the amount of recovery acceleration achieved by a particular countermeasure applied to a particular situation when the allowable dose constraints are specified. The amount of acceleration is measured by the "time saved" in resuming or initiating an activity. As will become apparent, interest is centered in activities to be recovered after the first few days following detonation and during the first few months thereafter.

B. Dose Rate

The expression for dose rate that will be used in the subsequent development is

$$I(t) = Ht^{-1.2} \text{ roentgens/hour,} \quad (D-1)$$

where t is the time after detonation in hours and H is independent of time. This expression for dose rate will be used to determine the dose that will be received by an individual while he is performing the activity of interest.

In this expression, Equation D-1, the constant H depends on the particular situation and on the intent of the analyst. This constant relates the activity characteristics (location in the fallout field, structure

PF,...) to the dose received in performing the activity. The scope and flexibility of the results produced by the subsequent analysis are critically dependent on the imagination utilized in interpreting H in a broad and flexible manner. In the simplest case of pre-attack planning the constant H may be set equal to $\frac{I(1)}{PF}$ where I(1) is the unit time reference intensity in the activity area and PF is the protection factor of the structure in which the activity is performed. If at the same time the activity has a sequential characteristic that involves several structures with different PF's, then H might be set equal to $\frac{I(1)}{P_e}$ where P_e is the equivalent protection factor.* In the simplest case of postattack planning, H might be set equal to $Iy^{1.2}$ where I is the measured dose rate where the activity will be performed and y is the time after detonation when the measurement is made. These examples are presented to illustrate simple interpretations of H. More complicated or flexible interpretations will arise as the individual's (or individuals') behavior pattern becomes a complicated function of time. Irrespective of the particular interpretation, two rules must be followed. First, H must be independent of time; and second, if the activity is performed from time t_0 to time $t_0 + \Delta t$, where Δt is the activity duration, then H must be chosen so that the total dose** received by the individual in performing the activity is:

*See Reference D-1, page 56.

**Throughout this appendix, D_T will refer to total dose, D_R will refer to equivalent residual dose (ERD), and D will refer to a dose that is either total dose or ERD. In both cases, D_T and D_R are calculated assuming zero prior dose. This assumption does not restrict the usefulness of the analysis. Prior dose enters into the application of the analysis when a determination is made of the allowable subsequent dose.

$$D_T = H \int_{t_e}^{t_e + \Delta t} x^{-1.2} dx \text{ roentgens.} \quad (D-2)$$

C. Countermeasure Effectiveness

In the preceding section the constant H in the dose rate equation was chosen to relate the effect of the activity characteristics (location, structure, FF, ...) to the total dose received in performing the activity, Equation D-2. A similar constant, f_d , is chosen to show the effect of a countermeasure on the dose received in performing the activity. This constant, f_d , is chosen so that if the activity, which is the object of the countermeasure, is performed from time t_e to time $t_e + \Delta t$, then the total dose received by the individual in performing the activity when the countermeasure is not activated will be

$$D_T = H \int_{t_e}^{t_e + \Delta t} x^{-1.2} dx \text{ roentgens,} \quad (D-3)$$

and when the countermeasure is activated and completed before time t_e , will be

$$D_T = f_d H \int_{t_e}^{t_e + \Delta t} x^{-1.2} dx \text{ roentgens.} \quad (D-4)$$

Values of f_d that lie between zero and one ($0 \leq f_d \leq 1$) will be considered in this appendix. Notice that when f_d is set equal to 1, the countermeasure is, in effect, not activated.

D. Activity Performance Dose

While performing a given activity, the individual will receive a certain

dose of radiation. Because it is not clear how hazardous a certain dose of radiation is to an individual, two approaches to the dose received will be taken in the subsequent development. The first approach will be to determine the total dose received,

$$D_T = f_d H \int_{t_e}^{t_e + \Delta t} x^{-1.2} dx \text{ roentgens,} \quad (D-4)$$

when the activity is performed from time t_e to time $t_e + \Delta t$. The second approach will be to determine the maximum equivalent residual dose received when the activity is performed from time t_e to time $t_e + \Delta t$,

$$D_R = \text{maximum } f_d H \int_{t_e}^t W(t-x) x^{-1.2} dx \text{ roentgens,} \quad (D-5)$$

$$t_e \leq t \leq t_e + \Delta t$$

where $W(t-x)$ is a function used to weight the dose rate in order to simulate the effect of possible biological repair and recovery.

For the first approach, the total dose received, from Equation D-4, is,

$$D_T = f_d H 5(t_e^{-0.2} - (t_e + \Delta t)^{-0.2}) \text{ roentgens.} \quad (D-6)$$

It has been shown* that this expression can be approximated as follows:

$$D_T = f_d H \Delta t (t_e + \frac{\Delta t}{2})^{-1.2} \text{ roentgens.} \quad (D-7)$$

The concomitant error is less than 1 per cent when $\frac{t_e}{\Delta t} \geq 2.85$ and is less than 5.2 per cent when $\frac{t_e}{\Delta t} \geq 1.0$.* Because this error is small and its bounds

*See Reference D-2.

are known, Equation D-7 will be used to determine the total dose received in the performance of the activity. This equation is graphed in Figure D-1 where $\frac{D_T/\Delta t}{F_d H}$ is displayed as a function of activity entry time, t_e , for selected activity durations, Δt , = 1 day, 4 days, 16 days, and 32 days. In this figure and in the following discussion, the quantity $D/\Delta t$ will be called the activity "effective intensity" and will be referred to as I_e . Therefore, in Figure D-1 the normalized effective intensity, $\frac{I_e}{F_d H}$, is displayed as a function of t_e .

For the second approach, the maximum ERD received is determined from Equation D-5 for two separate cases: Case I, where the maximum occurs at the end of the activity or when $t = t_e + \Delta t$ and Case II, where the maximum occurs before the end of the activity or when $t < t_e + \Delta t$. In both cases it is necessary to begin by selecting the appropriate weighting function $W(t)$. The weighting function most commonly used to approximate the effect of biological repair and recovery is:*

$$W(t) = .1 + 9e^{-.024t} \quad , \quad (D-8)$$

where t is in days. This approximation is shown in Figure D-2 along with the function

$$W(t) = 1 - .016t \quad , \quad (D-9)$$

which will be used in this discussion to approximate the biological effect for Case I when $t \leq 35$ days. Substituting Equation 9 in Equation 5, the maximum ERD for Case I becomes:

* See Reference D-1.

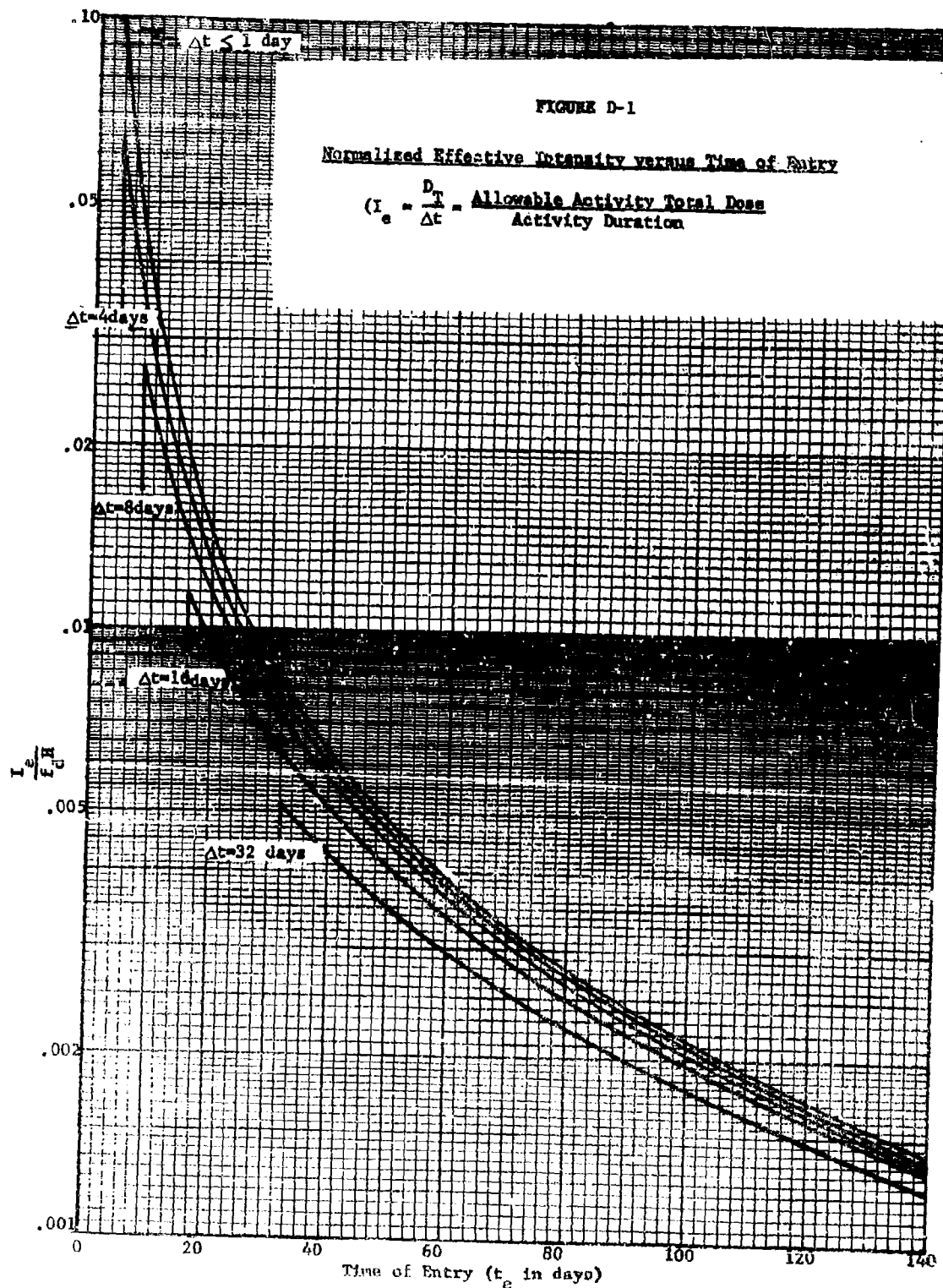
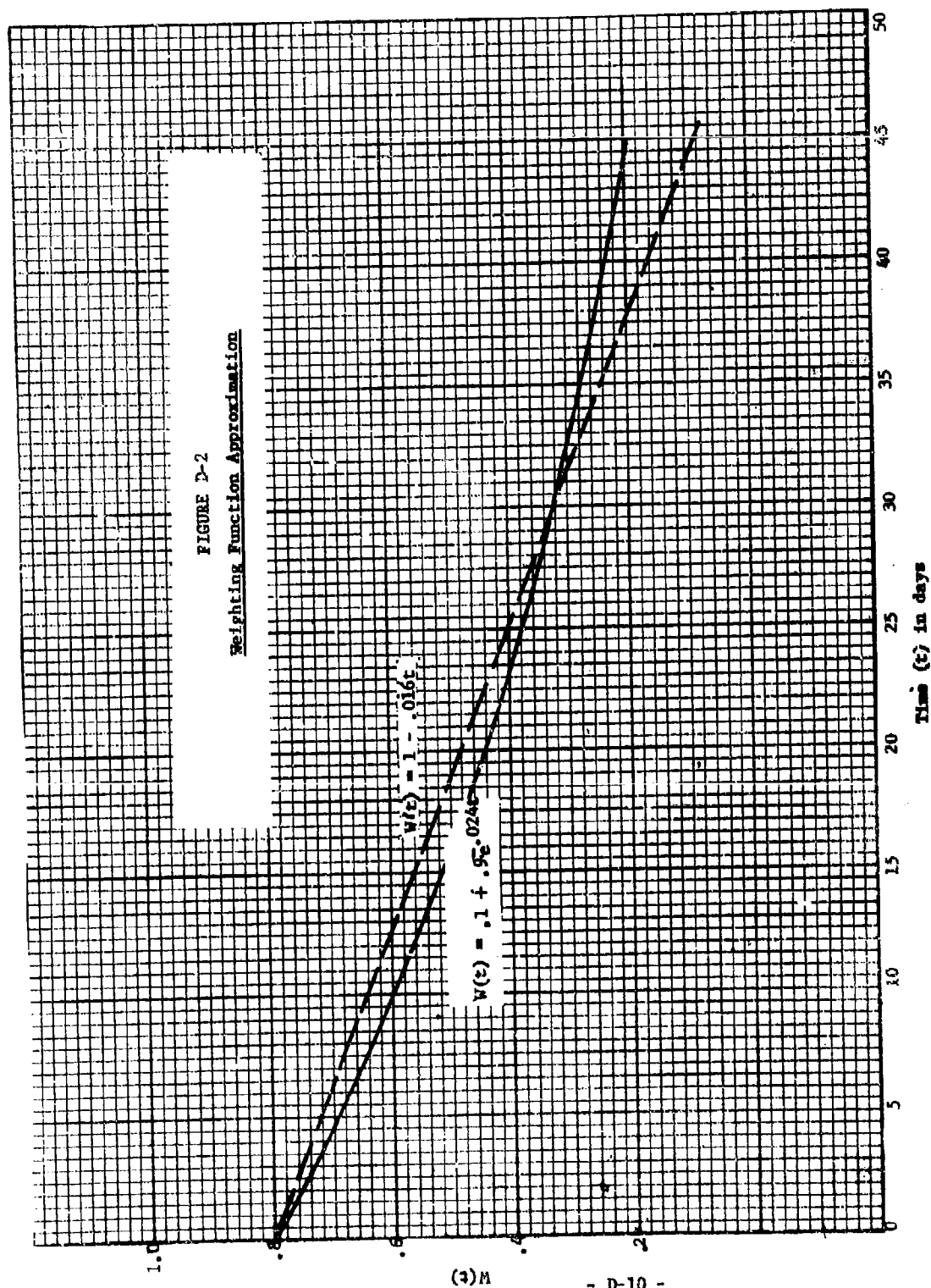


FIGURE D-2
Weighting Function Approximation



$$D_R = f_d H \int_{t_e}^{t_e + \Delta t} (1 - .016(t_e + \Delta t - x)) x^{-1.2} dx \quad (D-10)$$

$$= f_d H (1 - .016 t_e - .016 \Delta t) \int_{t_e}^{t_e + \Delta t} x^{-1.2} dx$$

$$= f_d H .016 \int_{t_e}^{t_e + \Delta t} x^{-1.2} dx \text{ roentgens,} \quad (D-11)$$

which can be approximated to the same accuracy as D_T (in Equation D-7) as follows:

$$D_R = f_d H (1 - .016(t_e + \Delta t)) \Delta t (t_e + \frac{\Delta t}{2})^{-1.2}$$

$$+ f_d H .016 (t_e + \frac{\Delta t}{2}) \Delta t (t_e + \frac{\Delta t}{2})^{-1.2} \quad (D-12)$$

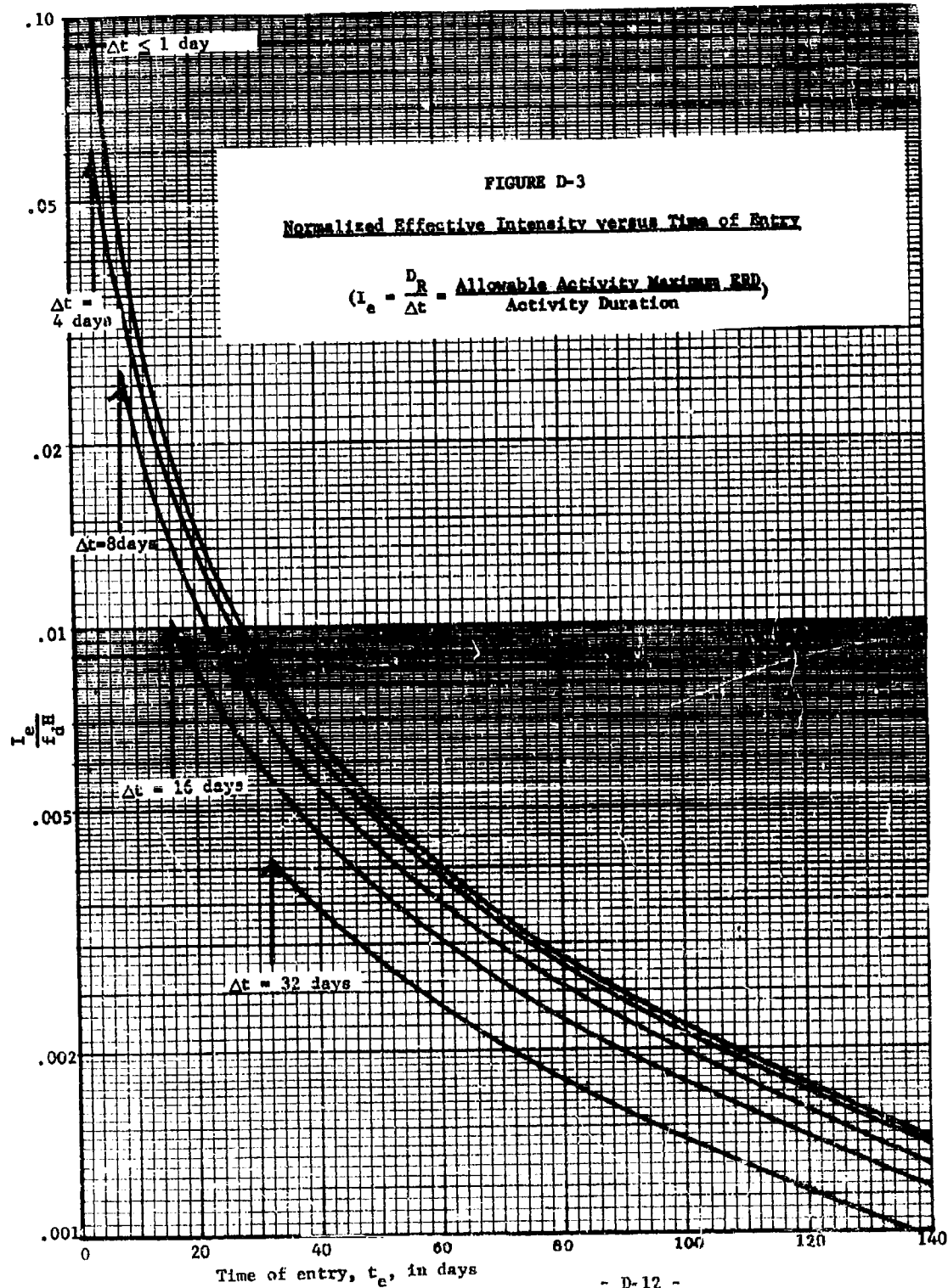
$$= f_d H \Delta t (1 - .008 \Delta t) (t_e + \frac{\Delta t}{2})^{-1.2} \text{ roentgens.} \quad (D-13)$$

Combining Equation D-7 with Equation D-13, this becomes:

$$D_R = (1 - .008 \Delta t) D_T \text{ roentgens.} \quad (D-14)$$

This equation will be used to determine the ERD in Case I where it reaches a maximum at the conclusion of the activity performance. This equation is graphed in Figure D-3 where $\frac{D_R/\Delta t}{f_d H} = \frac{I_e}{f_d H}$ is displayed as a function of activity entry time, t_e , for selected activity durations, $\Delta t = 1, 4, 8, 16, 32$ days.

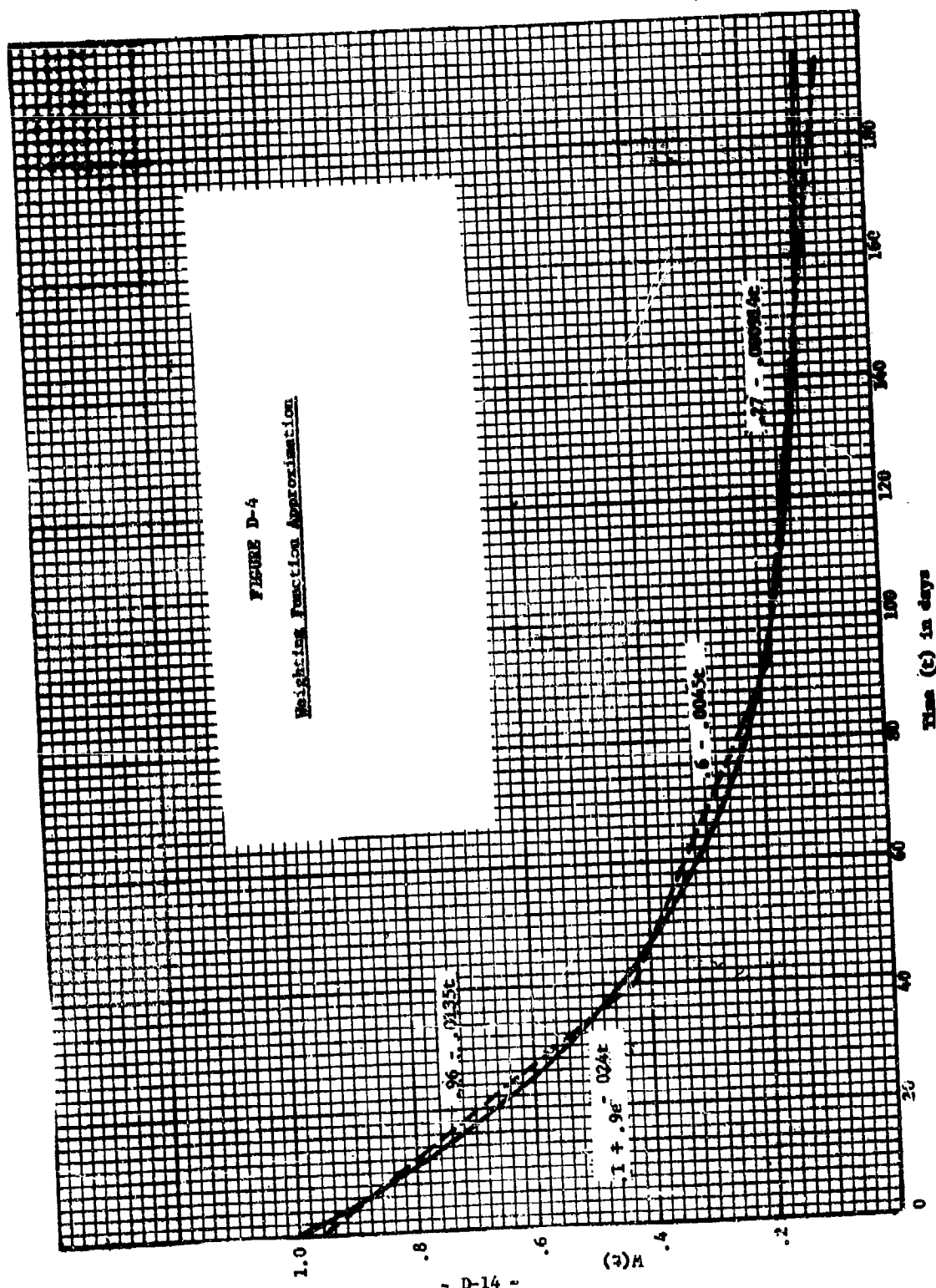
In Case II, where the maximum (Equation D-5) occurs for $t < t_e + \Delta t$, a slightly different approach will be used. First, it is necessary to use an approximation for $W(t)$ that is applicable over a wider range of Δt 's. The function which will be used is

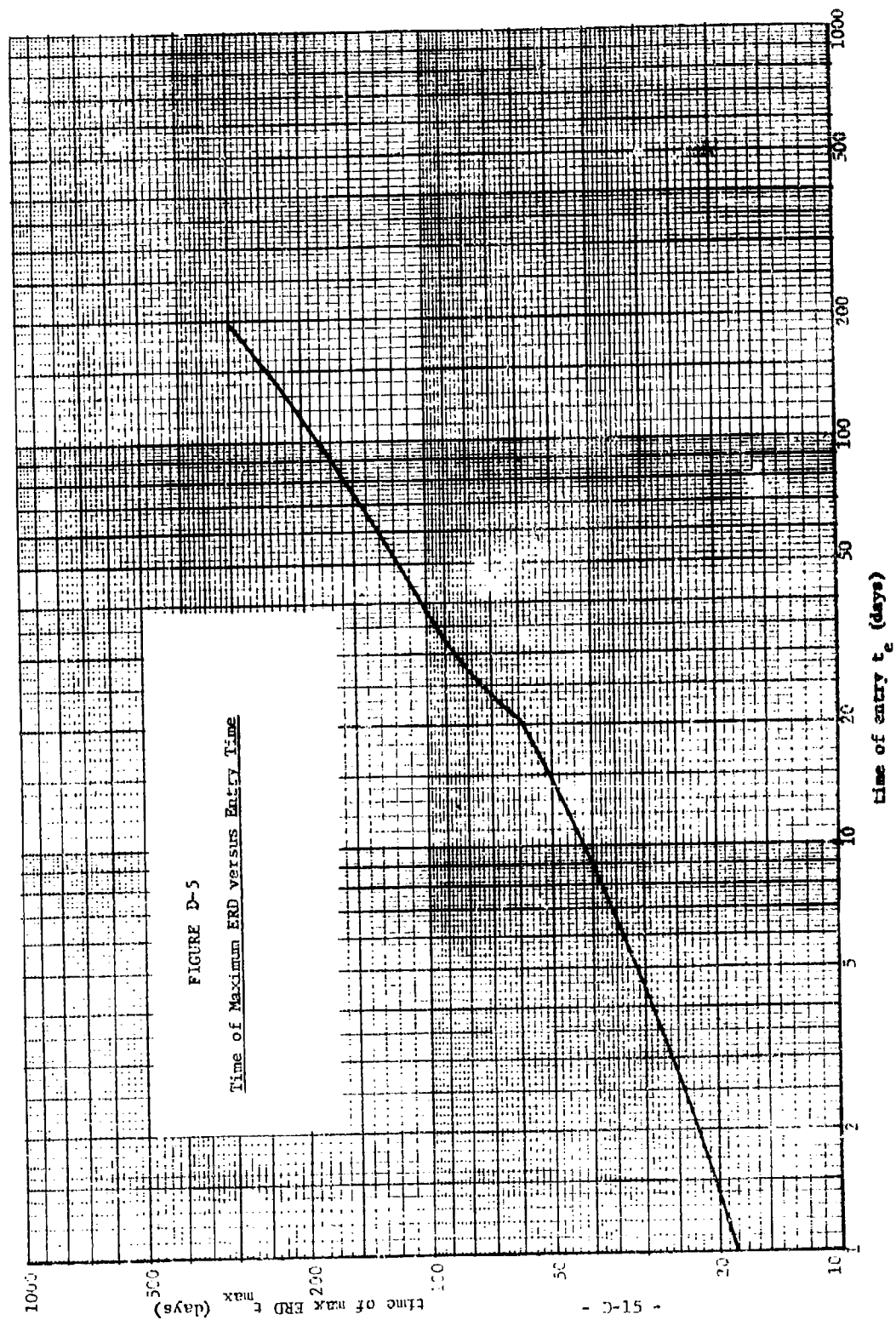


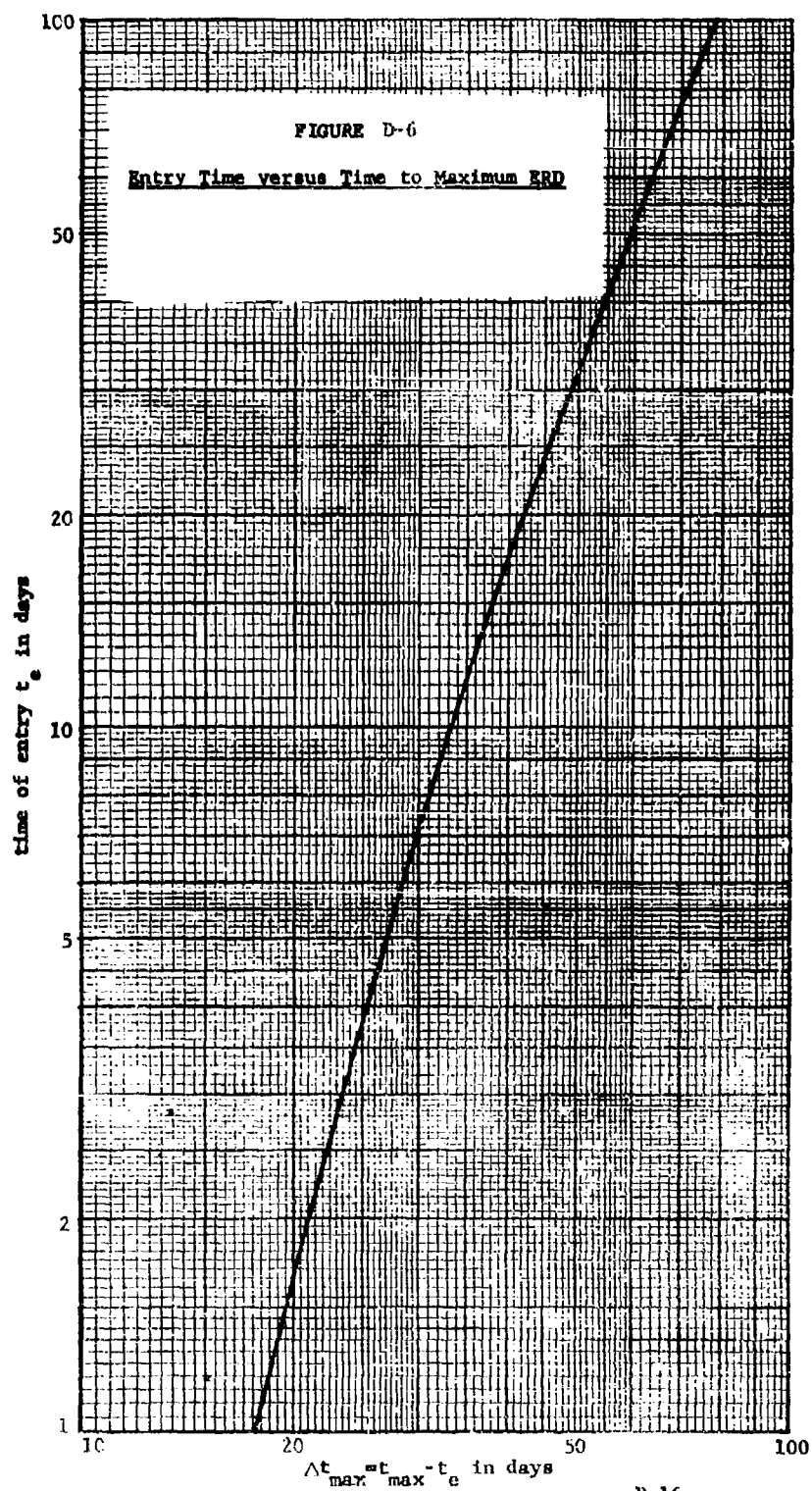
$$W(t) = \begin{cases} .96 - .0135t & 0 \leq \frac{t}{24} \leq 40 \\ .6 - .0045t & 40 < \frac{t}{24} \leq 92 \\ .27 - .000914t & 92 < \frac{t}{24} \end{cases} \quad (D-15)$$

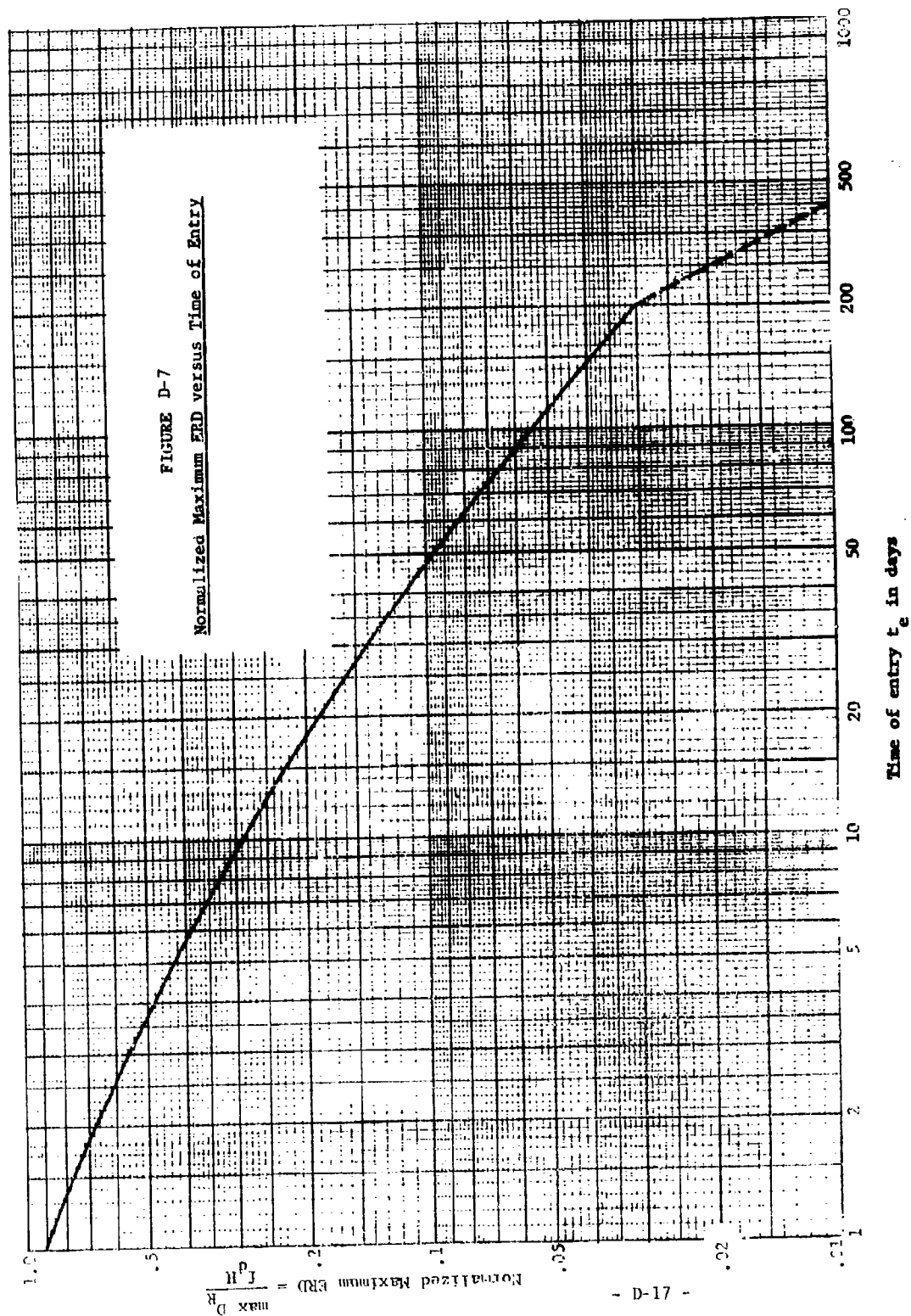
where t is in hours. This function is shown in Figure D-4 along with the common approximation given as Equation D-8. If this expression, with $t-x$ substituted for t , is used to replace $W(t-x)$ in Equation D-5, then the integration can be performed and the derivative of D_R with respect to t can be taken. Setting this derivative, $\frac{dD_R}{dt}$, equal to zero produces the t 's that maximize the dose D_R . These t 's (denoted by t_m) are graphed in Figure D-5 as a function of t_e . The discontinuity in the first derivative of this function that appears when t_e is 21 days in Figure D-5 is the result of the discontinuity in the first derivative of $W(t)$ as given in Equation D-15. It is useful to smooth the function in the region surrounding $t_e = 21$ days and replot the function. This has been done to arrive at Figure D-6, which presents $t_m - t_e = \Delta t_m$ (that is, the time interval between t_e and the time when the ERD becomes a maximum) as a function of t_e . The value of the corresponding maximum ERD is presented in Figure D-7 as a function of t_e . This illustration, Figure D-7, presents the normalized maximum ERD, $\frac{D_R}{f_d H}$, as a function of the activity entry time, t_e , for the Case II situations where the maximum occurs before the activity is completed. Therefore, Figure D-7 applies to situations where the activity durations, Δt , are greater than the $t_m - t_e = \Delta t_m$.

To compare the Case II approach to ERD that produced Figure D-7 with







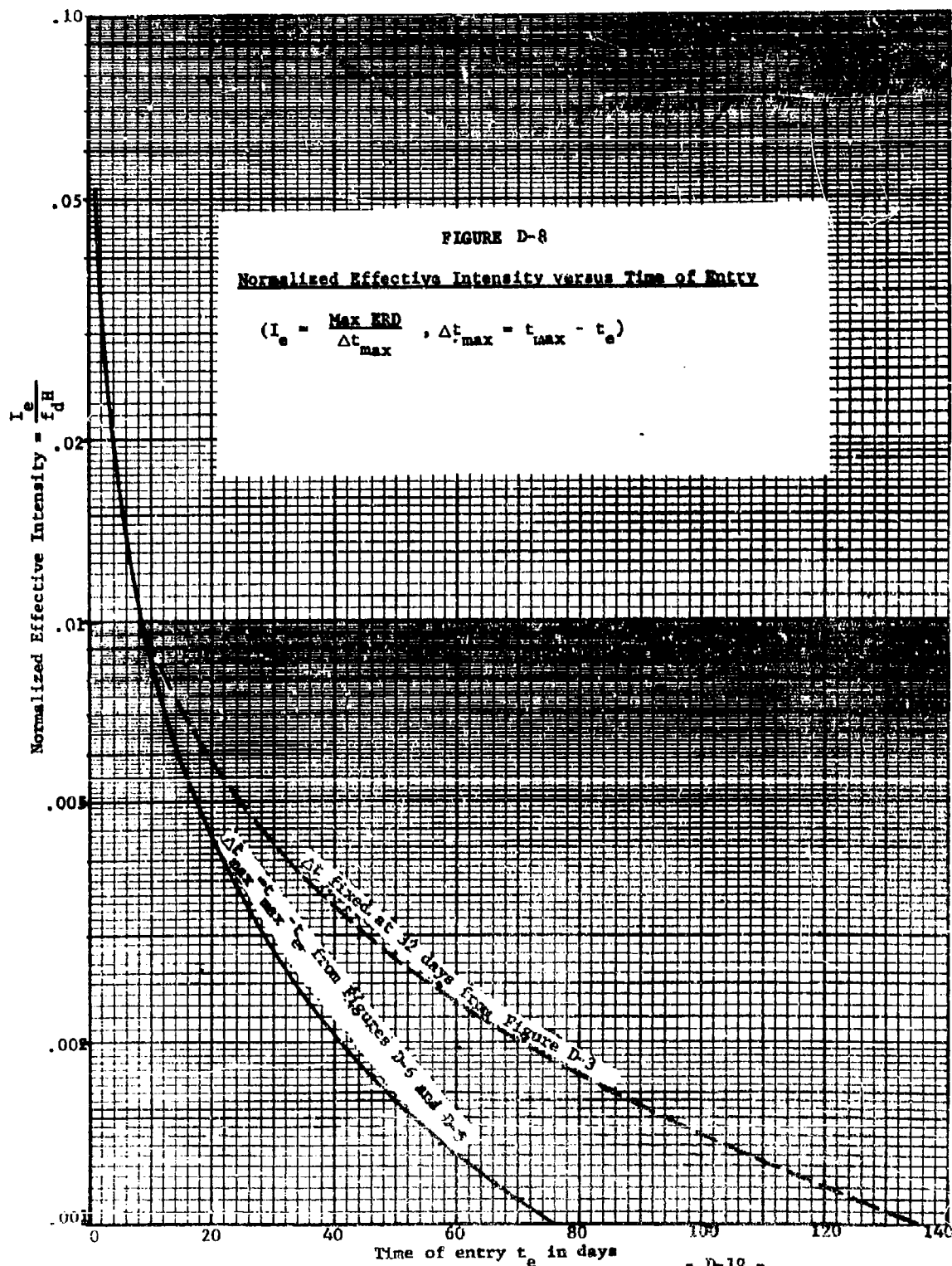


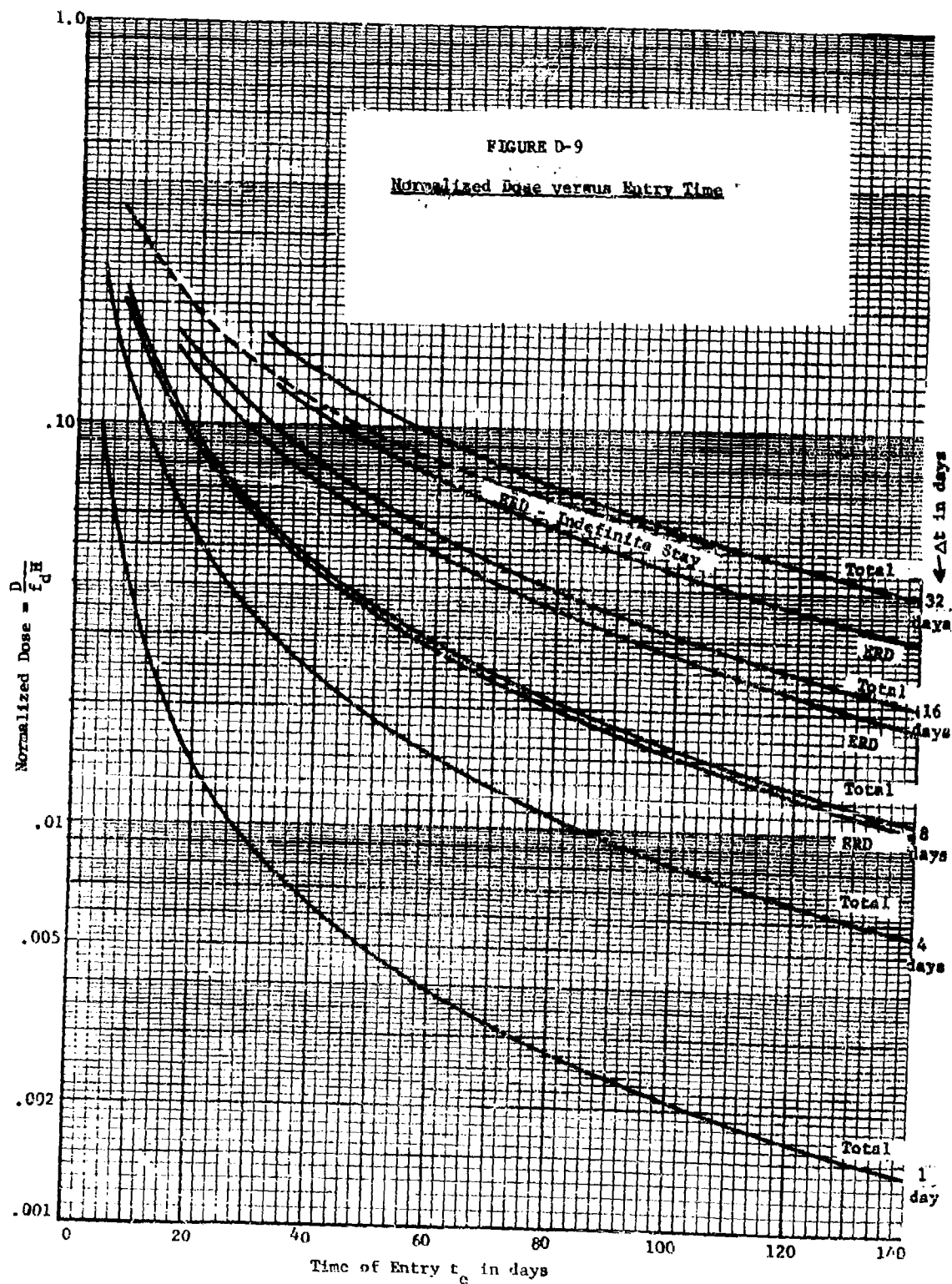
the Case I approach to ERD that produced Figure D-3, it is necessary to introduce a fictitious Δt into Figure D-7. If this is done, then the Case II result can be redrawn as $\frac{D_R/\Delta t}{f_d H} = \frac{I_e}{f_d H}$ versus t_e and then compared with the Case I graph in Figure D-3. To do this, the most logical Δt to use in the Case II approach is $\Delta t_m = t_m - t_e$ as presented in Figure D-6 as a function of t_e . Figure D-8 was obtained for such a comparison by dividing the $\frac{D_R}{f_d H}$ values in Figure D-7 by the $t_m - t_e$ values in Figure D-6. The dashed line included in Figure D-8 is the curve for $\Delta t = 32$ from Figure D-3 extended to intersect the solid line (Case II approach) at the proper position.

This completes the second approach to the dose received in the performance of a certain activity. The results of the two approaches (Figures D-1, D-3, and D-7) are summarized in Figure D-9 where the normalized total dose $\frac{D_T}{f_d H}$, and normalized maximum ERD, $\frac{D_R}{f_d H}$, are displayed as a function of activity entry time, t_e , and activity duration, Δt . In the following section, these functions will be inverted to display the activity entry time when the duration, Δt , and the dose to be received, D_R or D_T , are specified.

E. Activity Entry Lead Time

The activity entry lead time is the time before which the activity cannot begin if the duration, Δt , and the dose, D_R or D_T , are specified. In the previous discussion the dose was determined in terms of the activity entry time, t_e , and the activity duration, Δt . These same expressions can be inverted to give the entry time, t_e , in terms of the dose and the duration. Expressed in this manner, t_e is the activity entry lead time.





The lead time will depend on the normalized dose, the type of dose (ERD or total dose), and the duration. If the interest is in a specified total dose, then from Equation D-7, the lead time is:

$$t_e = \left(\frac{f_d H \Delta t}{D_T} \right)^{.833} - \frac{\Delta t}{2} \text{ hours.} \quad (D-16)$$

If the interest is in a specified maximum ERD occurring at the time $t_e + \Delta t$, Case I, then from Equation D-13 the lead time is:

$$t_e = \left(\frac{f_d H \Delta t}{D_R} \right)^{.833} (1 - .008 \Delta t)^{.833} - \frac{\Delta t}{2} \text{ hours.} \quad (D-17)$$

If the interest is in a specified maximum ERD occurring before time $t_e + \Delta t$, Case II, then the lead time is graphically determined from Figure D-7.

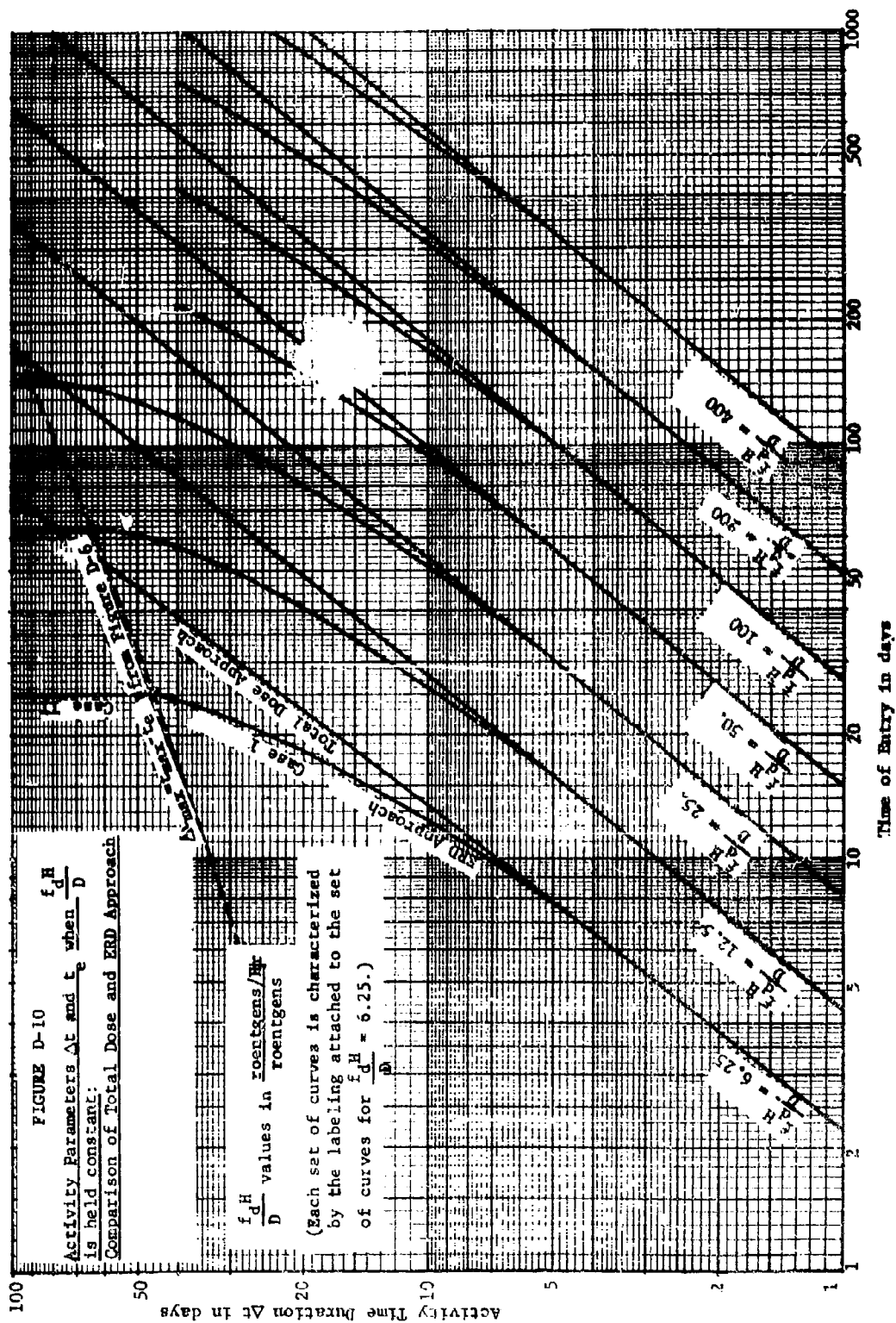
These three approaches to the activity entry lead time are shown in Figure D-9 (t_e versus normalized dose) and in Figure D-10 (t_e versus activity duration Δt). These two figures and Equations D-16 and D-17 will be used in the following discussion to determine the effect of the countermeasure, f_d , on reducing the lead time.

F Countermeasure Effect on Lead Time

From the lead time equations (Equations D-16 and D-17) it can be seen that as the countermeasure effectiveness increases (that is, as f_d decreases) the lead time, t_e , decreases. This effect can be viewed as the lead time saved, T , as follows:

$$T = t_e^* - t_e \text{ hours} \quad (D-19)$$

where t_e^* is the lead time without the countermeasure (a result of setting f_d equal to 1) and t_e is the lead time with the countermeasure. Therefore,



the time saved when the total dose is specified is, from Equation D-16,

$$T = \left(\frac{H}{I_e} \right)^{.833} (1 - f_d^{.833}) \text{ hours.} \quad (D-20)$$

From Equation D-17, the time saved when maximum ERD occurring at time $t_e + \Delta t$ is specified, Case I, is

$$T = (1 - .008\Delta t)^{.833} \left(\frac{H}{I_e} \right)^{.833} (1 - f_d^{.833}) \text{ hours.} \quad (D-21)$$

In these two equations (Equation D-20 and Equation D-21) care must be exercised in estimating the error. The error arises out of the error that is contained in t_e^* and in t_e in Equation D-19. Because these two terms in Equation D-19 are of opposite sign, the errors are also of opposite sign. Therefore, the error in T is less than either the error in t_e^* or the error in t_e . Because both t_e^* and t_e involve the same time interval, Δt , and because t_e is less than t_e^* , the dominant error arises out of the t_e term. This error increases as t_e decreases and hence, increases as f_d decreases (see Equations D-16 and D-17). Therefore, Equations D-20 and D-21 cannot be used as f_d approaches zero. (The actual error in T is less than the error in t_e , which is less than the error in D_T as given in the paragraph following Equation D-7.) If one is careful not to apply Equation D-20 when f_d approaches zero (and, normally, when f_d is less than .2), then Equation D-20 can be interpreted as the product of potential maximum time saved,

$$T_m = \left(\frac{H}{I_e} \right)^{.833} \quad (D-22)$$

and the fraction realized due to imperfect countermeasure effectiveness,

$$F = (1 - f_d)^{.833} \quad , \quad (D-23)$$

as follows:

$$T = T_m F \quad . \quad (D-24)$$

Similarly, Equation D-21 can be interpreted as the product of T_m , F , and the result of biological recovery,

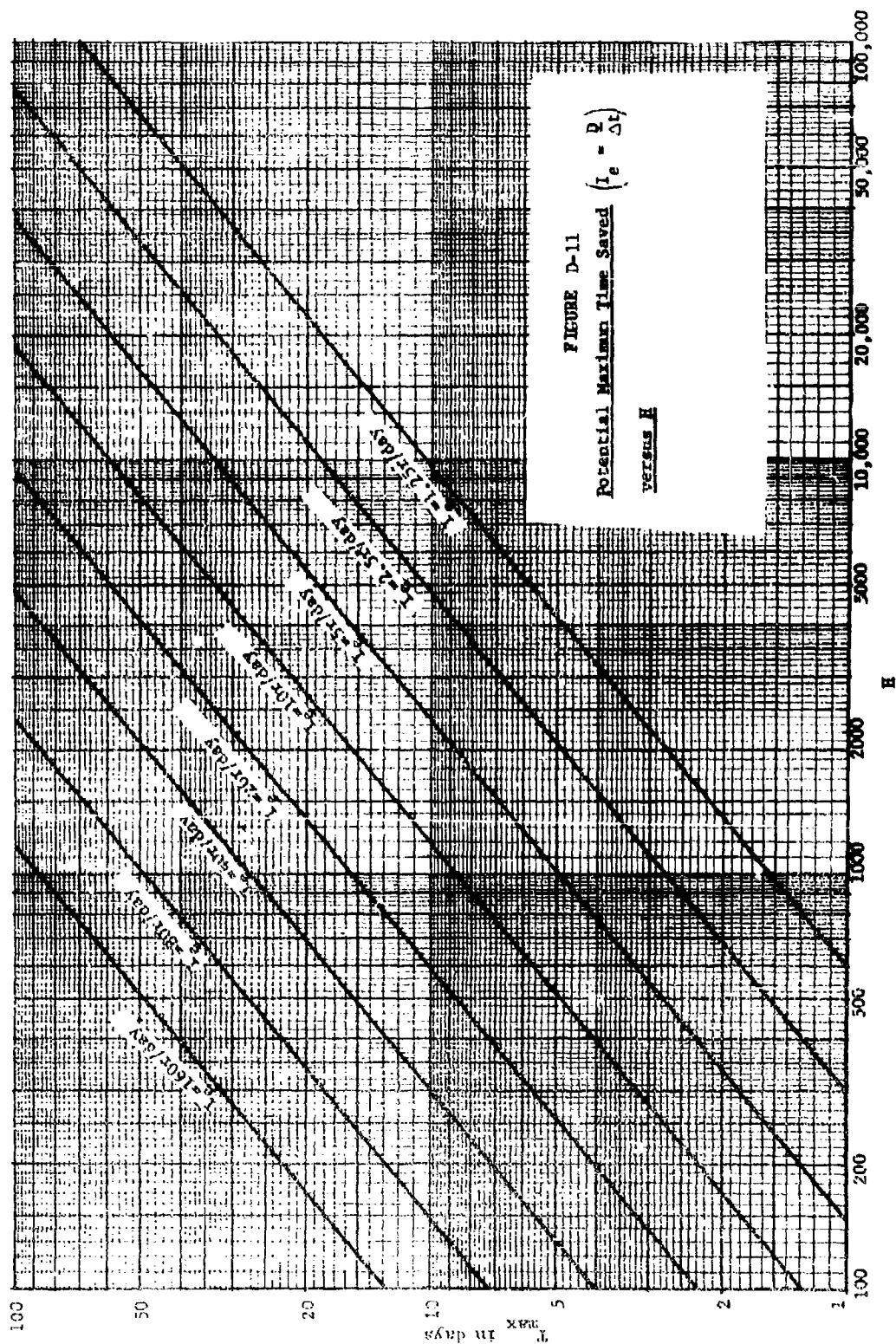
$$B = (1 - .008 \Delta t)^{.833} \quad , \quad (D-25)$$

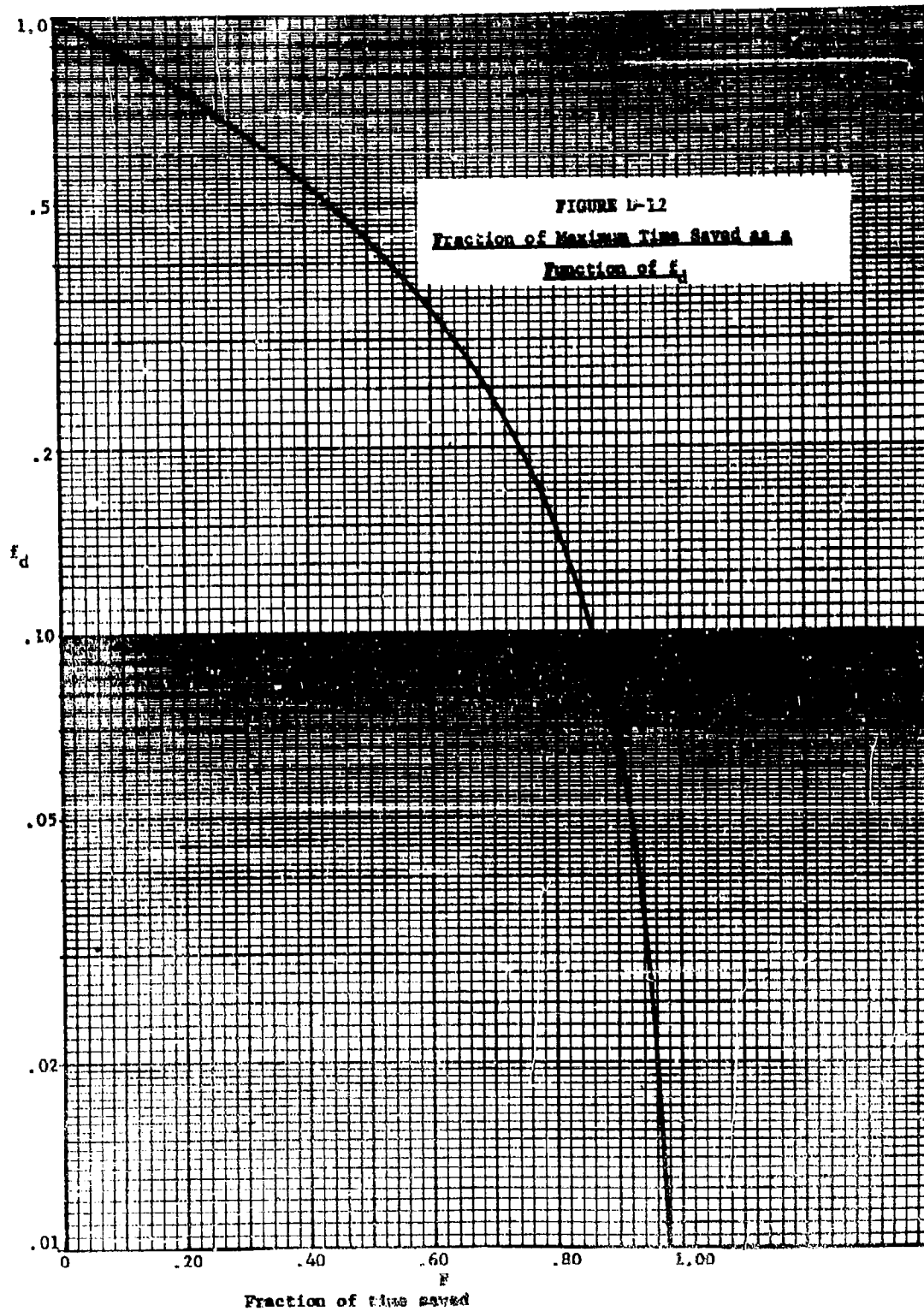
as follows:

$$T = T_m FB \quad . \quad (D-26)$$

By interpreting Equations D-20 and D-21 in this manner it is easy to quickly determine the effectiveness of f_d , of allowable ERD or total dose constraints, and of $\frac{H}{I_e}$ in reducing the lead time to activity resumption with countermeasure activities. For this purpose, the three pertinent relationships, Equations D-22, D-23, and D-25, are displayed in Figures D-11, D-12 and D-13 respectively.

The effect of f_d and $\frac{H}{I_e}$ on the time saved, T , when allowable total dose is specified, can be summarized by combining Figures D-11 and D-12 as indicated by Equation D-24. The resultant composite is displayed as Figure D-14. This figure presents the time saved in days as a function of the countermeasure effectiveness, f_d , when the other variables are constrained in a particular manner. Two different methods of constraining the variables are used to produce two sets of curves. In the first set of curves (solid lines), the normalized intensity, $\frac{I_e}{H}$ is fixed. If this is viewed as $\frac{I_e}{f_d H}$





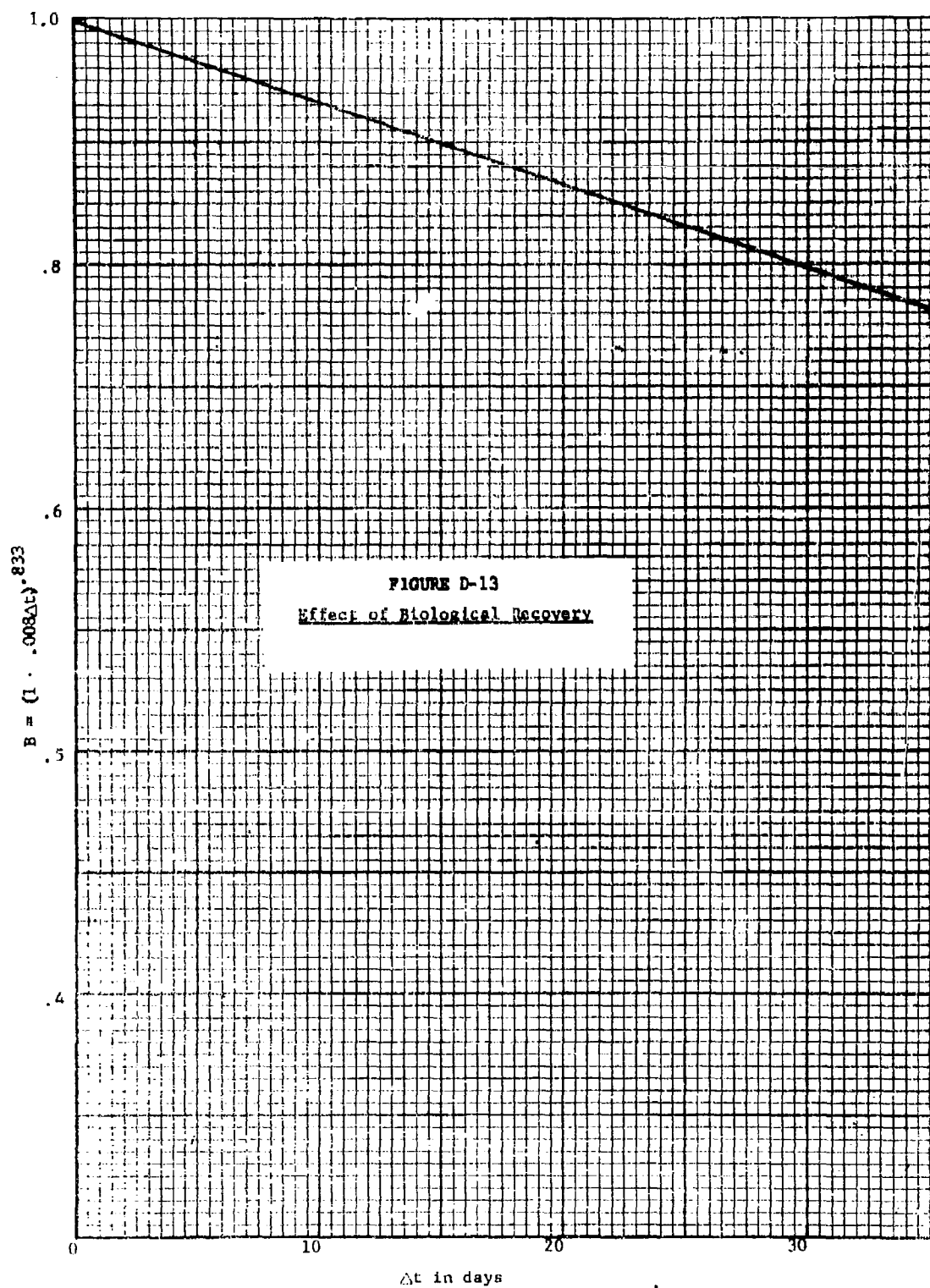


FIGURE D-13
Effect of Biological Recovery

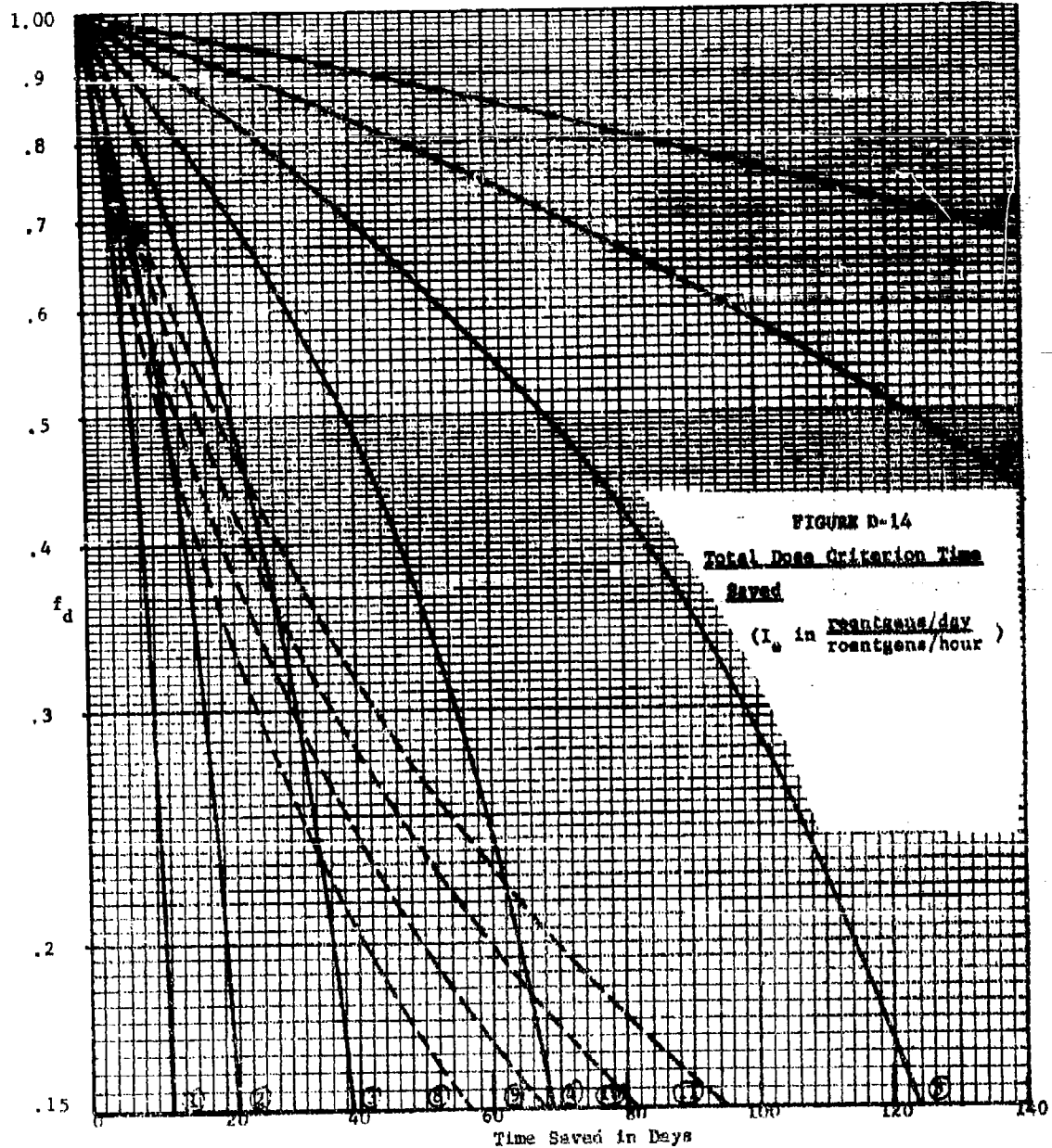
with f_d set equal to unity, then the corresponding solid curves relate the time saved to f_d when the time to the center of the performance interval, $t_e + \frac{\Delta t}{2}$, is held constant. This interpretation follows directly from Equation D-7, which has $t_e + \frac{\Delta t}{2}$ equal to $\left(\frac{f_d H}{I_e}\right)^{.833}$ times a constant. Because $f_d=1$, the above time of entry, t_e , is the time the activity may commence when the countermeasure is not activated. In summary, when the activity-intensity characteristics, H , the allowable dose, D_T , and the activity duration, Δt , are specified, the solid curve for $\frac{D_T}{H \Delta t} = \frac{I_e}{H}$ defines that situation and shows how the time saved in commencing the activity depends on the countermeasure effectiveness, f_d . For the same situation, the actual time of entry can be determined from Figure D-1.

The second set of curves (dashed lines) in Figure D-14 is developed by holding constant the time of entry with the countermeasure activated. This is accomplished by altering the form of Equation D-20 as follows:

$$T = \left(\frac{H}{I_e}\right)^{.833} (1 - f_d^{.833}) \quad (D-20)$$

$$= \left(\frac{f_d H}{I_e}\right)^{.833} (f_d^{-.833} - 1) \quad (D-27)$$

In the dashed curves, the first factor, $\left(\frac{f_d H}{I_e}\right)^{.833}$, has been held constant. From Equation D-7, this factor is equal to $t_e + \frac{\Delta t}{2}$, which is the time to the center of the performance interval when the countermeasure is activated. In Figure D-14, these dashed lines were developed for the case where no activity would be recovered before the end of a two week



$$① \frac{I_e}{H} = .02, t_e^* + \frac{\Delta t}{2} = 15.3 \text{ days}$$

$$② \frac{I_e}{H} = .01, t_e^* + \frac{\Delta t}{2} = 27.4 \text{ days}$$

$$③ \frac{I_e}{H} = .005, t_e^* + \frac{\Delta t}{2} = 48.8 \text{ days}$$

$$④ \frac{I_e}{H} = .0025, t_e^* + \frac{\Delta t}{2} = 86.7 \text{ days}$$

$$⑤ \frac{I_e}{H} = .00125, t_e^* + \frac{\Delta t}{2} = 155. \text{ days}$$

$$⑥ \frac{I_e}{H} = .000625, t_e^* + \frac{\Delta t}{2} = 276. \text{ days}$$

$$⑦ \frac{I_e}{H} = .0003125, t_e^* + \frac{\Delta t}{2} = 494. \text{ days}$$

$$⑧ t_e = 14 \text{ days}, \Delta t = 1 \text{ day}$$

$$⑨ t_e = 14 \text{ days}, \Delta t = 7 \text{ days}$$

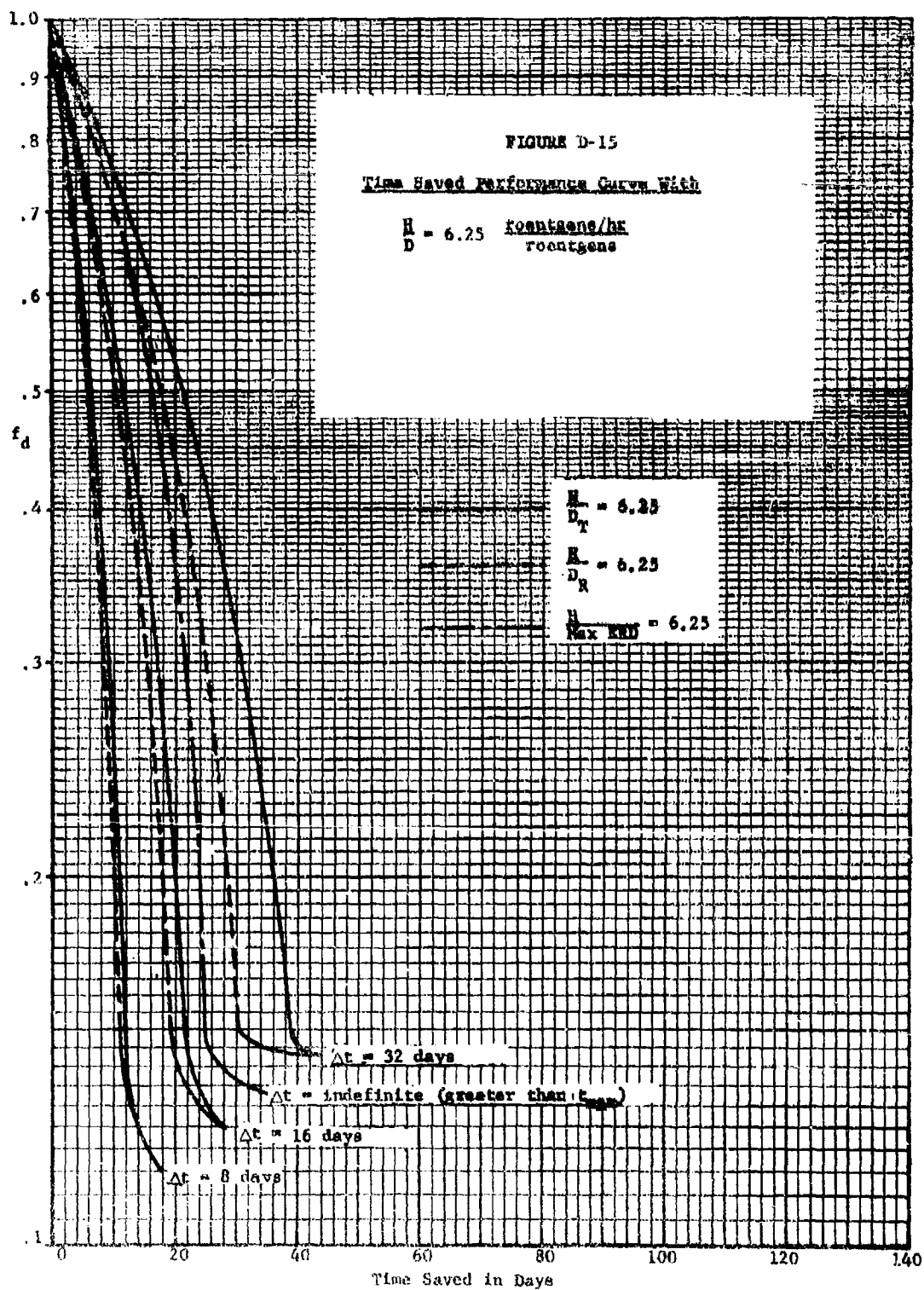
$$⑩ t_e = 14 \text{ days}, \Delta t = 14 \text{ days}$$

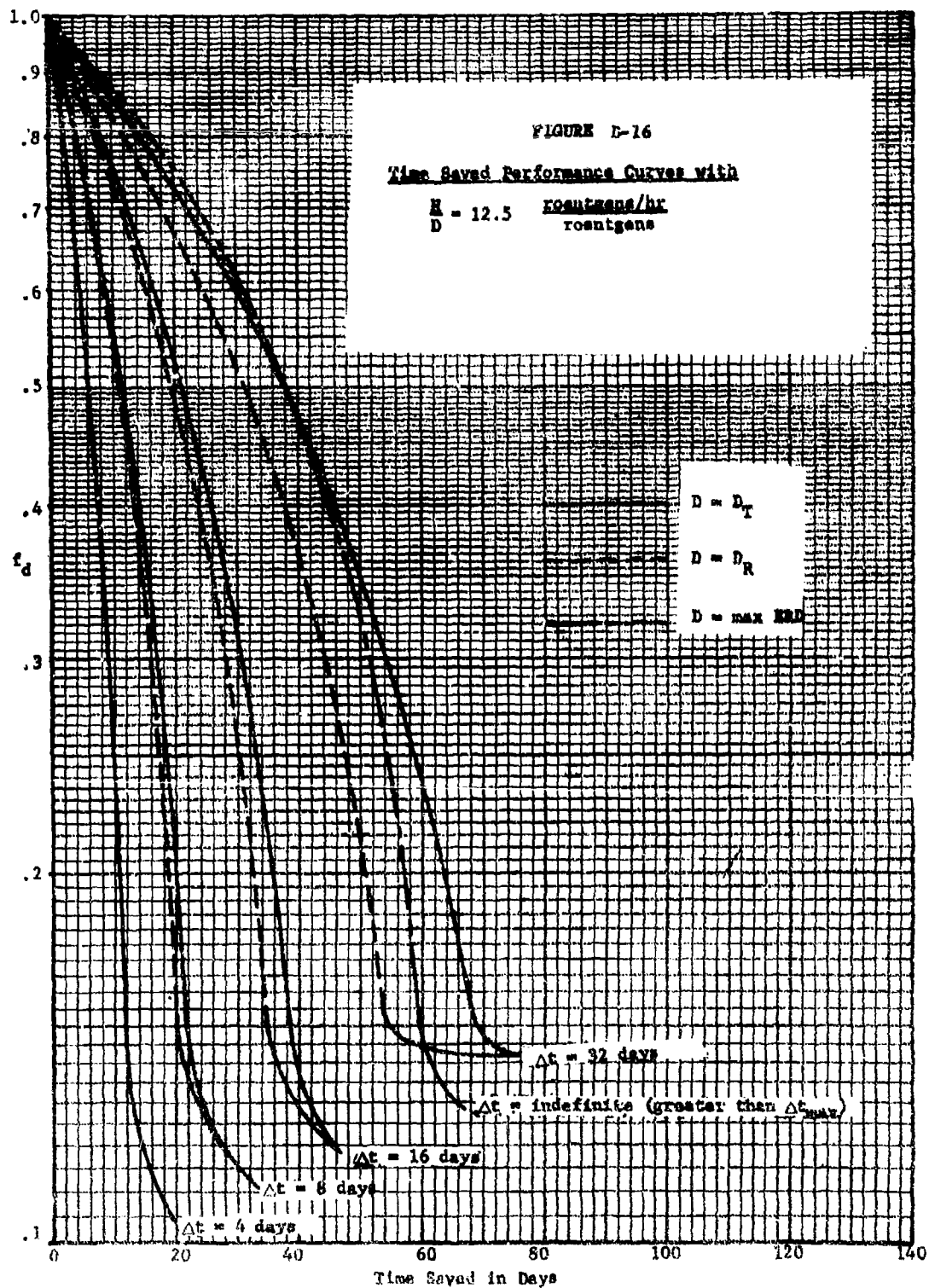
$$⑪ t_e = 14 \text{ days}, \Delta t = 21 \text{ days}$$

shelter period, independent of any countermeasure activation. This was accomplished by setting t_e equal to 14 days. The four curves were then selected by varying the performance interval, Δt . The four curves, therefore, represent the bound of useable f_d , or T , when the time of entry with the countermeasure activated is fixed.

To determine the time saved when maximum ERD occurs during the performance of the activity (rather than at the conclusion of the activity), Case II, Equation D-19 is solved graphically by using Figure D-7. That is, for a given normalized dose, $\frac{D_R}{H}$, the entry time without the countermeasure, t_e^* , is determined from Figure D-7. Then the effect of the countermeasure is determined by obtaining from Figure D-7 the entry time t_e when the normalized dose, $\frac{D_R}{f_d H}$, is used. The difference, $t_e^* - t_e$ is the time saved for the situation defined by the given value of $\frac{D_R}{H}$.

The three approaches to time saved are combined and presented in a set of performance curves, Figures D-15 through D-22. Each figure shows how the time saved varies as a function of f_d , the activity duration, Δt , and the manner in which the dose (total dose or ERD) is defined when the normalized dose, $\frac{D}{H}$, is specified. The figures cover normalized doses from .16 to .00125 in seven steps. The activity durations considered are 1, 2, 4, 8, 16, and 32 days (total dose and maximum ERD occurring before the end of the activity, Case I), and an infinite duration (maximum ERD occurring before the end of the activity, Case II). In addition, any curve not explicitly presented can be quickly obtained in the manner discussed in the preceding paragraphs of this section.





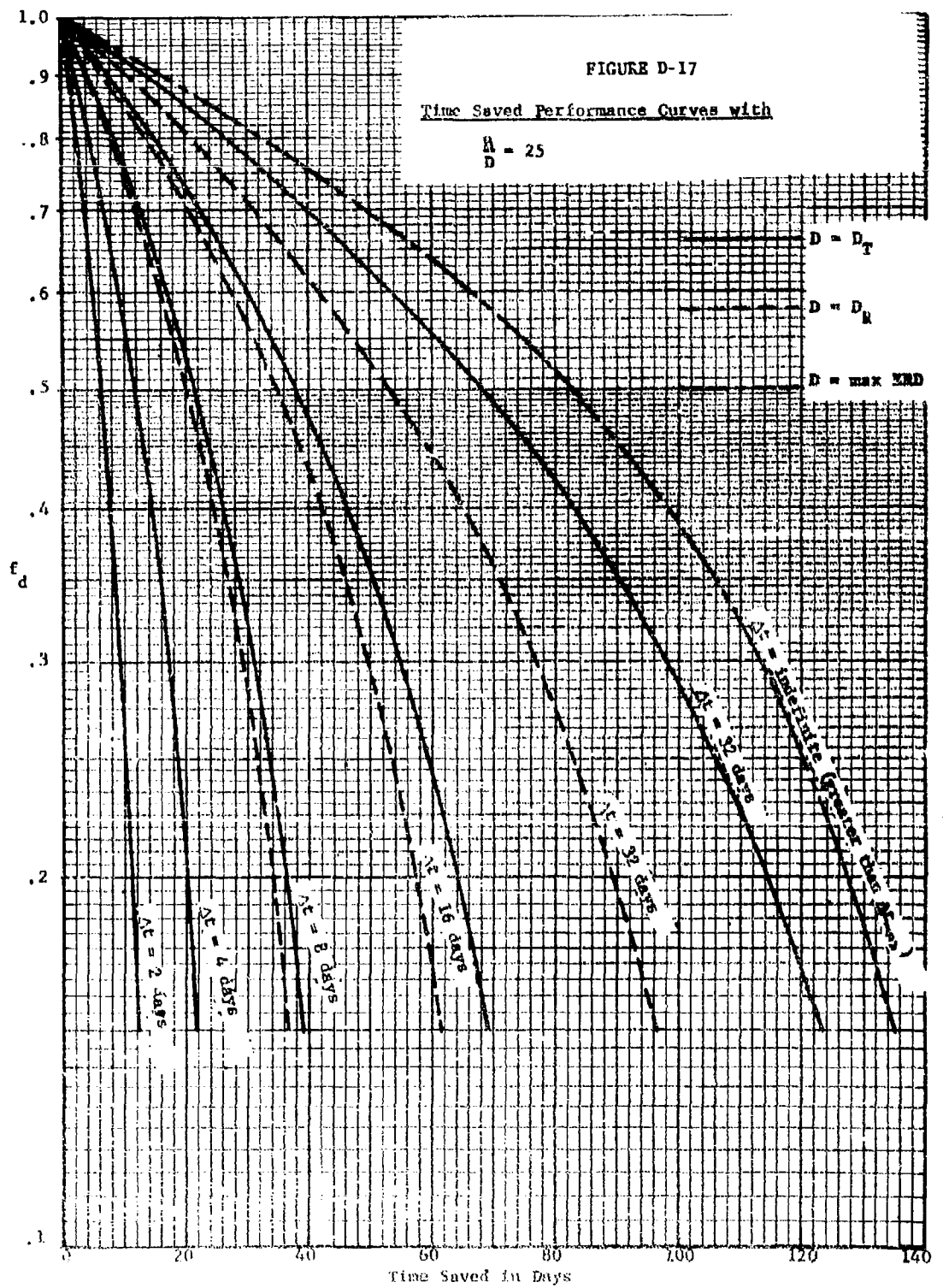


FIGURE D-18

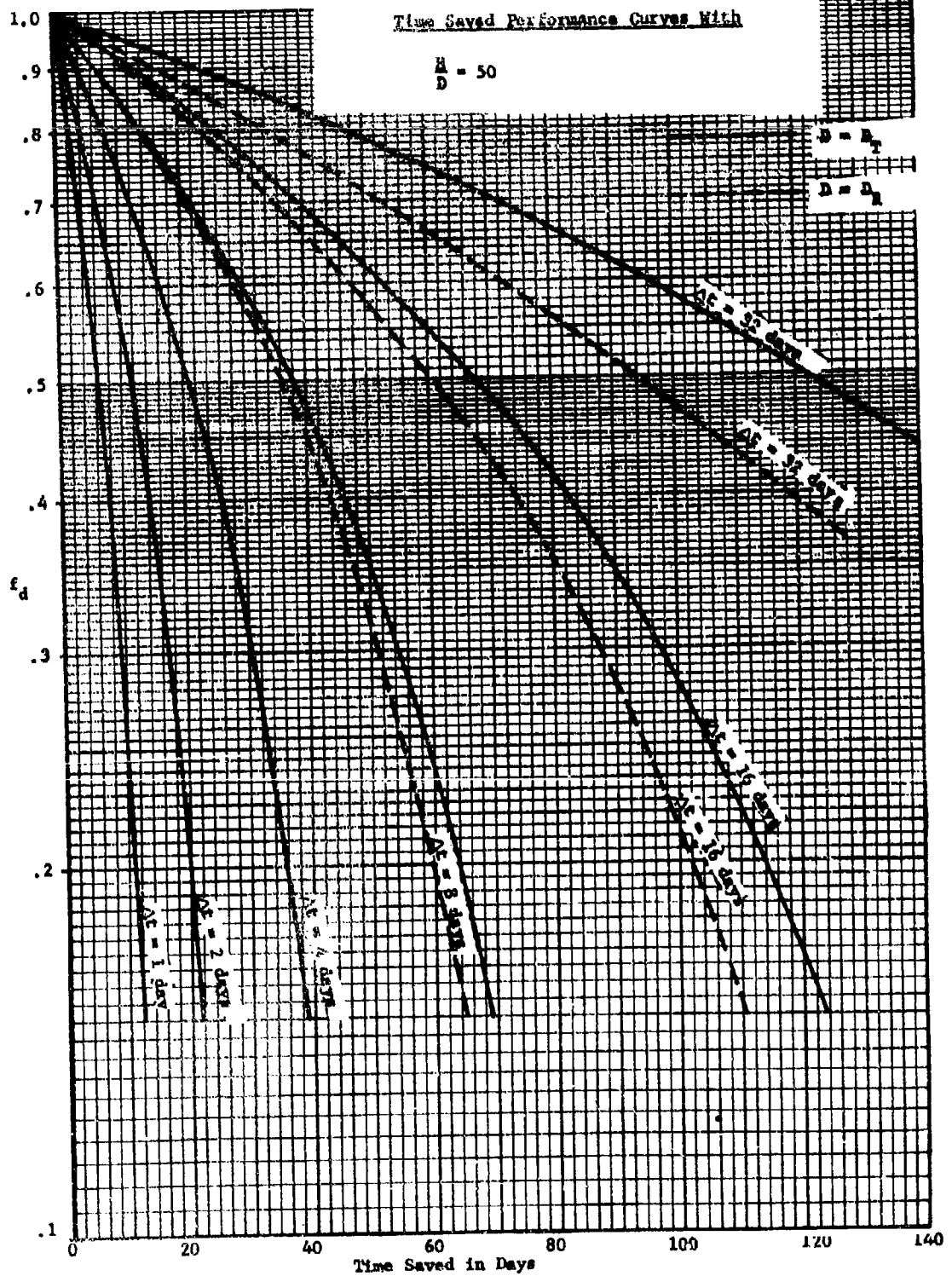
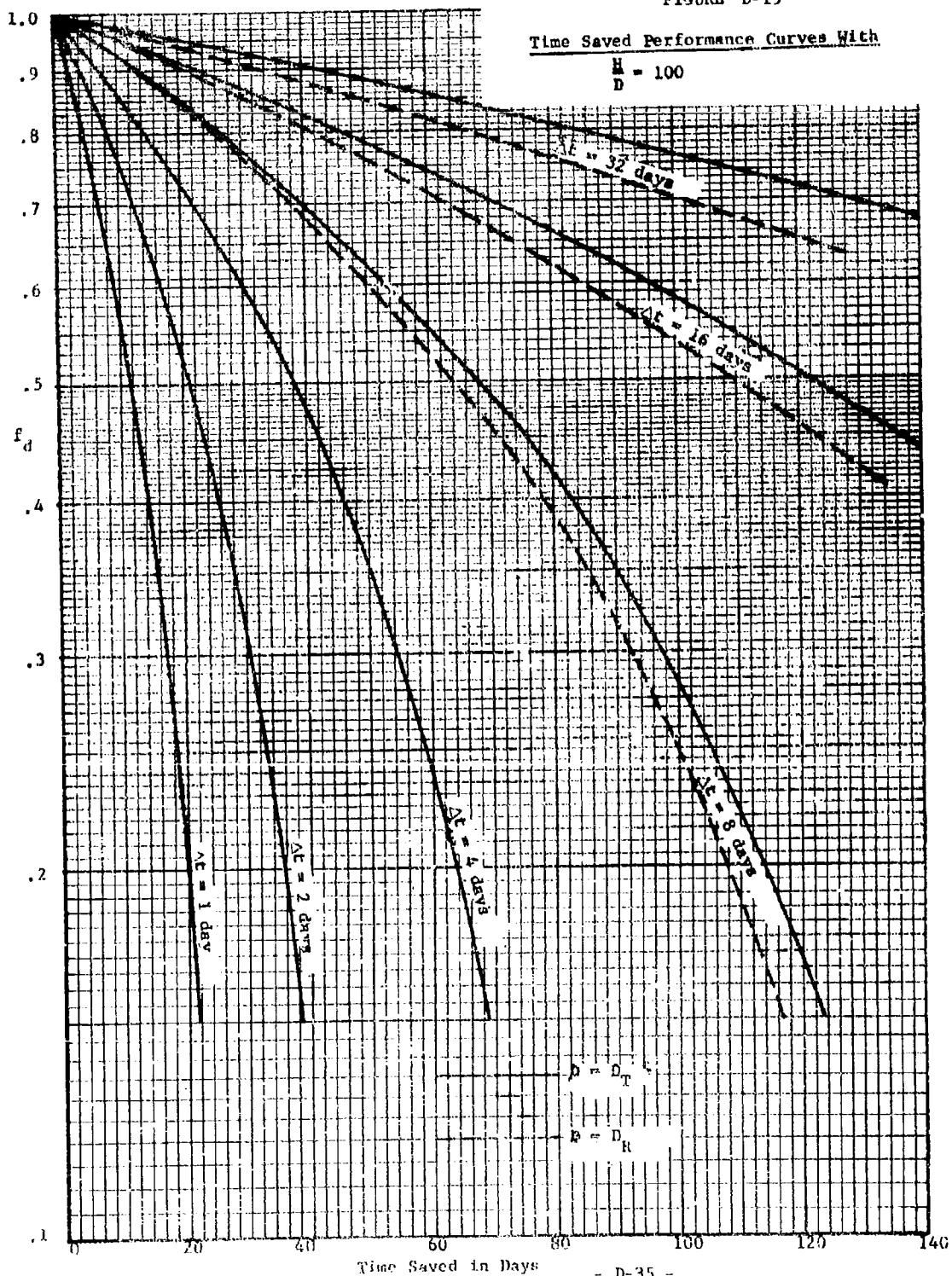


FIGURE D-19

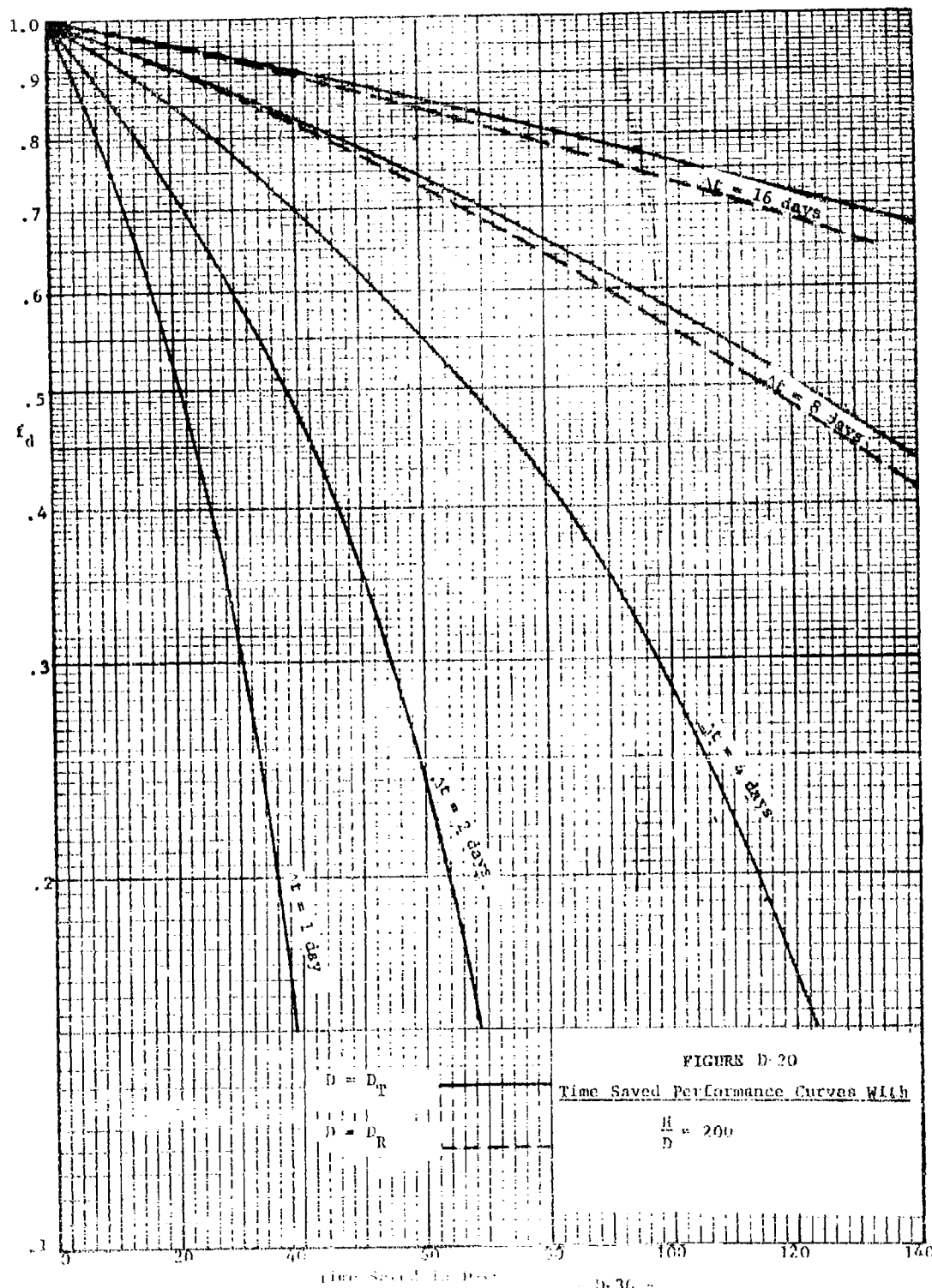
Time Saved Performance Curves With

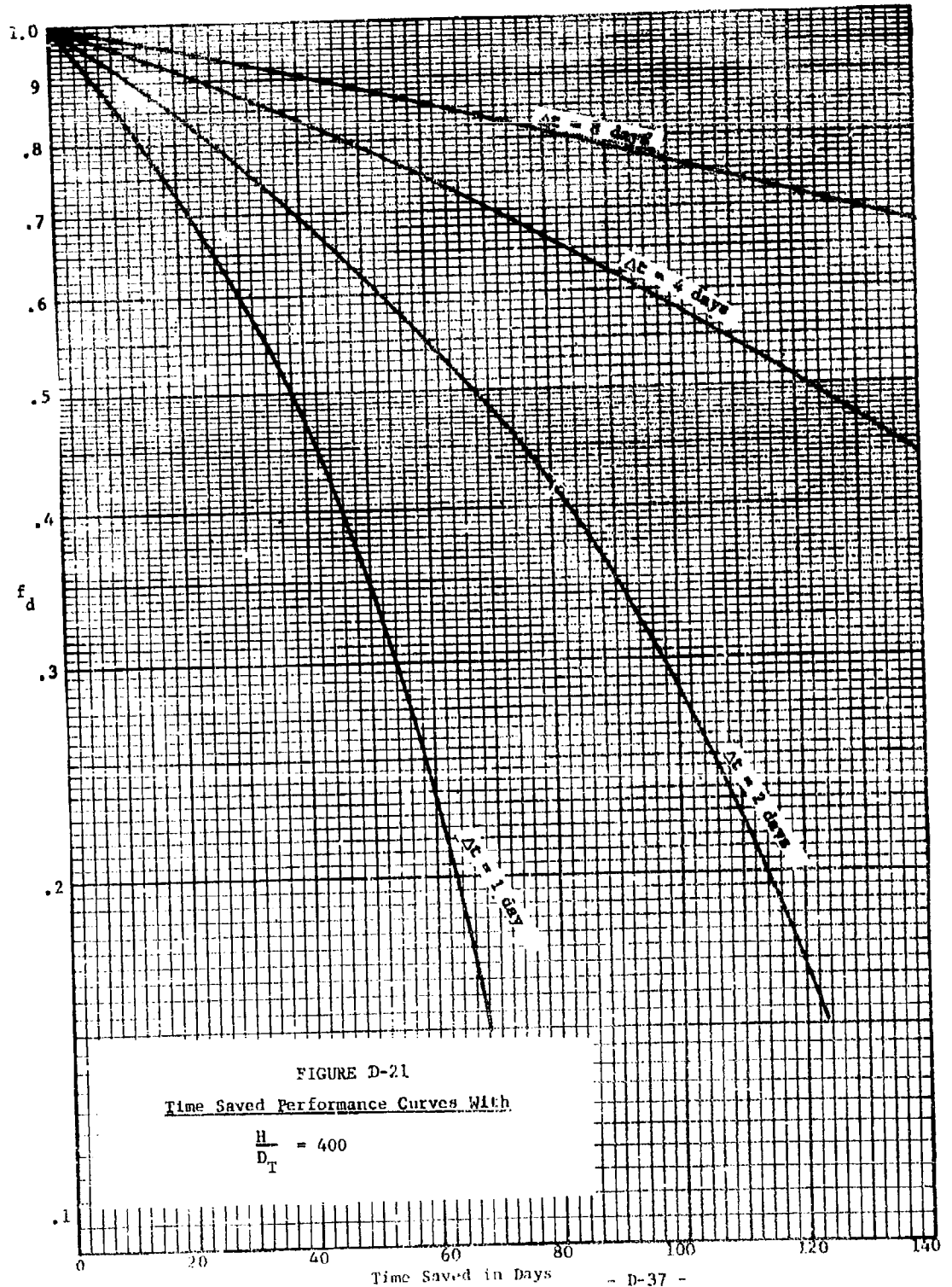
$$\frac{H}{D} = 100$$

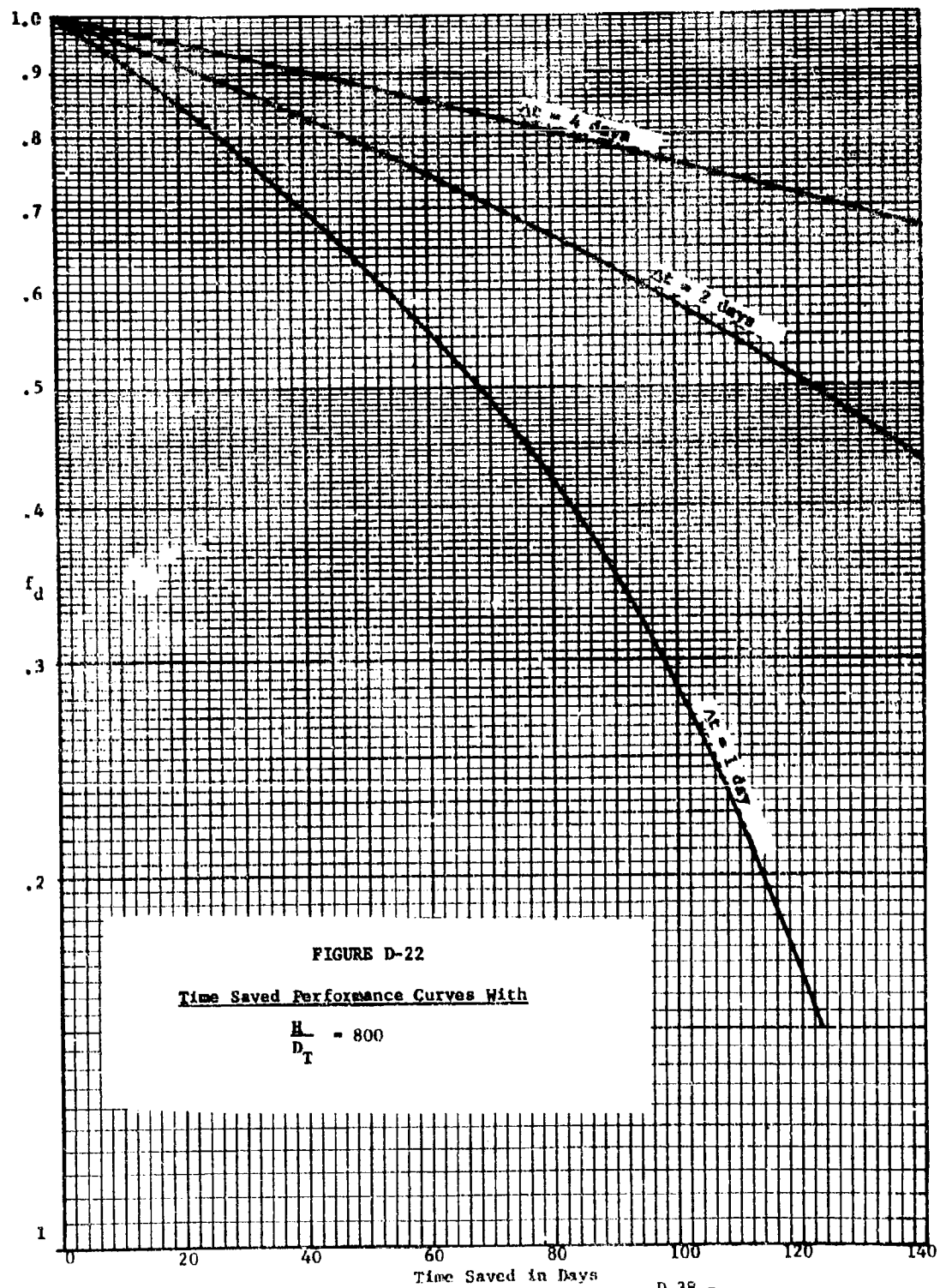


$D = D_T$

$D = D_R$







An additional set of performance curves, Figures D-23 through D-29, are included to illustrate the H , I_e , f_d trade-offs available when the time to be saved is specified and total dose is the constraint. Figure D-23 shows the effect of f_d and I_e on the relationship between H and T . Each of Figures D-24 through D-29 show, for a fixed f_d , the H , I_e trade-offs when the time to be saved is specified as 1, 2, 4, 7, 14, 21, 28, 35, or 42 days. This set of curves is presented to help delimit the range of situations where countermeasure activities are potentially useful in accelerating the recovery process. A general discussion of this range of situations is presented in the following section.

III. DISCUSSION OF RESULTS

The preceding section developed and presented curves that define the recovery lead time, t_e , and the amount by which the lead time is reduced, T , as a function of:

- (1) H , the activity radiation characteristics;
- (2) Δt , the duration of the activity;
- (3) D , the allowable dose received in performing the activity;
- (4) $\frac{D}{\Delta t} = I_e$, the effective dose rate while performing the activity;
and,
- (5) f_d , the effectiveness of the radiological countermeasure.

Having determined the effect of the above parameters, it is worthwhile to examine their combined effect for the purpose of estimating the range of situations where recovery-oriented countermeasures appear to be most useful. This final section will present such an examination in a

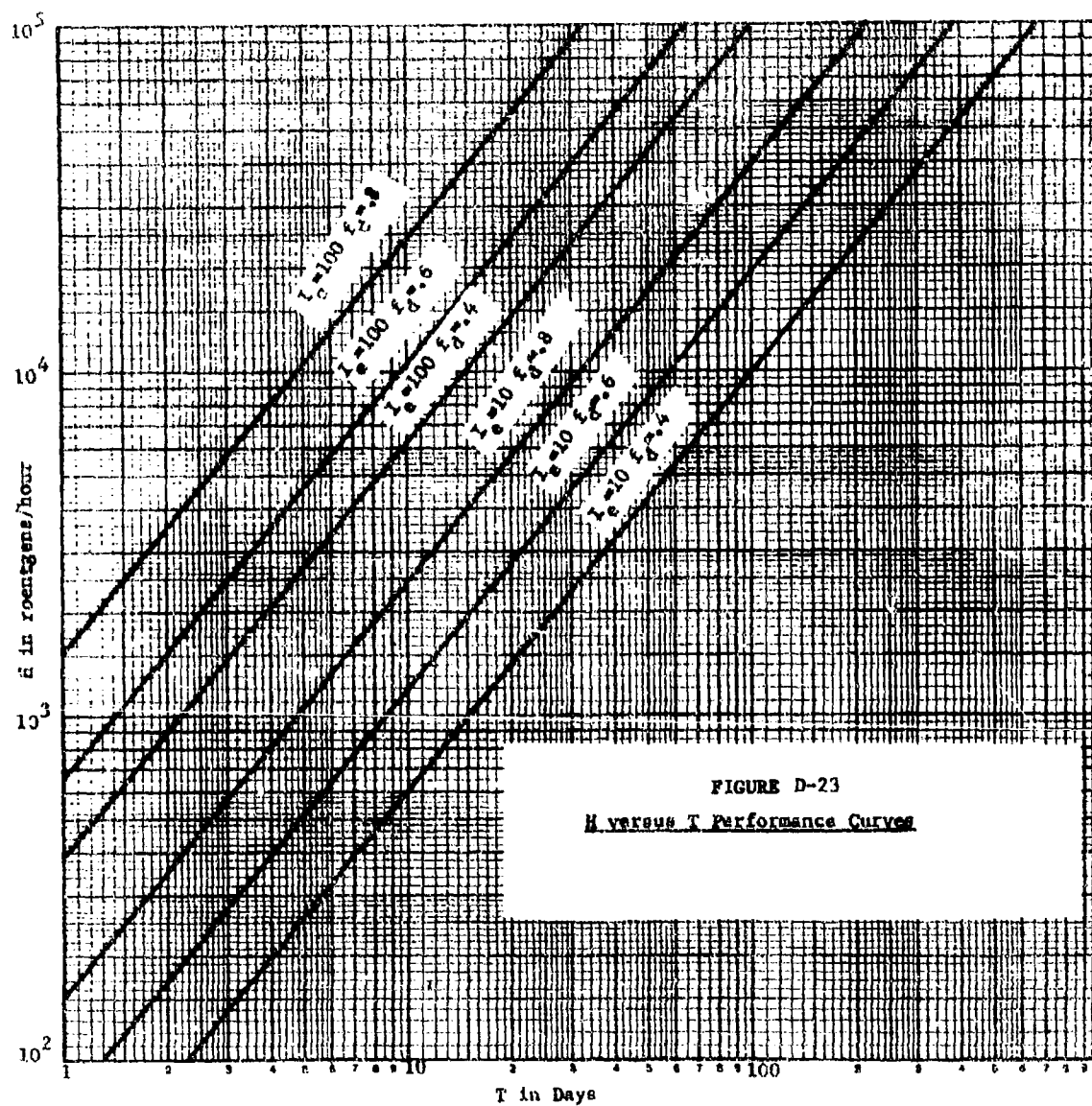
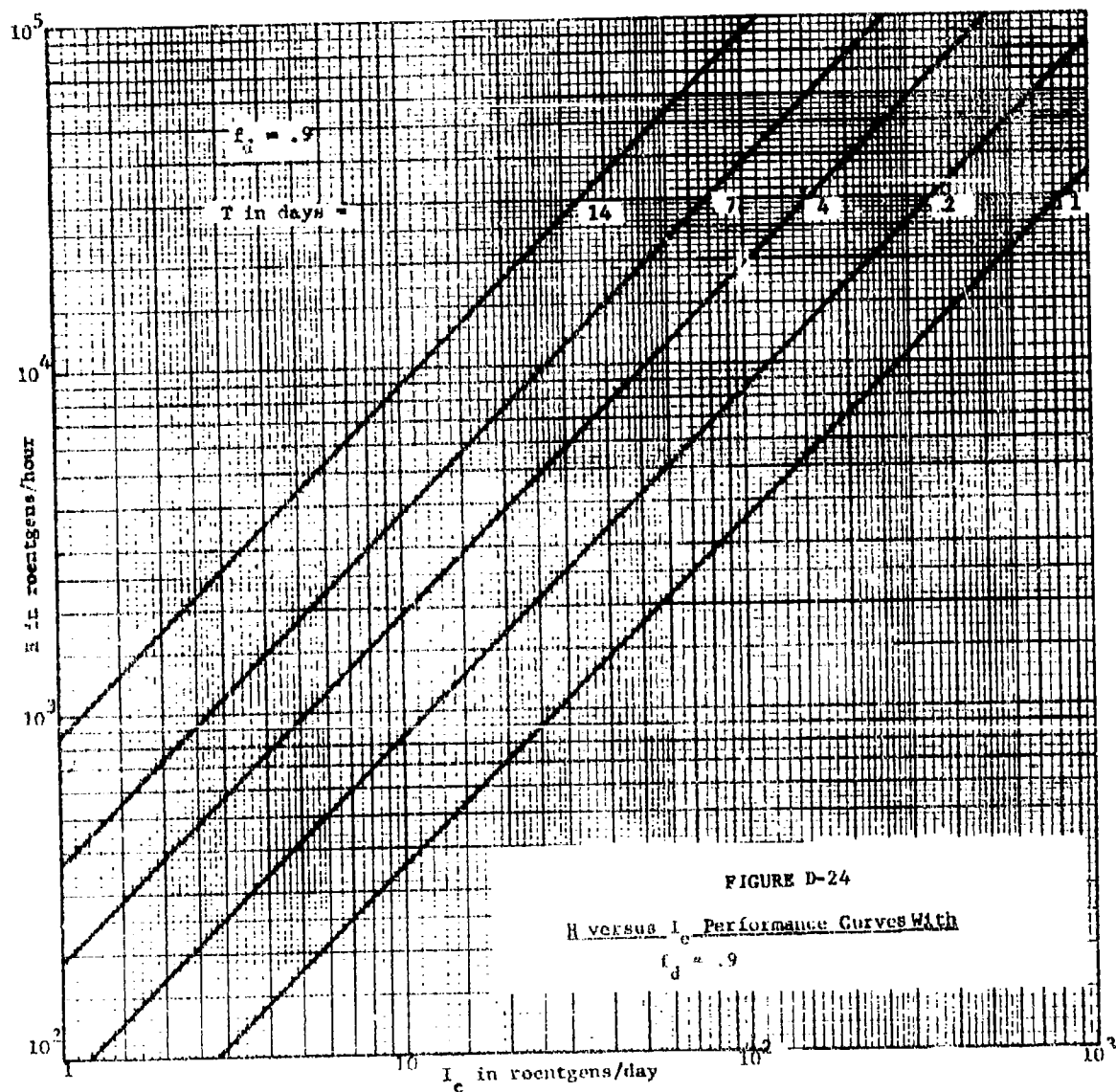
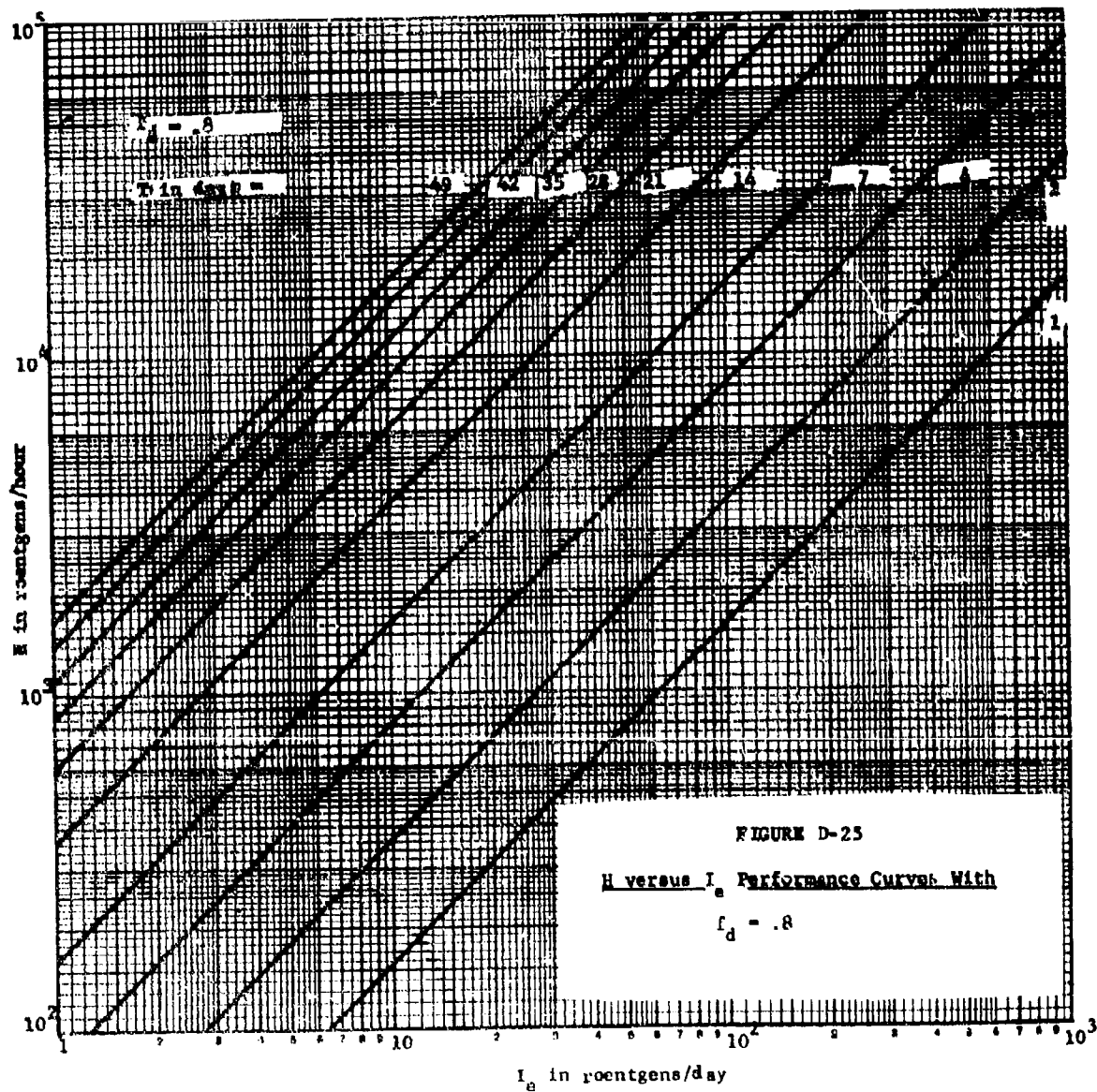
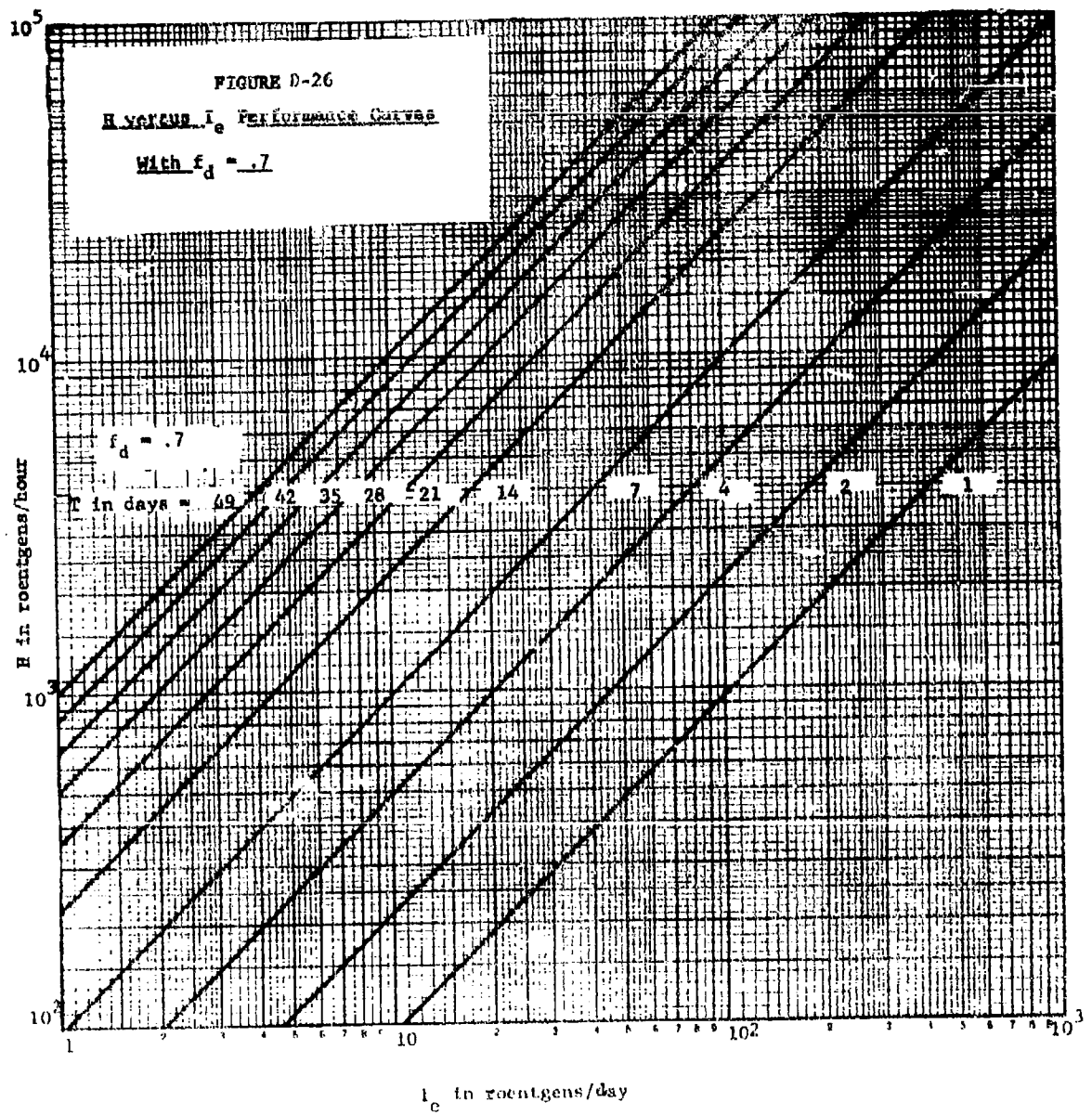
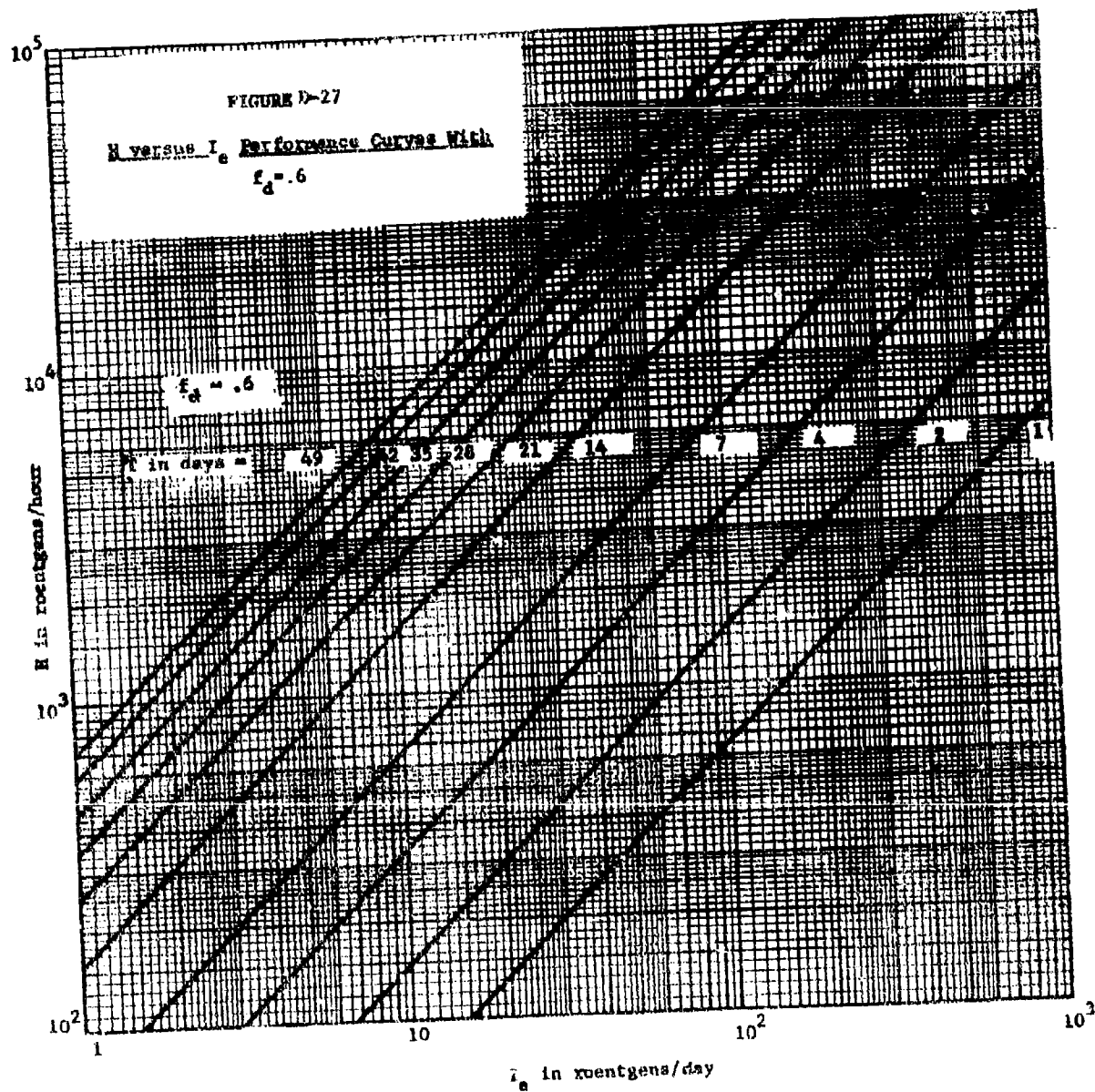


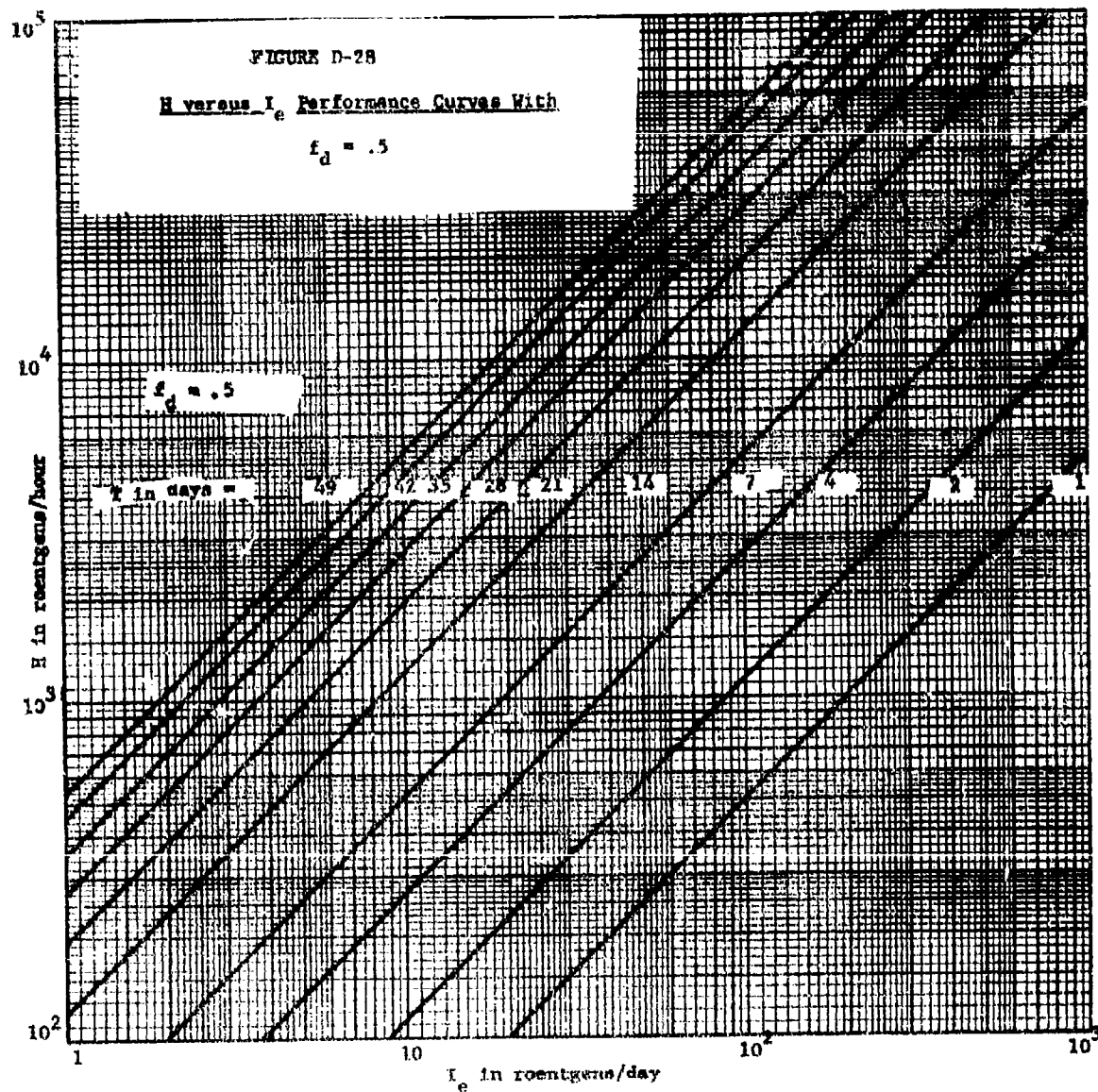
FIGURE D-23
H versus T Performance Curves

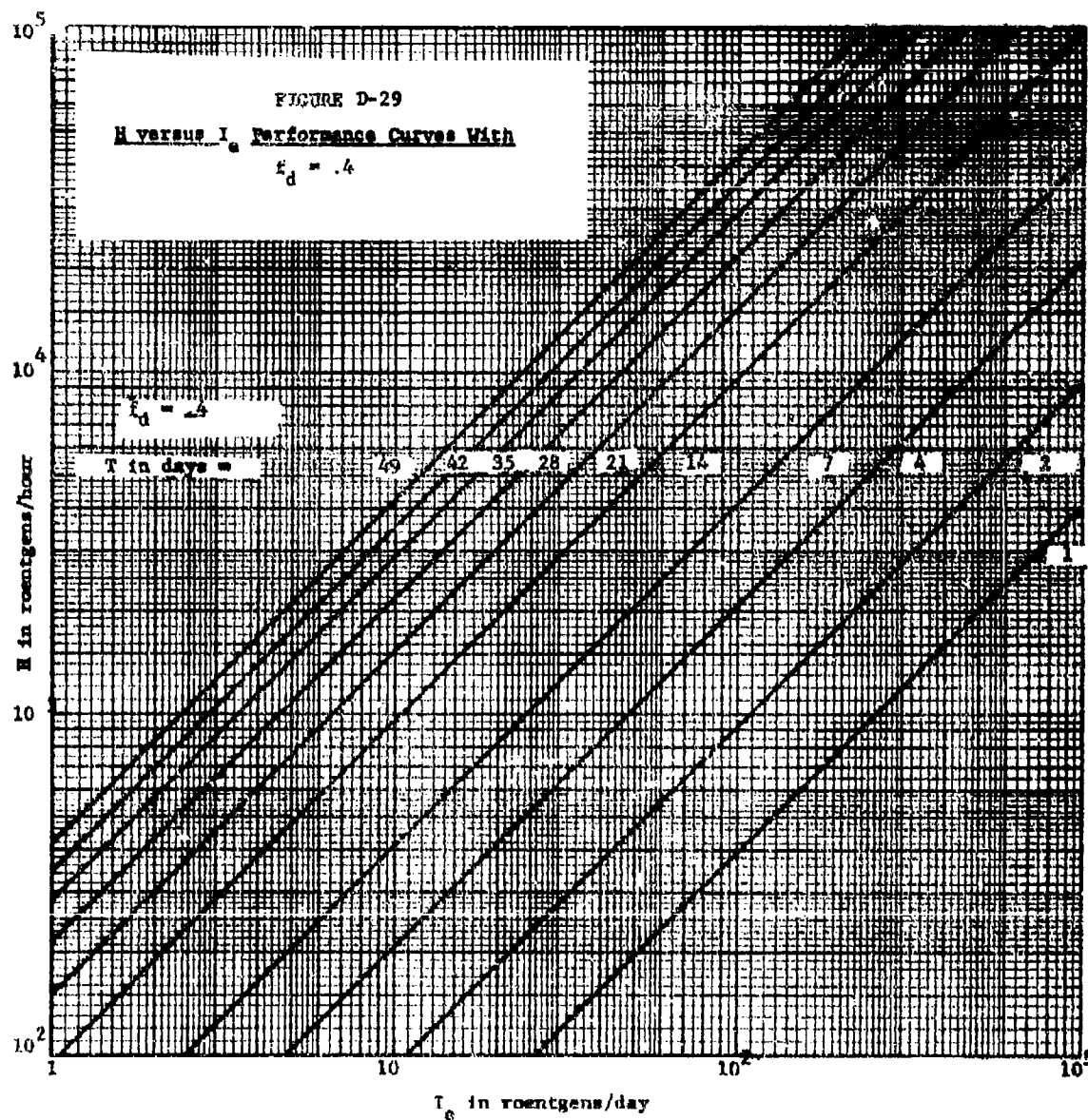












general manner without reference to specific applications or examples. The object here is to develop a picture of the time and place of valuable countermeasure applications.

Three factors that will receive direct attention are:

- (1) The relation of T to the lead time without decontamination, t_o^* ;
- (2) The absolute value of T ; and,
- (3) The relation of T to the activity performance dose rate,

$$L_o = \frac{D}{\Delta t}$$

A fourth factor, very important and difficult to evaluate, is the value of f_d that can be achieved with a given amount of effort (manpower). This factor relates the countermeasure manpower effort to the activity of interest. Because this appendix has concerned itself with the effectiveness, f_d , and not with the manpower effort required to achieve that effectiveness, this factor will not be discussed in this appendix.*

The first factor listed above can be interpreted as follows: If T is to be valuable, then it must at least be a given per cent (say 20%, 30%, or 40%) of the activity lead time without use of the countermeasure (t_o^*). That is, in general, if the normal lead time was 20 days, it would probably not be too great an accomplishment to reduce it to 18 days. If the activity was performed earlier, without using any countermeasure (that is, by increasing the allowable dose), then the fractional increase in dose would be the reciprocal of the countermeasure effectiveness required to perform

*For a discussion of this factor when decontamination is the countermeasure, see Appendix E.

the activity earlier without increasing the dose. Because the dose cannot be reliably predicted or measured to closer than 25 to 35 per cent of the true value,** one might insist that the value of f_d should be small enough so that if the activity was recovered without using the countermeasure then the resultant increase in dose would be at least 35 per cent. This means that f_d would have to be less than .74.

If at the same time, one decided that, in order for the countermeasure to be valuable, the lead time would have to be shortened by at least 30%, then f_d should be less than .65. This can be seen by forming the ratio $\frac{T}{t_e^*}$. This is accomplished either by combining Equations D-16 and D-20 (total dose) or by combining Equations D-17 and D-21 (ERD). Regardless of which combination is used, the following result is obtained:

$$\frac{T}{t_e^*} = (1 + \frac{\Delta t}{2t_e^*}) (1 - f_d^{.833}) \quad (D-28)$$

For a given situation, Δt and t_e^* , this becomes

$$\frac{T}{t_e^*} = K (1 - f_d^{.833}) \quad (D-29)$$

where K approaches unity as $\frac{\Delta t}{t_e^*}$ increases. If $K=1$, then T is 20% of t_e^* when $f_d=.76$, T is 30% of t_e^* when $f_d=.65$, and T is 40% of t_e^* when $f_d=.54$ (see Figure D-10). These percentages increase as K increases and,

** See Reference 2.

hence, as $\frac{\Delta E}{t_e}$ increases. If, therefore, a 20% return was considered marginal, then one might insist on a 30% return for the worst case (where $K=1$) and hence would consider only those countermeasures whose effectiveness was at least .65 (that is, consider only those situations where f_d was less than or equal to .65).

Combining these two approaches, the greatest value of f_d that is of general use will be set at .7, midway between .65 and .74. Note, that the trade-offs among H, T, and $\frac{D_T}{\Delta t} = I_e$ for this boundary case where $f_d=.7$ are presented in Figure D-26.

The second factor in the list can be interpreted as follows: If T is measured in hours is it significant? Or, should it be measured in days or in weeks to be significant? This is another value judgement required in assessing the practicality of countermeasure operations. In general, it would appear that T should be greater than one week if the operation is to be feasible. If a minimum T of 7 days is necessary and a maximum f_d of .7 is necessary, then the range of H and I_e where use of the countermeasure is feasible can be seen in Figure D-26. In Figure D-26, the boundary case where $f_d=.7$, it can be seen that $T \geq 1$ week if $\frac{H}{I_e} \geq 100$. That is, if $H=1000$, then I_e should be less than 10. Because $I_e = \frac{D_T}{\Delta t}$, if $D_T=200$, then Δt should be longer than 20 days for the countermeasure, in general, to be worthwhile.

As another example, assume the countermeasure efficiency, f_d was .5. Then, from Figure D-28, $\frac{H}{I_e}$ should be greater than 50 if T is to be greater than one week. Let $H=1000$ r/hr. In this case $\frac{H}{I_e} > 50$ implies that

$\frac{D_T}{\Delta t} < 20$, or that $D_T < 20 \Delta t$. Thus, if $D_T = 200r$, then $\Delta t > 10$ days is a situation where the countermeasure is potentially valuable. Obviously, the range of applicability $\Delta t > 10$ days, is considerably wider than the range when $f_d = .7$, which was $\Delta t > 20$ days.

In summary, if T_{\min} is the minimum useful T , and if f_d is given, then from the proper f_d figure (one of Figures D-24 through D-29) a constant $K(f_d, T_{\min})$ can be determined such that $\frac{H}{I_e} > K(f_d, T_{\min})$ insures that T will be greater than T_{\min} . Therefore, the progression,

$$\frac{H}{I_e} > K(f_d, T_{\min}) \quad , \quad (D-30)$$

$$\frac{\Delta t}{D_T} > \frac{K(f_d, T_{\min})}{H} \quad , \quad (D-31)$$

$$\Delta t > \frac{K(f_d, T_{\min})}{H} D_T \quad , \quad (D-32)$$

and in particular, the last inequality, defines the corresponding range of situations, Δt , D_T , and H , where the countermeasure is potentially valuable.

In regards to the third factor on the list, it is interesting to examine only the ratio $\frac{T}{\Delta t}$ and obtain an indication of its value. As was done in the case of the first factor, Equations D-16 and D-20 may be combined to yield:

$$\frac{T}{\Delta t} = \frac{1}{2} + \frac{t_e^*}{\Delta t} (1 - f_d^{.833}) \quad . \quad (D-33)$$

This relation is probably most important when Δt is small, (say, less than 5 days). In such cases, one might investigate under what conditions $T/\Delta t$ would be greater than 1. To do this set f_d equal to .65. Then, if

$\frac{t_e^*}{\Delta t} = 2, \frac{T}{\Delta t} = .75.$ and similarly, if $\frac{t_e^*}{\Delta t} = 5, \frac{T}{\Delta t} = 1.65.$ In this manner
 it is easy to determine the range of $\frac{t_e^*}{\Delta t}$ if a minimum value of $\frac{T}{\Delta t}$ is
 specified.

The above is presented as a brief treatment of several factors of
 general interest when assessing the applicability of countermeasures used
 to speed recovery. In order to arrive at specific conclusions, rather
 than broad, general ones, it is necessary to study specific examples of
 various countermeasures applied to particular situations. It is for this
 type of study or operations planning that the curves in the preceding
 sections are presented.

APPENDIX D REFERENCES

- D-1 J. F. Devaney. Operations in Fallout. OCEM-SA-61-13. Washington: Office of Civil Defense Mobilization, June 1961.
- D-2 National Committee on Radiation Protection and Measurements. Exposure to Radiation in an Emergency. Report No. 29. Chicago: University of Chicago, Department of Pharmacology, Section of Nuclear Medicine, January 1962.

Appendix E

Studies of Decontamination Effectiveness

The material in this
Appendix was originally
submitted to OCD in
Research Memorandum
RM 156-11*.

*J. T. Egan and J. D. Douglass, Jr., Studies of Decontamination Effectiveness,
Research Memorandum RM 156-11. Durham, North Carolina: Research Triangle
Institute, Operations Research Division, 5 August 1964.

Appendix E

Studies of Decontamination Effectiveness

I. INTRODUCTION

A. Objectives

As a radiological countermeasure, decontamination can be employed to achieve one or more different operational objectives. For example, it may be used to accelerate the re-entry and recovery of a contaminated building or building complex. It may be used to reduce the radiation hazard associated with a continuing operation such as a power station or communication link. It may be used to reduce the radiation dose associated with a change in operations, such as 14-2 week shelter emergence. In each of these applications and others that may arise, decontamination achieves the objective by removing fallout material and thus reducing the radiation intensity in the neighboring space. The degree to which a particular operational objective is achieved, depends on the effectiveness with which decontamination reduces the intensity. This in turn depends on the amount of fallout material removed from specific contaminated planes as a result of decontaminating those planes, and on the importance of each plane as a contributor to the intensity at the point where the intensity reduction is measured or desired.

This report examines the reduction in intensity that is achieved in a variety of circumstances as a function of the manner in which planes are decontaminated and of the importance of each plane to the intensity at the detector location. In particular, the analyses are formulated to accomplish

the following primary objectives:

1. Determine the intensity reductions that can be achieved by decontamination methods applied to practical situations involving real physical structures.
2. Determine the intensity reductions that can be achieved when the detector is located inside a structure and when the detector is located outside the structure.
3. Determine the decontamination costs (equipment, water expended, radiation dose received by the decontamination crews) in achieving the intensity reductions.
4. Determine the sensitivity of the achieved intensity reduction to the cleaning efficiency of the decontamination operation (and, therefore, to the type of decontamination method).
5. Determine the relative importance of the various surfaces (roofs, paved roads, parking lots, etc.) that can be decontaminated to the intensity reduction that can be achieved.

To accomplish the above objectives, ten situations were analysed. Each analysis forms the basis of one of the sections of Chapter II. Nine analyses, Chapter II, Sections B through J, investigate the effect on the intensity reduction, inside and outside existing NFSS shelters, of decontaminating the various accessible contaminated areas on and around the shelter structure. These analyses are summarized in Table E-IV in Chapter II of this appendix. The tenth analysis, Chapter II, Section K, is a parametric study that investigates the effects of certain structural parameters (floor and wall weights, apertures, story of the detector, etc.) on the intensity

reduction resulting from decontaminating a variety of contiguous contaminated planes. Chapter II, Section I is a parametric study that investigates the width and length effects on outside intensity reductions as a result of decontaminating various street segments in an urban area.

All analyses are formulated so that the effect of decontaminating selected subsets of the accessible areas (roofs, street segments, parking lots, etc.) with any level of decontamination effort may be determined quickly and easily. Although the analysis assumes a uniform distribution of fallout material, a method by which the results can be modified (or interpreted) for the situation involving non-uniform distribution, is also presented (Chapter I, Section F).

B. Decontamination Data

Decontamination efforts are applied to relevant contaminated surfaces and the fallout material removed is estimated using the information developed at USNRDL (References E-1, E-2, E-4, and E-5) and Curtiss-Wright (Reference E-6). The decontamination effort is measured in terms of the resources required to decontaminate, to a given level, a specified area (square feet) of a specified material (asphalt, concrete, tar paper, ground, etc.). The resources employed are specified by describing:

1. The type of equipment used (street flushers, firehoses, etc.);
2. The number of working personnel required;
3. The resources expended (gallons of water, fuel); and,
4. The time required for the decontamination activity.

This specification is restricted to the actual decontaminating activity and hence does not include such items as:

1. The time required to transport people and equipment to and from the site;
2. Resources required for the above transportation;
3. Requisite coordinating command and control activities such as radiological monitoring; and,
4. When appropriate, additional resources required to transport the collected fallout material away from the decontaminated site.

In general, when decontaminating a specified structure, three types of surfaces are investigated. First, the roof of the structure itself is decontaminated using firehose teams. This effort normally requires a seven-man team working .1 to .4 hours per thousand square feet to remove 90 to 98 per cent of the fallout material deposited on the roof (Reference E-6). Second, the paved ground surfaces (roads, parking lots, and playgrounds) adjacent to the structure are decontaminated. In this case various methods including firehose teams, street flushers, mechanical sweepers, and vacuum sweepers are employed. When equipment other than firehoses is used, it normally requires a one-man team working .01 to .04 hours per thousand square feet to remove 90 to 98 per cent of the fallout material deposited on the surface (Reference E-6). When firehoses are used to clean the paved areas, it normally requires a five-man team working .04 to .2 hours per thousand square feet to remove about 95 per cent of the fallout material deposited on the surface (Reference E-6). Third, when appropriate, the roofs of adjacent buildings are decontaminated using six- or seven-man firehose teams. For each surface in each study, the methods employed, times required, and fraction of the fallout material removed are specified.

C. Structures Analyzed

As stated earlier, one purpose of this facet of research is to apply decontamination efforts and efficiencies to real physical structures and to estimate the intensity reductions that can be accomplished in practical situations. To accomplish this, nine structures were selected from a previous study of NFSS buildings where building protection factors (PF) are computed (Reference E-3) using the Engineering Manual (Reference E-7).

In addition to the nine real structures, a tenth hypothetical structure is included to examine the effect on the intensity reduction of certain factors such as:

1. The inclusion of interior partitions;
2. The floor on which the detector is located;
3. The percentage of apertures; and
4. The mass thickness (psf) of the exterior walls.

In this parametric study, and also in Chapter II, Sections B, G, and H, the intensity reduction is studied first with the detector located inside the structure, and second with the detector located outside the structure. When the detector is located at ground level outside the structure, it is interesting to note that no intensity contribution is received from contaminated roofs of the surrounding structures. This characteristic (from Reference E-7) is not expected to be valid when the surrounding structures have low PF's (such as might be encountered in analyzing a shopping center).

D. Intensity Reduction Calculation

The determination of intensity reduction brought about by decontamination efforts involves the use of several terms (or definitions) whose meaning should

be clarified before entering into the individual analyses. These terms will be developed and explained using a simple example whose layout is presented in Figure E-1. The structure of interest occupies one-half of a city block and has paved surfaces (roads and parking lots) on all four sides. As in the actual analyses, detailed dimensions will not be included on the map. Two detector locations will be considered: Number 1 location is inside the structure, and Number 2 location is outside the structure in the center of an adjacent street. The effect of decontaminating three surfaces - a roof, a parking lot, and a street segment (numbers 1, 2, and 3, respectively) - on the intensity at the two detector locations will be determined.

The first factor to consider in an analysis is the extent to which a contaminated surface is cleaned. When decontamination resources are applied to a specified area, the effect of the effort is measured by the achieved reduction in residual mass level of fallout material. This effect is specified by the fraction of the fallout material deposited on the area that remains on the area after the decontamination operation is completed. Each surface decontaminated will have an associated fraction. The i^{th} fraction, associated with the i^{th} area, is called the mass reduction factor, E_i , of the i^{th} area.

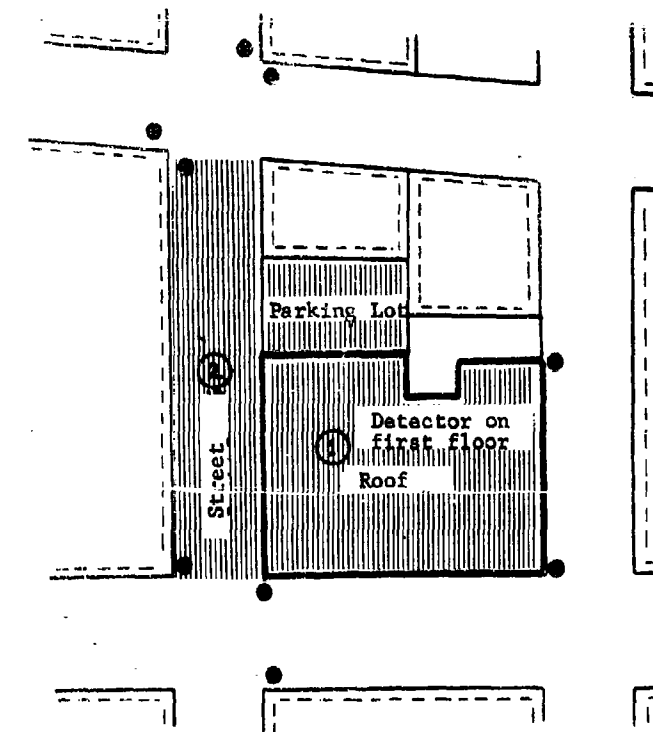
It is defined as follows:

$$E_i = \frac{m_i^a}{m_i} \quad , \quad (E-1)$$


where m_i = mass deposited on the i^{th} area, and m_i^a = mass remaining on the i^{th} area after the area has been decontaminated. Both m_i and m_i^a are assumed to be uniformly distributed over the surface of interest.


FIGURE E-1. Location Map of Decontamination Areas

EXAMPLE




● fire hydrants

 principal building

 adjacent buildings

① detector location 1

 Area 1 decontamination area

Ideal Intensity
Reduction Factors

detector location 1	detector location 2
$f_{1,1}^* = .70$	$f_{1,2}^* = 1.0$
$f_{2,1}^* = .88$	$f_{2,2}^* = .92$
$f_{3,1}^* = .75$	$f_{3,2}^* = .13$
$F_1^* = .33$	$F_2^* = .05$

If no material is removed during the decontamination operation, then $E_i = 1$. If all of the fallout material is removed in the process, then $E_i = 0$. In general, E_i is a function of the level of decontamination effort applied to the i^{th} area; it will be less than one and greater than zero. In Figure E-1, there are three areas to be decontaminated, and, therefore, there are three mass reduction factors to be considered. If 85 per cent of the fallout material is removed from the roof, surface 1, then $E_1 = .15$. If 95 per cent of the fallout material is removed from the street segment, then $E_3 = .05$. If 90 per cent of the fallout material is removed from the parking lot, then $E_2 = .10$. Numerical values of these factors are found in curves that relate the mass removed to the effort expended. Examples of such curves, taken from Reference E-6, are presented in Figure E-2.

Removing a portion of the fallout material deposited on the i^{th} area will decrease the radiation intensity in and around the structure. The magnitude of the resultant decrease will depend on both the location of the point where the intensity is measured and on the type and location of structures in the locality. Therefore, in Figure E-1, the effect of $E_2 = .1$ on the intensity at detector location one will be different from the effect of $E_2 = .1$ on the intensity at detector location two.

In addition to depending on the detector locations, the fraction by which the intensity* decreases will depend on the intensity contribution from fallout material remaining on the other contaminated areas. To determine the composite effect of E_i on the intensity at detector location j , it is necessary to calculate or measure the point intensity at location j , I_j , and the portion of the point intensity that is due to the contamination on the i^{th} area, $I_{i,j}$.

* All intensities are assumed corrected to eliminate the effect of decay.

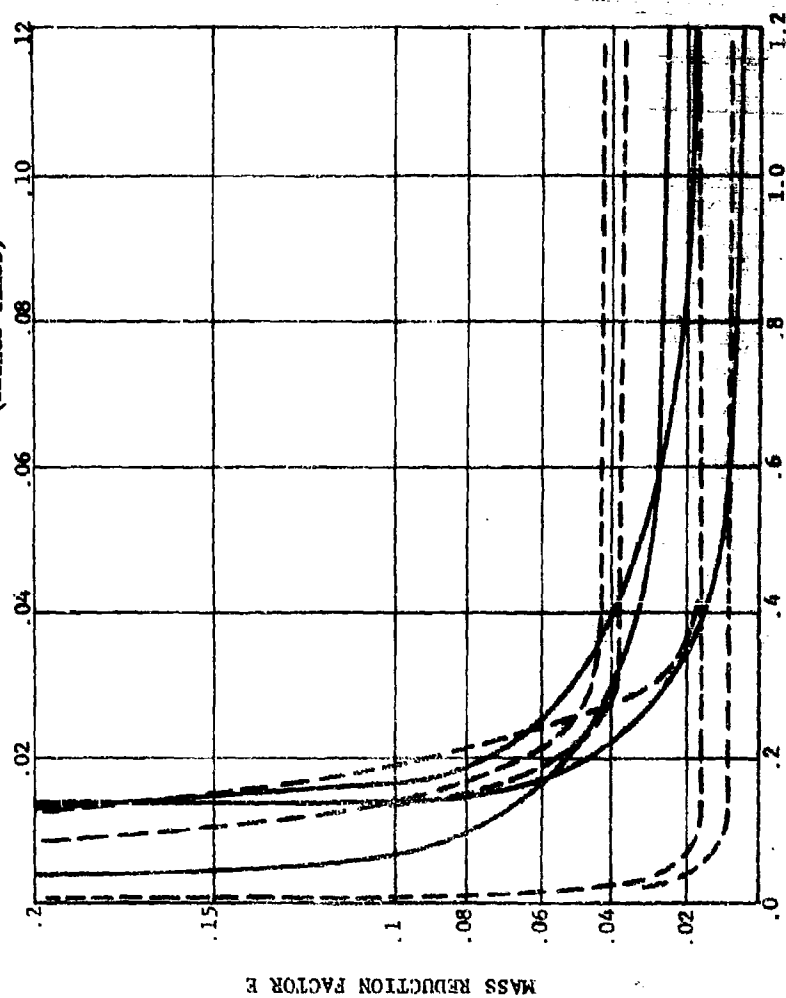
FIGURE E-2: Efficiencies of Decontamination Methods

(curves from Reference E-6)

H+1 reference intensity applicable to all curves is 1000 r/hr.

Man Hours/1000 Sq. Ft. - Sweepers & Flushers

(dashed lines)



Man Hours/1000 Sq. Ft. - Firehose
(Solid Lines)

When the distribution of fallout material in neighboring space is specified, these intensities, I_j and $I_{i,j}$, can be calculated using the methods presented in the OCD Engineering Manual (Reference E-6). Because:

1. all contaminated areas contribute independently to the intensity at location j (that is, $I_j = \sum_{i=1}^n I_{i,j}$ where n = number of contributing contaminated areas); and
2. the intensity due to the i^{th} area is directly proportional to the fallout material on the i^{th} area,

the intensity at location j after only the k^{th} area is decontaminated, I_j^k , is

$$I_j^k = I_j - (1 - E_k) I_{k,j} \quad (E-2)$$

Obviously, if all fallout material is removed from the k^{th} area (the ideal case where $E_k = 0$) then

$$I_j^k = I_j - I_{k,j} \quad (E-3)$$

In this ideal situation, the fractional reduction that has occurred is called $f_{k,j}^*$, the ideal intensity reduction factor of the k^{th} contaminated area relative to the j^{th} detector location, and is defined as follows:

$$f_{k,j}^* = \frac{I_j - I_{k,j}}{I_j} = 1 - \frac{I_{k,j}}{I_j} \quad (E-4)$$

For each contaminated area and detector location, this factor $f_{k,j}^*$ may be calculated using the methods outlined in the OCD Engineering Manual (Reference E-6). The factor represents the fractional reduction in intensity that can be achieved at detector location j by perfectly decontaminating only the k^{th}

contaminated surface ($E_k = 0$). In the studies presented in Chapter II, these factors were calculated using a computer program developed at RTI for calculating the protection factors of fallout shelters. In Figure E-1, these factors have been assigned the following representative values:

at detector location 1

surface 1	$f_{1,1}^* = .70$
surface 2	$f_{2,1}^* = .88$
surface 3	$f_{3,1}^* = .75$

at detector location 2

surface 1	$f_{1,2}^* = 1.0$
surface 2	$f_{2,2}^* = .92$
surface 3	$f_{3,2}^* = .13$

Let the intensity at detector location one be I_1 and the intensity at detector location two be I_2 . Thus, if surface 3, the street segment, is perfectly decontaminated ($E_3 = 0$), then the new intensity at detector one, I_1^3 , is

$$I_1^3 = f_{3,1}^* I_1 = .75 I_1 \quad (E-5)$$

and the new intensity at detector location two, I_2^3 , is

$$I_2^3 = f_{3,2}^* I_2 = .13 I_2 \quad (E-6)$$

That is, by removing all fallout material from surface 3 (and only surface 3), the intensity at detector location one (two) is reduced to 75 per cent (13 per cent) of its former value. In contrast, if all fallout material is removed from surface 1 (and only from surface 1), then the intensity at detector location one is reduced to 70% of its former value while the intensity at detector location two is not affected ($f_{1,2}^* = 1.0$).

The ideal intensity reduction factors, $f_{i,j}^*$, form the core of the intensity reduction analyses. At the beginning of each analysis, they are determined for each surface of interest relative to each detector point of interest. In terms of these (the $f_{i,j}^*$'s) and the mass reduction factors, E_i , the intensity reduction at any detector location can be determined for any combination of decontaminated surfaces. To develop the appropriate expression for this, first consider the intensity reduction achieved at detector location j when surface k (and only surface k) is decontaminated with $E_k \neq 0$. In this realistic situation, the fractional reduction that has occurred is called $f_{k,j}$, the intensity reduction factor of the k^{th} contaminated area relative to the j^{th} detector location, and is defined, using Equation E-2, as follows:

$$f_{k,j} = \frac{I_j - (1-E_k) I_{k,j}}{I_j} \quad (E-7)$$

This factor is more conveniently expressed in terms of E_k and $f_{k,j}^*$ as follows:

$$f_{k,j} = f_{k,j}^* + (1-f_{k,j}^*) E_k \quad (E-8)$$

In Figure E-1, as before, let the intensity at detector location one be I_1 , and the intensity at detector location two be I_2 . In addition, assume that 95% of the fallout material deposited on surface 3 is removed. That is, let $E_3 = .05$. As a result of this operation, the new intensity at detector one, I_1^3 , is

$$I_1^3 = (.75 + .25 \times .05) I_1 \\ = .7625 I_1 \quad (E-9)$$

$$\begin{aligned}
 F_j^* &= 1 - f_{n,j} = 1 - (n-1 - \sum_{i=1}^{n-1} f_{i,j}^*) \\
 &= 1 - n + \sum_{i=1}^n f_{i,j}^* \quad , \quad (E-14)
 \end{aligned}$$

where $f_{n,j}$ represents the contribution from the surfaces not decontaminated.

Returning to the example in Figure E-1, consider the best intensity reductions that can be achieved at each detector location when the three surfaces are perfectly decontaminated.

At detector location 1,

$$\begin{aligned}
 F_1^* &= \sum_{i=1}^3 f_{i,1}^* + 1 - 3 \\
 &= .70 + .88 + .75 - 2 \\
 &= .33 \quad (E-15)
 \end{aligned}$$

At detector location 2,

$$\begin{aligned}
 F_2^* &= \sum_{i=1}^3 f_{i,2}^* + 1 - 3 \\
 &= 1 + .92 + .13 - 2 \\
 &= .05 \quad (E-16)
 \end{aligned}$$

That is, if the intensities before any decontamination is performed are I_1 and I_2 , and if surfaces 1, 2, and 3 are perfectly decontaminated, then the intensities after the decontamination is performed are $.33 I_1$ and $.05 I_2$, respectively.

In the realistic situation, where the mass reduction factors are not equal to zero, it is a simple process to show that the combined intensity

reduction factor, F_j , may be obtained from Equation E-14 by merely substituting $f_{i,j}$ in place of $f_{i,j}^*$, and F_j in place of F_j^* . That is,

$$F_j = \sum_{i=1}^m f_{i,j} + 1-m, \quad (E-17)$$

where, as previously stated, $f_{i,j}$ is equal to $f_{i,j}^* + (1-f_{i,j}^*) E_i$. Equation E-17 is the expression that gives the fractional reduction in intensity that results when several surfaces are decontaminated.

To see how closely the ideal situation is approached when practical decontamination methods are employed in Figure E-1, let $E_1 = .15$, $E_2 = .10$, and $E_3 = .05$. Using Equation E-8, the intensity reduction factors are:

At detector location one,

$$\begin{aligned} f_{1,1} &= .70 + .30 \times .15 = .75 \\ f_{2,1} &= .88 + .12 \times .10 = .892 \\ f_{3,1} &= .75 + .25 \times .05 = .7625 \end{aligned} \quad (E-18)$$

Therefore

$$F_1 = .75 + .892 + .7625 - 2 = .4045 \quad (E-19)$$

out of a possible $F_1^* = .33$ as determined in Equation E-15.

At detector location two,

$$\begin{aligned} f_{1,2} &= 1.0 \\ f_{2,2} &= .92 + .08 \times .1 = .928 \\ f_{3,2} &= .13 + .87 \times .05 = .1735 \end{aligned} \quad (E-20)$$

Therefore

$$\begin{aligned} F_2 &= .1735 + .928 - 1 \\ &= .1015 \end{aligned} \quad (E-21)$$

out of a possible $F_2^* = .05$ as determined in Equation E-16.

On the other hand, if only the ground level surfaces (2 and 3) were decontaminated with $E_2 = .10$ and $E_3 = .05$, the following results would be obtained:

At detector location one,

$$\begin{aligned} f_{2,1} &= .88 + .12 \times .10 = .892 \\ f_{3,1} &= .75 + .25 \times .05 = .7625 \end{aligned} \quad (E-22)$$

Therefore

$$\begin{aligned} F_1 &= .7625 + .892 - 1 \\ &= .6545 \end{aligned} \quad (E-23)$$

At detector location two,

$$\begin{aligned} f_{2,2} &= .92 + .08 \times .1 = .928 \\ f_{3,2} &= .13 + .87 \times .05 = .1735 \end{aligned} \quad (E-24)$$

Therefore

$$\begin{aligned} F_2 &= .1735 + .928 - 1 \\ &= .1015 \end{aligned} \quad (E-25)$$

In the above calculations, the factors that are necessary are (1) the $f_{i,j}^*$'s and (2) the E_i 's. The E_i 's are obtained from curves, and the $f_{i,j}^*$'s are calculated with the techniques used to calculate the protection factor of the structure itself (Reference E-7). The

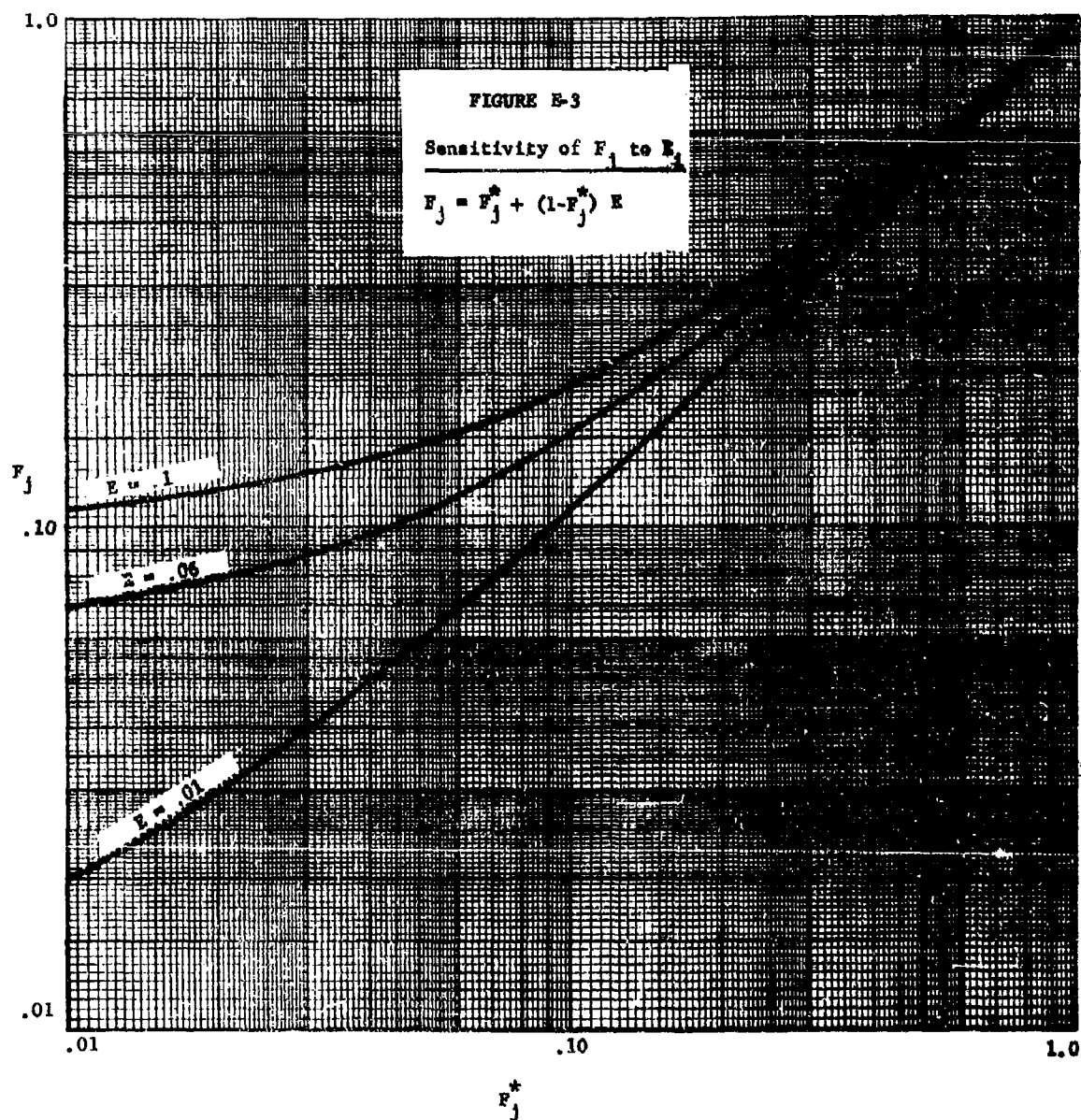
combining of these two sets of factors is the primary portion of the analyses presented in Chapter II, Sections B through J.

E. Practical Considerations

In this final section, three topics are discussed: (1) on-site postattack measurement of $f_{i,j}^*$; (2) sensitivity of $f_{i,j}$ and F_i to the value of the mass reduction factor E_i and appropriate simplified expressions for F_j ; and (3) analysis adjustments to account for weathering in calculations of F_j . Each topic will be discussed using the example presented in Figure E-1 and the definitions presented in Section D of this chapter.

Using the methods presented in Reference E-7, the UCD Engineering Manual, the pertinent ideal intensity reduction factors, $f_{i,j}^*$ and F_j^* , can be determined for a specific building just as the protection factor itself can be calculated. In the postattack environment, however, these factors will be unknown, and one must conduct an on-site measurement of the factors $f_{i,j}^*$ in order to decontaminate in the most effective manner. An additional reason for this measurement is that expected weathering will cause a redistribution of fallout material. As a result of this redistribution, the values of the $f_{i,j}^*$ factors (and, incidentally, the protection factor itself) will change, and therefore the effect of decontaminating specified areas with respect to specified detector locations will change. What previously were important areas to decontaminate may become unimportant (and, also, the reverse). Therefore, it would be desirable to check values of the $f_{i,j}^*$'s by measurement prior to commencing decontamination operations.

An on-site estimate of important $f_{i,j}^*$ factors can be made with appropriate directional detectors. This can be seen from the equation for

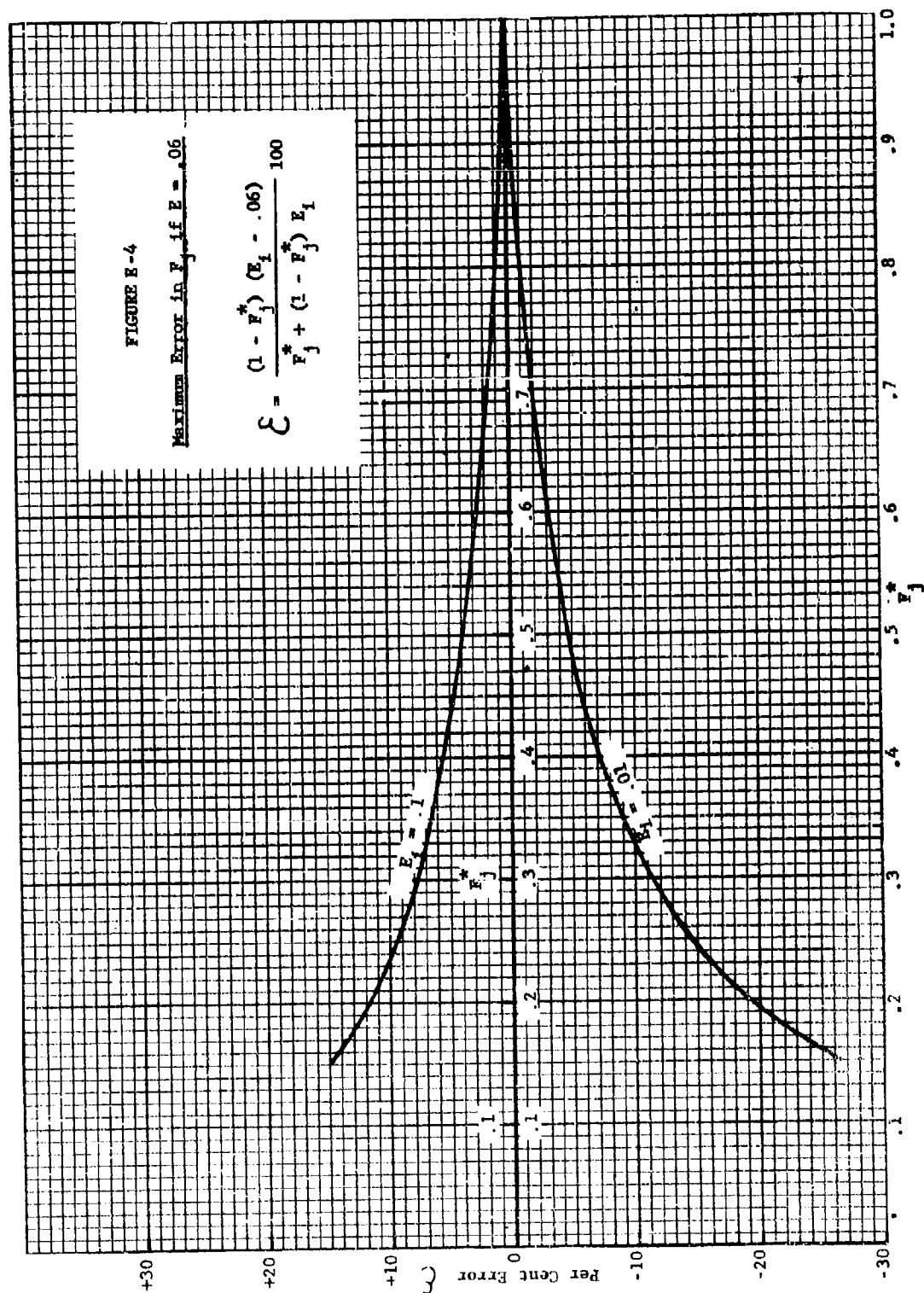


.1 > E_1 > .01). These two errors - using $E = .06$ rather than $E_1 = .1$ or $E_1 = .01$ - are displayed as a function of F_j^* in Figure E-4. Based on Figures E-3 and E-4, it is evident that the actual values of E_1 are not very significant in determining F_j when F_j^* is greater than .2. Therefore, when F_j^* is greater than .2, the approximation

$$\begin{aligned} F_j &\approx F_j^* + (1 - F_j^*) .06 \\ &= .94 F_j^* + .06 \end{aligned} \quad (E-27)$$

is useful for quickly estimating F_j . This approximation is appropriate in situations where the detector is located inside the building. In that situation, there are several contributing planes - ground and roof - of contamination. Each plane will have an appropriate mass reduction factor, E_1 , that is less than .1, and, for most cases (from Figure E-2), greater than .01. If E_1 was assumed equal to .06 for all planes, then the maximum error in the calculated F_j would arise in the equally unlikely situation where all E_1 's were actually .1 (or .01). In actual situations where all E_1 's were assumed equal to .06, the actual value of E_1 would lie between .01 and .1, on both sides of .06, and the errors that result from setting $E_1 = .06$ would tend to cancel out, resulting in an error much less than the maximum errors shown in Figure E-4.

In contrast to the above situation, when the detector is located externally, there are very few contributing planes - ground-level surfaces only (Reference E-7) - of contamination. In particular, the plane above which the detector is located is so significant a contributor that F_j^* can often be assumed equal to the $f_{i,j}^*$ of that plane. In addition, this $f_{i,j}^*$



tends to be less than .2, and, in many cases, less than .03. For such circumstances, it is convenient to set $f_{i,j}$ equal to $f_{i,j}^* + E_i$ rather than $f_{i,j}^* + (1-f_{i,j}^*) E_i$. When $f_{i,j}^*$ is less than .1, and E_i is less than .1, the error that results from using this approximation, $f_{i,j} = f_{i,j}^* + E_i$ is always less than 5.3% as shown in Figure E-5.

F. Non-Uniform Distributions

When it is desired to predict the effects of weathering or redistribution of fallout material, the preceding discussions are applicable if the value of $f_{i,j}^*$ is properly modified. The adjustment of $f_{i,j}^*$ is developed from the basic equation for the intensity at detector location j .

$$I_j = \sum_i I_{i,j} \quad (E-28)$$

If the fallout material is shifted about, the intensity at j becomes

$$I_j^0 = \sum_i k_i I_{i,j} \quad (E-29)$$

where k_i is the fractional increase or decrease in material deposited on the i^{th} plane. This expression can also be written as

$$I_j^0 = k_j \sum_i I_{i,j} \quad (E-30)$$

where k_j is the fractional increase or decrease in intensity at location j due to the redistribution. From Equation E-4,

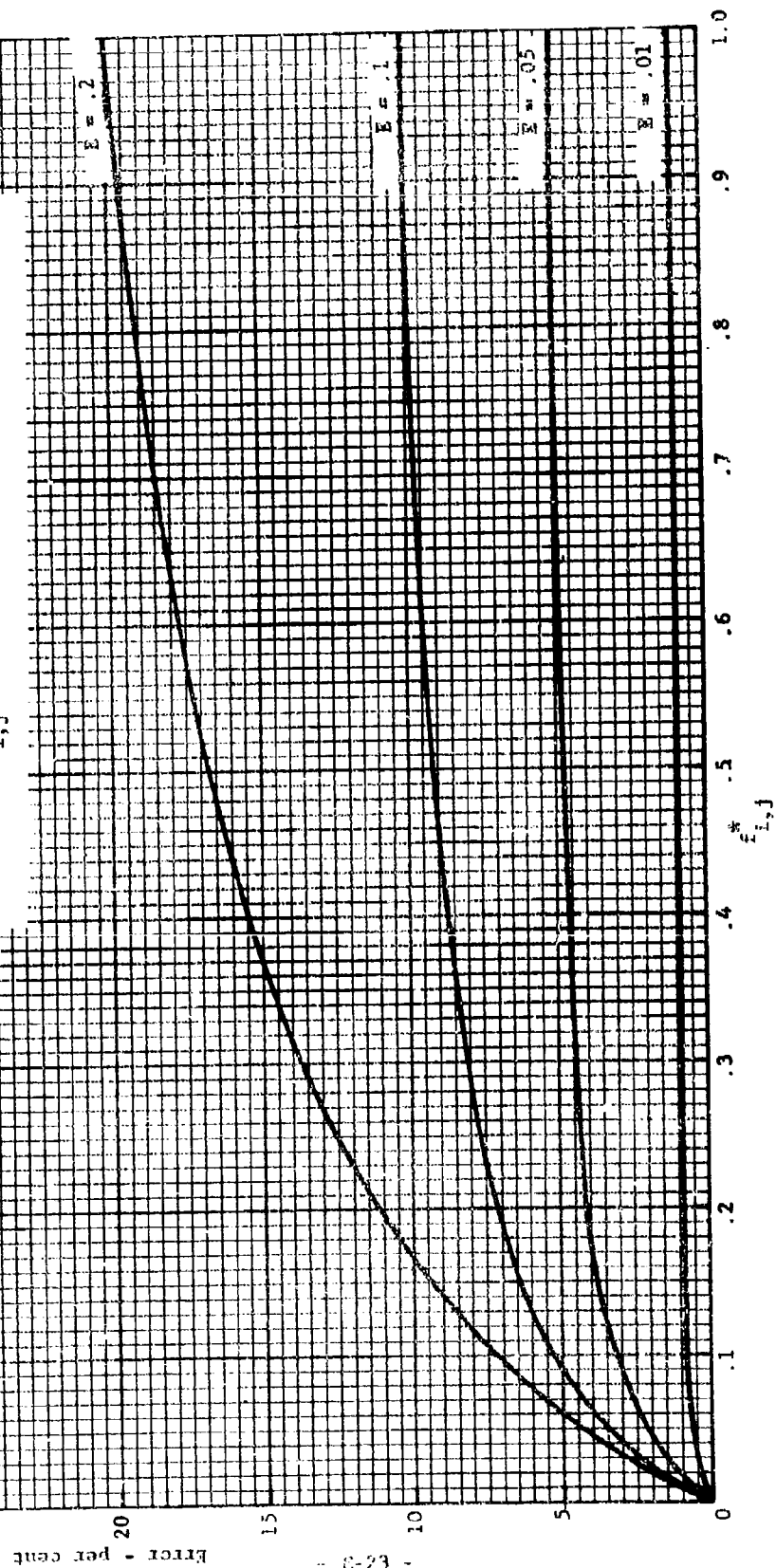
$$f_{i,j}^* = \frac{I_{i,j}}{I_j} \quad (E-4)$$

FIGURE E-5

Error in f_j using the Approximation $f_{i,j} = f_{i,j}^* + E_i$

$$\text{Error} = \frac{100}{\frac{1}{E_i} + \frac{1}{f_{i,j}^*} - 1} \text{ per cent}$$

$$= \frac{f_{i,j} - f_{i,j}^*}{f_{i,j}} 100 \text{ where } f_{i,j}^* = f_{i,j} + (1 - f_{i,j}^*) E_i$$



the appropriate $f_{i,j}^*$ after weathering has occurred, $f_{i,j}^{**}$ becomes

$$f_{i,j}^{**} = 1 - \frac{k_i I_{i,j}}{k_j \sum_i I_{i,j}}, \quad (E-31)$$

or

$$f_{i,j}^{**} = 1 - \frac{k_i}{k_j} (1 - f_{i,j}^*). \quad (E-32)$$

Naturally, if the weathering does not change the intensity at location j ($k_j = 1$), then the ideal intensity reduction factors become

$$f_{i,j}^{**} = 1 - k_i + k_i f_{i,j}^*. \quad (E-33)$$

II. INDIVIDUAL DECONTAMINATION STUDIES

A. Introduction

1. Contents

This chapter presents the results of the application of decontamination efforts to some real and hypothetical situations. The first nine studies, Sections B through J, primarily investigate the effect on the intensity reduction inside of nine NFSS shelters as a result of decontaminating accessible contaminated areas in and around these structures. The structures are as follows:

Section B	Six-Story Apartment Building 81 West 182nd Street Bronx, New York City New York
Section C	Six-Story Apartment Building 362 West 52nd Street Manhattan, New York City New York
Section D	Twenty-one-Story Office Building 310 Park Avenue Manhattan, New York City New York
Section E	General Dyestuff Corporation Building 435 Hudson Street Manhattan, New York City New York
Section F	High School Gymnasium Bennett Street Boston, Massachusetts
Section G	Simonds Press Building 37-49 South Avenue Rochester, New York
Section H	Department of the Interior Building 18th and C Streets, N. W. Washington, D. C.
Section I	Three-Story Department Store Building 619 Main Street Houston, Texas
Section J	Bell Telephone Building 1010 Pine Street St. Louis, Missouri

These buildings were selected from a group of NFSS buildings for which data necessary for the various calculations were readily available.

For each structure, the intensity reduction is determined for each accessible area individually, and for all areas combined, for various levels of selected decontamination methods. In addition, these studies show:

decontamination man-hours for each intensity reduction; the sensitivity of the achieved reduction to the cleaning efficiency of the decontamination operation; and the relative importance of decontaminating various accessible areas. The costs in water and fuel can be calculated for each case study by using the expenditure rates in Tables E-I and E-II.

In addition to the above structures, a tenth structure,

Section K	Five-Story Parametric Study Building Fictitious Location
-----------	-------------------------------------------------------------

is included to examine, in a controlled parametric manner, the effect on radiation intensity reduction of several structural features important in radiation shielding.

Section L is a parametric study of the effects on outside intensity reductions of decontaminating street segments of various lengths and widths.

Also included in three of the nine studies are data for detector locations outside of the structures.

2. Presentation of the Data

The detailed results of decontamination studies for each of the nine real structures are presented in Sections B through J. For each structure, the following analysis material is presented:

- (a) Building address, detector location in the structure, and the protection factor (see Section 2a-2c for each structure, paragraphs B through K below);

- (b) Description of the relevant decontamination areas, including identification (e.g., 1. roof, 2. parking lot), surface material (e.g., tar and gravel), and area in square feet (see Section 2d for each structure);
- (c) Ideal intensity reduction factor ($f_{i,j}^*$) associated with each decontamination area. These values indicate the relative importance of each area to the intensity reduction that can be achieved for the structure. In addition, the ideal combined intensity reduction factor, F_1^* , is given. This value is the best possible intensity reduction factor that can be achieved for the particular structure by perfectly decontaminating all selected areas (see Section 2e for each structure);
- (d) Man-hours, and effectiveness data for each individual area. Effectiveness data are expressed in terms of the practical intensity reduction factor which can be achieved as a result of applying various levels of decontamination effort for selected methods of decontamination. Corresponding decontamination costs in water and fuel may be derived from Tables E-I and E-II, extracted from a draft of a Federal Civil Defense Guide (Reference E-8);
- (e) Combined practical intensity reduction factors, F_1 , resulting from decontaminating one or more of the selected areas associated with the structure (see Section 2g for each structure);

TABLE E-1
Cost and Effectiveness Data for Selected Mass Reduction Factors for Various
Decontamination Methods - Decontamination of Pavements (Asphalt or Concrete)

Method	Identification Symbol	Effort in Man-hours per 1000 sq. feet	Rate in 1000 sq. feet per hour	Team Size	Water Rate in gals. per square foot	Fuel Rate in gal. per 1000 square feet	Mass Reduction Factor (E ₁)
Regular Street Sweepers	SS1	0.04	25	1		.0125	0.04
	SS2	0.02	50	1			0.06
	SS3	0.013	75	1			0.09
	SS4	0.01	100	1			0.15
Vacuumized Sweepers	VS1	0.04	25	1		0.125	0.02
	VS2	0.02	50	1			0.09
	VS3	0.01	100	1			0.25
Motorized Plusher	MF1	0.01	100	1	0.3	.008	0.02
	MF2	0.003	300	1	0.15		0.04
Firehosing	F1	1.0	5	5	2.3		0.02
	F2	0.5	10	5	1.1		0.03
	F3	0.2	25	5	0.5		0.07

TABLE E-II
Cost and Effectiveness Data for Selected Mass Reduction Factors
for Various Decontamination Methods - Decontamination of Roofs

Method	Identification Symbol	Effort in Man-hours per 1000 sq. feet	Rate in 1000 sq. feet per hour	Team Size	Water Rate in gals. per square foot	Mass Reduction Factor (E_i)
Firehosing Tar and Gravel Roofs	FTG1	1.0	7	7	2.0	0.01
	FTG2	0.5	14	7	1.0	0.03
	FTG3	0.3	23	7	0.6	0.07
	FTG4	0.2	35	7	0.4	0.12
Firehosing Composition Shingle	FCS1	0.5	12	6	1.2	0.03
	FCS2	0.2	30	6	0.5	0.05
	FCS3	0.1	50	6	0.25	0.08

- (f) A discussion of unusual factors or items encountered in the analysis, when appropriate (Section 1 for each structure);
- (g) A map showing the location of the building, the location of the areas to be decontaminated, and the location of the detector (Section 3 for each structure); and
- (h) Photographs, when available, showing the building, its surroundings, and the areas to be decontaminated (Section 4 for each structure).

For certain selected structures (Sections B, G, and H), an outside detector as well as an inside detector was considered. For these studies, the following additional information is included:

- (a) The location of the outside detector;
- (b) The original PF at the site of the detector; and
- (c) Some ideal intensity reduction factors ($f_{i,j}^*$ values) associated with the outside detector and the contributing planes of contamination.

3. Manner of Analysis

a. Effectiveness

Specifically, a particular area (contaminated plane) is selected, and a decontamination method (e.g., street sweeper) applied at one or more levels of effort to achieve one or more mass reduction factors, F_i , for the area. The relations between

effort and mass reduction factors are given in Tables E-I and E-II, extracted from Reference E-8.

The practical intensity reduction factor achieved in applying a particular E_1 to the area is computed by use of Equation E-8 and the ideal intensity factor, $f_{1,j}^*$, of the area.

For combined strategies (more than one area decontaminated), the reduction factors are computed by combining the intensity reduction factors for the various individual areas in the manner indicated by Equation E-26. Each combination of E_1 and decontamination method is identified by a strategy identification symbol (e.g., FTG1-1, fire hose on tar and gravel roof with $E_1 = .01$). These may be interpreted by reference to Tables E-I and E-II. Results of these calculations are summarized in Table E-IV (see page E-35).

These strategies were selected to provide an indication of the sensitivity of the practical intensity reduction factor to the E_1 (and thus the associated effort) for the given area and decontamination method. Further, the combined strategies portray the range of practical intensity reductions obtainable for real structures by decontamination, along with their costs. In addition, they illustrate the sensitivity of intensity reduction in the structure to the manner in which effort is allocated among the various areas.

b. Costs

Cost data for single and combined strategies are given in

terms of total man-hours of effort, water and fuel usage, and crew dose.* Man-hour costs are calculated by relating the unit effort (Tables E-I and E-II) to the size of the areas (defined in Section 2d for each structure) for each single strategy (listed in Section 2f for each structure) and summing for all decontaminated areas. Other kinds of costs (e.g., gallons of water) can be computed by similar use of the data in Sections 2d and 2f for each structure, and Tables E-I and E-II. Should the reader want to make similar calculations of the per cent of fallout removed by decontamination, he is reminded that the initial mass loading of fallout material affects the per cent of fallout removed for a specified effort. Further considerations and experimental results are contained in Reference E-4.

4. Summary of Results from Decontamination Studies

a. The Nine Real Structures

(1) General

The purpose of this section is to summarize the detailed analysis data associated with the nine real structure studies presented in Sections B through J. In interpreting these results, it should be noted that since these structures were selected from actual NFSS data, they may not be representative of those buildings which it would be desirable to decontaminate in the postattack period. Further, inferences drawn from

* For each of the nine structures, a sample calculation of crew dose for each strategy is given corresponding to an initial reference intensity of 10,000 r/hr and a decontamination time of H+2 weeks. Since an initial intensity of 10,000 r/hr will approximately decay to an intensity of 10 r/hr in two weeks, these crew doses were calculated simply by multiplying the team hours of effort by 10.

these individual structures may not be applicable to larger complexes of buildings or isolated buildings not surrounded by other structures.

(2) Ideal Reduction Factors (Perfect Decontamination)

Table E-III summarizes the combined ideal reduction factors (F_1^* 's) computed for each of the nine structures and provides an indication of the increased protection brought about by perfectly decontaminating the accessible areas. For seven of the nine structures, the intensity which can be removed ranges from 86 to 99.9%; this is equivalent to increasing the protection by factors ranging from 7 to 1000. For the other two structures, 68 per cent and 79 per cent can be removed. This corresponds to an increase in protection by factors of 3.1 and 4.8.

(3) Reduction Factors Achievable in Practice

Although practical values of intensity reduction factors approaching those F_1^* 's given in Table E-III could be achieved, it may not be desirable to expend the effort necessary to achieve "perfect" decontamination. The data in Table E-IV provide an indication of practical combined intensity reduction factors, F_1 , that could be achieved for these structures for selected decontamination strategies. For each structure, the F_1 's and their corresponding costs in man-hours of effort are given for three sets of selected strategies. These

TABLE E-III

Combined Ideal Intensity Reduction Factors for Nine Selected Structures

Structure	Normal PF	F ₁ [*]	Protection Increased By a Factor of
B	45	.135	7.4
C	73	.143	7.0
D	276	.044	22.7
E	126	.001	1×10^3
F	116	.017	58.2
G	47	.007	1.43×10^2
H	1090	.210	4.8
I	26	.001	1×10^3
J	127	.322	3.1

TABLE E-IV

Summary of Combined Practical Intensity Reduction Factor and Associated Costs for Nine Selected Structures

Structure	Combined Strategy Number	Symbol	Description of Strategies	Mass Reduction Factor (E_1) [*]	Combined Intensity Reduction Factor (F_1)	Man-Hours of Effort [*]
B	1	FTC1-1 SSI-2	Firehose on Roof Street Sweeper on Ground	.01 .04	.159	11.69
	2	FTG4-1 SS4-2	Same as Combined Strategy #1	.12 .15	.254	2.40
	3	SSI-2	Street Sweeper on Ground	.04	.514	1.76
C	1	FCS1-1 VS1-2 VS1-3	Firehose on Primary Roof Vacuum Sweeper on Alleys Vacuum Sweeper on Road	.03 .02 .02	.215	1.50
	2	FCS3-1 VS2-2 VS2-3	Same as Combined Strategy #1	.08 .09 .09	.261	0.39
	3	PCS1-1	Firehose on Primary Roof	.03	.595	1.08
D	1	SSI-1 SSI-2	Street Sweeper on Primary Roads and Sidewalks Street Sweeper on other Roads and Sidewalks	.04 .04	.083	6.56
	2	SS4-1 SS4-2	Same as Combined Strategy #1	.15 .15	.187	1.64
	3	SSI-1	Street Sweeper on Primary Roads and Sidewalks	.04	.456	4.88

^{*} see Reference E-8.

-continued-

TABLE E-IV (continued)

Structure	Combined Strategy Number	Symbol	Description of Strategies	Mass Reduction Factor (E_1)*	Combined Intensity Reduction Factor (F_1)	Man-Hours of Effort*
E	1	SS1-1 FCS1-3	Street Sweeper on Roads Firehose on Adjacent Roof	.04 .03	.048	6.38
	2	SS4-1 FCS3-3	Same as Combined Strategy #1	.15 .08	.145	1.50
	3	SS1-1	Street Sweeper on Roads	.04	.158	4.40
F	1	FCS1-4 SS4-1 SS1-3 SS3-2	Firehose on Roof Street Sweeper on Roads Street Sweeper on Playground Street Sweeper on Parking Lot	.03 .15 .04 .09	.066	3.25
	2	FCS3-4 SS4-1 SS3-3 SS3-2	Same as Combined Strategy #1	.08 .15 .09 .09	.092	0.89
	3	FCS1-4	Firehose on Roof	.03	.528	2.34
G	1	FCS1-1 MF2-2	Firehose on Roof Motor Flusher on Ground Levels	.03 .04	.038	4.68
	2	FCS3-1 MF2-2	Same as Combined Strategy #1	.08 .04	.082	1.22
	3	FCS3-1	Firehose on roof	.03	.138	4.00

* see Reference E-8.

-continued-

TABLE E-IV (continued)

Structure	Combined Strategy Number	Symbol	Description of Strategies	Mass Reduction Factor (E_I)*	Combined Intensity Reduction Factor (F_I)	Man-Hours of Effort*
H	1	FI-1	Firehose on Interior Courts	.02		
		FI-2	Firehose on Roads	.02	.226	33.40
	2	F3-1 F3-2	Same as Combined Strategy #1	.07 .07	.265	6.70
	3	FI-1	Firehose on Interior Courts	.02	.404	23.40
I	1	FTG1-1 SS1-2	Firehose on Roof Street Sweeper on Roads	.01 .04	.022	12.11
	2	FTG4-1 SS4-2	Same as Combined Strategy #1	.12 .15	.132	2.57
	3	FTG-1	Firehose on Roof	.01	.388	1.34
J	1	FCS1-1 FCS1-2 VS2-3 VS2-4	Firehose on Roof #1 Firehose on Roof #2 Vacuum Sweeper on Roads Vacuum Sweeper on Parking Lots	.03 .03 .09 .09	.367	9.36
	2	FCS3-1 FCS3-2 VS2-3 VS2-4	Same as Combined Strategy #1	.08 .08 .09 .09	.386	8.70
	3	FCS1-1	Firehose on Roof #1	.03	.740	3.54

* see Reference E-8.

strategies are formed by the cleaning of one or more of the accessible decontamination areas. The individual strategies which make up each combined strategy are identified by a symbol in Tables E-I and E-II and in the detailed results in Sections B through J.

(4) Effect of Level of Decontamination Effort

The first two sets of combined strategies are identical except that a smaller E_1 (more fallout is removed) is applied to each area for the first set of strategies than for the second. For the second set of strategies (lesser decontamination), it can be seen that from 61 per cent to 92 per cent of the intensity could be removed from these structures at a cost varying from 0.4 to 8.7 man-hours. For seven of the nine structures (excluding H and J) from 74 per cent to 92 per cent can be removed at a cost from 0.4 to 2.6 man-hours. For the first set of strategies, from 63 per cent to 98 per cent of the intensity can be removed with costs ranging from 1.5 to 33.4 man-hours. In seven of nine cases, from 78 per cent to 98 per cent can be removed at a cost varying from 1.5 to 12.1 man-hours. The maximum amount of time any crew member spends decontaminating for either the first set or second of combined strategies is 6.7 hours (Building H). It should be noted that firehose teams consist of more than one man and that team-hours of work will be less than man-hours.

It can be seen by comparing the second set of strategies to the first set for each structure that, in general, the cost increases considerably as one attempts to decrease F_1 toward F_1^* . For example, for structure G, 75 per cent of the intensity can be removed for a cost of 2.4 man-hours; however, to remove 84 per cent (i.e., 9 per cent more) would require 11.7 man-hours. Thus, by applying more effort to achieve a lower E_1 , the protection is increased from a factor of 4 to a factor of 6.25--or the protection is raised by an additional 56 per cent by applying more effort. On the other hand, the cost is increased by an additional 388 per cent in order to achieve this protection.

(5) Allocation of Decontamination Effort

The importance of properly allocating decontamination effort among the various accessible contaminated areas can be inferred by comparing the third set of combined strategies with the second set. The third set of strategies is the use of a single decontamination method on the single area that contributes the most intensity to the detector. The decontamination method used on the area is the same as that used in the second set of combined strategies. The method is, however, applied more extensively (i.e., E_1 is smaller) in the third set than it is in the second. In the second set, a smaller effort is applied to this area, but effort is

applied to other areas as well. It can be seen by comparing the third set of combined strategies with the second set in Table E-IV that, in general, considerably more of the intensity will be removed for these buildings with much less cost if the effort is allocated over more than one accessible area (as in Set 2), rather than applying extensive effort to one area (Set 3). For example, for Structure D, 4.88 man-hours with a street sweeper are applied extensively to just the primary roads and sidewalks (Set 3); 54 per cent of the intensity will be removed. However, if 1.64 man-hours with a street sweeper are applied less extensively to the same area and to other accessible areas (other roads and sidewalks), 81 per cent of the intensity will be removed.

(6) Effect of Decontamination on Outside Detectors

For outside detectors, considerably lower F^* values were calculated. Table E-V summarizes the pertinent data calculated for the three outside detector locations.

TABLE E-V

Summary of Outside Detector Analysis Data

Analysis Structure	Detector Location	Original PF at Site of Detector	Ideal Intensity Reduction Factor Associated with the Detector Surface*	Ideal Combined Intensity Reduction Factor (F*)
6-Floor Apartment Building (B)	Center of Playground	1.39	.056	.019
Simonds Press Building (G)	Center of Street	1.40	.029	.001
Department of the Interior Building (H)	Center of Interior Court	1.61	0	0

As is seen from this table, the most significant contributing plane of contamination is the surface above which the detector is located. By decontaminating that surface alone, the intensity can be reduced by a factor of 20 or more.

b. Parametric Studies:(1) Introduction

Several parametric studies were undertaken to provide inferences regarding the relationship between intensity reduction (due to decontamination) and several factors associated with the contaminated planes and the shielding

This is the $f_{i,j}^$ factor (perfect decontamination) associated with outside detector location j and the surface above which the detector is located (designated as surface i).

afforded the detector. Both inside and outside detector locations were considered.

(2) Indoor Locations

For the studies of intensity reduction indoors, a ten-story structure was hypothesized and a detector placed on each of the first five stories. In these cases, there was no roof contribution to these detectors. One of the basic purposes of this study was to determine which physical factors were most influential in determining the relative importance of the contributing planes of contamination. As might be expected, the distance between the detector and the contaminated plane weighs most heavily for the detectors positioned on the first and second floors. For the higher floors, this factor was less important, inasmuch as the floors themselves provided some shielding from the nearer contaminated planes. This is seen most easily by observing (from section K below) that the $f_{i,j}^*$ values for $i = 7$ and 8 (representing the two nearest planes) increase fairly consistently as one ascends from floor to floor. This is the case in all four tables (Tables E-VIII through E-XI of Section K).

One important fact should be noted: The $f_{i,j}^*$ represent only the fraction of intensity remaining, so that $f_{i,j_1}^* > f_{i,j_2}^*$ does not imply that there is a higher intensity at detector j_1 on floor i than at j_2 on floor i . The detector at j_2 may

have had a much higher intensity reading than the detector at j_1 , before plane 1 was decontaminated. Thus, the intensity after decontamination may still be higher at the detector at j_2 even though the fraction of intensity remaining is less.

(3) Outdoor Locations

The parametric studies involving unshielded detectors placed on streets lined by buildings (Section 1 below) led to one rather interesting conclusion: The intensity measured in the center of a street will not change appreciably as (say) an unshielded person passes through intersections or passes by other ground-level planes of contamination (parking lots, playgrounds, parks, etc.). Considering only roads, 40 feet wide and 60 feet wide, the calculated protection factors were always between 1.47 and 1.72. (See Tables E-XII through E-XV). This means that the postattack planner can safely use 1.5 or 1.6 as the protection factor afforded unshielded persons on streets.

B. Six-Floor Apartment Building

1. Discussion

This building is situated on the corner of two paved streets and across the street from a school building and playground area. Prior to an on-site inspection it was assumed that the playground was completely paved. However, a portion of the school ground has been fenced off for a garden as is shown on the map (Figure E-6) and in the photograph (Figure E-13). The analysis which was accomplished prior to the visit assumes that this area is paved and is a part of the school playground. Inasmuch as this playground is directly in front of the building housing the detector, it was included in the total ground surface area to be decontaminated. The areas behind the building consisting primarily of smaller structures, alleyways, and a backyard, with many obstructions, were not considered suitable for decontamination.

For a first-floor detector, if only the roof of the building were decontaminated, about one-third of the radiation intensity would be removed; if only the ground surfaces (streets and playground) were decontaminated, about one-half of the radiation intensity would be removed. If both of these areas (roof and ground) were decontaminated, more than four-fifths of the radiation intensity would be removed.

2. Analysis Data

(a) Address: 81 West 182nd Street
Bronx, New York City
New York

(b) Detector Location: First-floor (Three feet high)

(c) Normal Protection Factor: PF = 45

(d) Decontamination Areas:

(1) Roof: 9918 sq. ft. tar paper surface.
(assumed equivalent to tar and gravel)

(2) Ground Level: 15,000 sq. ft. (asphaltic concrete on
West 182nd Street)
16,000 sq. ft. (asphaltic concrete on
Aqueduct Avenue)
13,000 sq. ft. (asphalt on P.S. 91
playground)

(Roof = Area Number 1; Ground Level = Area Number 2)

(e) Ideal Intensity Reduction Factors:

(1) Roof: $f_{1,1}^* = .641$

(2) Ground Level: $f_{2,1}^* = .494$

(3) Roof and Ground Combined: $F_1^* = f_{1,1}^* + f_{2,1}^* - 1 = .135$

(f) Cost and Effectiveness Data for Selected Methods on Individual Areas:

Strategy Identifi- cation Symbol*	Area (Use Nos. from (d) above)	Mass Reduction Factor (E_i)	Intensity Reduction Factor ($f_{i,j}$)	Team Hours of Effort	Crew Dose in Roentgens **
FTG1	1	.01	.645	1.42	14.2
FTG2	1	.03	.652	.71	7.1
FTG3	1	.07	.666	.43	4.3
FTG4	1	.12	.684	.28	2.8
SS1	2	.04	.514	1.76	17.6
SS4	2	.15	.570	.44	4.4
VS1	2	.02	.504	1.76	17.6
MF1	2	.02	.504	.44	4.4
F1	2	.02	.504	8.80	88.0

* See Tables E-I and E-II for description of symbols.

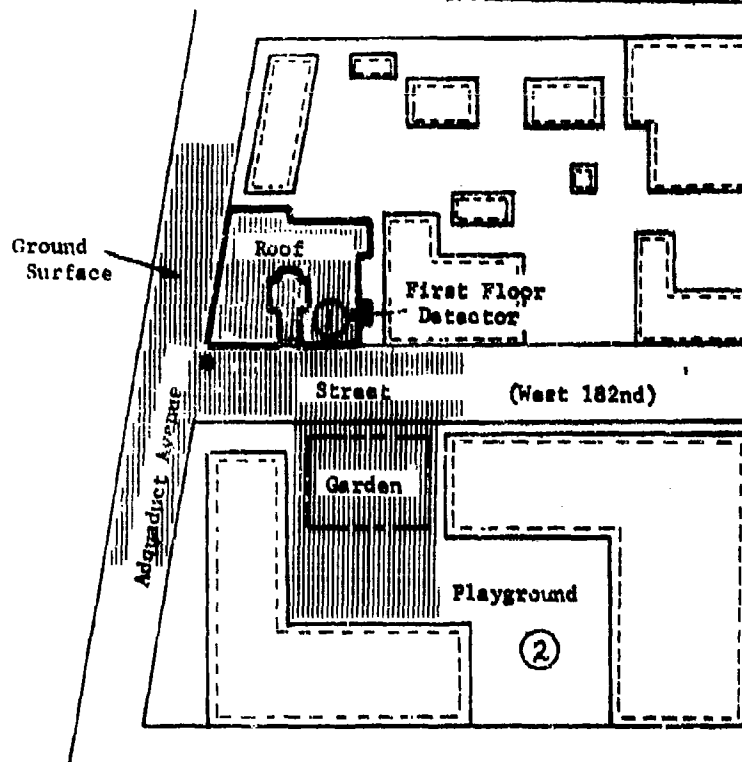
** Crew dose in roentgens is calculated assuming decontamination at H+2 weeks
with an H+1 reference intensity of 10,000 r/hr.




(g) Combined Strategies:

Strategy Identification Symbol and Area	Intensity Reduction Factor, F_1	Total Man- Hours of Effort
FTG1-1 + SS1-2	.159	11.69
FTG1-1 + F1-2	.149	53.92
FTG4-1 + VS1-2	.188	3.72
FTG4-1 + SS4-2	.254	2.40

3. Map

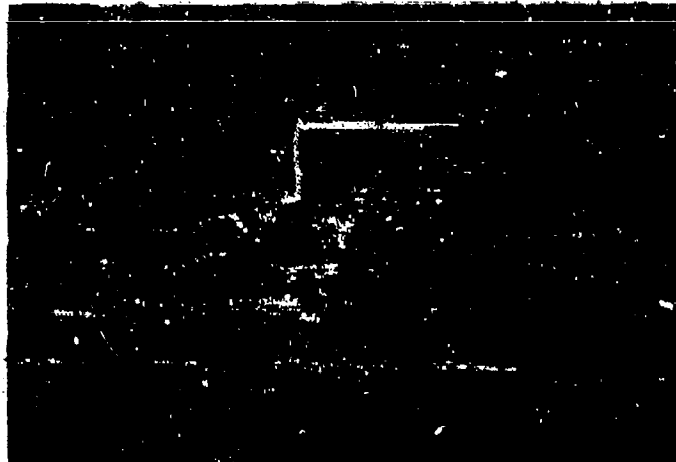
FIGURE E-6. Location Map of Decontamination Area



- fire hydrants
-  principal building
-  adjacent buildings
- ① detector location 1
-  Area 1 decontamination area

4. Some Photographs of the Associated Contaminated Surfaces

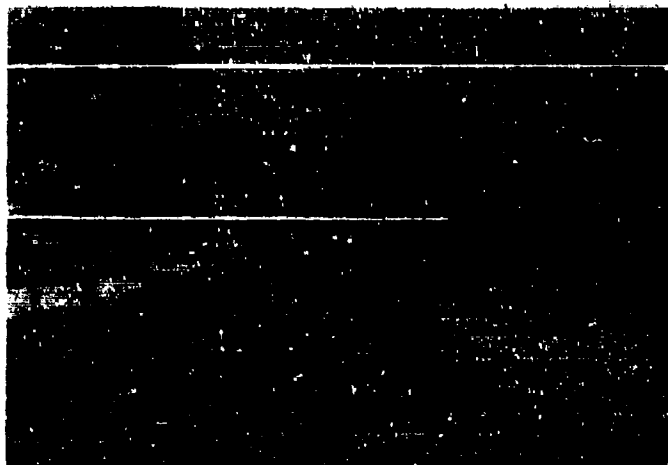
FIGURE E-7



View of Building from West 182nd Street

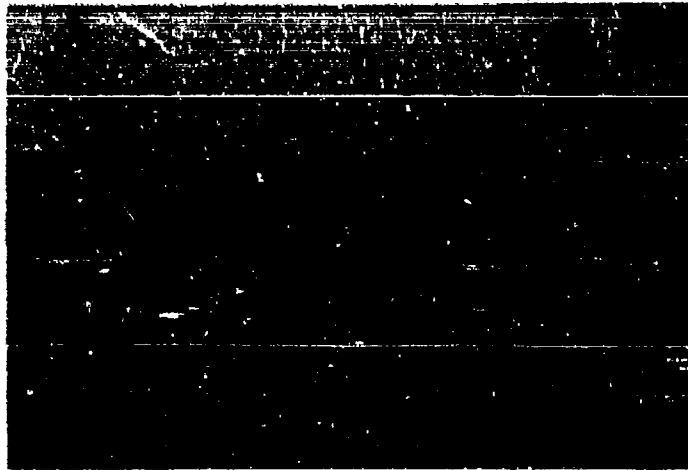
(Note: Fireplug)

FIGURE E-8



West 182nd Street (Note: large drain on corner)

FIGURE E-9



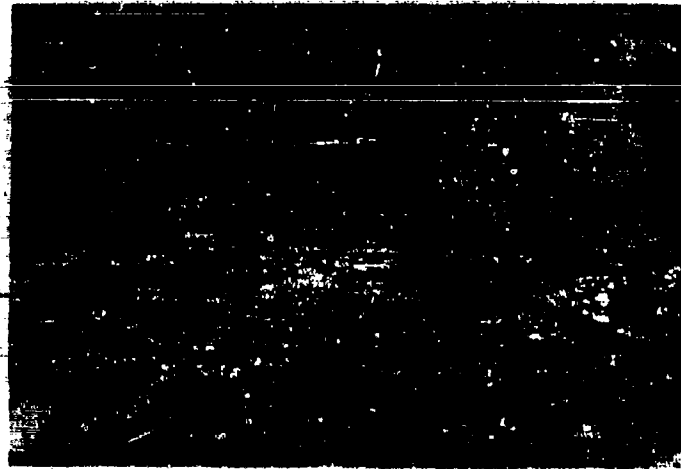
View of Roof

FIGURE E-10



View of Side Alley

FIGURE E-11



View of Adjacent Roofs

FIGURE E-12



View of Playground and Garden Area

(Note: iron fence around garden)

5. Outside Detector

(a) Location of Detector: In center of playground across the street from original building studied. (Three feet off ground).

(b) Original FF at site of detector -----1.39

(c) f^* 's for individual planes

$f_{1,2}^*$: (playground, i.e., plane above which detector is located) ----- .056

$f_{2,2}^*$: Street in front of building ----- .963

$$F_2^* = f_{1,2}^* + f_{2,2}^* - 1 = .019$$

C. Six-Floor Apartment Building

1. Discussion

This building is typical of many multi-family dwellings located in densely populated areas. It is surrounded by other buildings, narrow alleys, and congested paved areas. In order to provide for a complete decontamination operation, these areas, particularly the parking lot shown in Figure E-16, would have to be cleared of parked vehicles and other obstructions. In this instance, however, all but about one-fifth of the radiation intensity at the second floor can be removed by decontaminating the building's roof, the paved alley, and street directly adjacent to the building. The garage roof, parking lot, and other paved areas account for an additional five per cent of the radiation intensity.

2. Analysis Data

- (a) Address: 362 West 52nd Street
Manhattan, New York City
New York
- (b) Detector Location: Second Floor
- (c) Normal Protection Factor: PF = 73
- (d) Decontamination Areas:
 - (1) Roof (Primary): 2,400 sq. ft. composition shingle.
 - (2) Alleys: 1,400 sq. ft. asphaltic concrete (behind building and garage).
 - (3) Road Area Directly in Front of Building: 6,000 sq. ft. asphaltic concrete (West 52nd Street).
 - (4) Parking Lot, Garage Roof, Road Area in Front of Parking Lot:
 - 9,200 sq. ft. (asphaltic concrete parking lot).
 - 2,100 sq. ft. (composition shingle garage roof).
 - 7,500 sq. ft. (asphaltic concrete road in front of parking lot)

(e) Ideal Intensity Reduction Factors:

- (1) Roof (Primary): $f_{1,1}^* = .583$
- (2) Alleys: $f_{2,1}^* = .774$
- (3) Road Area in Front of Building: $f_{3,1}^* = .636$
- (4) Parking Lot and Associated Road Area, Garage Roof:
 $f_{4,1}^* = .950$
- (5) All Decontamination Areas Combined:
 $F_1^* = f_{1,1}^* + f_{2,1}^* + f_{3,1}^* + f_{4,1}^* - 3 = .143$

(f) Cost and Effectiveness Data for Selected Methods on Individual Areas:

Strategy Identification Symbol*	Area (Use Nos. from (d) above)	Mass Reduction Factor (E_1)	Intensity Reduction Factor ($f_{1,j}$)	Team Hours of Effort	Crew Dose in Roentgens
FCS1	1	.03	.596	.20	2.0
FCS3	1	.08	.616	.04	.4
VS1	2	.02	.780	.06	.6
VS2	2	.09	.794	.03	.3
SS1	2	.04	.783	.06	.6
SS3	2	.09	.794	.02	.2
SS1	3	.04	.843	.24	2.4
SS4	3	.09	.851	.06	.6
VS1	3	.02	.839	.24	2.4
VS2	3	.09	.851	.12	1.2
MF2	3	.04	.843	.02	.2
F1	3	.02	.839	1.20	12.0
F3	3	.07	.847	.24	2.4

(g) Combined Strategies:

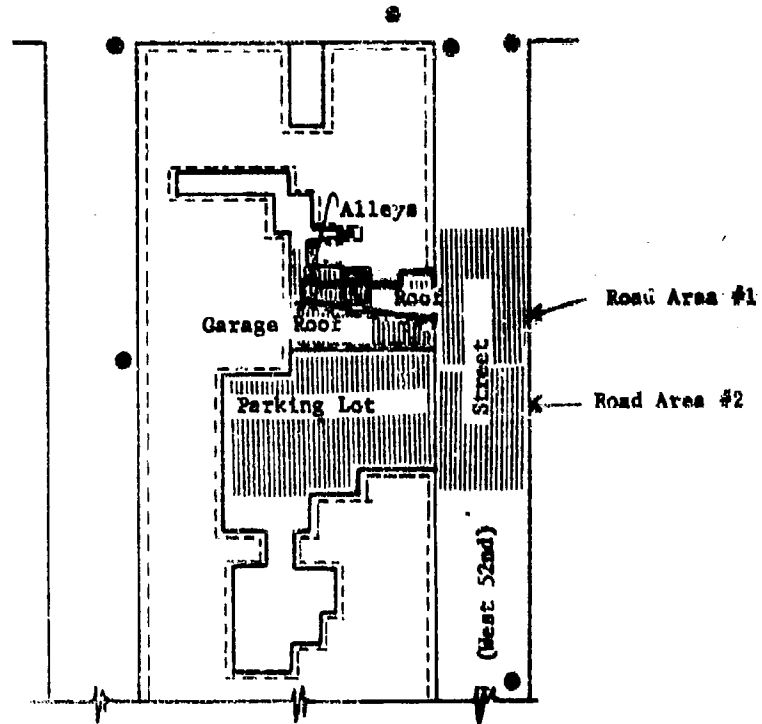
Strategy Identification Symbol and Area	Intensity Reduction Factor, F_1	Total Man-Hours of Effort
FCS1-1 + VS1-2 + VS1-3	.215	1.50
FCS3-1 + VS2-2 + VS2-3	.261	.39
VS2-2 + VS2-3	.645	.15
SS1-2 + SS1-3	.626	.30
FCS1-1 + F1-3	.435	7.20
FCS1-1 + MF2-3	.439	1.22

* See Tables E-I and E-II for description of symbols.

** Crew Dose in roentgens is calculated assuming decontamination at H+2 weeks with an H+1 reference intensity of 10,000 r/hr.

3. Map

FIGURE E-13. Location Map of Decontamination Areas



● fire hydrants

▭ principal building

▭ adjacent buildings

① detector location 1
(First Floor Detector)

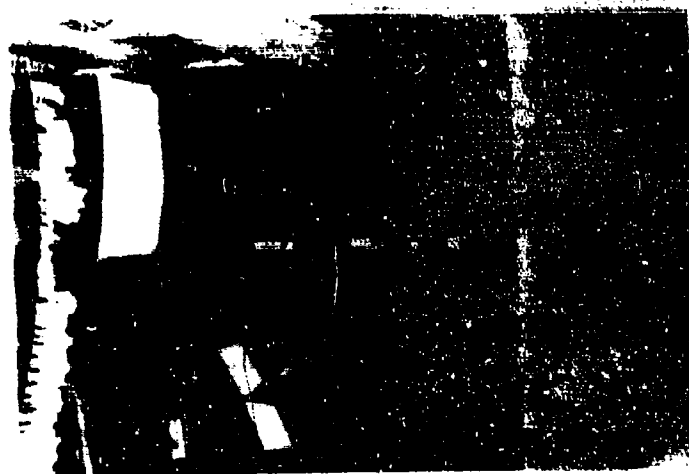
▨ Area 1
decontamination area

FIGURE E-14



A View of West 22nd Street

FIGURE E-15



A View of the Narrow Alley Behind Building

FIGURE E-16



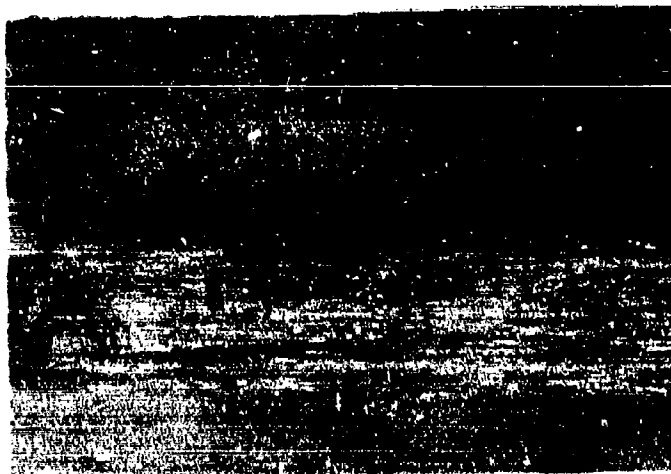
View of Garage Roof and Parking Lot

FIGURE E-17



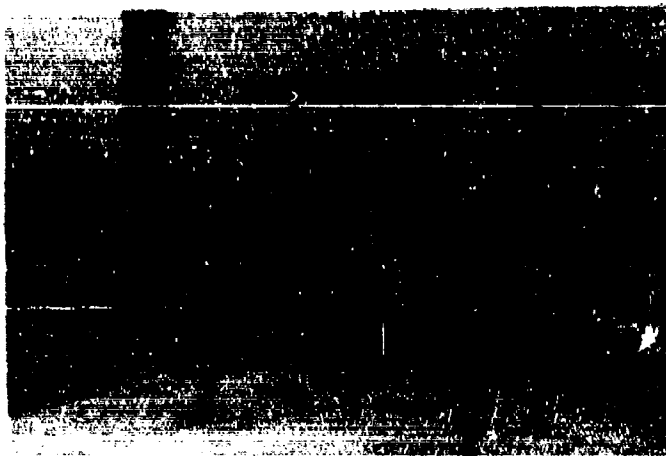
View of Tunnel to Rear Alley

FIGURE E-18



View of Building from West 52nd Street

FIGURE E-19



View of Roof (Note: three foot lip at edge)

D. Twenty-one Story Office Building

1. Discussion

The Palmolive Trust Building on Park Avenue in New York City is a twenty-one story office building situated among other tall buildings which would provide considerable shielding from radiation intensity. The fourth floor detector is sufficiently far from the roof so that none of the intensity received at the detector comes from the roof. Almost all of the radiation intensity comes from the paved roads and sidewalks directly adjacent to the building itself. A small part of the intensity would come from the garden island areas in the middle of Park Avenue. It is believed that this area could not be decontaminated easily.

2. Analysis Data

(a) Address: 310 Park Avenue
Manhattan, New York City
New York

(b) Detector Location: Fourth Floor - (Three feet off floor)

(c) Normal Protection Factor: $PF = 276$

(d) Decontamination Areas:

(1) Park Avenue: 110,000 sq. ft. asphaltic concrete road
and cement sidewalk

12,000 sq. ft. asphaltic concrete road
and cement sidewalk.

(2) Other Roads: 42,000 sq. ft. asphaltic concrete road
and cement sidewalk.

(e) Ideal Intensity Reduction Factors

(1) Park Avenue: $f_{1,1}^* = .439$

(2) Other Roads: $f_{2,1}^* = .611$

(3) All Road Surfaces: $F_1^* = .044$

(f) Cost and Effectiveness Data for Selected Methods on Individual Surfaces:

Strategy Identification, Symbol	Area (Use Nos. from (d) above)	Mass Reduction Factor (R_1)	Intensity Reduction Factor ($F_{1,j}$)	Team Hours of Effort	Crew Dose in roentgens
SS1	1	.04	.456	4.88	48.8
SS4	1	.15	.518	1.22	12.2
VS1	1	.02	.442	4.88	48.8
VS3	1	.25	.575	1.22	12.2
MF1	1	.02	.442	1.22	12.2
F3	1	.07	.473	4.88	48.8
SS1	2	.04	.627	1.68	16.8
SS4	2	.15	.669	0.42	4.2
VS1	2	.02	.619	1.68	16.8
VS3	2	.25	.708	0.42	4.2
MF1	2	.02	.619	0.42	4.2
F3	2	.07	.638	1.68	16.8

(g) Combined Strategies:

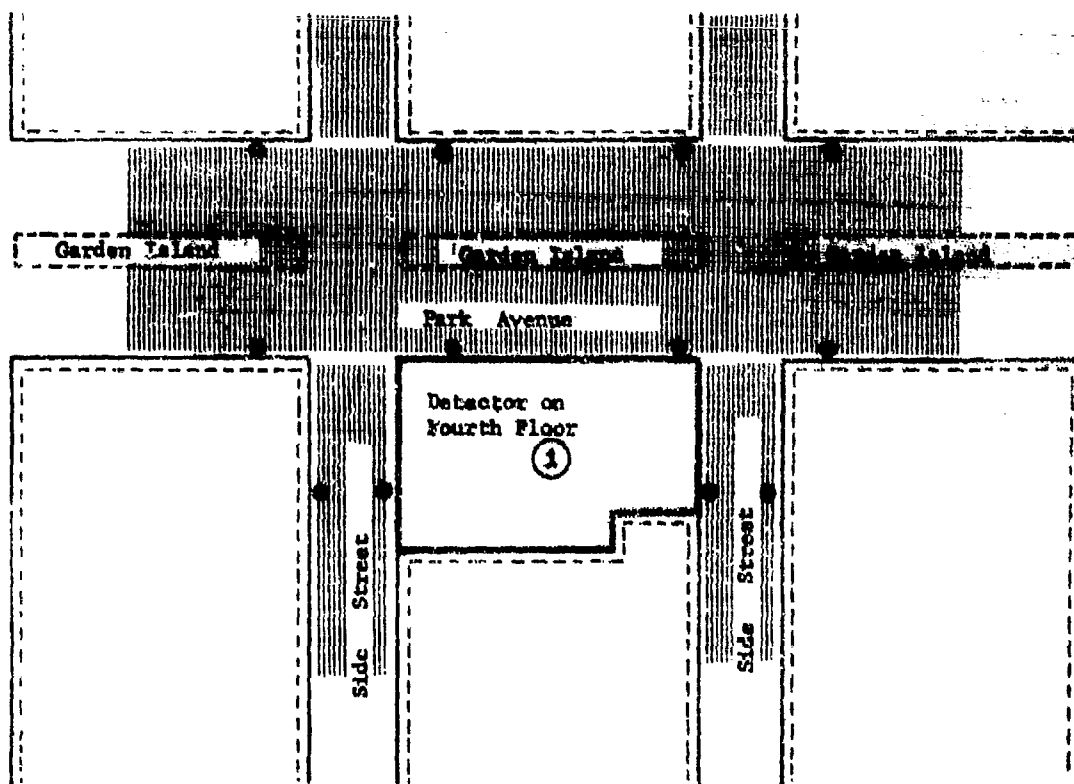
Strategy Identification Symbol and Area	Intensity Reduction Factor, F_1	Total Man-Hours of Effort
SS4-1 + SS4-2	.187	1.64
SS1-1 + SS1-2	.083	6.56
MF1-1 + MF1-2	.061	1.64
F3-1 + F3-2	.111	32.80

* See Tables E-I and E-II for description of symbols

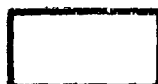
** Crew dose in roentgens is calculated assuming decontamination at H+2 weeks with an H+1 reference intensity of 10,000 r/hr.

3. Map

FIGURE E-20. Location Map of Decontamination Areas

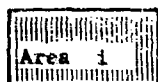


● fire hydrants

 principal building

 adjacent building

① detector location 1

 Area 1 decontamination Area

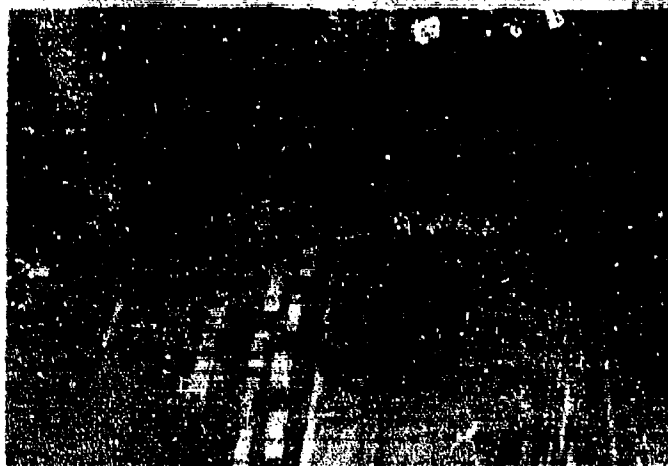
4. Some Photographs of the Associated Contaminated Surfaces

FIGURE E-21



View of Park Avenue (Note: Island
with Garden in Center of Road)

FIGURE E-22



View of East 49th Street

FIGURE E-23



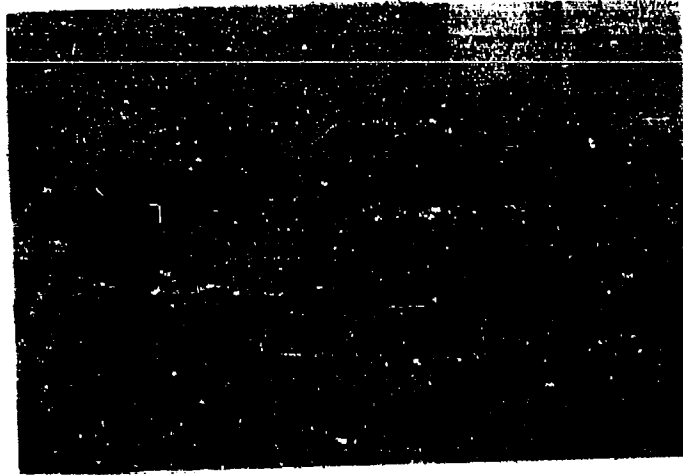
View of Park Avenue Showing Iron Gate Around
Center Island

FIGURE E-24



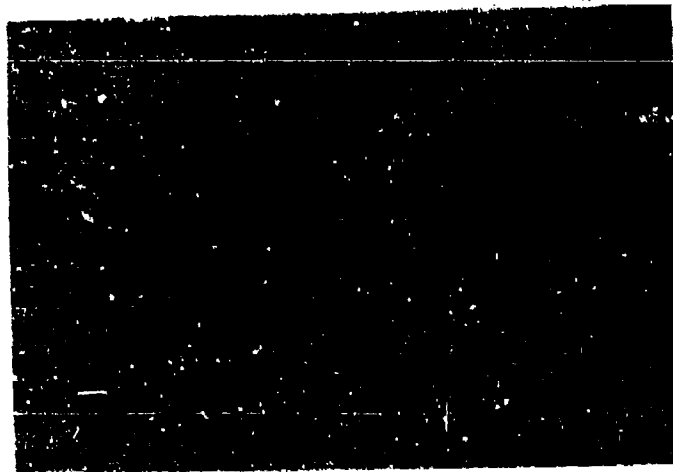
View of Sidewalk and Fireplug on
East 49th Street

FIGURE E-25



View of Roof (Non-contributing surface)

FIGURE E-26



A Drain on the Roof

E. General Dyestuffs Corporation

1. Discussion

The General Dyestuffs Corporation is similar to the building in Section C in that a garage roof is one of the decontamination surfaces. Here, this roof accounts for more than one-tenth of the radiation intensity on the fourth floor and is therefore distinguished as a separate decontamination area in the analysis.

All brick pavements were assumed to be equivalent to asphaltic concrete when estimating the effectiveness of the decontamination equipment.

2. Analysis Data

(a) Address: 435 Hudson Street
Manhattan, New York City
New York

(b) Detector Location: Fourth Floor

(c) Normal Protection Factor: PF = 126

(d) Decontamination Areas:

(1) All Roads: 110,000 sq. ft.

(2) Parking Lot and Playground: 36,000 sq. ft.

(3) Roof of Adjacent Garage: 4,000 sq. ft.

(e) Ideal Intensity Reduction Factors:

(1) Roads: $f_{1,1}^* = .123$

(2) Parking Lot and Playground: $f_{2,1}^* = .991$

(3) Roof of Adjacent Garage: $f_{3,1}^* = .887$

(4) Above Combined: $F_1^* = .001$

(f) Cost and Effectiveness Data for Selected Methods on
Individual Areas:

Strategy Identifi- cation, Symbol	Area (Use Nos. from (d) above)	Mass Reduction Factor (R_1)	Intensity Reduction Factor ($f_{1,j}$)	Team Hours of Effort	Crew Dose in Roentgens **
SS1	1	.04	.158	4.40	44.0
SS4	1	.15	.255	1.10	11.0
VS1	1	.02	.141	4.40	44.0
VS3	1	.25	.342	1.10	11.0
F3	1	.07	.184	4.40	44.0
SS1	2	.04	.991	1.44	14.4
VS1	2	.02	.991	1.44	14.4
MF1	2	.02	.991	0.36	3.6
F1	2	.02	.991	7.20	72.0
FCS1	3	.03	.890	.33	3.3
FCS3	3	.08	.896	.07	.7

(g) Combined Strategies:

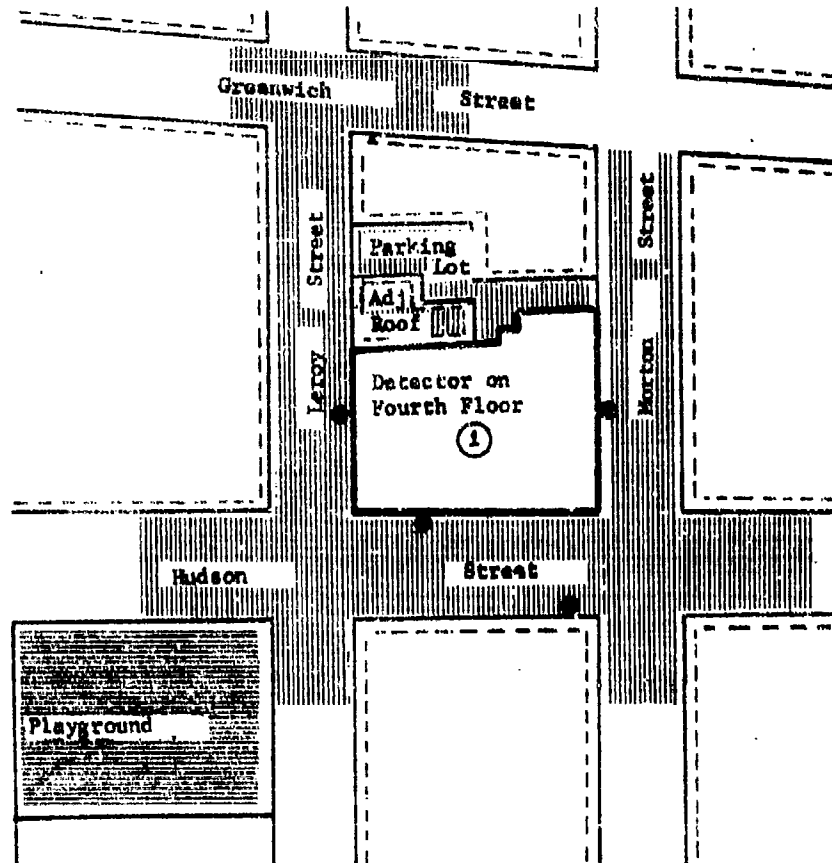
Strategy Identification Symbol and Area	Intensity Reduction Factor, F_1	Total Man- Hours of Effort
SS4-1 + SS1-2 + FCS1-3	.136	4.52
SS4-1 + FCS1-3	.145	3.08
F3-1 + F1-2 + FCS1-3	.065	59.78
SS1-1 + FCS1-3	.048	6.38

* See Tables E-I and E-II for description of symbols.

** Crew dose in roentgens is calculated assuming decontamination at H+2 weeks with an H+1 reference intensity of 10,000 r/hr.

3. Map

FIGURE E-27. Location Map of Decontamination Areas



● fire hydrants



principal building



adjacent buildings



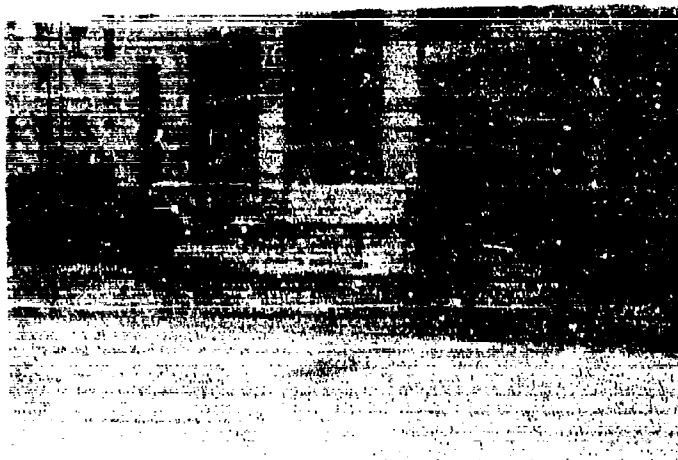
detector location



decontamination area

4. Some Photographs of the Associated Contaminated Surfaces

FIGURE E-28



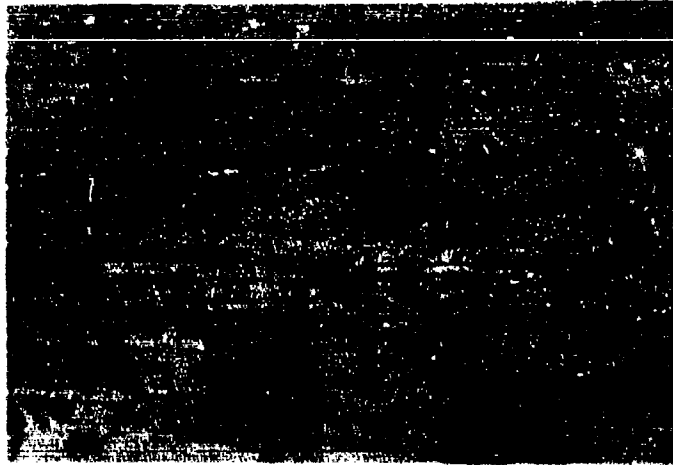
View of Building from Hudson Street.
(Note: Sewer drain)

FIGURE E-29



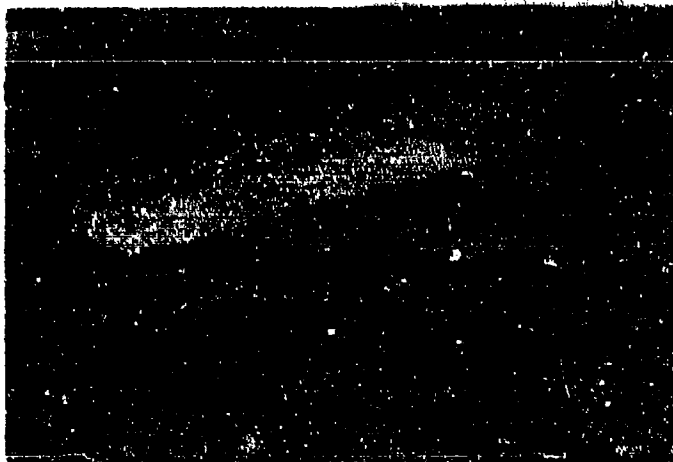
View of Intersection of Hudson Street and
Morton Street. (Note: brick pavement, fire-
plug and sewer)

FIGURE E-30



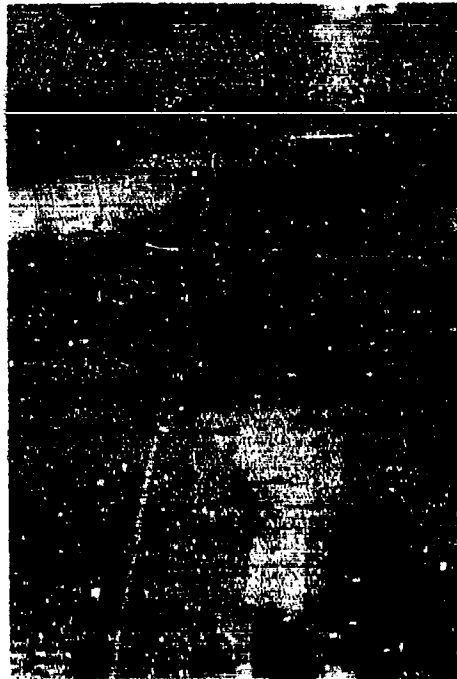
View of Building Roofs Across Laroy Street

FIGURE E-31



Playground (Note: two drains in center)

FIGURE E-32



View of Hudson Street and Sidewalk
Area from Roof

FIGURE E-33



View of Parking Lot and Adjacent Garage
Roof. (Note: depression area on garage roof)

F. High School Gymnasium

1. Discussion

This building is surrounded by large paved areas which could easily be decontaminated. About half of the radiation intensity on the second floor could be removed by decontamination of the paved ground-level areas around the building. A complete decontamination of the roof and the paved areas near the building would remove more than 95% of the radiation intensity.

2. Analysis Data

(a) Address: Bennett Street
Boston, Massachusetts

(b) Detector Location: Second Floor (Three feet off floor)

(c) Normal Protection Factor: $PF = 116$

(d) Decontamination Areas:

(1) Roads: 5,000 sq. ft. (asphaltic concrete)

(2) Parking Lot: 10,000 sq. ft. (asphalt)

(3) Playground: 23,750 sq. ft. (asphalt)

(4) Roof: 4,700 sq. ft. (assumed to be tar and gravel)

(e) Ideal Intensity Reduction Factors:

(1) Roads: $F_{1,1}^* = .948$

(2) Parking Lot: $F_{2,1}^* = .789$

(3) Playground: $F_{3,1}^* = .767$

(4) Roof: $F_{4,1}^* = .513$

(5) Ground Areas (1,2,3): $F_1^* = .504$

(6) All Areas (1,2,3,4): $F_1^* = .017$

(f) Cost and Effectiveness Data for Selected Methods on

Individual Areas:

Strategy Identifi- cation, Symbol	Area (Use Nos. from (d) above	Mass Reduction Factor (E_1)	Intensity Reduction Factor ($I_{1,j}$)	Team Hours of Effort	Crew Dose in Roentgens **
SS4	1	.15	.954	.05	.5
MF1	1	.02	.949	.05	.5
SS3	2	.09	.808	.13	1.3
V83	2	.25	.842	.10	1.0
MF1	2	.02	.793	.10	1.0
SS3	3	.09	.788	.31	3.1
SS1	3	.04	.776	.95	9.5
V83	3	.25	.825	.24	2.4
MF1	3	.02	.772	.24	2.4
FC81	4	.03	.538	.39	3.9
FC83	4	.08	.552	.07	.7

(g) Combined Strategies:

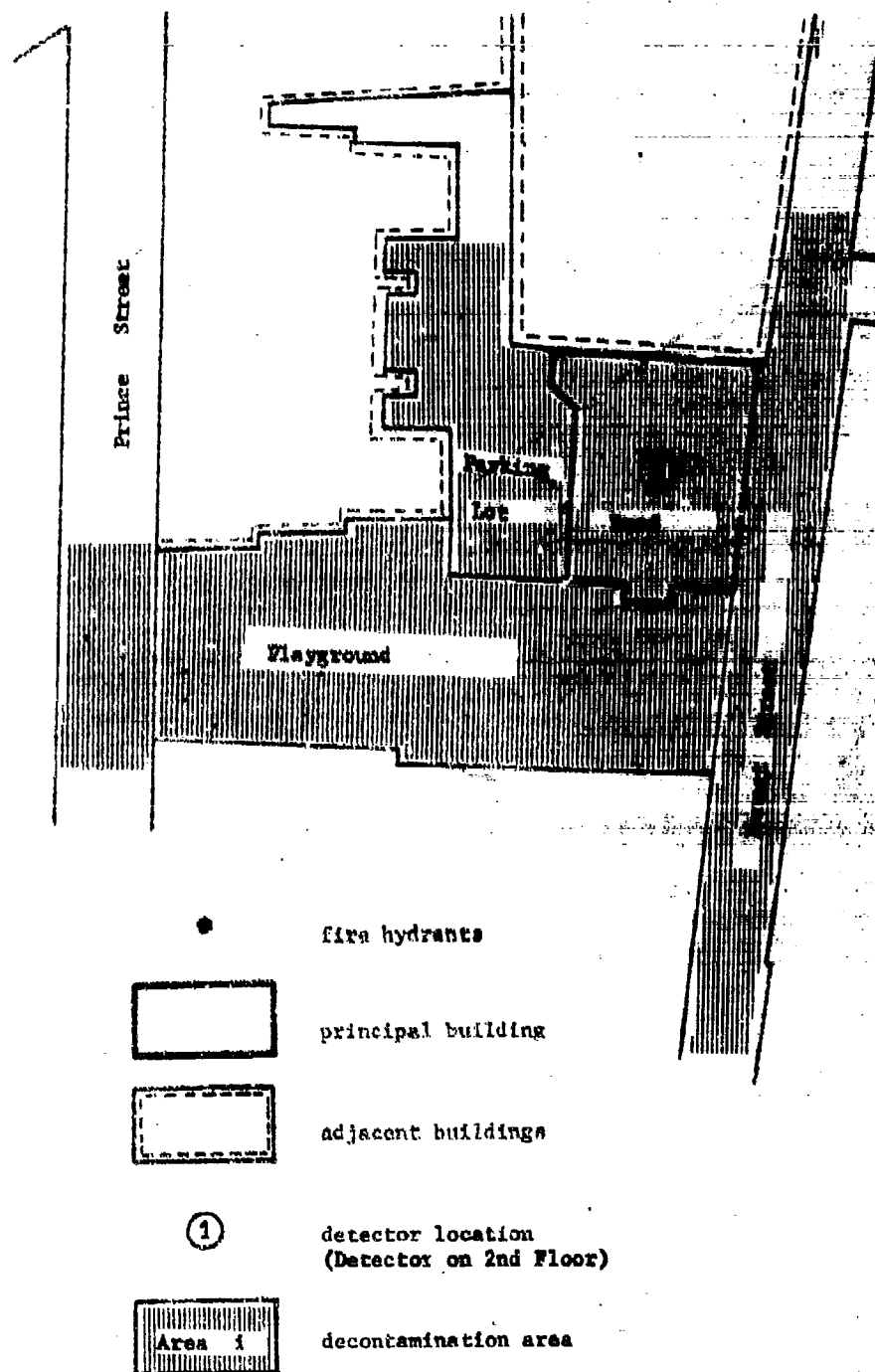
Strategy Identification Symbol and Area	Intensity Reduction Factor, F_1	Total Man- Hours of Effort
V83-2 + V83-3	.667	.34
SS4-1 + V83-2 + V83-3	.621	.39
SS3-3 + SS3-2	.596	.44
MF1-1 + MF1-2 + MF1-3	.514	.39
FC81-4	.528	2.36
SS4-1 + SS3-2 + SS3-3 + FC83-4	.092	.89

* See Tables E-I and E-II for description of symbols.

** Crew dose in roentgens is calculated assuming decontamination at H+2 weeks with an H+1 reference intensity of 10,000 r/hr.

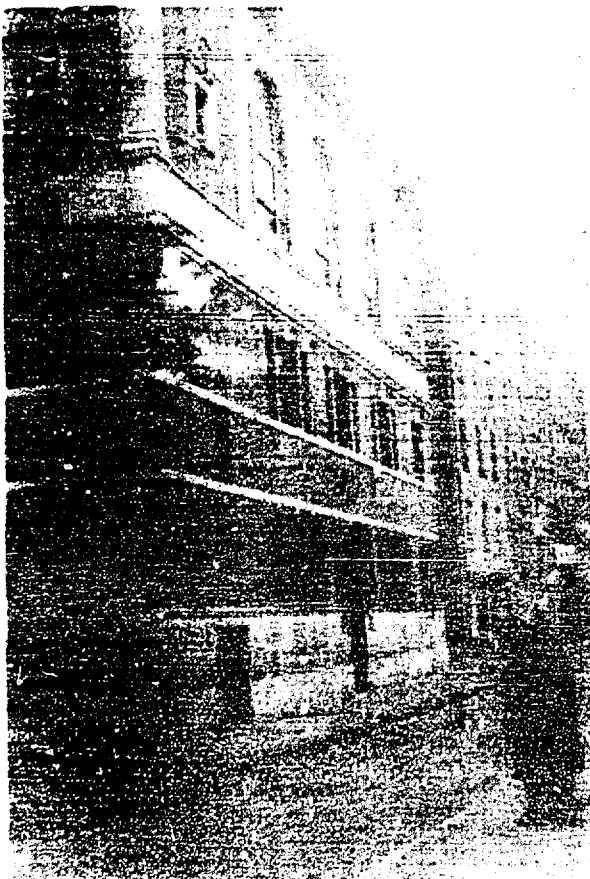
3. Map

FIGURE E-34. Location Map of Decontamination Areas



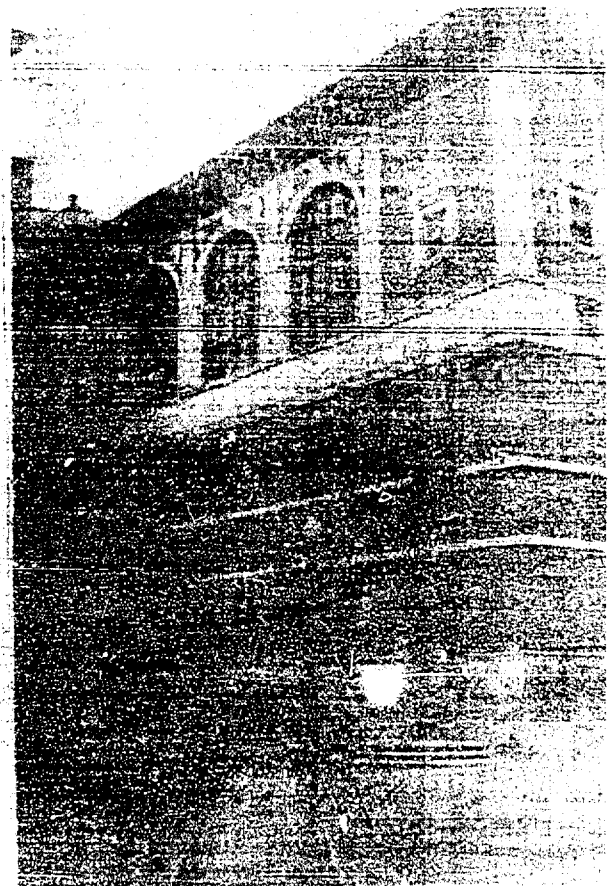
4. Some Photographs of the Associated Contaminated Surfaces

FIGURE E-35



View of Building from Bennett Street

FIGURE E-36



Playground

G. Simonds Press Building

1. Discussion

Here, the detector is located in the basement of the Simonds Press Building. Because the detector is located below the ground level, almost all (89 per cent) of the radiation intensity comes from the roof. The five degree pitch of the roof and the sharp incline of Ely Street might provide excellent drain-off for wet decontamination methods.

2. Analysis Data

(a) Address: 37-49 South Avenue
Rochester, New York

(b) Detector Location: Basement

(c) Normal Protection Factor: $1F = 47$

(d) Decontamination Areas:

(1) Roof: 10,000 sq. ft. (composition shingle - 5° pitch)

(2) Ground Level: 25,000 sq. ft. (asphaltic concrete -
South Avenue)

8,930 sq. ft. (brick - South Water Street)

1,960 sq. ft. (brick - Ely Street)

2,800 sq. ft. (asphaltic concrete - parking
lots)

880 sq. ft. (asphaltic concrete - Ely
Street extension).

(e) Ideal Intensity Reduction Factors:

(1) Roof: $f_{1,1}^* = .111$

(2) Ground Level: $f_{2,1}^* = .896$

(3) Roof and Ground Combined: $F_1^* = .007$

(f) Cost and Effectiveness Data for Selected Methods on
Individual Areas:

Strategy Identifi- cation* Symbol	Area (Use Nos. from (d) above)	Mass Reduction Factor (E_1)	Intensity Reduction Factor ($f_{i,j}$)	Team Hours of Effort	Crew Dose in Roentgens**
FCS1	1	.03	.138	.83	8.3
FC83	1	.08	.182	.17	1.7
F3	2	.07	.903	1.58	15.8
MF2	2	.04	.900	.12	1.2

(g) Combined Strategies:

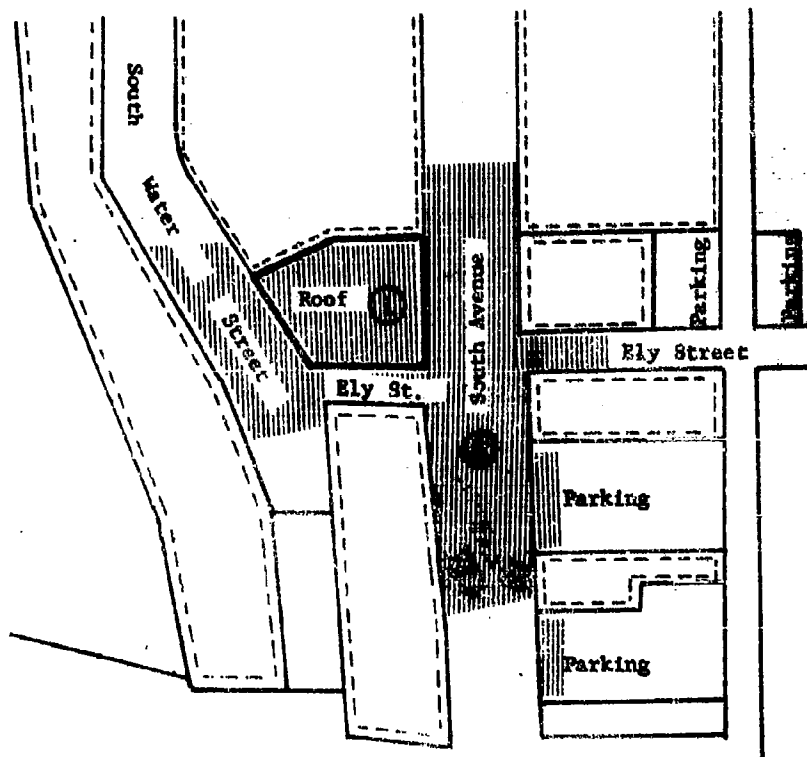
Strategy Identification Symbol and Area	Intensity Reduction Factor, F_1	Total Man- Hours of Effort
FCS1-1 + MF2-2	.038	4.68
FCS3-1 + MF2-2	.082	1.22
FCS3-1 + F3-2	.085	8.92
FCS3-1	.138	4.00





* See Tables E-I and E-II for description of symbols.

** Crew dose in roentgens is calculated assuming decontamination at H+2 weeks with an H+1 reference intensity of 10,000 r/hr.

3. Map

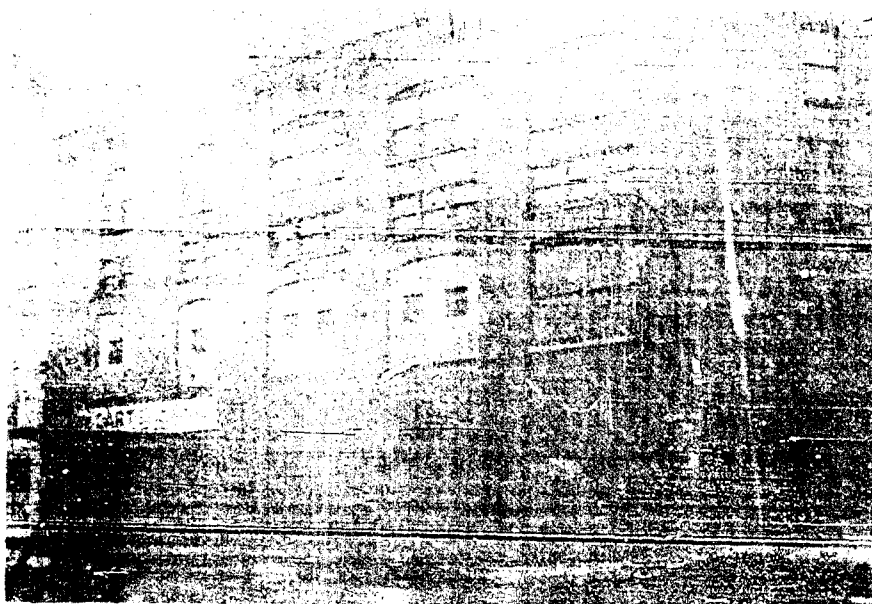
FIGURE E-37. Location Map of Decontamination Areas



- fire hydrants
-  principal building
-  adjacent buildings
-  detector location 1
-  Area 1 decontamination area

4. Some Photographs of the Associated Contaminated Surfaces

FIGURE E-38



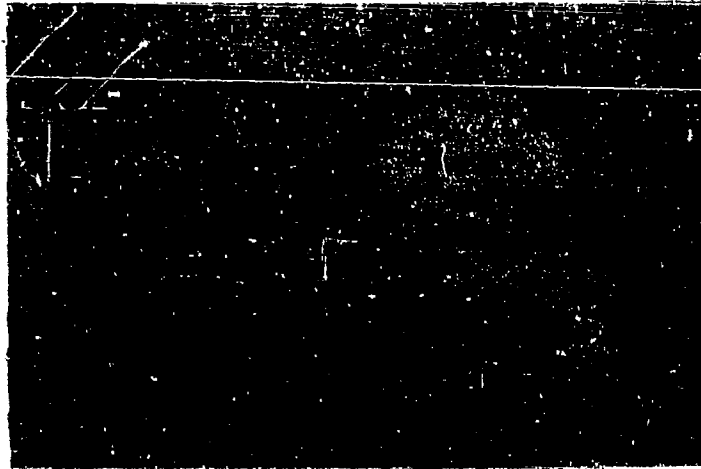
View of Building from South Water Street

FIGURE E-39



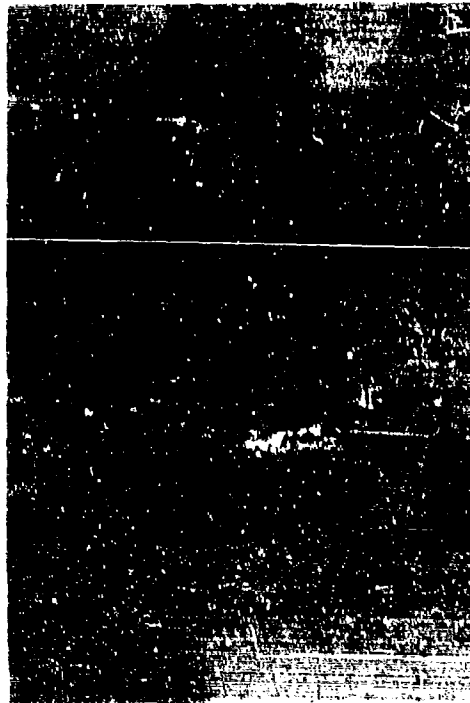
View of Building from Fly Street -
(Notes: green grass)

FIGURE E-40



View of Building from South Avenue

FIGURE E-41



View of Building from Intersection of
South Avenue and Ely Street

H. Department of Interior*

1. Discussion

The original protection factor of this building on the third floor is quite high. Furthermore, most of the intensity would be from fallout in four inner court areas (See map, Figure E-42).

If the inner courts are decontaminated, almost 99 per cent of, all radiation intensity is removed from a location in the center of the court itself.

2. Analysis Data

(a) Address: 18th and C Streets, N. W.
Washington, D. C.

(b) Detector Location: Third Floor

(c) Normal Protection Factor: PF = 1090

(d) Decontamination Areas:

(1) Interior Courts: 23,400 sq. ft. (assumed to be concrete)

(2) Roads: 800 sq. ft. (assumed to be asphaltic concrete -
19th Street, N. W.)

1200 sq. ft. (assumed to be asphaltic concrete -
18th Street, N. W.)

(e) Ideal Intensity Reduction Factors:

(1) Interior Courts: $f_{1,1}^* = .392$

(2) Roads: $f_{2,1}^* = .818$

(3) Courts and Roads Combined: $F_1^* = .210$

* Sub-section 4 not included in this section inasmuch as no photographs were available.

(f) Cost and Effectiveness Data for Selected Methods on
Individual Surfaces:

Strategy Identification Symbol*	Area (Use Nos. from (d) above)	Mass Reduction Factor (R_1)	Intensity Reduction Factor ($f_{i,j}$)	Team Hours of Effort	Crew Dose in Roentgens**
F1	1	.02	.404	4.68	46.8
F3	1	.07	.434	.94	9.4
F1	2	.02	.822	2.02	20.2
F3	2	.07	.831	.40	4.0
MF2	2	.04	.825	.01	.1
V83	2	.25	.864	.02	.2
SS4	2	.15	.845	.02	.2

(g) Combined Strategies:

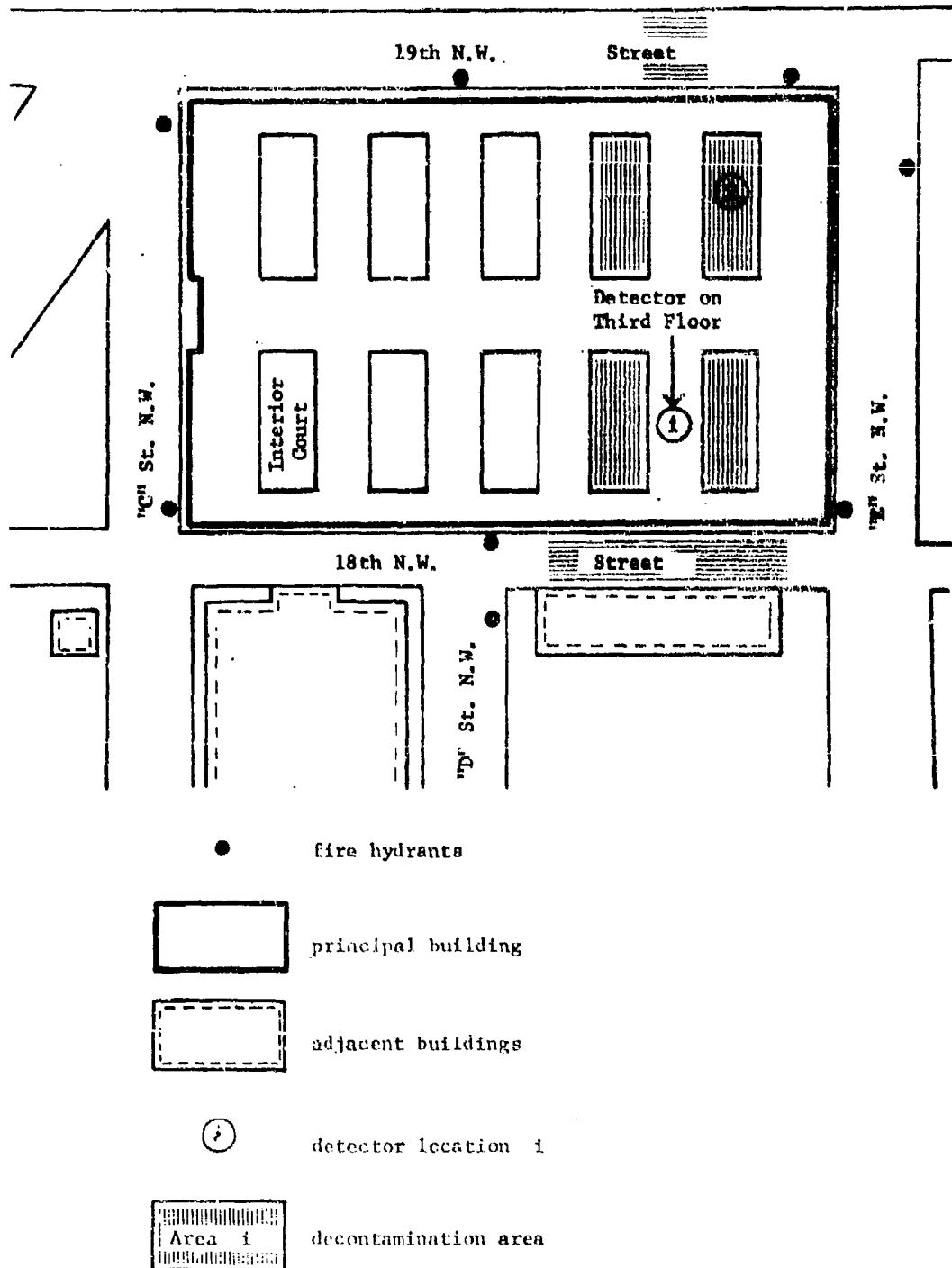
Strategy Identification Symbol and Area	Intensity Reduction Factor, F_1	Total Man- Hours of Effort
F1-1 + F1-2	.226	33.40
F3-1 + F3-2	.265	6.70
F1-1	.404	23.40

* See Tables E-I and E-II for description of symbols.

** Crew dose in roentgens is calculated assuming decontamination at H+2 weeks with an H+1 reference intensity of 10,000 r/hr.

3. Map

FIGURE E-42. Location Map of Decontamination Areas



5. Outside Detector

(a) Location of Detector: The center of any of the interior court sections.

(b) Original PF at site of detector----- 1.61

(c) F_2^* for court = 0 (all of the dose rate contribution comes from fallout in the court itself).

1. A Three-Story Department Store Building

1. Discussion

This three-story building can be effectively decontaminated. All but about one-one thousandth of the intensity reaches the second-floor detector from the roof and the streets in front of and on two sides of the building. There are no narrow alleys, trees, or other sources of stray contamination in the area.

2. Analysis Data

(a) Address: 619 Main Street
Houston, Texas

(b) Detector Location: Second Floor

(c) Normal Protection Factor: $PF = 26$

(d) Decontamination Areas:

(1) Roof: 9,400 sq. ft. (assumed tar and gravel)

(2) Roads: 68,300 sq. ft. (assumed asphaltic concrete)

(e) Ideal Intensity Reduction Factors:

(1) Roof: $f_{1,1}^* = .382$

(2) Roads: $f_{2,1}^* = .619$

(3) Roof and Roads Combined: $F_1^* = .001$

(f) Cost and Effectiveness Data for Selected Methods
and Individual Surfaces:

Strategy Identifi- cation,* Symbol	Area (Use Nos. from (d) above)	Mass Reduction Factor (E_1)	Intensity Reduction Factor ($E_{1,j}$)	Team Hours of Effort	Crew Dose in Roentgen. **
FTG1	1	.01	.388	1.34	13.4
FTG4	1	.12	.456	0.27	2.7
SS1	2	.04	.634	2.73	27.3
SS4	2	.15	.676	0.68	6.8
VS2	2	.09	.653	1.37	13.7
MF1	2	.02	.627	0.68	6.8
MF2	2	.04	.634	0.20	2.0

(g) Combined Strategies:

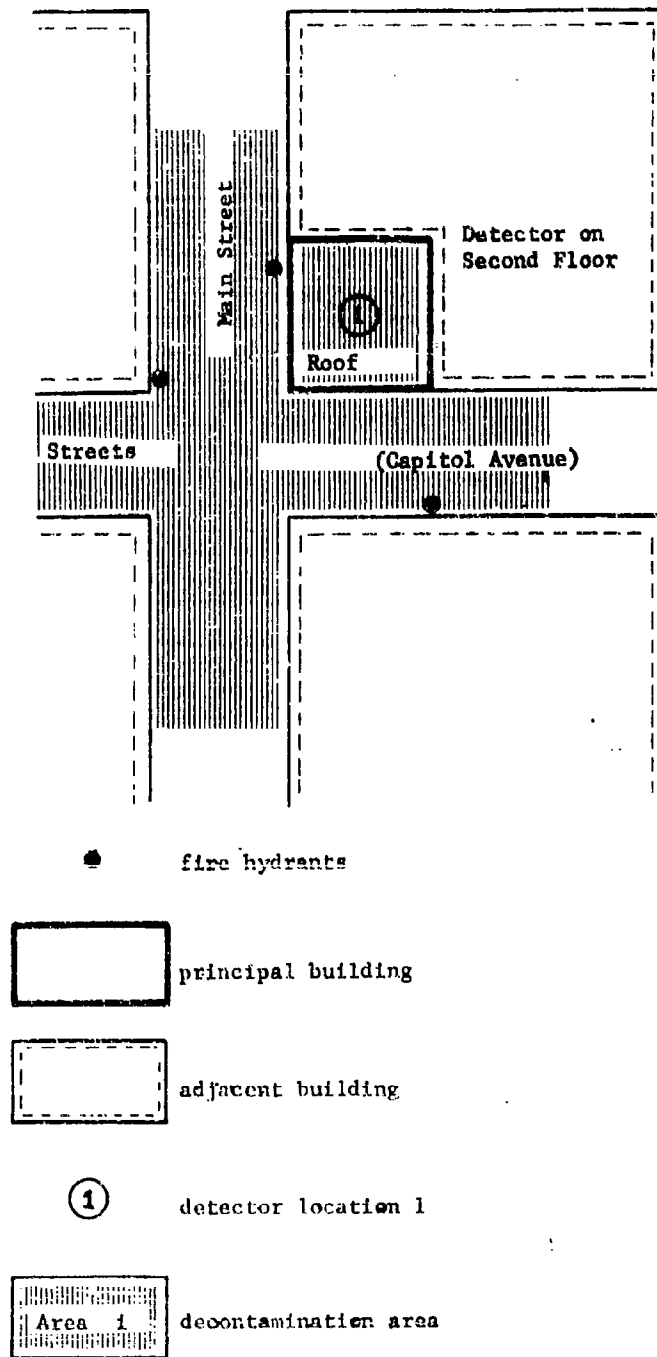
Strategy Identification Symbol and Area	Intensity Reduction Factor, F_1	Total Man- Hours of Effort
FTG4-1 + SS4-2	.132	2.57
FTG1-1 + SS1-2	.022	12.11
FTG1-1 + MF1-2	.015	10.06
FTG4-1 + VS2-2	.109	3.26

* See Tables E-I and E-II for a description of symbols.

** Crew dose in roentgens is calculated assuming decontamination at H+2 weeks with an H+1 reference intensity of 10,000 r/hr.

3. Map

FIGURE E-43. Location Map of Decontamination Areas



(e) Ideal Intensity Reduction Factors:

- (1) 4th Floor Roof: $f_{1,1}^* = .732$
- (2) 14th Floor Roof: $f_{2,1}^* = .885$
- (3) Roads: $f_{3,1}^* = .843$
- (4) Parking Lots: $f_{4,1}^* = .870$
- (5) Grass Lawns: $f_{5,1}^* = .992$
- (6) All above: $F_1^* = .322$

(f) Cost and Effectiveness Data for Selected Methods on Individual Surfaces:

Strategy Identification* Symbol	Area (Use Nos. from (d) above)	Mass Reduction Factor (E_1)	Intensity Reduction Factor ($f_{i,j}$)	Team Hours of Effort	Crew Dose in Roentgens**
FCS1	1	.03	.740	.59	5.9
FCS3	1	.08	.753	.12	1.2
FCS1	2	.03	.888	.06	.6
FCS3	2	.08	.894	.01	.1
SS1	3	.04	.849	8.04	80.4
SS4	3	.15	.867	2.01	20.1
VS2	3	.09	.857	4.02	40.2
MF2	3	.04	.849	.60	6.0
SS1	4	.04	.875	2.92	29.2
SS4	4	.15	.890	.72	7.2
VS2	4	.09	.882	1.44	14.4
MF2	4	.04	.875	.22	2.2

(g) Combined Strategies:

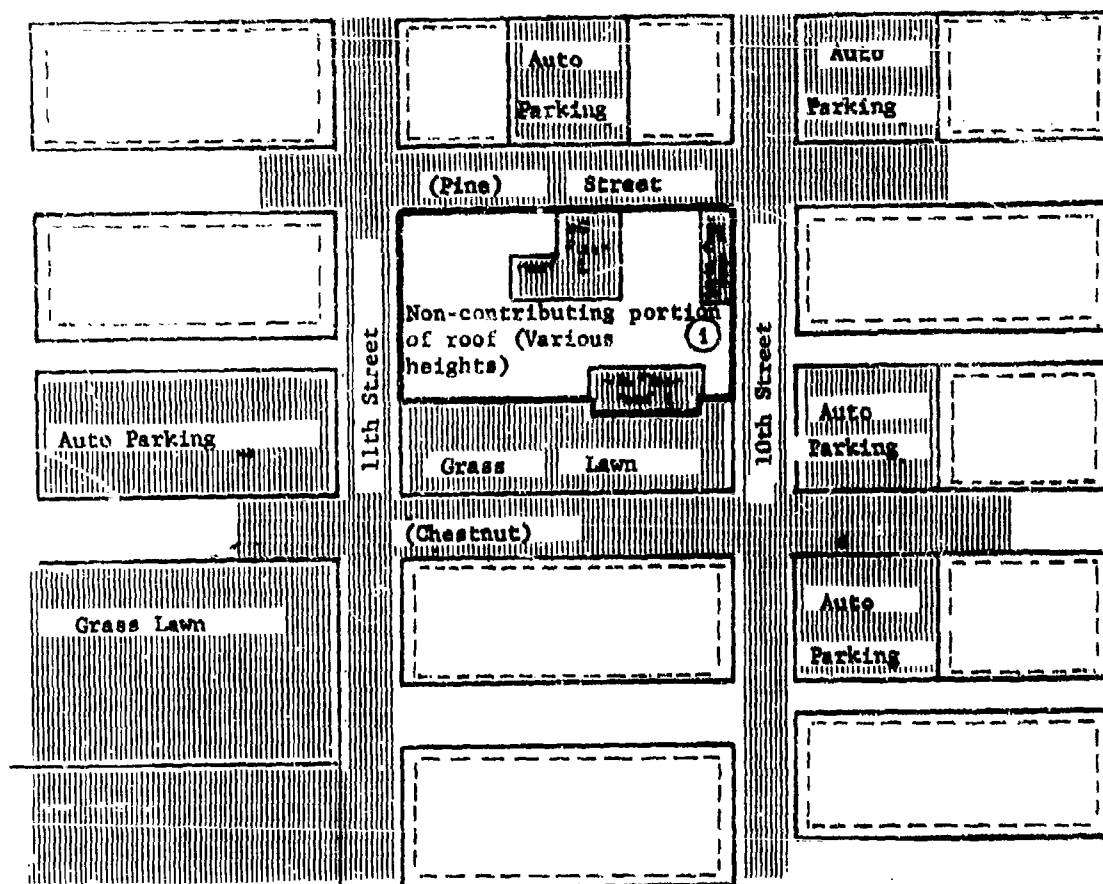
Strategy Identification Symbol and Area	Intensity Reduction Factor, F_1	Total Man-Hours of Effort
FCS3-1 + FCS3-2 + VS2-3 + VS2-4	.386	8.70
FCS1-1 + FCS1-2 + VS2-3 + VS2-4	.367	9.36
FCS1-1 + FCS1-2	.628	3.90
MF2-3 + MF2-4	.724	0.82

* See Tables E-I and E-II for a description of symbols.

** Crew dose in roentgens is calculated assuming decontamination at H+2 weeks with an H+1 reference intensity of 10,000 r/hr.

3. Map

FIGURE E-46. Location Map of Decontamination Areas



● fire hydrants

▭ principal building

▭ adjacent buildings

① detector location
(Detector on 13th Floor)

▭ Area 1 decontamination area

4. Some Photographs of the Associated Contaminated Surfaces

FIGURE E-47



View of Building from Intersection of 11th Street
and Chestnut Street

FIGURE E-48



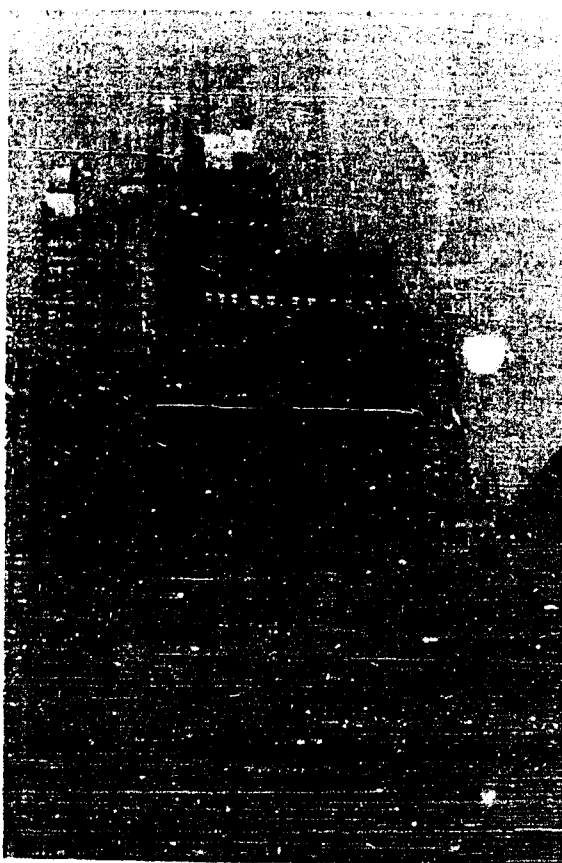
View of Building from Pine Street

FIGURE E-49



View of the Building from 10th Street and Chestnut Street

FIGURE E-50



View of the Building from 11th Street

K. Fictitious Building - Parametric Study

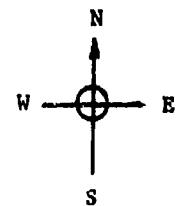
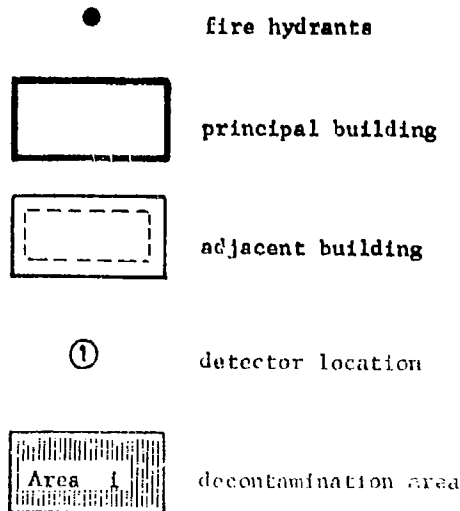
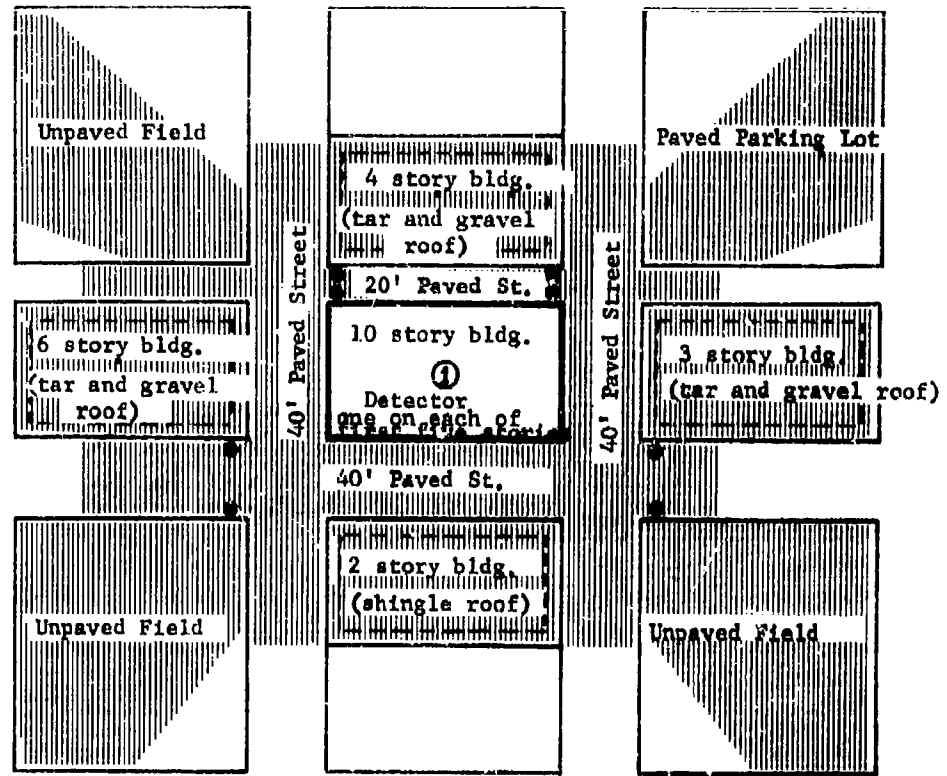
1. Discussion

This study is included in order to analyze the effects that certain physical parameters have on the intensity reduction of decontaminating a variety of individual contaminated planes. For this study, a fictitious ten-story structure was conceived, and a detector was placed on each of the first five floors. These detectors are centered in the building as is shown on the map (Figure E-51). They are three feet from the floor in each case. The map also shows the individual surfaces which can be decontaminated. Table E-VI assigns a Surface Number to each of these potential contaminated planes.

Table E-VII shows all of the pertinent building data necessary to calculate the reduction of radiation intensity due to removing all of the contamination from any single contaminated plane. Tables E-VIII through E-XI show the $f_{i,j}^*$ values for all of the parametric studies. These studies are designated Parametric Studies I, II, III, and IV. The conclusions drawn from these tables are included in Section A-3 of this chapter. The $f_{i,j}^*$ factor is simply the fraction of radiation intensity remaining at the detector on floor j when the contaminated plane referenced by Surface Number i is decontaminated perfectly. The original residual number and PF associated with each detector are also shown on Tables E-VIII through E-XI.

3. Map

FIGURE E-11. Location Map of Parametric Study



2. Analysis Data

TABLE E-VI

Designation of Surfaces which can be Decontaminated

<u>Surface Number</u> (See Figure 2-44)	<u>Description</u>
1	9 story building north of detector location (120 ft. x 60 ft.)
2	3 story building east of detector location (120 ft. x 60 ft.)
3	2 story building south of detector location (120 ft. x 60 ft.)
4	6 story building west of detector location (120 ft. x 60 ft.)
5	40 ft. wide road west of detector location
6	40 ft. wide road east of detector location
7	40 ft. wide road south of detector location
8	20 ft. wide alley north of detector location
9	Parking lot in NE corner
10	The three unpaved fields

All pavement in the intersections are considered part of the two north-south roadways.

TABLE E-VII

Building Data for Hypothetical Building Study

Building Data for Parametric Studies I, II, and III

1. number of stories----- 10 (detector located on first five floors)
2. number of azimuthal sectors----- 12
3. total height of building----- 100'
4. height of each story----- 10'
5. roof weight----- 60 psf
6. exterior wall weight----- 80 psf
7. windows: sill height----- 3'
top of window height----- 8'
(window widths total to about 50% of the exterior wall width)
8. building dimensions----- 60' x 120'
9. Floor weights are shown on individual charts.

Building Data for Parametric Study IV.

This building is like that for studies I, II, and III except for the following:

1. The north wall of the building has no windows
2. The west side of the detector has additional protection from an interior partition (10 psf).

TABLE E-VIII

The $f_{i,j}^*$ Values for Parametric Study I*

Parametric Study I: All Floor Weights = 37 psf

		<u>Values of $f_{i,j}^*$</u>				
	floor j	1	2	3	4	5
Surface number i						
1		1	1	1	1	1
2		1	1	.999	.965	.955
3		1	.998	.930	.921	.918
4		1	1	1	1	1
5		.803	.849	.885	.913	.919
6		.787	.826	.860	.847	.874
7		.795	.797	.795	.984	.844
8		.843	.899	.951	.957	.972
9		.956	.930	.912	.958	.920
10		.815	.731	.684	.680	.699

floor (j)	original residual number	original PF
1	.0322	31.07
2	.0265	37.71
3	.0234	42.79
4	.0225	44.42
5	.0209	47.88

* See Table E-VII

TABLE E-IX

The f_{ij}^* Values for Parametric Study II*

Parametric Study II: All Floor Weights = 17 psf

Surface number i	floor j	1	2	3	4	5
1		1	1	1	1	1
2		1	1	.998	.970	.946
3		1	.996	.941	.902	.901
4		1	1	1	1	1
5		.805	.859	.891	.924	.930
6		.788	.835	.869	.884	.894
7		.790	.797	.810	.837	.869
8		.848	.891	.931	.971	.976
9		.956	.928	.901	.905	.913
10		.814	.695	.655	.645	.676

floor (j)	original residual number	original PF
1	.0340	29.37
2	.0352	28.38
3	.0289	34.57
4	.0282	35.50
5	.0270	37.08

*See Table E-VII

TABLE E-X

The $f_{1,j}^*$ Values for Parametric Study III*

Parametric Study III: All Floor Weights = 57 psf

	floor j	1	2	3	4	5
Surface number i						
1		1	1	1	1	1
2		1	1	.999	.961	.961
3		1	.999	.923	.934	.931
4		1	1	1	1	1
5		.803	.843	.881	.906	.911
6		.786	.819	.855	.855	.860
7		.797	.797	.785	.821	.827
8		.842	.906	.950	.965	.969
9		.957	.931	.920	.924	.925
10		.816	.703	.703	.703	.715

floor (j)	original residual number	original PF
1	.0315	31.73
2	.0226	44.25
3	.0209	47.78
4	.0200	49.98
5	.0182	55.03

* See Table E-VII

TABLE E-XI

The $f_{i,j}^*$ Values for Parametric Study IV^{*}

Parametric Study IV: All Floor Weights = 37 psf

	floor j	1	2	3	4	5
Surface number i						
1		1	1	1	1	1
2		1	1	1	1	.998
3		1	.999	.936	.910	.941
4		1	1	1	1	1
5		.879	.893	.914	.931	.932
6		.791	.818	.869	.891	.887
7		.737	.734	.737	.772	.793
8		.838	.917	.965	.979	.986
9		.951	.923	.908	.910	.957
10		.817	.694	.680	.658	.657

floor (j)	original residual number	original PF
1	.0317	31.51
2	.0250	39.98
3	.0221	45.33
4	.0200	49.88
5	.0175	57.29

^{*} See Table E-VII

1. Unshielded Detector on Streets - Parametric Study

i. Straight Road

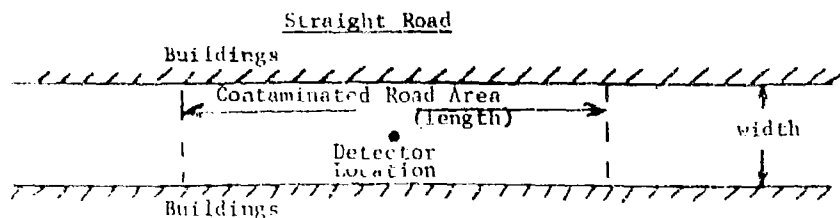
Table E-XII shows computed protection factors for persons standing in the middle of an asphalt* street as shown in Figure E-45 for various widths and lengths of contaminated roadway. All of the radiation intensity at the point is received from fallout on this single piece of road (i.e., within the areas designated in Figure E-52. This would be the case if buildings lined both sides of the street.

TABLE E-XII

Equivalent PF Obtained by Removing all Contamination Except on Straight Road.

<u>Length (feet)</u>	<u>Width (feet)</u>	<u>PF</u>
1000	60	1.57
200	60	1.57
100	60	1.59
50	60	1.71
1000	40	1.67
200	40	1.67
100	40	1.68
50	40	1.79

FIGURE E-52



*The ground roughness factors used were those associated with asphalt.

2. T - Intersections

Table E-XIII shows computed protection factors for person-standing in a T - shaped street intersection as shown in Figure E-53 for various lengths and widths of the intersecting roads.

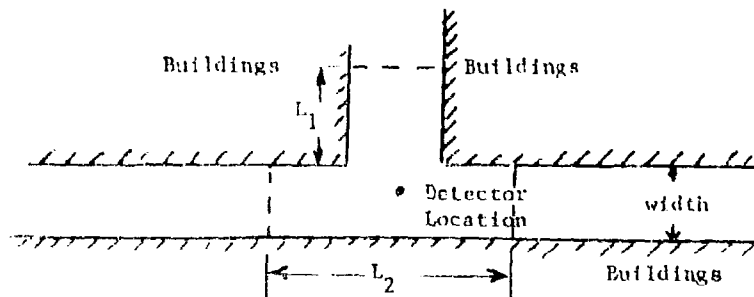
TABLE E-XIII

Equivalent PF Obtained by Removing all Contamination
Except that on T - Shaped Intersection

<u>Length L_1 (feet)</u>	<u>Length L_2 (feet)</u>	<u>Width (feet)</u> <u>Both Streets</u>	<u>PF</u>
500	1000	60	1.54
100	1000	60	1.54
50	1000	60	1.55
0	1000	60	1.57
50	200	60	1.55
50	100	60	1.56
50	50	60	1.57
500	1000	40	1.63
100	1000	40	1.63
50	1000	40	1.64
0	1000	40	1.67

FIGURE E-53

T - Shaped Street Intersection



3. Full Four-way Street Intersections

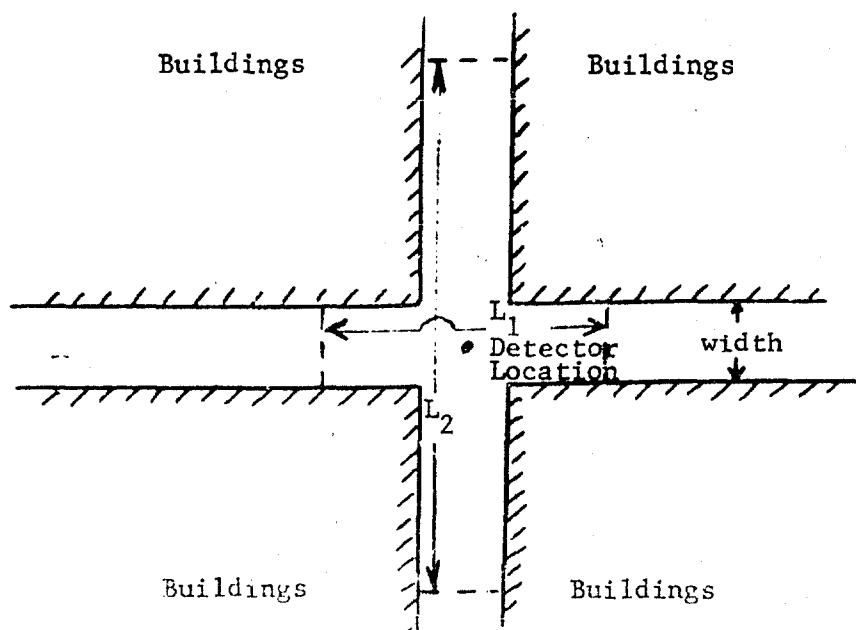
Table E-XIV shows computed protection factors for persons standing in the center of a full four-way intersection for various road widths and lengths as designated in Figure E-54.

TABLE E-XIV
Equivalent PF Obtained by Removing all Contamination
Except that on Four-way Intersection

Length L_1 (feet)	Length L_2 (feet)	Width (feet) Both Streets	PF
1000	1000	60	1.47
1000	200	60	1.47
1000	100	60	1.50
1000	60	60	1.57
1000	1000	40	1.50
1000	200	40	1.51
1000	100	40	1.54
1000	40	40	1.67

FIGURE E-54

Full Four-way Intersection



4. Typical Protection Factors of Unshielded Detectors on Streets

Table E-XV shows some typical protection factors afforded to unshielded individuals located in the center of various streets and intersections. These values were selected from the preceding sections.

TABLE E-XV

Equivalent PF from
Typical Contaminated Streets *

<u>Road Width (feet)</u>	<u>Detector Location</u>	<u>PF</u>
60	Center of Straight Road	1.57
60	Center of T - Shaped Intersection	1.54
60	Center of Four-way Intersection	1.47
40	Center of Straight Road	1.67
40	Center of T - Shaped Intersection	1.63
40	Center of Four-way Intersection	1.50

* All roads are assumed to be asphalt and are lined with sufficiently tall buildings so that all of the contributing fallout is on the street itself.

APPENDIX E REFERENCES

- E-1 W. L. Owen, V. D. Sartor, and W. H. VanHorn. Stoneman II Test of Reclamation Performance, Vol. II: Performance Characteristics of Wet Decontamination Procedures. USNRDL-TR-335. San Francisco: United States Naval Radiological Defense Laboratory, July 1960.
- E-2 H. Lee, V. D. Sartor, and W. H. VanHorn. Stoneman II Test of Reclamation Performance, Vol. III: Performance Characteristics of Dry Decontamination Procedures. USNRDL-TR-336. San Francisco: United States Naval Radiological Defense Laboratory, June 1959.
- E-3 E. L. Hill, et. al. Analysis of Survey Data, R-OU-81, Final Report. Durham, North Carolina: Research Triangle Institute, Operations Research Division, 15 February 1964.
- E-4 C. F. Miller. Theory of Decontamination. Part I, USNRDL-460. San Francisco: United States Naval Radiological Defense Laboratory, July 1958.
- E-5 W. L. Owen and J. D. Sartor. Radiological Recovery of Land Target Components - Complex I and Complex II. USNRDL-TR-570. San Francisco: United States Naval Radiological Defense Laboratory, 25 May 1960.
- E-6 M. V. Cammarano, C. H. Wheeler, and G. S. Wing. A Prototype Civil Defense Manual for Radiological Decontamination of Municipalities. 2nd Edition. Caldwell, New Jersey: Environmental Systems, Curtiss Division, Curtiss-Wright Corporation, May 1964.
- E-7 Office of Civil Defense. Shelter Design and Analysis. (The Engineering Manual) TR-20. Revised edition. Washington: Office of Civil Defense, Volume I, November 1962 and Volume 2, September 1963.
- E-8 Office of Civil Defense. Federal Civil Defense Guide (Draft). Washington: Office of Civil Defense, August 1964.

DISTRIBUTION LIST

ADDRESSEE

No. of Copies

Office of Civil Defense, DOD
Pentagon, Washington, D. C.
Attn: Director for Research

remainder

Army Library
Civil Defense Unit
Washington 25, D. C.

3

Assistant Secretary of the Army (R&D)
Washington 25, D. C.
Attn: Assistant for Research

1

Chief of Naval Research (Code 104)
Department of the Navy
Washington 25, D. C.

1

Chief of Naval Operations (OP-07T10)
Department of the Navy
Washington 25, D. C.

1

Chief, Bureau of Naval Weapons (Code RRRE-5)
Department of the Navy
Washington 25, D. C.

1

Chief, Bureau of Medicine and Surgery
Department of the Navy
Washington 25, D. C.

1

Chief, Bureau of Supplies & Accounts (Code L12)
Department of the Navy
Washington 25, D. C.

1

Chief, Bureau of Yards and Docks
Office of Research (Code 74)
Department of the Navy
Washington 25, D. C.

1

U. S. Naval Civil Engineering Laboratory
Port Hueneme, California

1

Defense Documentation Center
Cameron Station
Alexandria, Virginia

20

Advisory Committee on Civil Defense
National Academy of Sciences
2101 Constitution Avenue, N. W.
Washington 25, D. C.
Attn: Mr. Richard Park

1

Chief, Bureau of Ships (Code 335)
Department of the Navy
Washington 25, D. C.

2

Chief, Bureau of Ships (Code 203)
Department of the Navy
Washington 25, D. C.

1

Coordin, Marine Corps
Landing Force
Development Activities
Quantico, Virginia

1

Dr. Wayne Bell
General Dynamics Corp.
P. O. Box 5
Old San Diego Station
San Diego 10, California

1

Dr. Eric Clarke
Technical Operations, Inc.
Burlington, Massachusetts

1

Dr. Carl F. Miller
Stanford Research Institute
Menlo Park, California

1

Cdr. W. J. Christensen
Naval Civil Engineering Laboratory
Port Hueneme, California

1

Dr. J. Laurence Kulp
Isotopes Incorporated
123 Woodlawn Avenue
Westwood, New Jersey

1

Dr. Louis Gavantman
Naval Radiological Defense Laboratory
San Francisco, California

1

Mr. Joseph Maloney
Nuclear Defense Laboratory
Army Chemical Center
Edgewood, Maryland

1

Dr. Wayne A. McRae
Ionics Incorporated
152 Sixth Street
Cambridge, Massachusetts

1

Mr. R. P. Schmidt
U. S. Army Material Office
Directorate of Research & Development
Fort Belvoir, Virginia

1

Dr. Edgar A. Parsons
Research Triangle Institute
P. O. Box 490
Durham, North Carolina

1

Mr. Wheeler & Cammarano
2 Field Stone Lane
Upper Saddle River, New Jersey

1

Mr. Olaf Fernald
Advance Research Inc.
19 Brook Road
Needham Heights 94, Massachusetts

1

Mr. Harvey Ludwig
Engineering Science, Inc.
150 East Foothills Boulevard
Arcadia, California

1

Dr. Eugene Sevin
IIT Research Institute
10 West 35th Street
Chicago 16, Illinois

1

Dr. Paul Parrino
Public Health Service, DHEW
Washington 25, D. C.

1

Mr. Herman Kahn
Hudson Institute
Quaker Ridge Road
Harmon-on-Hudson, New York

1

Dr. Robert McGinnis
Cornell University
Ithaca, New York

1

Lt. Col. Converse R. Lewis
Office of the Surgeon General
Main Navy Building
Washington 25, D. C.

1

Col. F. H. Whitley
Medical Division
Hq. USAREUR
APO 403
New York, New York

1

Dr. Frank Todd
Assistant to the Administrator
Agricultural Research
U. S. Department of Agriculture
Washington 25, D. C.

1

Dr. Luna Leopold Water Resources Division U. S. Geological Survey Washington 25, D. C.	1
Col. Stanley J. Widenkaph Hq. Medical R&D Command Main Navy Building Washington 25, D. C.	1
Water & Sewage Industry and Utilities Division U. S. Department of Commerce Washington 25, D. C.	1
Mr. Gordon E. McCallum Water Supply & Pollution Control Public Health Service, DHEW Washington 25, D. C.	1
Mr. George W. Burke, Jr. Div. of Water Supply & Pollution Control Public Health Service, DHEW Washington 25, D. C.	1
Prof. Thomas deS. Furman Civil Engineering Department University of Florida Gainesville, Florida	1
American Institute for Research 410 Amberson Avenue Pittsburgh, Pennsylvania	1
Dr. Frederick Bellinger School of Engineering Georgia Institute of Technology Atlanta, Georgia	1
Dr. W. Fulton Abercrombie U. S. Public Health Service Division of Health Mobilization Washington 25, D. C.	1
Dr. Ken Kaplan 1811 Trousdale Avenue United Research Services Burlingame, California	1
Dr. Frank Parker Health Physics Division Oak Ridge National Laboratory Oak Ridge, Tennessee	1

<p> PARM Project 7th Floor 1424 16th St., N. W. Washington, D. C. </p>	1
<p> Dr. Joseph Coker Office of Emergency Planning Washington 25, D. C. </p>	1
<p> Dr. Ray Edwards Nuclear Science & Engineering Corp. P. O. Box 10901 Pittsburgh 36, Pennsylvania </p>	1
<p> Mr. H. Malcolm Childers 708 North West Street Alexandria 14, Virginia </p>	1
<p> Technical Information Service U. S. Atomic Energy Commission Oak Ridge, Tennessee </p>	1
<p> Mr. Jim O. Terrell, Jr. Radiological Health Division U. S. Public Health Service, DHEW Washington 25, D. C. </p>	1
<p> Dr. Werner N. Grune Professor of Civil Engineering Merrimack College North Andover, Massachusetts </p>	1
<p> Mr. Walter Wood Dikewood Corporation 4803 Monaul Blvd. N. E. Albuquerque, New Mexico </p>	1
<p> U. S. Atomic Energy Commission Hdq. Reports Library G-017 Germantown, Md. </p>	1
<p> Commander, Field Command Defense Atomic Support Agency Sandia Base Albuquerque, New Mexico </p>	1
<p> Dr. Morgan Seal U. S. Public Health Service Box 684 Las Vegas, Nevada </p>	1

<p>Defense Logistics Studies Information Exchange U. S. Army Logistics Management Center Attn: Col. L. A. Robbins Fort Lee, Virginia</p>	2
<p>NASA Headquarters Office of Advanced Research & Technology 1512 H Street, N. W. Washington, D. C.</p>	1
<p>Commanding General Combat Developments Command Material Requirements Division Fort Belvoir, Virginia</p>	1
<p>Assistant Secretary of the Air Force (R&D) Room 4E968 The Pentagon Washington 25, D. C.</p>	1
<p>Advanced Research Projects Agency Department of Defense The Pentagon Washington 25, D. C.</p>	1
<p>Dr. Vincent Schulta Division of Biology and Medicine U. S. Atomic Energy Commission Washington, D. C.</p>	1
<p>Dr. Arnold H. Sparrow Biology Department Brookhaven National Laboratory Upton, Long Island, New York</p>	1
<p>Dr. John D. Spikes Department of Experimental Biology University of Utah Salt Lake City, Utah</p>	1
<p>Dr. William S. Osborn, Jr. Institute of Arctic and Alpine Research University of Colorado Boulder, Colorado</p>	1
<p>Mr. Stanley Auerbach Oak Ridge National Laboratory Oak Ridge, Tennessee</p>	1
<p>Mr. Gene Odum University of Georgia Athens, Georgia</p>	1

Mr. John Wolf
U. S. Atomic Energy Commission
Oak Ridge, Tennessee

1

Mr. Edward G. Struxness
Deputy Director
Health Physics Division
Oak Ridge National Laboratory
Oak Ridge, Tennessee

1

Mr. Kermit Larson
UCLA Medical School
Los Angeles, California

1

Mr. L. K. Bustad
Biology Laboratory
Hanford Laboratories
Richland, Washington

1

Department of Sanitary Engineering
Walter Reed Army Institute of Research
Washington, D. C. 20012

1

Naval Command Systems Support Agency
U. S. Naval Station
Washington Navy Yard Annex
Building 196
Washington 25, D. C.
Attn: N. L. Richardson, Code 22

1

Lt. Morgan S. Ely
Navy Training Publications Center
Navy Yard Annex
Washington, D. C. 20390

1

THE RESEARCH TRIANGLE INSTITUTE, Durham, North Carolina
OCD Subtask 3233B - Final Report R-OU-156, Volume II

16 October 1964 (UNCLASSIFIED) 299 pp. Joseph T. Ryan, et al.

This is Volume II of two volumes which contain the analysis and conclusions reached under OCD Subtask 3233B, Radiological Recovery Concepts, Requirements and Structures. This report contains five studies concerned with determining the costs and effectiveness of decontamination applied to postattack recovery in a fallout environment. These studies cover the following subjects: (1) The Effect of Early Decontamination on Total Dose: This study describes the effect of a single (discrete) reduction in radiation intensity (i.e., by decontamination) on an individual's dose history in a $t^{-1.2}$ radiation field; (2) The Effect of Early Decontamination on ERD: This analysis is like the first in describing the effect of a single reduction in radiation intensity, except that an individual's dose is measured in terms of his ERD; (3) Total Dose Approximations for Brief Exposure in a Fallout Environment: Two approximations to the expression used to calculate total dose for a finite exposure time in a $t^{-1.2}$ radiation field are developed and the resultant error is estimated; (4) The Effectiveness of Radiological Countermeasures in Accelerating Postattack Recovery: This study develops the parametric relationships that determine which radiological countermeasures could accelerate the postattack recovery process; (5) Studies of Decontamination Effectiveness: This analysis determines the costs and effectiveness of decontamination on and around nine NTSS structures.

CIVIL DEFENSE, DECONTAMINATION, RECOVERY, RADIOACTIVE FALLOUT, POSTATTACK OPERATIONS, CONTAMINATION, RADIOLOGICAL CONTAMINATION, RADIATION HAZARDS, DOSE RATE, CLEANING, STRUCTURES, PROTECTION FACTOR, CIVIL DEFENSE SYSTEMS.

THE RESEARCH TRIANGLE INSTITUTE, Durham, North Carolina
OCD Subtask 3233B - Final Report R-OU-156, Volume II

16 October 1964 (UNCLASSIFIED) 299 pp. Joseph T. Ryan, et al.

This is Volume II of two volumes which contain the analysis and conclusions reached under OCD Subtask 3233B, Radiological Recovery Concepts, Requirements and Structures. This report contains five studies concerned with determining the costs and effectiveness of decontamination applied to postattack recovery in a fallout environment. These studies cover the following subjects: (1) The Effect of Early Decontamination on Total Dose: This study describes the effect of a single (discrete) reduction in radiation intensity (i.e., by decontamination) on an individual's dose history in a $t^{-1.2}$ radiation field; (2) The Effect of Early Decontamination on ERD: This analysis is like the first in describing the effect of a single reduction in radiation intensity, except that an individual's dose is measured in terms of his ERD; (3) Total Dose Approximations for Brief Exposure in a Fallout Environment: Two approximations to the expression used to calculate total dose for a finite exposure time in a $t^{-1.2}$ radiation field are developed and the resultant error is estimated; (4) The Effectiveness of Radiological Countermeasures in Accelerating Postattack Recovery: This study develops the parametric relationships that determine which radiological countermeasures could accelerate the postattack recovery process; (5) Studies of Decontamination Effectiveness: This analysis determines the costs and effectiveness of decontamination on and around nine NTSS structures.

CIVIL DEFENSE, DECONTAMINATION, RECOVERY, RADIOACTIVE FALLOUT, POSTATTACK OPERATIONS, CONTAMINATION, RADIOLOGICAL CONTAMINATION, RADIATION HAZARDS, DOSE RATE, CLEANING, STRUCTURES, PROTECTION FACTOR, CIVIL DEFENSE SYSTEMS.

THE RESEARCH TRIANGLE INSTITUTE, Durham, North Carolina
OCD Subtask 3233B - Final Report R-OU-156, Volume II

16 October 1964 (UNCLASSIFIED) 299 pp. Joseph T. Ryan, et al.

This is Volume II of two volumes which contain the analysis and conclusions reached under OCD Subtask 3233B, Radiological Recovery Concepts, Requirements and Structures. This report contains five studies concerned with determining the costs and effectiveness of decontamination applied to postattack recovery in a fallout environment. These studies cover the following subjects: (1) The Effect of Early Decontamination on Total Dose: This study describes the effect of a single (discrete) reduction in radiation intensity (i.e., by decontamination) on an individual's dose history in a $t^{-1.2}$ radiation field; (2) The Effect of Early Decontamination on ERD: This analysis is like the first in describing the effect of a single reduction in radiation intensity, except that an individual's dose is measured in terms of his ERD; (3) Total Dose Approximations for Brief Exposure in a Fallout Environment: Two approximations to the expression used to calculate total dose for a finite exposure time in a $t^{-1.2}$ radiation field are developed and the resultant error is estimated; (4) The Effectiveness of Radiological Countermeasures in Accelerating Postattack Recovery: This study develops the parametric relationships that determine which radiological countermeasures could accelerate the postattack recovery process; (5) Studies of Decontamination Effectiveness: This analysis determines the costs and effectiveness of decontamination on and around nine NTSS structures.

CIVIL DEFENSE, DECONTAMINATION, RECOVERY, RADIOACTIVE FALLOUT, POSTATTACK OPERATIONS, CONTAMINATION, RADIOLOGICAL CONTAMINATION, RADIATION HAZARDS, DOSE RATE, CLEANING, STRUCTURES, PROTECTION FACTOR, CIVIL DEFENSE SYSTEMS.

THE RESEARCH TRIANGLE INSTITUTE, Durham, North Carolina
OCD Subtask 3233B - Final Report R-OU-156, Volume II

16 October 1964 (UNCLASSIFIED) 299 pp. Joseph T. Ryan, et al.

This is Volume II of two volumes which contain the analysis and conclusions reached under OCD Subtask 3233B, Radiological Recovery Concepts, Requirements and Structures. This report contains five studies concerned with determining the costs and effectiveness of decontamination applied to postattack recovery in a fallout environment. These studies cover the following subjects: (1) The Effect of Early Decontamination on Total Dose: This study describes the effect of a single (discrete) reduction in radiation intensity (i.e., by decontamination) on an individual's dose history in a $t^{-1.2}$ radiation field; (2) The Effect of Early Decontamination on ERD: This analysis is like the first in describing the effect of a single reduction in radiation intensity, except that an individual's dose is measured in terms of his ERD; (3) Total Dose Approximations for Brief Exposure in a Fallout Environment: Two approximations to the expression used to calculate total dose for a finite exposure time in a $t^{-1.2}$ radiation field are developed and the resultant error is estimated; (4) The Effectiveness of Radiological Countermeasures in Accelerating Postattack Recovery: This study develops the parametric relationships that determine which radiological countermeasures could accelerate the postattack recovery process; (5) Studies of Decontamination Effectiveness: This analysis determines the costs and effectiveness of decontamination on and around nine NTSS structures.

CIVIL DEFENSE, DECONTAMINATION, RECOVERY, RADIOACTIVE FALLOUT, POSTATTACK OPERATIONS, CONTAMINATION, RADIOLOGICAL CONTAMINATION, RADIATION HAZARDS, DOSE RATE, CLEANING, STRUCTURES, PROTECTION FACTOR, CIVIL DEFENSE SYSTEMS.

Security Classification

DOCUMENT CONTROL DATA - R&D

(Security classification of title, body of abstract and indexing annotation must be entered when the overall report is classified)

1. ORIGINATING ACTIVITY (Corporate author) Research Triangle Institute Post Office Box 490 Durham, North Carolina		2a. REPORT SECURITY CLASSIFICATION UNCLASSIFIED	
		2b. GROUP -----	
3. REPORT TITLE <u>Radiological Recovery Concepts, Requirements and Structures</u> Volume II - Specific Considerations and Supporting Documents			
4. DESCRIPTIVE NOTES (Type of report and inclusive dates) Volume II of a 2 volume final report			
5. AUTHOR(S) (Last name, first name, initial) Ryan, J. T. Douglass, Joseph D. Campbell, H. E.			
6. REPORT DATE October 16, 1964	7a. TOTAL NO. OF PAGES 299	7b. NO. OF REFS 31	
8a. CONTRACT OR GRANT NO. OCD-PS-64-56	9a. ORIGINATOR'S REPORT NUMBER(S) R-OJ-156		
b. PROJECT NO. OCD 3233B Subtask			
c. Postattack Research Division	9b. OTHER REPORT NO(S) (Any other numbers that may be assigned this report)		
d. OCD Research Directorate	Volume 2		
10. AVAILABILITY/LIMITATION NOTICES Qualified Requestors may obtain copies of this report from DDC			
11. SUPPLEMENTARY NOTES		12. SPONSORING MILITARY ACTIVITY Office of Civil Defense Department of the Army Washington, D. C. 20310	

13. ABSTRACT

This is Volume II of two volumes which contain the analysis and conclusions reached under OCD Subtask 3233B, Radiological Recovery Concepts, Requirements and Structures. This report contains five studies concerned with determining the costs and effectiveness of decontamination applied to postattack recovery in a fallout environment. These studies cover the following subjects: (1) The Effect of Early Decontamination on Total Dose: This study describes the effect of a single (discrete) reduction in radiation intensity (i.e., by decontamination) on an individual's dose history in a $t^{-1.2}$ radiation field; (2) The Effect of Early Decontamination on ERD: This analysis is like the first in describing the effect of a single reduction in radiation intensity, except that an individual's dose is measured in terms of his ERD; (3) Total Dose Approximation: Brief Exposure in a Fallout Environment: Two approximations to the equation used to calculate total dose for a finite exposure time in a t^{-k} rad field developed and the resultant error is estimated. (4) The Effectiveness of Radiological Countermeasures in Accelerating Postattack Recovery: This study develops the parametric relationships that determine which radiological countermeasures could accelerate the postattack recovery process; (5) Study of Decontamination Effectiveness: This analysis determines the costs and effectiveness of decontamination on and around nine NFSS structures.

Best Available Copy